

APPENDIX A

A.1	GENERAL INFORMATION.....	A.1-1
A.1.1	Introduction.....	A.1-2
A.1.2	General Description and Operational Features of the NUHOMS® MATRIX.....	A.1-3
	A.1.2.1 NUHOMS® MATRIX Characteristics	A.1-3
	A.1.2.2 Transfer Equipment	A.1-4
	A.1.2.3 Operational Features	A.1-5
A.1.3	Drawings.....	A.1-7
A.1.4	NUHOMS® EOS System Contents.....	A.1-8
A.1.5	Qualification of TN Americas, LLC (Applicant).....	A.1-9
A.1.6	Quality Assurance.....	A.1-10
A.1.7	References	A.1-11
A.1.8	Supplemental Data.....	A.1-12
	A.1.8.1 Generic Storage Arrays	A.1-12
A.2	PRINCIPAL DESIGN CRITERIA.....	A.2-1
A.2.1	SSCs Important to Safety.....	A.2-2
	A.2.1.1 Dry Shielded Canisters	A.2-2
	A.2.1.2 HSM-MX	A.2-2
	A.2.1.3 ISFSI Basemat and Approach Slabs	A.2-2
	A.2.1.4 Transfer Equipment	A.2-2
	A.2.1.5 Auxiliary Equipment	A.2-2
A.2.2	Spent Fuel To Be Stored.....	A.2-3
A.2.3	Design Criteria for Environmental Conditions and Natural Phenomena.....	A.2-4
	A.2.3.1 Tornado Wind and Tornado Missiles for HSM-MX	A.2-4
	A.2.3.2 Tornado Wind and Tornado Missiles for EOS-TC	A.2-4
	A.2.3.3 Water Level (Flood) Design.....	A.2-5
	A.2.3.4 Seismic Design	A.2-5
	A.2.3.5 Snow and Ice Loading.....	A.2-6
	A.2.3.6 Tsunami.....	A.2-6

	<i>A.2.3.7 Lightning.....</i>	<i>A.2-6</i>
A.2.4	<i>Safety Protection Systems.....</i>	<i>A.2-7</i>
	<i>A.2.4.1 General</i>	<i>A.2-7</i>
	<i>A.2.4.2 Structural</i>	<i>A.2-7</i>
	<i>A.2.4.3 Thermal.....</i>	<i>A.2-7</i>
	<i>A.2.4.4 Shielding/Confinement/Radiation Protection</i>	<i>A.2-8</i>
	<i>A.2.4.5 Criticality.....</i>	<i>A.2-8</i>
	<i>A.2.4.6 Material Selection.....</i>	<i>A.2-8</i>
	<i>A.2.4.7 Operating Procedures.....</i>	<i>A.2-9</i>
	<i>A.2.4.8 Acceptance Tests and Maintenance</i>	<i>A.2-9</i>
	<i>A.2.4.9 Decommissioning.....</i>	<i>A.2-9</i>
A.2.5	<i>References</i>	<i>A.2-10</i>
A.3	<i>STRUCTURAL EVALUATION.....</i>	<i>A.3-1</i>
A.3.1	<i>Structural Design</i>	<i>A.3-2</i>
	<i>A.3.1.1 Design Criteria</i>	<i>A.3-2</i>
A.3.2	<i>Weight and Centers of Gravity</i>	<i>A.3-3</i>
A.3.3	<i>Mechanical Properties of Materials.....</i>	<i>A.3-4</i>
	<i>A.3.3.1 EOS-37PTH DSC/EOS-89BTH DSC.....</i>	<i>A.3-4</i>
	<i>A.3.3.2 HSM-MX.....</i>	<i>A.3-4</i>
	<i>A.3.3.3 EOS-TC.....</i>	<i>A.3-4</i>
A.3.4	<i>General Standards for NUHOMS® MATRIX System.....</i>	<i>A.3-5</i>
	<i>A.3.4.1 Chemical and Galvanic Reaction</i>	<i>A.3-5</i>
	<i>A.3.4.2 Positive Closure</i>	<i>A.3-5</i>
	<i>A.3.4.3 Lifting Devices</i>	<i>A.3-5</i>
	<i>A.3.4.4 Heat.....</i>	<i>A.3-5</i>
	<i>A.3.4.5 Cold.....</i>	<i>A.3-7</i>
A.3.5	<i>Fuel Rods General Standards for NUHOMS® MATRIX System.....</i>	<i>A.3-8</i>
A.3.6	<i>Normal Conditions of Storage and Transfer</i>	<i>A.3-9</i>
	<i>A.3.6.1 EOS-37PTH DSC/89BTH DSC.....</i>	<i>A.3-9</i>
	<i>A.3.6.2 HSM-MX.....</i>	<i>A.3-9</i>
	<i>A.3.6.3 EOS-TC.....</i>	<i>A.3-10</i>

A.3.7	<i>Off-Normal and Hypothetical Accident Conditions of Storage and Transfer</i>	<i>A.3-11</i>
A.3.7.1	<i>EOS-37PTH DSC/89BTH DSC.....</i>	<i>A.3-11</i>
A.3.7.2	<i>HSM-MX.....</i>	<i>A.3-11</i>
A.3.7.3	<i>EOS-TC.....</i>	<i>A.3-11</i>
A.3.8	<i>References</i>	<i>A.3-12</i>
A.3.9.1	<i>DSC SHELL STRUCTURAL ANALYSIS</i>	<i>A.3.9.1-1</i>
A.3.9.1.1	<i>General Description</i>	<i>A.3.9.1-1</i>
A.3.9.1.2	<i>DSC Shell Assembly Stress Analysis.....</i>	<i>A.3.9.1-1</i>
A.3.9.1.3	<i>DSC Shell Buckling Evaluation.....</i>	<i>A.3.9.1-4</i>
A.3.9.1.4	<i>DSC Fatigue Analysis.....</i>	<i>A.3.9.1-4</i>
A.3.9.1.5	<i>DSC Weld Flaw Size Evaluation.....</i>	<i>A.3.9.1-4</i>
A.3.9.1.6	<i>Conclusions.....</i>	<i>A.3.9.1-4</i>
A.3.9.1.7	<i>References</i>	<i>A.3.9.1-5</i>
A.3.9.2	<i>EOS-37PTH AND EOS-89BTH BASKET STRUCTURAL ANALYSIS</i>	<i>A.3.9.2-1</i>
A.3.9.3	<i>NUHOMS® EOS SYSTEM ACCIDENT DROP EVALUATION</i>	<i>A.3.9.3-1</i>
A.3.9.4	<i>HSM-MX STRUCTURAL ANALYSIS.....</i>	<i>A.3.9.4-1</i>
A.3.9.4.1	<i>General Description</i>	<i>A.3.9.4-1</i>
A.3.9.4.2	<i>Material Properties</i>	<i>A.3.9.4-1</i>
A.3.9.4.3	<i>Design Criteria.....</i>	<i>A.3.9.4-1</i>
A.3.9.4.4	<i>Load Cases.....</i>	<i>A.3.9.4-2</i>
A.3.9.4.5	<i>Load Combination.....</i>	<i>A.3.9.4-2</i>
A.3.9.4.6	<i>Finite Element Models.....</i>	<i>A.3.9.4-2</i>
A.3.9.4.7	<i>Normal Operation Structural Analysis</i>	<i>A.3.9.4-4</i>
A.3.9.4.8	<i>Off-Normal Operation Structural Analysis</i>	<i>A.3.9.4-5</i>
A.3.9.4.9	<i>Accident Condition Structural Analysis.....</i>	<i>A.3.9.4-6</i>
A.3.9.4.10	<i>Structural Evaluation</i>	<i>A.3.9.4-11</i>
A.3.9.4.11	<i>Conclusions.....</i>	<i>A.3.9.4-21</i>
A.3.9.4.12	<i>References</i>	<i>A.3.9.4-22</i>

A.3.9.5	NUHOMS® EOS-TC BODY STRUCTURAL ANALYSIS	A.3.9.5-1
A.3.9.6	NUHOMS® EOS FUEL CLADDING EVALUATION.....	A.3.9.6-1
A.3.9.7	NUHOMS® MATRIX STABILITY ANALYSIS.....	A.3.9.7-1
A.3.9.7.1	General Description	A.3.9.7-1
A.3.9.7.2	HSM-MX Stability Analyses.....	A.3.9.7-4
A.3.9.7.3	EOS Transfer Cask Missile Stability and Stress Evaluation	A.3.9.7-14
A.3.9.7.4	References	A.3.9.7-15
A.4	THERMAL EVALUATION.....	A.4-1
A.4.1	Discussion of Decay Heat Removal System.....	A.4-2
A.4.2	Material and Design Limits.....	A.4-3
	A.4.2.1 Summary of Thermal Properties of Materials	A.4-3
A.4.3	Thermal Loads and Environmental Conditions	A.4-4
A.4.4	Thermal Evaluation for Storage	A.4-5
	A.4.4.1 EOS-37PTH DSC and Basket Type 4H - Description of Load Cases for Storage.....	A.4-6
	A.4.4.2 EOS-37PTH DSC with Basket Type 4H - Thermal Model for Storage in HSM-MX.....	A.4-7
	A.4.4.3 EOS-37PTH DSC with Basket Type 4H for HLZC 7 – Storage Evaluation.....	A.4-17
	A.4.4.4 EOS-37PTH DSC with Basket Type 4L/5 - Storage in HSM-MX	A.4-22
	A.4.4.5 EOS-89BTH DSC with Basket Type 3 - Storage in HSM-MX	A.4-26
A.4.5	Thermal Evaluation for Storage in Updated HSM-MX.....	A.4-27
	A.4.5.1 Design Changes in Updated HSM-MX.....	A.4-27
	A.4.5.2 Description of Load Cases for Storage in Updated HSM-MX	A.4-28
	A.4.5.3 Thermal Model for Storage in Updated HSM-MX	A.4-28
	A.4.5.4 EOS-37PTH DSC with Basket Type 4H – Storage in Updated HSM-MX	A.4-29
	A.4.5.5 EOS-37PTH DSC with Basket Type 4L/5 – Storage in Updated HSM-MX	A.4-31

	<i>A.4.5.6 EOS-89BTH DSC with Basket Type 3 - Storage in Updated HSM-MX</i>	<i>A.4-32</i>
	<i>A.4.5.7 Sensitivity Study</i>	<i>A.4-33</i>
A.4.6	<i>References</i>	<i>A.4-38</i>
A.5	<i>CONFINEMENT.....</i>	<i>A.5-1</i>
A.6	<i>SHIELDING EVALUATION.....</i>	<i>A.6-1</i>
A.6.1	<i>Discussions and Results.....</i>	<i>A.6-2</i>
A.6.2	<i>Source Specification</i>	<i>A.6-4</i>
	<i>A.6.2.1 Computer Programs.....</i>	<i>A.6-4</i>
	<i>A.6.2.2 PWR and BWR Source Terms</i>	<i>A.6-4</i>
	<i>A.6.2.3 Axial Source Distributions and Subcritical Neutron Multiplication.....</i>	<i>A.6-4</i>
	<i>A.6.2.4 Control Components</i>	<i>A.6-4</i>
	<i>A.6.2.5 Blended Low Enriched Uranium Fuel</i>	<i>A.6-4</i>
	<i>A.6.2.6 Reconstituted Fuel</i>	<i>A.6-4</i>
	<i>A.6.2.7 Irradiation Gases</i>	<i>A.6-4</i>
A.6.3	<i>Model Specification.....</i>	<i>A.6-5</i>
	<i>A.6.3.1 Material Properties.....</i>	<i>A.6-5</i>
	<i>A.6.3.2 MCNP Model Geometry for the EOS-TC</i>	<i>A.6-5</i>
	<i>A.6.3.3 MCNP Model Geometry for the HSM-MX.....</i>	<i>A.6-5</i>
A.6.4	<i>Shielding Analysis.....</i>	<i>A.6-8</i>
	<i>A.6.4.1 Computer Codes.....</i>	<i>A.6-8</i>
	<i>A.6.4.2 Flux-to-Dose Rate Conversion</i>	<i>A.6-8</i>
	<i>A.6.4.3 EOS-TC Dose Rates</i>	<i>A.6-8</i>
	<i>A.6.4.4 HSM-MX Dose Rates</i>	<i>A.6-8</i>
A.6.5	<i>Supplemental Information.....</i>	<i>A.6-11</i>
	<i>A.6.5.1 References</i>	<i>A.6-11</i>
A.7	<i>CRITICALITY EVALUATION</i>	<i>A.7-1</i>
A.8	<i>MATERIALS EVALUATION.....</i>	<i>A.8-1</i>
A.8.1	<i>General Information.....</i>	<i>A.8-2</i>
	<i>A.8.1.1 HSM-MX Materials.....</i>	<i>A.8-2</i>

A.8.1.2	<i>Environmental Conditions</i>	A.8-2
A.8.1.3	<i>Engineering Drawings</i>	A.8-2
A.8.2	<i>Materials Selection</i>	A.8-3
A.8.2.1	<i>Applicable Codes and Standards and Alternatives</i>	A.8-3
A.8.2.2	<i>Material Properties</i>	A.8-4
A.8.2.3	<i>Materials for ISFSI Sites with Experience of Atmospheric Chloride Corrosion</i>	A.8-5
A.8.2.4	<i>Weld Design and Inspection</i>	A.8-5
A.8.2.5	<i>Galvanic and Corrosive Reactions</i>	A.8-6
A.8.2.6	<i>Creep Behavior of Aluminum</i>	A.8-6
A.8.2.7	<i>Bolt Applications</i>	A.8-7
A.8.2.8	<i>Protective Coatings and Surface Treatments</i>	A.8-7
A.8.2.9	<i>Neutron Shielding Materials</i>	A.8-7
A.8.2.10	<i>Materials for Criticality Control</i>	A.8-7
A.8.2.11	<i>Concrete and Reinforcing Steel</i>	A.8-7
A.8.2.12	<i>Seals</i>	A.8-7
A.8.2.13	<i>Low Temperature Ductility of Ferritic Steels</i>	A.8-7
A.8.3	<i>Fuel Cladding</i>	A.8-8
A.8.4	<i>Prevention of Oxidation Damage During Loading of Fuel</i>	A.8-9
A.8.5	<i>Flammable Gas Generation</i>	A.8-10
A.8.6	<i>DSC Closure Weld Testing</i>	A.8-11
A.8.7	<i>References</i>	A.8-12
A.9	<i>OPERATING PROCEDURES</i>	A.9-1
A.9.1	<i>Procedures for Loading the DSC and Transfer to the HSM-MX</i>	A.9-2
A.9.1.1	<i>TC and DSC Preparation</i>	A.9-2
A.9.1.2	<i>DSC Fuel Loading</i>	A.9-2
A.9.1.3	<i>DSC Drying and Backfilling</i>	A.9-2
A.9.1.4	<i>DSC Sealing Operations</i>	A.9-2
A.9.1.5	<i>TC Downending and Transfer to ISFSI</i>	A.9-2
A.9.1.6	<i>DSC Transfer to the HSM-MX</i>	A.9-2
A.9.1.7	<i>Monitoring Operations</i>	A.9-4
A.9.2	<i>Procedures for Unloading the DSC</i>	A.9-5

A.9.2.1	<i>DSC Retrieval from the HSM-MX</i>	A.9-5
A.9.2.2	<i>Removal of Fuel from the DSC</i>	A.9-7
A.9.3	<i>References</i>	A.9-8
A.10	<i>ACCEPTANCE TESTS AND MAINTENANCE PROGRAM</i>	A.10-1
A.10.1	<i>Acceptance Tests</i>	A.10-2
A.10.1.2	<i>Leak Tests</i>	A.10-2
A.10.1.3	<i>Visual Inspection and Non-Destructive Examinations</i>	A.10-2
A.10.1.4	<i>Shielding Tests</i>	A.10-2
A.10.1.5	<i>Neutron Absorber Tests</i>	A.10-2
A.10.1.6	<i>Thermal Acceptance Tests</i>	A.10-3
A.10.1.7	<i>Low Alloy High Strength Steel for Basket Structure</i>	A.10-3
A.10.1.8	<i>Cask Identification</i>	A.10-3
A.10.2	<i>Maintenance Program</i>	A.10-4
A.10.3	<i>Repair, Replacement, and Maintenance</i>	A.10-5
A.10.4	<i>References</i>	A.10-6
A.11	<i>RADIATION PROTECTION</i>	A.11-1
A.11.1	<i>Radiation Protection Design Features</i>	A.11-2
A.11.2	<i>Occupational Dose Assessment</i>	A.11-3
A.11.2.1	<i>EOS-DSC Loading, Transfer, and Storage Operations</i>	A.11-3
A.11.2.2	<i>EOS-DSC Retrieval Operations</i>	A.11-3
A.11.2.3	<i>Fuel Unloading Operations</i>	A.11-4
A.11.2.4	<i>Maintenance Operations</i>	A.11-4
A.11.2.5	<i>Doses during ISFSI Expansion</i>	A.11-4
A.11.3	<i>Offsite Dose Calculations</i>	A.11-5
A.11.3.1	<i>Normal Conditions (10 CFR 72.104)</i>	A.11-5
A.11.3.2	<i>Accident Conditions (10 CFR 72.106)</i>	A.11-8
A.11.4	<i>Ensuring that Occupational Radiation Exposures Are ALARA</i>	A.11-9
A.11.4.1	<i>Policy Considerations</i>	A.11-9
A.11.4.2	<i>Design Considerations</i>	A.11-9
A.11.4.3	<i>Operational Considerations</i>	A.11-9
A.11.5	<i>References</i>	A.11-10

A.12	ACCIDENT ANALYSES.....	A.12-1
A.12.1	Introduction.....	A.12-1
A.12.2	Off-Normal Events.....	A.12-2
	A.12.2.1 Off-Normal Transfer Load.....	A.12-2
	A.12.2.2 Extreme Temperatures.....	A.12-4
A.12.3	Postulated Accidents.....	A.12-5
	A.12.3.1 EOS-TC Drop.....	A.12-5
	A.12.3.2 Earthquake.....	A.12-7
	A.12.3.3 Tornado Wind and Tornado Missiles Effect on HSM-MX.....	A.12-7
	A.12.3.4 Tornado Wind and Tornado Missiles Effect on EOS-TC.....	A.12-9
	A.12.3.5 Flood.....	A.12-9
	A.12.3.6 Blockage of HSM-MX Air Inlet Openings.....	A.12-9
	A.12.3.7 Lightning.....	A.12-10
	A.12.3.8 Fire/Explosion.....	A.12-10
A.12.4	References.....	A.12-12
A.13	OPERATING CONTROLS AND LIMITS.....	A.13-1

APPENDIX A.1 GENERAL INFORMATION

Table of Contents

A.1 GENERAL INFORMATION.....	A.1-1
A.1.1 Introduction.....	A.1-2
A.1.2 General Description and Operational Features of the NUHOMS® MATRIX.....	A.1-3
A.1.2.1 NUHOMS® MATRIX Characteristics.....	A.1-3
A.1.2.2 Transfer Equipment	A.1-4
A.1.2.3 Operational Features	A.1-5
A.1.3 Drawings.....	A.1-7
A.1.4 NUHOMS® EOS System Contents.....	A.1-8
A.1.5 Qualification of TN Americas, LLC (Applicant)	A.1-9
A.1.6 Quality Assurance.....	A.1-10
A.1.7 References.....	A.1-11
A.1.8 Supplemental Data.....	A.1-12
A.1.8.1 Generic Storage Arrays.....	A.1-12

List of Tables

Table A.1-1	Key Design Parameters of the NUHOMS® MATRIX Components	A.1-13
-------------	--	--------

List of Figures

Figure A.1-1	NUHOMS® MATRIX Construction Joint Expansion	A.1-14
Figure A.1-2	NUHOMS® MATRIX Expansion Joint.....	A.1-15
Figure A.1-3	Not Used	A.1-16
Figure A.1-4	ISFSI Layout Drawing for Single Array.....	A.1-17
Figure A.1-5	ISFSI Layout Drawing for a Double Array	A.1-18
Figure A.1-6	ISFSI Layout Drawing for a Combined Single and Double Array.....	A.1-19
Figure A.1-7	NUHOMS® MATRIX System Components and Structures	A.1-20
Figure A.1-8	NUHOMS® MATRIX System Components and Structures	A.1-21
Figure A.1-9	NUHOMS® MATRIX System Components, Structures, and Transfer Equipment.....	A.1-22

A.1 GENERAL INFORMATION

Appendix A to the NUHOMS® EOS Updated Final Safety Analysis Report (UFSAR) addresses the Important to Safety aspects of adding the NUHOMS® MATRIX (HSM-MX) to the NUHOMS® EOS System described in the UFSAR. The HSM-MX is added to the UFSAR as an alternative to the EOS horizontal storage module (EOS-HSM). The primary reason for adding HSM-MX is to reduce the footprint of the current EOS-HSM, which will allow for greater storage capability on an independent spent fuel storage installation (ISFSI) pad than that currently available.

The HSM-MX is a two-tiered staggered, high-density horizontal storage module (HSM), which contains compartments to accommodate dry shielded canisters (DSCs) with various diameters and lengths (See Figure A.1-7 and Figure A.1-8). The HSM-MX provides an independent, passive system with heat removal capacity sufficient to ensure that peak cladding temperatures during long-term storage of spent fuel assemblies remain below acceptable limits to ensure fuel cladding integrity.

The format of this appendix has been prepared in compliance with the information and methods defined in Revision 1 to U.S. Nuclear Regulatory Commission (NRC) NUREG-1536 [A.1-2]. The analyses presented in this appendix demonstrate that the HSM-MX System meets all the requirements of 10 CFR Part 72 [A.1-1].

Note: References to sections or chapters within this appendix are identified with a prefix A (e.g., Section A.2.3, Appendix A.2.3, Chapter A.2, or Appendix A.2). References to sections or chapters of the UFSAR outside of this Appendix (i.e., main body of the UFSAR) are identified with the applicable UFSAR section or chapter number (e.g., Section 2.3 or Chapter 2).

Where the term “HSM” is used without distinction, this term shall be use applies to both the EOS-HSM and HSM-MX.

A.1.1 Introduction

This appendix adds the HSM-MX to the NUHOMS® EOS System. Only those features that are being revised or added to the NUHOMS® EOS System are addressed and evaluated in this appendix. Sections of this appendix that are not affected by the addition of the HSM-MX are indicated in this appendix with “No Change.” The various DSCs and transfer cask (TC) in the NUHOMS® EOS System remain generally unchanged.

The HSM-MX is a staggered, two-tiered reinforced monolithic structure, consisting of massive reinforced concrete compartments that increase resistance to earthquakes and offer significant self-shielding. The HSM-MX is capable of withstanding all normal condition loads, as well as the off-normal condition loads created by earthquakes, tornadoes, flooding, and other natural phenomena hazards. The DSCs are axially restrained to prevent movement during seismic events.

The system is equipped with special design features for enhanced shielding and heat rejection capabilities.

The HSM-MXs are arranged in arrays and fully expandable to permit modular expansion in support of operating power plants. The HSM-MX can be arranged in either a single-row or back-to-back arrangement. The thick concrete monolith of the HSM-MX provides substantial neutron and gamma shielding.

A.1.2 General Description and Operational Features of the NUHOMS® MATRIX

A.1.2.1 NUHOMS® MATRIX CHARACTERISTICS

The NUHOMS® MATRIX provides a staggered two-tiered self-contained modular structure for storage of spent fuel canistered in an EOS-37PTH or EOS-89BTH DSC. The HSM-MX is constructed from reinforced concrete and structural steel. Contact doses for the HSM-MX are designed to be as low as reasonably achievable (ALARA). The key design parameters of the HSM-MX are listed in Table A.1-1.

In lieu of a separate roof and separate shield walls, those features are integral to the monolith in the HSM-MX.

The HSM-MXs provide an independent, passive system with substantial structural capacity to ensure the safe dry storage of spent fuel assemblies (SFAs). To this end, the HSM-MXs are designed to ensure that normal transfer operations and postulated accidents or natural phenomena do not impair the DSC or pose a hazard to the public or plant personnel. Postulated accidents and natural phenomena affecting the HSM-MX are described in detail in Chapter A.12.

The HSM-MX provides a means of removing spent fuel decay heat by a combination of radiation, conduction, and convection. Ambient air enters the HSM-MX through ventilation inlet openings located on the lower tier of the HSM-MX, circulates around the DSC and the heat shields, then exits through the outlets of the HSM-MX. The HSM-MX is designed to remove up to 50.0 kW of decay heat from the bounding EOS-37PTH DSC, when loaded in an HSM-MX lower compartment.

Decay heat is rejected from the DSC to the HSM-MX air space by convection and then removed from the HSM-MX by natural circulation airflow. Heat is also radiated from the DSC surface to the heat shields and HSM-MX walls and roof, where the natural convection airflow and conduction through the walls and roof aid in the removal of the decay heat. The passive cooling system for the HSM-MX is designed to preserve fuel cladding integrity by maintaining SFA peak cladding temperatures below acceptable limits during long-term storage. The outlet vent covers installed on the top of the HSM-MX are designed to mitigate the effect of sustained winds.

Configurations of systems to be stored in the HSM-MX are determined based on heat load, basket type, etc. These configurations are detailed in Table 1-2.

The HSM-MXs are installed on a load-bearing foundation, which consists of a reinforced concrete basemat on a subgrade suitable to support the loads. The HSM-MXs are not tied to the basemat.

Dimensions of the HSM-MX components described in the text and provided in figures and tables of this UFSAR are, in general, nominal dimensions for general system description purposes. Actual design dimensions are contained in the drawings in Section A.1.3.

A.1.2.2 TRANSFER EQUIPMENT

Transfer Trailer:

The EOS DSC will be transferred to the HSM-MX using the same transfer trailer and ram as the transfer equipment transferring the EOS DSC to the EOS-HSM. Thus, there is no change from Section 1.2.2.

Cask Support Skid:

A universal support skid will be used for the transfer of the NUHOMS® EOS DSC to the HSM-MX and is shown in Figure A.1-9. The key design features from the EOS cask support skid are the same as those described in Section 1.2.2; however, in addition, the universal support skid also allows for a NUHOMS® MATRIX loading crane (MX-LC) to capture the skid with a grappling mechanism to raise and lower the TC/DSC for insertion into the HSM-MX.

Ram:

The EOS DSC will be transferred to the HSM-MX using the same ram as the transfer equipment transferring the EOS DSC to the EOS-HSM. Thus, there is no change from Section 1.2.2.

NUHOMS® MATRIX Loading Crane:

The MX-LC is the device used as part of the NUHOMS® transfer equipment, designed and built to assist in loading the DSC into the HSM-MX. The MX-LC is a Part 72 [A.1-1] important-to-safety (ITS)-related piece of transfer equipment. The MX-LC is designed, fabricated, installed, tested, inspected, and qualified in accordance with ASME NOG-1 [A.1-4], as a Type 1 gantry crane. In addition, the MX-LC is engineered to be “single-failure-proof” per NUREG-0612 [A.1-5]. The MX-LC is considered ITS as it supports the loaded TC/DSC during the DSC’s insertion and extraction both into and out of the HSM-MX, respectively, thus providing both a structural and retrieval function.

NUHOMS® MATRIX Retractable Roller Tray:

The NUHOMS® MATRIX retractable roller tray (MX-RRT) is part of the NUHOMS® transfer equipment and is a device used to support the DSC during transfer operations. There are two MX-RRT beams inserted into opposing channels below the DSC opening on the HSM-MX. Each of the MX-RRT beams are removed upon completion of the loading operation.

The MX-RRT is designed in accordance with ASME B30.1 [A.1-6] as a combination power-operated jack with industrial rollers. Structural acceptance criteria of the MX-RRT are in accordance with ASME NOG-1 [A.1-4]. In addition, the MX-RRT is engineered as “single-failure-proof” per NUREG-0612 [A.1-5]. The MX-RRT function is twofold, first to accept the DSC during its insertion, and second, to lower the DSC onto its permanent pillow blocks within the HSM-MX. The MX-RRT is a Part 72 ITS-related piece of transfer equipment. The MX-RRT is considered ITS since it supports the DSC during its insertion and extraction both into and out of the HSM-MX, respectively, thus providing both a structural and retrieval function.

MX-RRT Handling Device

The MX-RRT handling device (RHD) is part of the NUHOMS® Transfer Equipment and is a device used to allow insertion and extraction of the MX-RRT and the HSM-MX shield door shielding blocks. This is a NITS piece of equipment since it does not provide a safety function feature for the HSM-MX.

A.1.2.3 OPERATIONAL FEATURES

This section provides a discussion of the sequence of operations involving the HSM-MX components.

A.1.2.3.1 Spent Fuel Assembly Loading Operations

For the HSM-MX, there is no change from the primary operations listed in Steps 1 to 16 in Section 1.2.3.1. After those steps, the following operations occur, which replace Steps 17 to 20 in Section 1.2.3.1:

17. Move loaded TC to ISFSI
18. Position and align TC/HSM-MX
19. Insert DSC into HSM-MX
20. Close HSM-MX

These operations from Steps 17 to 20 are described in the following paragraphs. The descriptions are intended to be generic and are described in greater detail in Chapter A.9. Plant-specific requirements may affect these operations and are to be addressed by the licensee.

Move Loaded Transfer Cask to ISFSI:

The transfer trailer is moved to the ISFSI along a predetermined route on a prepared road surface. Upon entering the ISFSI, the cask is positioned in front of the HSM-MX loading crane.

Position and align TC/HSM-MX:

The trailer is moved inside the HSM-MX loading crane, and the crane grappling mechanism captures the TC along with the skid.

The HSM-MX loading crane travels laterally and vertically to position the TC in front of its storage compartment in the open HSM-MX with MX-RRTs installed.

Insert DSC into HSM-MX:

After final alignment of the TC, HSM-MX, and ram, the DSC is slid onto the MX-RRT beams inside the HSM-MX by the ram. The DSC is then lowered into place onto the front and rear DSC supports.

Close HSM-MX:

Install HSM-MX door.

A.1.3 Drawings

MX01-5000-SAR	NUHOMS® HSM-MX HORIZONTAL STORAGE MODULE – MATRIX Main Assembly (17 Sheets)
---------------	--

**Proprietary and Security Related Information
for Drawing MX01-5000-SAR, Rev. 0
Withheld Pursuant to 10 CFR 2.390**

A.1.4 NUHOMS® EOS System Contents

No change to Section 1.4.

A.1.5 Qualification of TN Americas, LLC (Applicant)

The prime contractor for design and procurement of the NUHOMS® MATRIX is TN Americas, LLC (TN). TN will subcontract the fabrication, testing, onsite construction, and quality assurance (QA) services, as necessary, to qualified firms on a project-specific basis, in accordance with TN's QA Program requirements.

The design activities for the SAR were performed by TN and subcontractors, in accordance with TN QA Program requirements. TN is responsible for the design and analysis of the HSM-MX and the associated transfer equipment.

A.1.6 Quality Assurance

TN Americas LLC's QA Program has been established in accordance with the requirements of 10 CFR Part 72, Subpart G [A.1-1]. The QA Program applies to the design, purchase, fabrication, handling, shipping, storing, cleaning, assembly, inspection, testing, operation, maintenance, repair, and modification of the NUHOMS® MATRIX and components identified as ITS and "safety-related." These components and systems are defined in Chapter A.2.

The complete description and specific commitments of the TN Americas LLC QA program are contained in the TN Americas LLC QA Program Description Manual [A.1-3]. This manual has been approved by the NRC for performing 10 CFR Part 72-related activities.

A.1.7 References

- A.1-1 Title 10, Code of Federal Regulations, Part 72, “Licensing Requirements for the Independent Storage of Spent Nuclear Fuel, High-Level Radioactive Waste, and Reactor-Related Greater Than Class C Waste.”
- A.1-2 NUREG-1536, “Standard Review Plan for Spent Fuel Dry Storage Systems at a General License Facility,” Revision 1, U.S. Nuclear Regulatory Commission, Office of Nuclear Material Safety and Safeguards, July 2010.
- A.1-3 TN Americas, LLC, “TN Americas LLC Quality Assurance Program Description Manual for 10 CFR Part 71, Subpart H and 10 CFR Part 72, Subpart G,” current revision.
- A.1-4 ASME NOG-1-2015, “Rules for Construction of Overhead and Gantry Cranes (Top Running Bridge Multiple Girder),” The American Society of Mechanical Engineers, New York, New York, 2015.
- A.1-5 NUREG-0612, “Control of Heavy Loads at Nuclear Power Plants,” U.S. Nuclear Regulatory Commission, July 1980.
- A.1-6 ASME B30.1-2015, “Jacks, Industrial Rollers, Air Casters, and Hydraulic Gantries,” The American Society of Mechanical Engineers, New York, New York, 2015.

A.1.8 Supplemental Data

A.1.8.1 GENERIC STORAGE ARRAYS

The DSC containing the SFAs is transferred to, and stored in, compartments of the HSM-MX. Multiple compartments are grouped together to form a staggered, two-tiered monolithic structure known as the HSM-MX. Multiple compartments are grouped together to form arrays whose size is determined to meet plant-specific needs. The HSM-MX is arranged within the ISFSI site on a concrete basemat(s) with the entire area enclosed by a security fence. Modules may be placed in a single-row array or in a back-to-back array for site dose and footprint optimization. Like the EOS-HSM, the decay heat within the HSM-MX DSC compartment is primarily removed by internal natural circulation flow through the inlet/outlet vents and conduction through the HSM-MX walls.

Figure A.1-1 and Figure A.1-2 show typical HSM-MX expansion layouts at ISFSIs that are capable of modular expansion to any capacity.

The expansion option shown in Figure A.1-1 allows the array to be expanded with a construction joint splitting the upper compartment at the end of the array. A minimum of five compartments are required in a monolith. End shield walls shall be installed at this location in the interim period between expansions; the shield walls will be removed to allow for expansion of the array. Two empty compartments (one upper and one lower), in addition to the partial empty compartment, are required at the end of an array during the interim period before expansion. At the end of the array, the end wall will be the same thickness as the wall at the beginning of the first array, and all compartments may be filled.

Figure A.1-2 shows the expansion joint used at ~100 feet into the array. This joint addresses the thermal growth due to cyclic temperatures in ambient conditions. When an array is expanded at the expansion joint, two empty compartments (one top and one bottom) are required at the end of the interim array prior to expansion. When the expansion joint is used, and construction continues past the expansion joint, the construction joint configuration can be used to further expand the array, or the array can terminate with an end wall the same thickness as the wall at the beginning of the first array. If using the construction joint configuration, the same requirements described above for the construction joint apply.

These are typical layouts only and do not represent limitations in number of modules, number of rows, and orientation of modules in rows. Back-to-back module configurations require expansion in sets of pairs. Expansion can be accomplished, as necessary, by the licensee, provided the criteria of 10 CFR 72.104, 10 CFR 72.106 and Chapter 14 are met. The parameters of interest in planning the installation layout are the configuration of the HSM-MX array and an area in front of each HSM-MX to provide adequate space for loading operations. Illustrations of typical HSM-MX ISFSI layouts are provided in Figure A.1-4 through Figure A.1-6.

Table A.1-1
Key Design Parameters of the NUHOMS® MATRIX Components

Horizontal Storage Module (HSM-MX):	
Overall length	23'-1" single array
	41'-4" back-to-back array
Overall width	36'-6"
Overall height (two-tiers without vent covers)	27'-1 3/8"
Total weight not including DSC (kips) (max. concrete density of 160 pcf.)	2,450 (single array)
	4,125 (double array)
Materials of construction	Reinforced concrete and structural steel
Heat removal	Conduction, convection, and radiation

Note: Dimensions are based on a single monolith of five compartments (see Figure A.1-2).

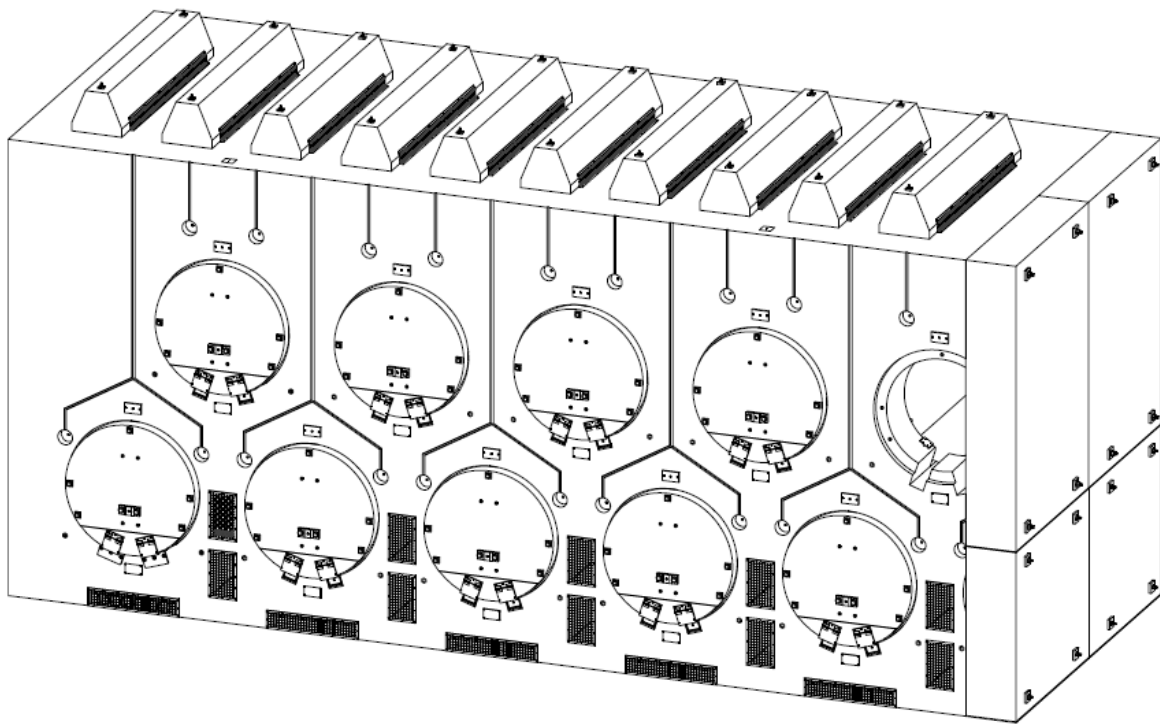


Figure A.1-1
NUHOMS® MATRIX Construction Joint Expansion

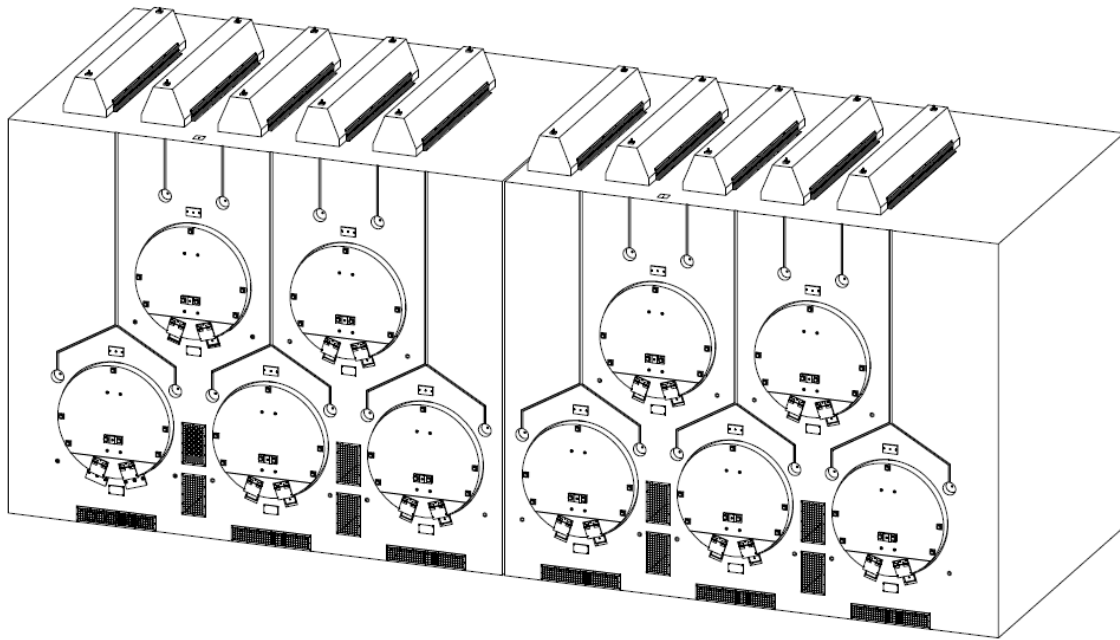


Figure A.1-2
NUHOMS® MATRIX Expansion Joint

Figure A.1-3
Not Used

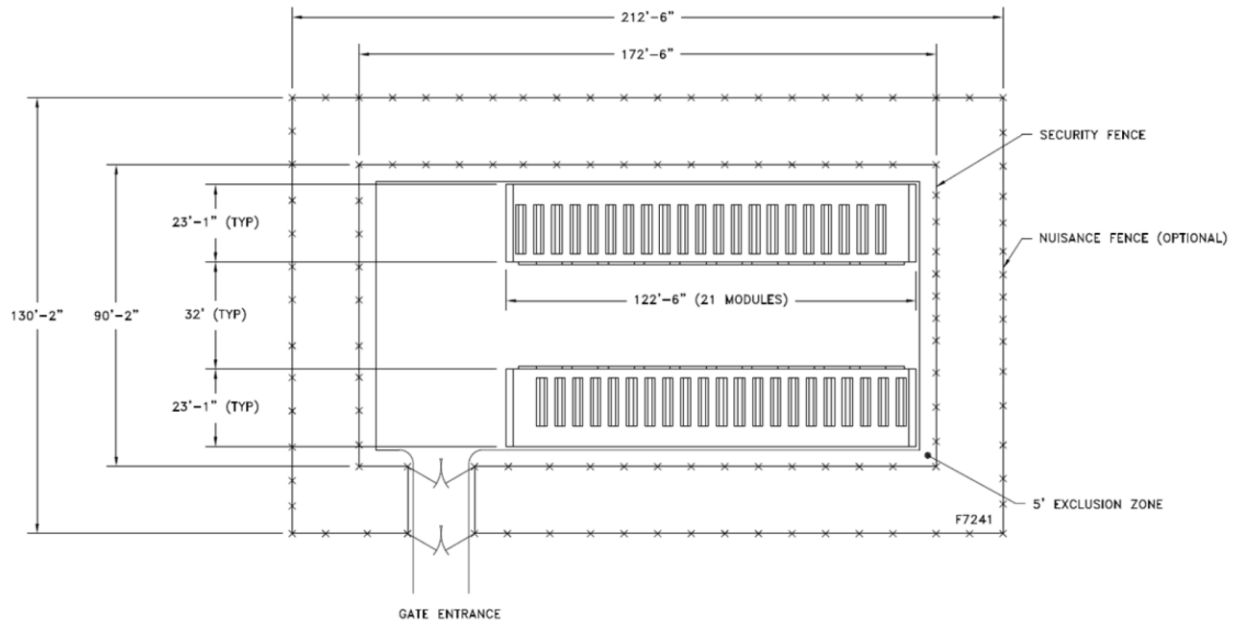


Figure A.1-4
ISFSI Layout Drawing for Single Array

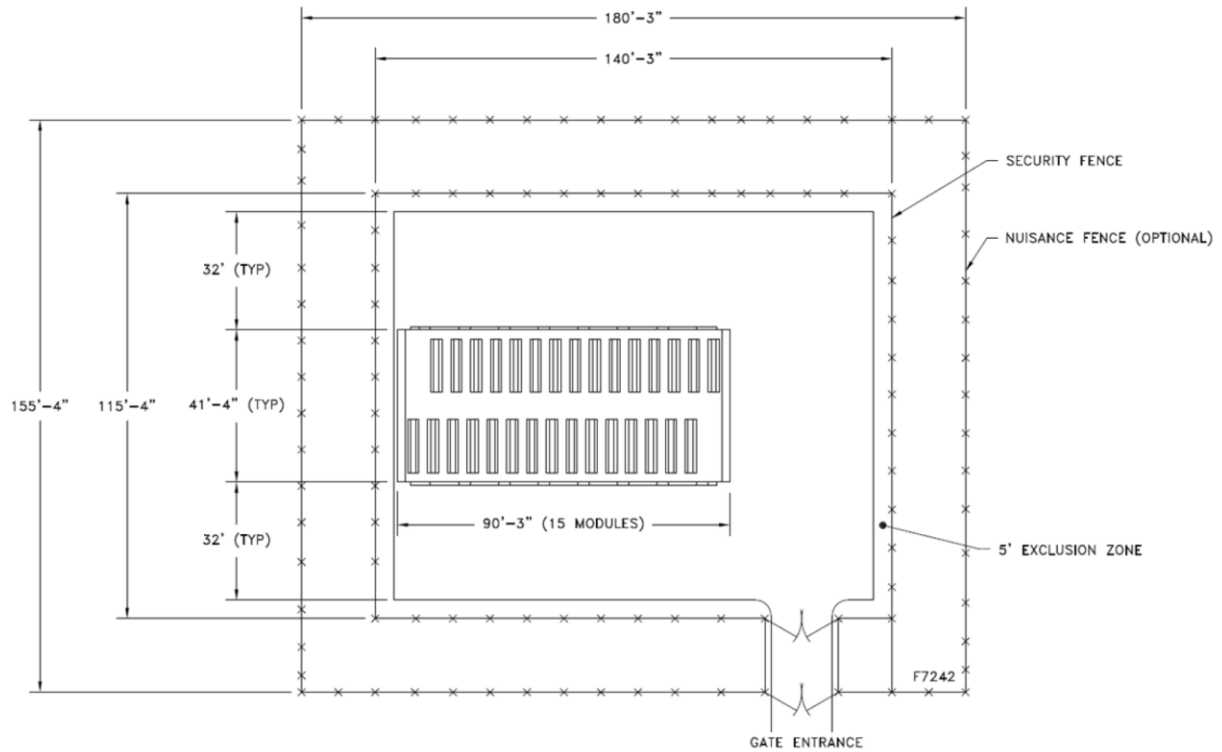


Figure A.1-5
ISFSI Layout Drawing for a Double Array

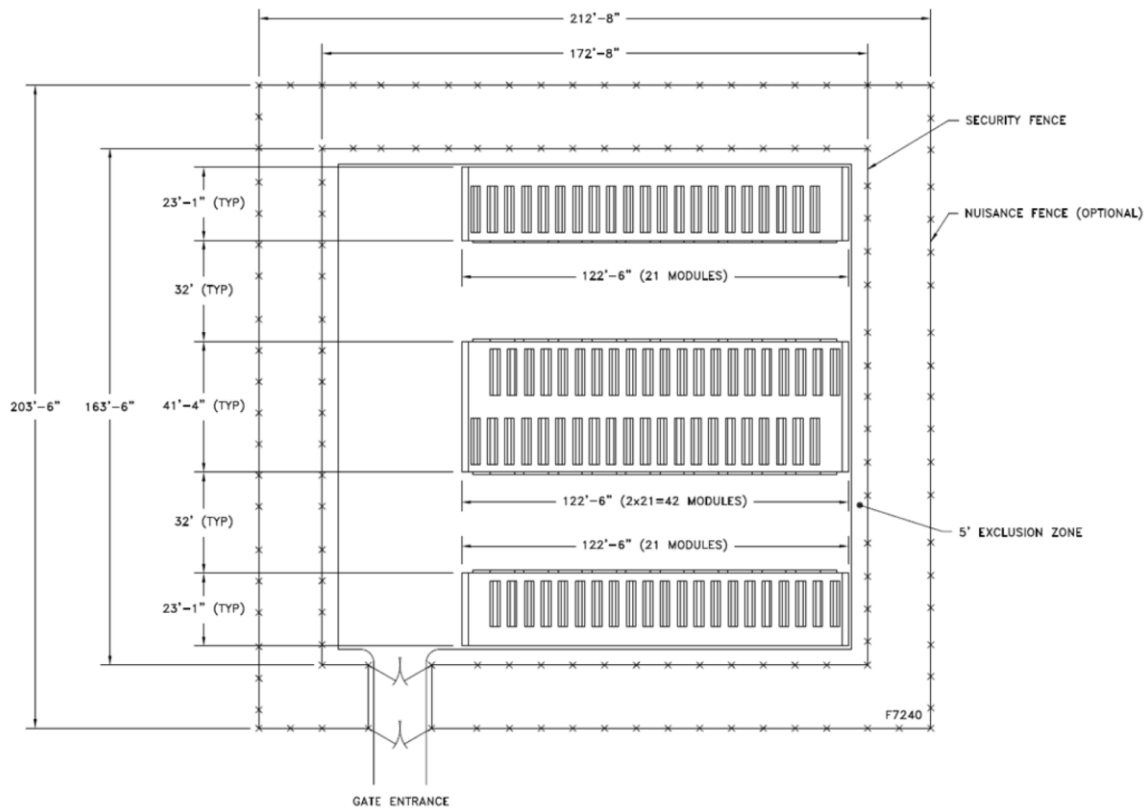


Figure A.1-6
ISFSI Layout Drawing for a Combined Single and Double Array

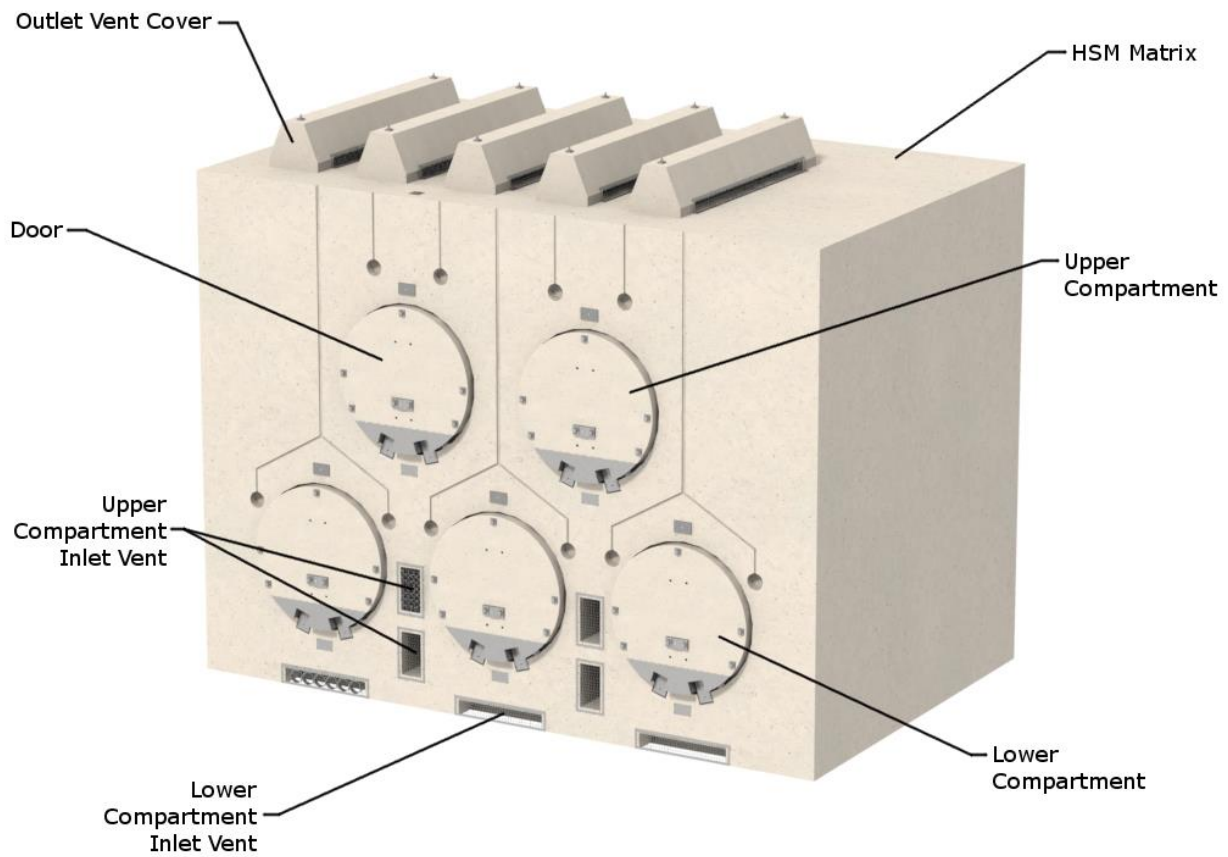


Figure A.1-7
NUHOMS® MATRIX System Components and Structures

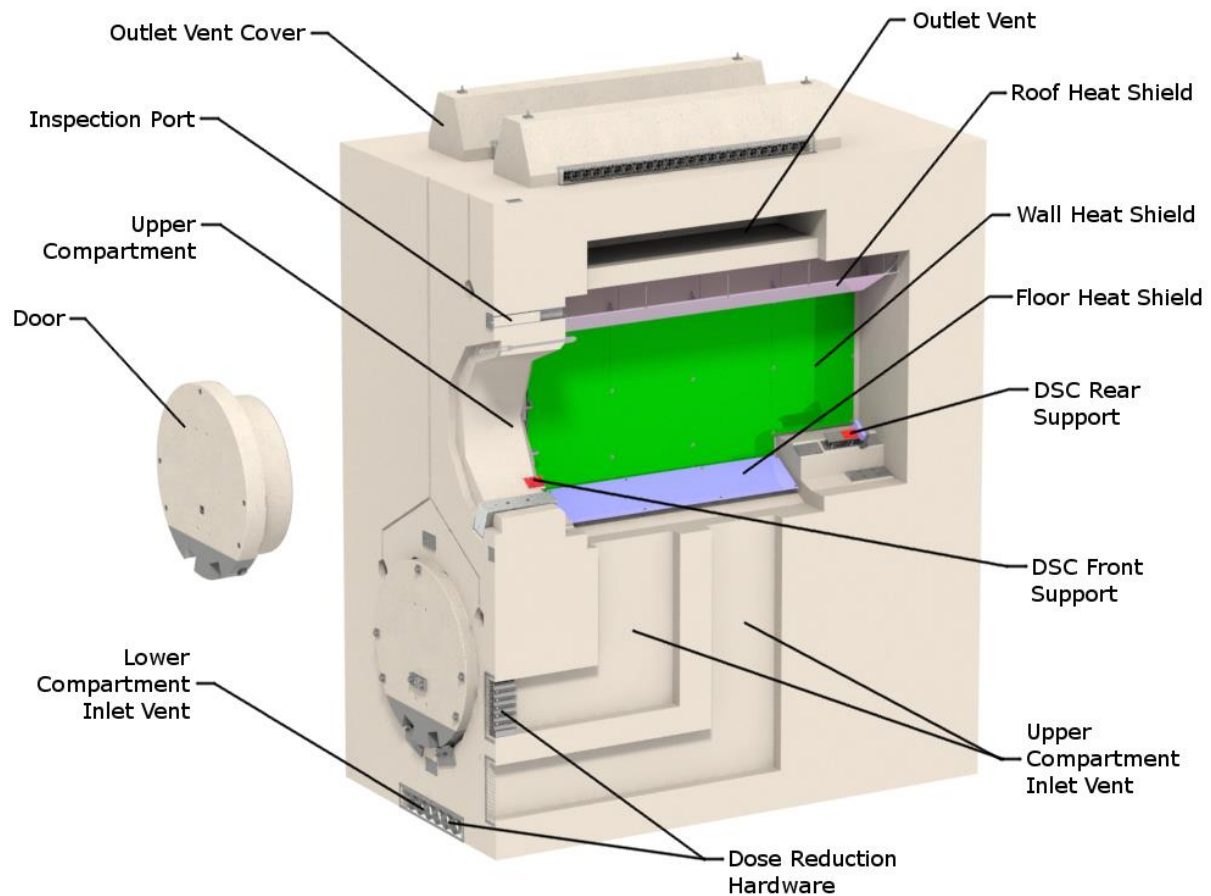


Figure A.1-8
NUHOMS® MATRIX System Components and Structures

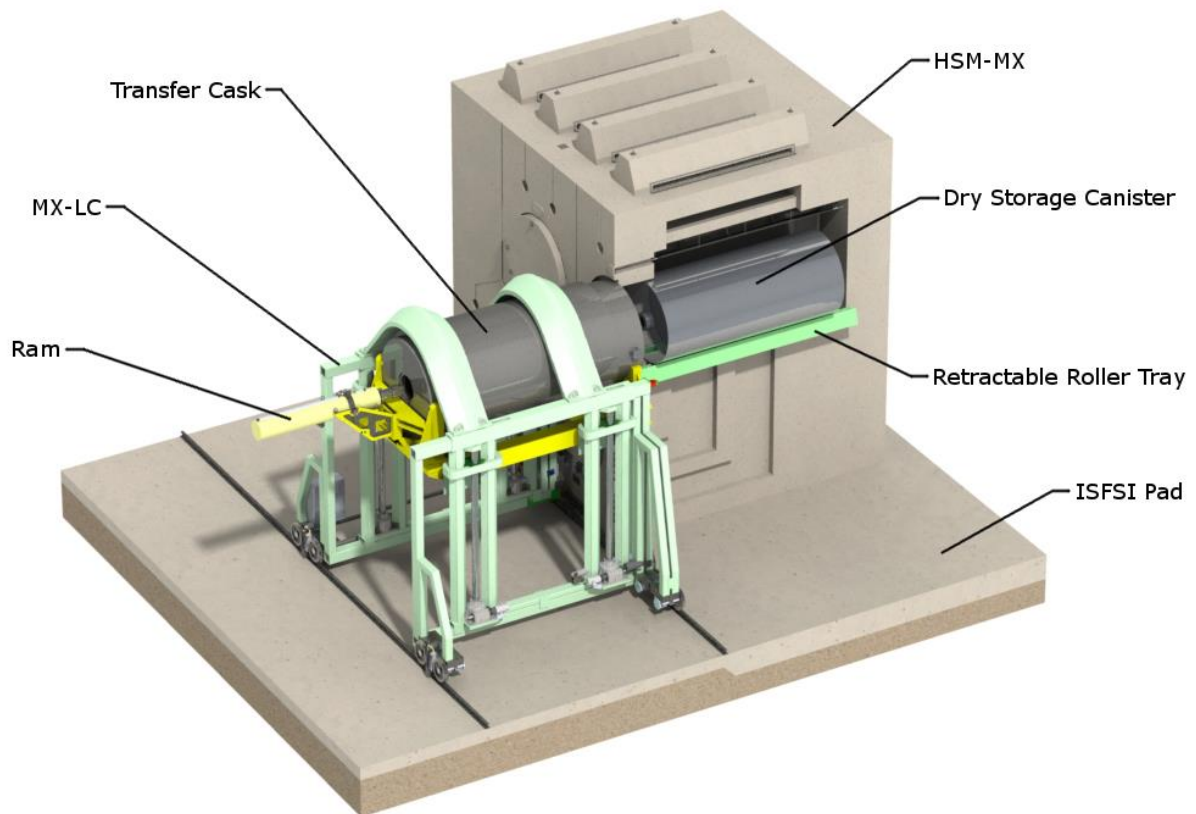


Figure A.1-9
NUHOMS® MATRIX System Components, Structures, and Transfer Equipment

APPENDIX A.2 PRINCIPAL DESIGN CRITERIA

Table of Contents

A.2	PRINCIPAL DESIGN CRITERIA	A.2-1
A.2.1	SSCs Important to Safety	A.2-2
A.2.1.1	Dry Shielded Canisters	A.2-2
A.2.1.2	HSM-MX	A.2-2
A.2.1.3	ISFSI Basemat and Approach Slabs	A.2-2
A.2.1.4	Transfer Equipment	A.2-2
A.2.1.5	Auxiliary Equipment.....	A.2-2
A.2.2	Spent Fuel To Be Stored.....	A.2-3
A.2.3	Design Criteria for Environmental Conditions and Natural Phenomena.....	A.2-4
A.2.3.1	Tornado Wind and Tornado Missiles for HSM-MX	A.2-4
A.2.3.2	Tornado Wind and Tornado Missiles for EOS-TC.....	A.2-4
A.2.3.3	Water Level (Flood) Design	A.2-5
A.2.3.4	Seismic Design.....	A.2-5
A.2.3.5	Snow and Ice Loading	A.2-6
A.2.3.6	Tsunami.....	A.2-6
A.2.3.7	Lightning.....	A.2-6
A.2.4	Safety Protection Systems	A.2-7
A.2.4.1	General.....	A.2-7
A.2.4.2	Structural.....	A.2-7
A.2.4.3	Thermal	A.2-7
A.2.4.4	Shielding/Confinement/Radiation Protection	A.2-8
A.2.4.5	Criticality	A.2-8
A.2.4.6	Material Selection	A.2-8
A.2.4.7	Operating Procedures.....	A.2-9
A.2.4.8	Acceptance Tests and Maintenance	A.2-9
A.2.4.9	Decommissioning	A.2-9
A.2.5	References	A.2-10

List of Tables

Table A.2-1	NUHOMS® EOS HSM-MX System Major Components and Safety Classification.....	A.2-12
Table A.2-2	Thermal Conditions for NUHOMS® HSM-MX System Analyses	A.2-13

List of Figures

Figure A.2-1	RG 1.60 Response Spectra with Enhancement in Frequencies above 9.0 Hz.....	A.2-14
--------------	---	--------

A.2 PRINCIPAL DESIGN CRITERIA

This section provides the principal design criteria for the NUHOMS® MATRIX (HSM-MX) described in Chapter A.1. Section A.2.1 identifies the structures, systems, and components (SSCs) important-to-safety (ITS) for the HSM-MX design. Section A.2.2 presents a general description of the spent fuel to be stored. Section A.2.3 provides the design criteria for environmental conditions and natural phenomena. Section A.2.4 discusses safety protection systems.

A.2.1 SSCs Important to Safety

Table 2-1 provides a list of major NUHOMS® EOS System independent spent fuel storage installation (ISFSI) components and their classification. In addition, Table A.2-1 provides a list of the major NUHOMS® MATRIX (HSM-MX) components and their classification. Components are classified in accordance with the criteria of 10 CFR Part 72. Structures, systems, and components (SSCs) classified as important-to-safety (ITS) are defined in 10 CFR 72.3 as the features of the ISFSI whose function is:

- To maintain the conditions required to store spent fuel safely.
- To prevent damage to the spent fuel container during handling and storage.
- To provide reasonable assurance that spent fuel can be received, handled, packaged, stored, and retrieved without undue risk to the health and safety of the public.

These criteria are applied to the HSM-MX components in determining their classification in the paragraphs that follow.

A.2.1.1 Dry Shielded Canisters

No Change to Section 2.1.1

A.2.1.2 HSM-MX

The HSM-MX is considered ITS since it provides physical protection and shielding for the dry shielded canister (DSC) during storage. The reinforced concrete HSM-MX is designed in accordance with American Concrete Institute (ACI) 349-06 [A.2-3] and constructed to ACI-318-08 [A.2-4]. The level of testing, inspection, and documentation provided during construction and maintenance is in accordance with the quality assurance requirements as defined in 10 CFR Part 72 [A.2-6], Subpart G and as described in Chapter 14. Thermal instrumentation for monitoring HSM-MX concrete temperatures is considered “not important-to-safety” (NITS).

A.2.1.3 ISFSI Basemat and Approach Slabs

The independent spent fuel storage installation (ISFSI) basemat and approach slabs and buildings for indoor storage are considered NITS and are designed, constructed, maintained, and tested as commercial-grade items.

Licensees are required to perform an assessment to confirm that the license seismic criteria described in Section A.2.3.4 are met.

A.2.1.4 Transfer Equipment

A.2.1.4.1 Transfer Cask and Yoke

No change to Section 2.1.4.1.

A.2.1.4.2 Other Transfer Equipment

The NUHOMS® EOS HSM-MX transfer equipment (i.e., ram, skid, transfer trailer, MATRIX loading crane (MX-LC), MATRIX retractable rolling tray (MX-RRT) and MX-RRT handling device (RHD)) are necessary for the successful loading of the DSCs into the HSM-MX.

MX-LC

The NUHOMS® MX-LC is the device used as part of the NUHOMS® transfer equipment, designed and built to assist in loading the DSC into the HSM-MX. The MX-LC is a Part 72 [A.2-6] ITS-related piece of transfer equipment. The MX-LC is designed, fabricated, installed, tested, inspected, and qualified in accordance with ASME NOG-1 [A.2-7], as a Type I gantry crane. In addition, the MX-LC is engineered as “single-failure-proof” per NUREG-0612 [A.2-9]. The MX-LC is considered ITS since it supports the loaded TC/DSC during the DSC’s insertion and extraction both into and out of the HSM-MX, respectively, thus providing both a structural and retrieval function.

MX-RRT

The MX-RRT is part of the NUHOMS® transfer equipment and is a device used to support the DSC, during transfer operations. There are two MX-RRT beams inserted into opposing channels below the DSC opening on the HSM-MX. Each of the MX-RRT beams are removed upon completion of the loading operation and replaced with the HSM-MX shield door shielding blocks. The MX-RRT is designed in accordance with ASME B30.1 [A.2-15] as a combination power-operated jack with industrial rollers. Structural acceptance criteria of the MX-RRT is in accordance with ASME NOG-1 [A.2-7]. In addition, the MX-RRT is engineered as “single-failure-proof” per NUREG-0612 [A.2-9]. The MX-RRT function is twofold, one to accept the DSC during its insertion and second, to lower the DSC onto its permanent pillow blocks within the HSM-MX. The MX-RRT is a Part 72 ITS-related piece of transfer equipment. The MX-RRT is considered ITS as it supports the DSC during its insertion and extraction both into and out of the HSM-MX, respectively, thus providing both a structural and retrieval function.

MX-RRT Handling Device

The MX-RRT handling device is part of the NUHOMS® Transfer Equipment and is a device used to allow insertion and extraction of the MX-RRT and the HSM-MX shield door shielding blocks. This is a NITS piece of equipment since it does not provide a safety function feature for the HSM-MX.

A.2.1.5 Auxiliary Equipment

No change to Section 2.1.5.

A.2.2 Spent Fuel To Be Stored

Spent fuel that is allowed for storage in the HSM-MX is described in Section 2.2.

A.2.3 Design Criteria for Environmental Conditions and Natural Phenomena

The HSM-MX ITS SSCs described in Section A.2.1 are designed consistent with the 10 CFR Part 72 [A.2-6] §122(b) requirement for protection against environmental conditions and natural phenomena. The criterion used in the design of the NUHOMS® EOS System ensures that exposure to credible site hazards does not impair their safety functions.

A.2.3.1 Tornado Wind and Tornado Missiles for HSM-MX

The HSM-MX and MX-LC are designed to safely withstand 10 CFR 72.122 (b)(2) tornado missiles. The tornado characteristics, as specified in NRC Regulatory Guide (RG) 1.76, Revision 1 [A.2-8], are used to qualify the HSM-MX and MX-LC. The missiles spectrum of NUREG-0800, Revision 3, Section 3.5.1.4 [A.2-10] with missile velocity for Region I is used to qualify the HSM-MX and MX-LC.

Extreme wind effects are much less severe than the specified design basis tornado (DBT) wind forces. The design basis extreme wind for the HSM-MX is calculated per [A.2-10].

However, since the MX-LC is specified per ASME NOG-1 [A.2-7] loading conditions, the design basis wind for the MX-LC is calculated per Region IV of [A.2-12]. Nonetheless, congruent with the HSM-MX, the design basis extreme wind (i.e., tornado wind) for the MX-LC is calculated per Region I of [A.2-10].

A.2.3.1.1 Tornado Wind Design Parameters

No change to Section 2.3.1.1.

A.2.3.1.2 Determination of Forces on Structures

No change to Section 2.3.1.2.

A.2.3.1.3 Tornado Missiles

No change to Section 2.3.1.3.

A.2.3.2 Tornado Wind and Tornado Missiles for EOS-TC

No change to Section 2.3.2.

A.2.3.2.1 Tornado Wind Design Parameters

No change to Section 2.3.2.1.

A.2.3.2.2 Tornado Missiles

No change to Section 2.3.2.2.

A.2.3.3 Water Level (Flood) Design

HSM-MX inlet vents are blocked when the depth of flooding is greater than 0.25 m (10 in.) for the lower compartment, and 2.29 m (7 ft-6 in.), for the upper compartments, above the level of the ISFSI basemat. The DSC in the lower and upper compartments are wetted when flooding exceeds a depth of 1.3 m (4 ft-2 in.), and 4.4 m (14 ft-5 in.), respectively, above ISFSI basemat. Greater flood heights result in submersion of the DSC and blockage of the HSM-MX outlet vents.

The DSC and HSM-MX are conservatively designed for an enveloping design basis flood. The flood is postulated to result from natural phenomena such as tsunamis and seiches, as specified by 10 CFR 72.122(b) [A.2-6]. A bounding assumption of a 15-meter (50-foot) flood height and water velocity of 4.6 m/sec (15 fps) is used for the flood evaluation. The HSM-MX is evaluated for the effects of the 4.6 m/sec (15 fps) water current impinging upon the side of the submerged HSM-MX. The DSC is subjected to an external pressure equivalent to a 15-meter (50-foot) head of water. These evaluations are presented in Section A.12.3.5. The effects of water reflection on DSC criticality safety are addressed in Chapter 7. Due to its short-term, infrequent use, the onsite EOS transfer cask (EOS-TC) is not explicitly evaluated for flood effects. Independent spent fuel storage installation procedures should ensure that the EOS-TC is not used for DSC transfer during flood conditions.

The plant-specific design basis flood (if the possibility for flooding exists at a particular ISFSI site) should be evaluated by the licensee and shown to be enveloped by the flooding conditions used for this generic evaluation of the HSM-MX.

A.2.3.4 Seismic Design

The seismic design criteria for the HSM-MX are based on the NRC RG 1.60 [A.2-13] response spectra anchored at a zero period acceleration (ZPA) of 0.85g in the horizontal direction and 0.80g in the vertical direction and enhanced frequency content above 9 Hz. The horizontal and vertical components of the design response spectra corresponding to a maximum horizontal ground acceleration of 1.0g are shown in Figure A.2-1. The seismic structural evaluations consider both stability evaluation and stress qualification of the HSM-MX. The stability criteria for seismic loading are based on the stability response of a five-compartment construction joint option of the HSM-MX module without the side shield walls attached.

The HSM-MX has no anchorage to the concrete basemat. The stability analyses consider the effects of sliding and rocking motions, and determine the maximum possible sliding of the HSM-MX. The HSM-MX will neither slide nor overturn at design ZPA of 0.48g in the horizontal direction and 0.32g in the vertical direction.

The licensee shall determine if, based on ISFSI-specific site investigations, a soil-structure interaction (SSI) analyses ought to be performed to assess potential site-specific amplifications. The SSI evaluations are based on ISFSI site-specific parameters (free-field accelerations, strain-dependent soil properties, HSM-MX array configurations, etc.). The SSI response spectra at the base of the HSM-MXs are to be bounded by the HSM-MX design basis seismic criteria response spectra, i.e., the RG 1.60 response spectra shape, with enhanced spectral accelerations above 9 Hz, and anchored at 0.85g horizontal and 0.80g vertical directions. The licensee shall reconcile spectral accelerations from the SSI analysis response spectra that exceed the seismic criteria spectra (if any); 5% damped response spectra may be used in making these determinations.

Since the DSC can be considered to act as a large diameter pipe for the purpose of evaluating seismic effects, the “Equipment and Large Diameter Piping System” category in NRC RG 1.61 [A.2-16], Table 1 is applicable. Therefore, a damping value of 3% of critical damping for the design bases safe shutdown earthquake is used. Similarly, from the same RG table, a damping value of 7% of critical damping is used for the reinforced concrete structural components of the HSM-MX.

The seismic criteria for the MX-LC are based on Figures 1 and 2 of NRC Regulatory Guide 1.60 [A.2-13], with enhanced spectral accelerations above 9 Hz, and anchored at 0.85g zero period acceleration (ZPA) in the horizontal direction and 0.80g ZPA in the vertical direction. The seismic structural calculations consider both a stability evaluation and stress qualification of the MX-LC for seismic loading criteria. The stability evaluations address the MX-LC rails and use of any shims under the MX-LC rails due to unevenness in the basemat and approach slab foundation.

The seismic criteria for the MX-RRTs is based on Figures 1 and 2 of NRC Regulatory Guide 1.60 [A.2-13], with enhanced spectral accelerations above 9 Hz, and anchored at 0.85g ZPA in the horizontal direction and 0.80g ZPA in the vertical direction. As required, the seismic structural calculations shall consider both a stability evaluation and stress qualification for the seismic loading criteria.

A.2.3.5 Snow and Ice Loading

No change to Section 2.3.5.

A.2.3.6 Tsunami

No change to Section 2.3.6.

A.2.3.7 Lightning

A lightning strike will not cause a significant thermal effect on the HSM-MX, MX-LC, MX-RRT, or stored DSC. The effects on the HSM-MX resulting from a lightning strike are discussed in Section 12.3.7.

A.2.4 Safety Protection Systems

A.2.4.1 General

No change to Section 2.4.1.

A.2.4.2 Structural

A.2.4.2.1 EOS-DSC Design Criteria

No change to Section 2.4.2.1.

A.2.4.2.2 HSM-MX Design Criteria

The principal design criteria for the HSM-MX, both the concrete and steel structures, are presented in Table 2-7.

The reinforced concrete HSM-MX is designed to meet the requirements of ACI 349-06 [A.2-3]. The ultimate strength method of analysis is utilized with the appropriate strength reduction factors as described in Appendix A.3.9.4. The load combinations specified in Section 6.17.3.1 of American National Standards Institute (ANSI) 57.9-1984 [A.2-20] are used for combining normal operating, off-normal, and accident loads for the HSM-MX. All seven load combinations specified are considered and the governing combinations are selected for detailed design and analysis. The resulting HSM-MX load combinations and the appropriate load factors are presented in Appendix A.3.9.4. The effects of duty cycle on the HSM-MX are considered and found to have negligible effect on the design.

A.2.4.2.3 EOS-TC Design Criteria

No change to Section 2.4.2.3.

A.2.4.2.4 MX-LC Design Criteria

The MX-LC is designed in accordance with the applicable portions of ASME NOG-1 [A.2-7], as a Type 1 gantry style crane. The MX-LC is engineered to provide high integrity handling (HIH) of the load, defined as a lifting/handling operation, wherein the risk of an uncontrolled lowering of the heavy load is considered non-credible. Demonstration of HIH of the MX-LC occurs when designed for “single-failure-proof” lifting operations per NUREG-0612 [A.2-9], maintaining the supported loads in a safe configuration during design basis events (e.g., seismic). Therefore, design requirements from ASME NOG-1 for Type 1 loading equipment are specified with an additional single failure proof handling capability. MX-LC single-failure-proof handling capability is achieved by ensuring that the applicable design factor is 200% of that required by ASME NOG-1 (i.e., NUREG-0612 application). Alternatively, other load carrying members may be designed with redundant devices to meet the single failure proof handling capability. Therefore, MX-LC HIH may be achieved by having either MX-LC subcomponent SSCs that comply with ASME NOG-1 stress limits plus the 200% NUREG-0612 design factor or with other MX -LC subcomponent SSCs having redundant safety basis protection features.

A.2.4.2.5 MX-RRT Design Criteria

Congruent with the MX-LC, the MX-RRT is engineered to provide HIH of the load. Demonstration of HIH of the MX-RRT occurs when designed for “single-failure-proof” lifting operations per NUREG-0612 [A.2-9], maintaining the supported loads in a safe configuration during design basis events (e.g., seismic). Therefore, applicable design acceptance criteria are provided by ASME NOG-1 [A.2-7], plus an additional single-failure-proof handling capability. MX-RRT single failure proof handling capability is achieved by ensuring that the design factor is 200% of that from ASME NOG-1 (i.e., NUREG-0612 application). In lieu of the 200% requirement, it is acceptable to have other load carrying members designed with redundant devices to meet the single failure proof handling. Therefore, MX-RRT HIH may be achieved by having either MX-RRT subcomponent SSCs that comply with ASME NOG-1 stress limits plus the 200% NUREG-0612 design factor or with other MX-RRT subcomponent SSCs having redundant safety-basis protection features.

A.2.4.3 Thermal

The NUHOMS® MATRIX relies on natural convection through the air space in the HSM-MX to cool the DSC. This passive convective ventilation system is driven by the pressure difference due to the stack effect (ΔP_s) provided by the height difference between the bottom of the DSC and the HSM-MX air outlet. This pressure difference is greater than the flow pressure drop (ΔP_f) at the design air inlet and outlet temperatures. The details of the ventilation system design are provided in Chapter A.4.

Thermal analysis is based on fuel assemblies with decay heat up to 50.0 kW per DSC for the EOS-37PTH and up to 34.4 kW per DSC for the EOS-89BTH. Zoning is used to accommodate high per assembly heat loads. The heat load zoning configurations for the DSCs are shown in Figure 1A through Figure 1I and Figure 2 of the Technical Specifications [A.2-18] for 37PTH and 89BTH DSC, respectively. Among the various HLZCs presented in Figure 1 for EOS-37PTH DSC, only HLZC # 7 through 9 presented in Figure 1G through Figure 1I are applicable for storage in HSM-MX. Similarly for the EOS-89BTH, among the various HLZCs presented in Figure 2 for EOS-89BTH DSC, only HLZC # 3 is permitted for storage in the HSM-MX.

The thermal analyses for storage are performed for the environmental conditions listed in Table A.2-2. The remainder of the environment conditions are provided in Table 2-9.

Peak clad temperature of the fuel at the beginning of the long-term storage does not exceed 400 °C for normal conditions of storage, and for short-term operations, including DSC drying and backfilling. Fuel cladding temperature shall be maintained below 570 °C (1058 °F) for accident conditions involving fire or off-normal storage conditions.

For onsite transfer in the EOS-TC, air circulation may be used, as a recovery action, to facilitate transfer operations in the EOS-37PTH DSC as described in the Technical Specifications [A.2-18].

A.2.4.4 Shielding/Confinement/Radiation Protection

The HSM-MX provides the bulk of the radiation shielding for the DSCs. The HSM-MX designs can be arranged in either a single-row or a back-to-back arrangement. The nominal thickness of the HSM-MX roof is 50 inches for biological shielding. Additionally, the front wall has a minimum thickness of 39 inches. Sufficient shielding is provided by thick concrete side walls between HSM-MXs in an array to minimize doses in adjacent HSM-MXs during loading and retrieval operations. Section A.11.3 provides a summary of the offsite dose calculations for representative arrays of design basis HSM-MXs providing assurance that the limits in 10 CFR 72.104 and 10 CFR 72.106(b) are not exceeded.

There are no radioactive releases of effluents during normal and off-normal storage operations. Also, there are no credible accidents that cause significant releases of radioactive effluents from the DSC. Therefore, there are no off-gas or monitoring systems required for the HSM-MX.

A.2.4.5 Criticality

No change to Section 2.4.5.

A.2.4.6 Material Selection

No change to Section 2.4.6.

A.2.4.7 Operating Procedures

The sequence of operations are outlined for the HSM-MX in Chapter A.9 for loading of fuel, closure of the DSC, transfer to the ISFSI using the TC, insertion into the HSM-MX, monitoring operations, and retrieval and unloading. Throughout Chapter A.9, CAUTION statements are provided at the step where special notice is needed to maintain as low as reasonably achievable (ALARA), protect the contents of the DSC, protect the public and/or ITS components of the HSM-MX.

A.2.4.8 Acceptance Tests and Maintenance

Chapter A.10 specifies the acceptance testing and maintenance program for ITS components of the HSM-MX.

A.2.4.9 Decommissioning

The exact decommissioning plan for the ISFSI will be dependent on the U.S. Department of Energy's fuel transportation system capability and requirements for a specific plant. Because of the minimal contamination of the outer surface of the DSC, no contamination is expected on the internal passages of the HSM-MX. It is anticipated that the prefabricated HSM-MXs can be dismantled and disposed of using commercial demolition and disposal techniques.

A.2.5 References

- A.2-1 Title 10, Code of Federal Regulations, Part 100, “Reactor Site Criteria.”
- A.2-2 American Society of Mechanical Engineers, “ASME Boiler and Pressure Vessel Code,” Section III, Division 1, Subsections NB, NF, ND and NCA, 2010 Edition with 2011 Addenda.
- A.2-3 ACI 349-06, “Code Requirements for Nuclear Safety Related Concrete Structures,” American Concrete Institute.
- A.2-4 ACI 318-08, “Building Code Requirements for Structural Concrete and Commentary,” American Concrete Institute.
- A.2-5 Title 10, Code of Federal Regulations, Part 50, “Domestic Licensing of Production and Utilization Facilities.”
- A.2-6 Title 10, Code of Federal Regulations, Part 72, “Licensing Requirements for the Independent Storage of Spent Nuclear Fuel, High-Level Radioactive Waste, and Reactor-Related Greater Than Class C Waste.”
- A.2-7 ASME NOG-1-2015, “Rules for Construction of Overhead and Gantry Cranes (Top Running Bridge Multiple Girder),” The American Society of Mechanical Engineers, New York, New York, 2015.
- A.2-8 U.S. Nuclear Regulatory Commission, Regulatory Guide 1.76, “Design Basis Tornado and Tornado Missiles for Nuclear Power Plants,” Revision 1, March 2007.
- A.2-9 NUREG-0612, “Control of Heavy Loads at Nuclear Power Plants,” U.S. Nuclear Regulatory Commission, July 1980.
- A.2-10 NUREG-0800, Standard Review Plan, Section 3.3.1 “Wind Loading,” Section 3.3.2 “Tornado Loads”, and Section 3.5.1.4 “Missiles Generated by Tornado and Extreme Winds,” Revision 3, March 2007.
- A.2-11 NUREG-0800, Standard Review Plan, Section 3.5.3 “Barrier Design Procedures,” Revision 3, March 2007.
- A.2-12 American Society of Civil Engineers, ASCE 7-10, “Minimum Design Loads for Buildings and Other Structures,” (formerly ANSI A58.1).
- A.2-13 NRC Regulatory Guide 1.60, “Design Response Spectra for Seismic Design of Nuclear Power Plants” Revision 1, December 1973.
- A.2-14 ANSI N14.6, “American National Standard for Special Lifting Device for Shipping Containers Weighing 10,000 lbs. or More for Nuclear Materials,” American National Standards Institute, Inc., 1993.
- A.2-15 ASME B30.1-2015, “Jacks, Industrial Rollers, Air Casters, and Hydraulic Gantries,” The American Society of Mechanical Engineers, New York, New York, 2015.
- A.2-16 U.S. Nuclear Regulatory Commission, Regulatory Guide 1.61, “Damping Values for Seismic Design of Nuclear Power Plants,” Revision 1, March 2007.
- A.2-17 NOT USED

A.2-18 CoC 1042 Appendix A, NUHOMS® EOS System Generic Technical Specifications, Amendment 1.

A.2-19 NOT USED

A.2-20 ANSI 57.9-1984, Design Criteria for an Independent Spent Fuel Storage Installation (Dry Type).

Table A.2-1
HSM-MX System Major Components and Safety Classification

Component	10 CFR Part 72 Classification⁽¹⁾
Horizontal Storage Module (HSM-MX)	
Reinforced Concrete	ITS
Thermal Instrumentation (if used)	NITS
Transfer Equipment	
MX-LC	ITS
MX-RRT	ITS
Universal Support Skid	ITS

Notes:

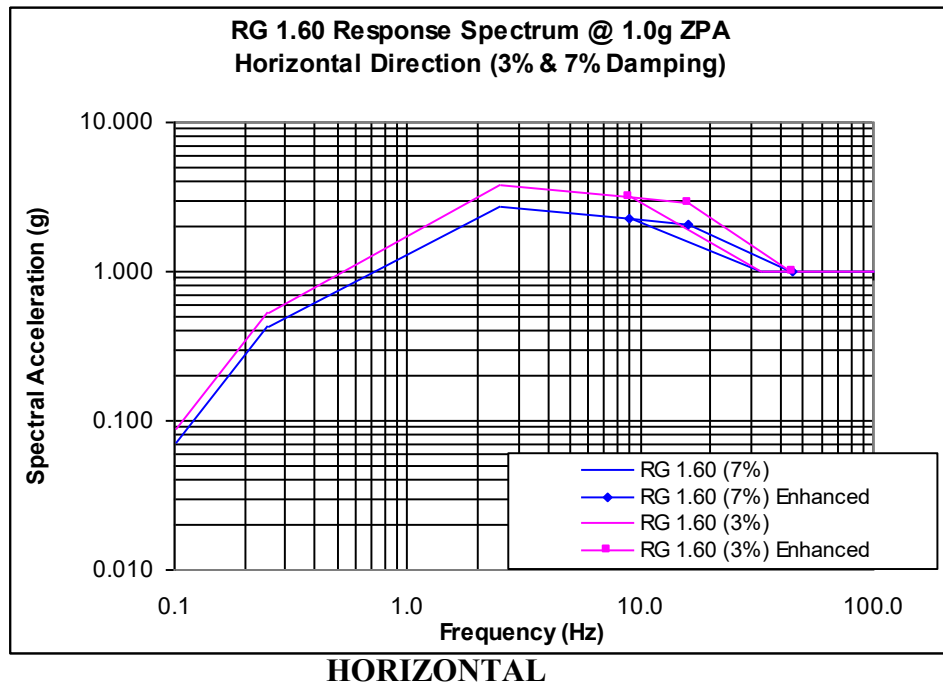
1. SSCs ITS are defined in 10 CFR 72.3 as those features of the ISFSI whose function is (1) to maintain the conditions required to store spent fuel safely, (2) to prevent damage to the spent fuel container during handling and storage, or (3) to provide reasonable assurance that spent fuel can be received, handled, packaged, stored, and retrieved without undue risk to the health and safety of the public.

Table A.2-2
Thermal Conditions for HSM-MX System Analyses

Operating Conditions	EOS-37PTH/EOS-89BTH DSC Location	Minimum Ambient Temperature	Maximum Ambient Temperature
Normal	HSM-MX	-20 °F	100 °F
Off-Normal	HSM-MX	-40 °F	117 °F
Accident	HSM-MX ⁽¹⁾	n/a	117 °F

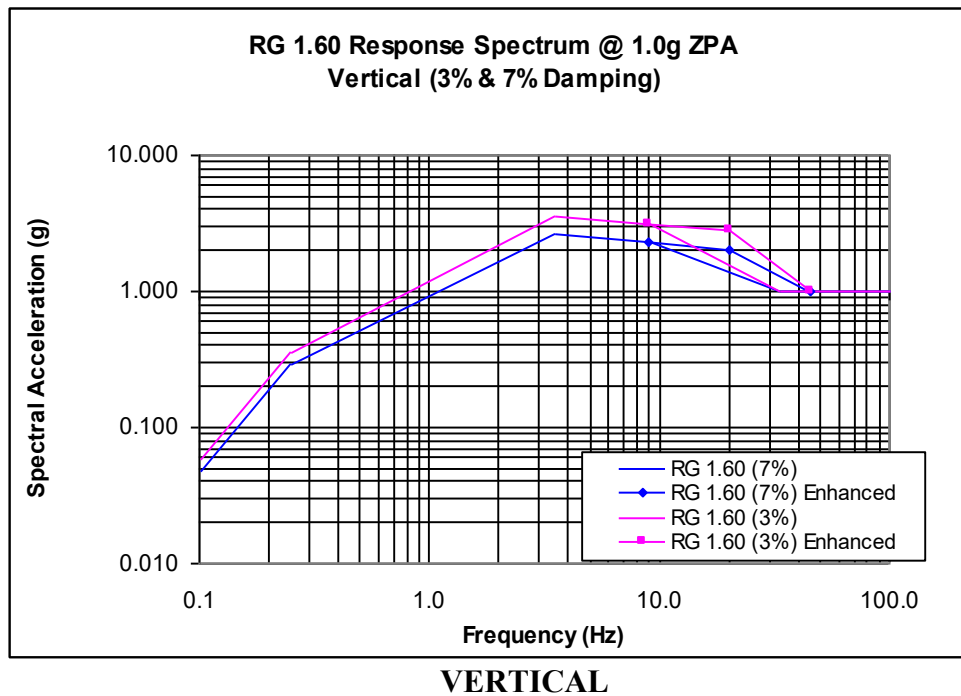
Notes:

1. 10% rod rupture is considered for this blocked vent accident condition for DSC internal pressure calculation.



RG 1.60 (3%, Horiz. Enhanced)	
Freq (Hz)	Acc. (g)
0.10	0.085
0.25	0.529
2.5	3.755
9.0	3.130
16.0	2.885
45.0	1.000
100.0	1.000

RG 1.60 (7%, Horiz. Enhanced)	
Freq (Hz)	Acc. (g)
0.10	0.069
0.25	0.432
2.5	2.720
9.0	2.270
16.0	2.093
45.0	1.000
100.0	1.000



RG 1.60 (3%, Vert. Enhanced)	
Freq (Hz)	Acc. (g)
0.10	0.056
0.25	0.353
3.5	3.577
9.0	3.130
20.0	2.797
45.0	1.000
100.0	1.000

RG 1.60 (7%, Vert. Enhanced)	
Freq (Hz)	Acc. (g)
0.10	0.046
0.25	0.287
3.5	2.590
9.0	2.270
20.0	2.030
45.0	1.000
100.0	1.000

Figure A.2-1
RG 1.60 Response Spectra with Enhancement in Frequencies above 9.0 Hz

APPENDIX A.3 STRUCTURAL EVALUATION

Table of Contents

A.3	STRUCTURAL EVALUATION.....	A.3-1
A.3.1	Structural Design	A.3-2
	A.3.1.1 Design Criteria	A.3-2
A.3.2	Weight and Centers of Gravity.....	A.3-3
A.3.3	Mechanical Properties of Materials	A.3-4
	A.3.3.1 EOS-37PTH DSC/EOS-89BTH DSC	A.3-4
	A.3.3.2 HSM-MX.....	A.3-4
	A.3.3.3 EOS-TC.....	A.3-4
A.3.4	General Standards for NUHOMS® MATRIX System	A.3-5
	A.3.4.1 Chemical and Galvanic Reaction.....	A.3-5
	A.3.4.2 Positive Closure	A.3-5
	A.3.4.3 Lifting Devices.....	A.3-5
	A.3.4.4 Heat	A.3-5
	A.3.4.5 Cold.....	A.3-7
A.3.5	Fuel Rods General Standards for NUHOMS® MATRIX System	A.3-8
A.3.6	Normal Conditions of Storage and Transfer.....	A.3-9
	A.3.6.1 EOS-37PTH DSC/89BTH DSC	A.3-9
	A.3.6.2 HSM-MX	A.3-9
	A.3.6.3 EOS-TC.....	A.3-10
A.3.7	Off-Normal and Hypothetical Accident Conditions of Storage and Transfer	A.3-11
	A.3.7.1 EOS-37PTH DSC/89BTH DSC	A.3-11
	A.3.7.2 HSM-MX	A.3-11
	A.3.7.3 EOS-TC.....	A.3-11
A.3.8	References	A.3-12

List of Tables

Table A.3-1	Summary of HSM-MX Weight and Center of Gravity	A.3-13
-------------	--	--------

A.3 STRUCTURAL EVALUATION

This chapter and its appendices describe the structural evaluation for the NUHOMS® MATRIX (HSM-MX), described in Appendix A.1, under normal and off-normal conditions, accident conditions, and natural phenomena events. Structural evaluations are provided for the important-to-safety components (ITS), which are the EOS-37PTH DSC, the EOS-89BTH DSC, and the HSM-MX monolith. The analyses in Chapter 3 of the EOS-TCs envelop the HSM-MX system and are therefore not provided in this chapter.

A.3.1 Structural Design

The HSM-MX is a staggered horizontal storage version of the NUHOMS® EOS System, which provides environmental protection and radiological shielding for the DSCs. The HSM-MX is designed to accommodate EOS-37PTH DSC and 89BTH DSC configurations. The HSM-MX provides heat rejection from the spent fuel decay heat. Sections in this section of the Appendix that do not have an effect on the evaluations presented in Chapter 3 of the Updated Final Safety Analysis Report (UFSAR) include a statement that there is no change. In addition, a complete evaluation of the HSM-MX has been performed and is summarized in this section and appendices, which are ITS in accordance with 10 CFR Part72 [A.3-1].

A.3.1.1 Design Criteria

A.3.1.1.1 EOS-37PTH DSC/EOS-89BTH DSC Design Criteria

No change to Section 3.1.1.1.

A.3.1.1.1.1 Stress Criteria

No change to Section 3.1.1.1.1.

A.3.1.1.1.2 Stability Criteria

No change to Section 3.1.1.1.2.

A.3.1.1.2 HSM-MX Design Criteria

The HSM-MX concrete and steel components are designed to the requirements of American Concrete Institute (ACI) 349-06 [A.3-2] and the American Institute of Steel Construction (AISC) Manual of Steel Construction [A.3-3], respectively, meeting the load combinations in accordance with the requirements of ANSI 57.9 [A.3-4]. The load combination and design criteria for concrete components are described in Appendix A.3.9.4.

A.3.1.1.3 EOS-TC Design Criteria

No change to Section 3.1.1.3.

A.3.2 Weight and Centers of Gravity

Table A.3-1 summarizes the weights of the HSM-MX. The dead weights of the components are determined based on the nominal dimensions.

A.3.3 Mechanical Properties of Materials

A.3.3.1 EOS-37PTH DSC/EOS-89BTH DSC

No change to Section 3.3.1.

A.3.3.2 HSM-MX

The material properties for the HSM-MX are summarized in Chapter A.8.

A.3.3.3 EOS-TC

No change to Section 3.3.3.

A.3.4 General Standards for NUHOMS® MATRIX System

A.3.4.1 Chemical and Galvanic Reaction

No change to Section 3.4.1 for the EOS System. Chemical and galvanic reactions for the HSM-MX System are presented in Chapter A.8.

A.3.4.2 Positive Closure

No change to Section 3.4.2.

A.3.4.3 Lifting Devices

No change to Section 3.4.3.

A.3.4.4 Heat

A.3.4.4.1 Summary of Pressures and Temperatures

Temperatures and pressures for the HSM-MX are described in Chapter A.4. The thermal evaluations for storage and transfer conditions are performed in Chapter A.4 for normal, off-normal, and accident conditions. The internal pressure evaluation is performed in Chapter A.4, Section A.4.5.

Maximum temperatures for the various components of the HSM-MX, loaded with an EOS-37PTH DSC or an EOS-89BTH DSC under normal, off-normal and accident conditions are summarized in Chapter A.4, Section A.4.5 for all the applicable heat zone loading configurations provided in Appendix A, Technical Specification [A.3-5].

These temperatures are used for the structural evaluations documented in Appendices A.3.9.1 and A.3.9.4. Stress allowables for the components are a function of component temperature. The temperatures used to perform the structural analyses are based on actual calculated temperatures or conservatively selected higher temperatures.

A.3.4.4.2 Differential Thermal Expansion

No change to Section 3.4.4.2.

A.3.4.4.2.1 Minimum Gaps within the Interlocking Slots

No change to Section 3.4.4.2.1.

A.3.4.4.2.2 Axial Gaps between the Basket Assembly Plates

No change to Section 3.4.4.2.2.

A.3.4.4.2.3 Radial Gap between the Basket Assembly and the DSC Shell

No change to Section 3.4.4.2.3.

A.3.4.4.2.4 Axial Gaps between Fuel Assemblies and the DSC Cavity

No change to Section 3.4.4.2.4.

A.3.4.4.2.5 Axial Gap between the Basket Assembly and the DSC Cavity

No change to Section 3.4.4.2.5.

A.3.4.4.2.6 Axial Gap between the Transition Rails and the DSC Cavity

No change to Section 3.4.4.2.6.

A.3.4.4.2.7 Axial Gap between the TC125/TC135 Cavity and the DSC Shell

No change to Section 3.4.4.2.7.

A.3.4.4.2.8 Axial Gap between the Rear DSC support, Axial Retainer and the HSM-MX cavity

A gap of 0.5 inch is provided between the rear DSC Support and the HSM-MX to accommodate any thermal growth. This section verifies that there is no interference when the rear DSC support increases from room temperature to accident temperature.

The maximum temperature of the rear DSC support is assumed to be 350°F. A mean thermal expansion coefficient of 7.0×10^{-6} in/in/°F for 350°F is used. The thermal growth of the rear DSC support is determined as:

$$\Delta L_{rs} = L_{cold} \times \alpha \times \Delta T$$

$$\Delta L_{rs} = 21.5 \times 7.0 \times 10^{-6} \times (350 - 70) = 0.042 \text{ in.}$$

The maximum thermal growth between the rear DSC Support and the HSM-MX is 0.042 inch and is less than the initial 0.5-inch gap.

Therefore, there is sufficient clearance for free thermal expansion between the rear DSC supports and HSM-MX.

A gap is provided between the axial retainer and DSC to accommodate any thermal growth. Shims are used to adjust the gap to be 0.1875 inch initially. The bounding thermal expansion temperature ranges from the normal operating temperature to the blocked vent accident temperature. The largest average temperature difference for the DSC is 396 °F - 293 °F = 103 °F. The axial retainer is conservatively assumed to experience the same temperature difference. The average HSM concrete temperature difference is 207 °F - 152 °F = 55 °F. Conservatively, a higher temperature difference of 105 °F is applied to the DSC and axial retainer, and a lower temperature difference of 50 °F is applied to the HSM concrete. Thermal expansion coefficients of 7.5×10^{-6} in/in/°F and 10.1×10^{-6} in/in/°F for 350 °F are used for the Axial Retainer and the DSC, respectively. The instantaneous coefficients of thermal expansion are used here as the initial temperatures are above 70 °F. A thermal expansion coefficient of 5.5×10^{-6} in/in/°F is used for the HSM concrete. The growth of the HSM is subtracted from the growth of the DSC and axial retainer as it increases the gap.

$$\Delta L = L_{DSC} \times \alpha_{DSC} \times \Delta T_{DSC} + L_{AR} \times \alpha_{AR} \times \Delta T_{AR} - L_{HSM} \times \alpha_{HSM} \times \Delta T_{HSM}$$

$$\Delta L = 199.5 \times 10.1 \times 10^{-6} \times (105) + 36.5 \times 7.5 \times 10^{-6} \times (105) - (199.5 + 36.5) \times 5.5 \times 10^{-6} \times (50) = 0.175 \text{ in}$$

The maximum thermal growth between the axial retainer and DSC is 0.175 inch and is less than a 0.1875-inch gap.

A.3.4.5 Cold

No change to Section 3.4.5.

A.3.5 Fuel Rods General Standards for NUHOMS[®] MATRIX System

No change to Section 3.5.

A.3.6 Normal Conditions of Storage and Transfer

This section presents the structural analysis of the EOS-37PTH DSC/ EOS-89BTH DSCs, the HSM-MX and the EOS-TC subjected to normal conditions of storage and transfer. The analyses performed evaluate the components for the design criteria described in Section A.3.1.1.

Numerical analyses have been performed for the normal and accident conditions. In general, numerical analyses have been performed for the regulatory events. The analyses are summarized in this section.

The detailed structural analyses of the HSM-MX are included in Appendices A.3.9.1 through A.3.9.7.

A.3.6.1 EOS-37PTH DSC/89BTH DSC

Details of the structural analysis of the DSC shell assemblies are provided in Appendix A.3.9.1, while the structural analysis for basket assemblies are provided in Appendix 3.9.2. There are no changes to the analysis described for the DSC shell except that the DSC shell is analyzed for dead weight and seismic load combinations, which are affected when the DSC is loaded into the HSM-MX and are provided in Appendix A.3.9.1. The design or loading conditions for the basket remain the same when loaded into the DSC shell and, therefore, results for the basket from Appendix 3.9.2 remain the same and are applicable.

A.3.6.2 HSM-MX

The HSM-MX design is able to accommodate different DSC lengths. For the structural evaluation, the HSM-MX with the longest DSC bounds all sizes. The following table shows how the bounding loads are used for structural evaluation of the HSM-MX.

Component	Weight (kips)	Thermal Heat Load
EOS-37PTH DSC (Loaded Weight)	134	50 kW
EOS-89BTH DSC (Loaded Weight)	120	43.6 kW
Bounding HSM-MX (Double Array)	4,125 ⁽²⁾	50 kW for lower compartment and 41.8 kW for upper compartment ⁽¹⁾

Notes:

1. The thermal loading condition of the HSM-MX is based on the most conservative thermal loading configuration.
2. For stability evaluation, several different combinations of DSC and HSM bounding weights are considered.

Detailed geometry descriptions, material properties, loadings, and structural evaluation for the HSM-MX are presented in Appendix A.3.9.4.

A.3.6.3 EOS-TC

No change to Section 3.6.3.

A.3.7 Off-Normal and Hypothetical Accident Conditions of Storage and Transfer

This section presents the structural analyses of the EOS-37PTH DSC, EOS-89BTH DSC and the HSM-MX subjected to off-normal and hypothetical accident conditions. These analyses are summarized in this section, and described in detail in Appendices A.3.9.1 through A.3.9.7.

A.3.7.1 EOS-37PTH DSC/89BTH DSC

Detailed geometry descriptions, material properties, loadings, and structural evaluation for the affected loads combinations of the DSC are presented in Appendix A.3.9.1. The design and loading conditions for the basket remain the same when loaded into the DSC shell and, therefore, results for the basket from Appendix 3.9.2 remain the same and are applicable.

A.3.7.2 HSM-MX

Detailed geometry descriptions, material properties, loadings, and structural evaluation for the HSM-MX are presented in Appendix A.3.9.4.

A.3.7.3 EOS-TC

No change to Section 3.7.3.

A.3.8 References

- A.3-1 Title 10, Code of Federal Regulations, Part 72, “Licensing Requirements for the Storage of Spent Fuel in the Independent Spent Fuel Storage Installation,” U.S. Nuclear Regulatory Commission.
- A.3-2 ACI 349-06, “Code Requirements for Nuclear Safety Related Concrete Structures,” American Concrete Institute, November 2006.
- A.3-3 American Institute of Steel Construction, “AISC Manual of Steel Construction,” 13th Edition or 14th Edition.
- A.3-4 ANSI/ANS 57.9-1984, “Design Criteria for an Independent Spent Fuel Storage Installation (Dry Storage Type),” American National Standards Institute.
- A.3-5 CoC 1042 Appendix A, NUHOMS® EOS System Generic Technical Specifications, Amendment 1.

Table A.3-1
Summary of HSM-MX Weight and Center of Gravity

Component	Description	
Empty HSM-MX	Total Weight (kips)	
	Single Array	2,448
	Double Array	4,125
	Center of Gravity from Bottom in Vertical Direction (inches)	
	Single Array	176.42
	Double Array	178.79
HSM-MX Loaded with EOS-37PTH DSC	Maximum Weight (kips)	
	Single Array	3,048
	Double Array	5,325
	Center of Gravity from Bottom in Vertical Direction (inches)	
	Single Array	168.68
	Double Array	169.39
HSM-MX Loaded with EOS-89BTH DSC	Maximum Weight (kips)	
	Single Array	3,053
	Double Array	5,335
	Center of Gravity from Bottom in Vertical Direction (inches)	
	Single Array	168.63
	Double Array	169.33

Notes:

1. The weight and center of gravity values listed in the table are corresponding to the maximum concrete density of 160 pcf.
2. The weight values are for the HSM-MX having three lower compartments and two upper compartments.

APPENDIX A.3.9.1 DSC SHELL STRUCTURAL ANALYSIS

Table of Contents

A.3.9.1 DSC SHELL STRUCTURAL ANALYSIS	A.3.9.1-1
A.3.9.1.1 General Description	A.3.9.1-1
A.3.9.1.2 DSC Shell Assembly Stress Analysis	A.3.9.1-1
A.3.9.1.3 DSC Shell Buckling Evaluation.....	A.3.9.1-4
A.3.9.1.4 DSC Fatigue Analysis.....	A.3.9.1-4
A.3.9.1.5 DSC Weld Flaw Size Evaluation	A.3.9.1-4
A.3.9.1.6 Conclusions.....	A.3.9.1-4
A.3.9.1.7 References.....	A.3.9.1-5

List of Tables

Table A.3.9.1-1	EOS-37PTH/EOS-89BTH DSC Shell Assembly Loads and Load Combinations	A.3.9.1-6
Table A.3.9.1-2	DSC Results - Load Combinations	A.3.9.1-9
Table A.3.9.1-3	DSC Weld Stress Results- Load Combinations.....	A.3.9.1-11
Table A.3.9.1-4	DSC-OTCP Maximum Radial Weld Stress (S_x) Results- Load Combinations	A.3.9.1-12
Table A.3.9.1-5	Controlling DSC Load Combination Results Summary	A.3.9.1-13

List of Figures

Figure A.3.9.1-1	DSC Supports and Axial Retainers.....	A.3.9.1-14
Figure A.3.9.1-2	DSC Dead Weight Equivalent Pressure.....	A.3.9.1-15
Figure A.3.9.1-3	DSC Boundary Conditions in HSM-MX.....	A.3.9.1-16
Figure A.3.9.1-4	Internals Seismic Equivalent Pressures with Internal Pressure, Load Case 2.....	A.3.9.1-17

A.3.9.1 DSC SHELL STRUCTURAL ANALYSIS

The purpose of this appendix is to present the structural evaluation of the shell assembly of the EOS-37PTH dry shielded canister (DSC) and the EOS-89BTH DSC under all applicable normal, off-normal and accident loading conditions during storage in the NUHOMS® MATRIX (HSM-MX).

The DSC shell is evaluated in Chapter 3.9.1 for all loads and load combinations. Only dead weight, and seismic load combinations affect the DSC when stored in the HSM-MX. Therefore, results from Chapter 3.9.1 are applicable to this chapter except for dead weight and seismic load combinations.

A.3.9.1.1 General Description

No change to Section 3.9.1.1.

A.3.9.1.2 DSC Shell Assembly Stress Analysis

No change to Section 3.9.1.2.

A.3.9.1.2.1 Material Properties

No change to Section 3.9.1.2.1.

A.3.9.1.2.2 DSC Shell Stress Criteria

No change to Section 3.9.1.2.2.

A.3.9.1.2.3 Finite Element Model Description

No change to Section 3.9.1.2.3 except that ANSYS version 17.1 [A.3.9.1-1] is used for the analysis in this appendix.

A.3.9.1.2.4 Mesh Sensitivity

No change to Section 3.9.1.2.4.

A.3.9.1.2.5 Post-Processing

No change to Section 3.9.1.2.5.

A.3.9.1.2.6 Stress Categorization Sensitivity Studies

No change to Section 3.9.1.2.6.

A.3.9.1.2.7 Load Cases for DSC Shell Stress Analysis

No change to Section 3.9.1.2.7, except the dead weight load as described in A.3.9.1.2.7.1 and the seismic loads as described in A.3.9.1.2.7.6.

A.3.9.1.2.7.1 Dead Weight

The dead weight is analyzed for the following basic configurations:

- When the DSC is vertical in the EOS-TC135 (No change to Section 3.9.1.2.7.1),
- When the DSC is horizontal in the EOS-TC135 (No change to Section 3.9.1.2.7.1),
- When the DSC is horizontal in the HSM-MX.

The model for the HSM-MX differs from EOS-HSM in boundary conditions representing the DSC supports. The DSC supports and axial retainers are shown in Figure A.3.9.1-1.

Horizontal Position in HSM-MX

When stored in the HSM-MX, the DSC shell is supported by the front and rear DSC supports. The inertial loads of the DSC internals are accounted for by applying an equivalent pressure onto the inner surface of the DSC shell. The magnitude of the pressure is determined based on the payload of 105 kips.

The interfaces between the DSC and the HSM-MX DSC supports, axial retainer and rear stop plate are modeled through node-to-node contact elements (CONTA178). The nodes representing the HSM-MX supports are constrained in all Degrees of Freedom (DOF). Similarly, the stop plate and axial retainer are also constrained in all degrees of freedom.

Figure A.3.9.1-2 and Figure A.3.9.1-3 show the pressure load and boundary conditions applied to the Finite Element Model (FEM).

Gaps for the contact elements are set to zero, placing the DSC and the HSM-MX DSC supports in initial contact.

A.3.9.1.2.7.2 Fabrication Pressure and Leak Testing

No change to Section 3.9.1.2.7.2.

A.3.9.1.2.7.3 Internal and External Pressure

No change to Section 3.9.1.2.7.3.

A.3.9.1.2.7.4 HSM-MX Loading/Unloading

No change to Section 3.9.1.2.7.4 except that the loads applied by the ram are balanced by the friction between the DSC shell and the EOS-TC and or MX-RRT support.

A.3.9.1.2.7.5 Transfer/Handling Load

No change to Section 3.9.1.2.7.5.

A.3.9.1.2.7.6 Seismic Load during Storage

The model described in Section A.3.9.1.2.7.1 for dead weight in HSM-MX is used and updated to reflect the effect of the vertical 0.8g load, transverse 1.7g load, axial (longitudinal) 1.7g load, and the internal pressure load of 20 psig.

Two elastic-plastic runs are performed for this load:

1. 0.8g vertical + 1.7g transverse + 1.7g axial with the weight of DSC internals modeled by equivalent pressure application on TSP with addition of internal pressure of 20 psig.
2. 0.8g vertical + 1.7g transverse + 1.7g axial with the weight of DSC internals modeled by equivalent pressure application on IBCP with addition of internal pressure of 20 psig.

The compound effect of dead weight, 0.8g vertical and 1.7g transverse, is modeled by multiplying the pressure from the dead weight case by a conservative factor of 4.

Seismic axial forces away from the HSM-MX door (load case 1 above) are resisted by the rear plates located at the ends of the DSC rear supports. The OTCP is recessed from the edge of the DSC shell, thus, the rear plate bears against the bottom edge of the DSC shell. The nodes of the top end of DSC shell, which come into contact with the rear stop plate, are restrained in the axial direction.

Seismic axial forces toward the HSM-MX door (load case 2 above) are resisted by the front axial retainers. The retainer is a steel bar located horizontally through the HSM-MX door. The retainer bears against the OBCP. The nodes of the OBCP, which bear against the area of the axial retainer bar, are restrained in the axial direction.

Figure A.3.9.1-4 shows the pressure load applied to the DSC while supported by the HSM-MX DSC supports.

The DSC shell and the OBCP experience compressive bearing stress in the vicinity of the axial retainer and rear plate. The bearing stresses experienced by the DSC shell and OBCP need not be evaluated for Service Level D loads.

A.3.9.1.2.7.7 Cask Drop

No change to Section 3.9.1.2.7.7.

A.3.9.1.2.7.8 Thermal Loads

Thermal analysis is performed to support the new HLZCs 4, 5, 6, 7, 8 and 9 as discussed in Technical Specification [A.3.9.1-2] (See Figure 1D through Figure 1I). For thermal stress analysis, temperature profiles and maximum component temperatures are based on thermal analysis of the EOS-37PTH DSC for transfer conditions. For transfer operations, HLZC 4 bounds HLZC 5, 6, 7, 8 and 9. The new HLZC 4 DSC maximum temperature is 480 °F (Chapter 4, Figure 4.9.6-4) which is below the temperatures of 484 °F (Chapter 4, Figure 4-32) for transfer operation. Therefore, new HZLC temperatures are bounded by the original thermal stress analysis. Therefore, no change to Section 3.9.1.2.7.8.

A.3.9.1.2.8 Load Combinations

No change to Section 3.9.1.2.8, except the dead weight and seismic load combinations described in Section A.3.9.1.2.7. Table A.3.9.1-1 provides the load combinations described in Section 3.9.1.2.8, in this chapter for information purpose. Only load combinations 9 and 10 affecting the DSC stored in HSM-MX on the front and rear DSC supports are analyzed.

A.3.9.1.3 DSC Shell Buckling Evaluation

No change to Section 3.9.1.3.

A.3.9.1.4 DSC Fatigue Analysis

No change to Section 3.9.1.4.

A.3.9.1.5 DSC Weld Flaw Size Evaluation

No change to Section 3.9.1.5.

A.3.9.1.6 Conclusions

The EOS DSC shell assembly has been analyzed for normal, off-normal, and accident load conditions using three dimensional finite element analyses. The load combinations provided in Section A.3.9.1.2.8 are used in the analysis of the EOS DSC. Analyses are performed only for the dead weight and seismic load combinations (9 and 10), which affect the DSC when stored in the HSM-MX. Stress intensities in different components of the DSC shell assembly, compared with ASME code stress intensity allowables and the resulting stress ratios, are summarized in Table A.3.9.1-2. The stress ratio is calculated by dividing the maximum stress intensity by the stress intensity allowable value, with the stress ratio required to be less than 1.

The DSC weld stresses are summarized in Table A.3.9.1-3. The maximum weld stress ratio is 0.87 and occurs at the DSC shell to ITCP weld for Load Combination 9. The maximum radial weld stress is summarized in Table A.3.9.1-4. The maximum radial stress between the DSC and OTCP is 4.22 ksi. Therefore, the flaw size evaluation from Section 3.9.1.5 still remains valid.

Table A.3.9.1-5 summarizes the stress results for the controlling load combination. The maximum component stress ratio remains the same as in the original analysis and is equal to 0.92 in the grapple ring support. The second maximum component stress ratio is equal to 0.87 and occurs in the confinement boundary area of the DSC shell during load combination 9 (storage condition in the HSM-MX, dead weight normal conditions).

The structural integrity of the DSC shell, including closure welds, is maintained since the maximum stress ratio is less than 1. Therefore, it is concluded that the EOS DSC is structurally adequate under all anticipated load conditions for service during the transfer and storage in the HSM-MX.

A.3.9.1.7 References

- A.3.9.1-1 ANSYS Computer Code and User's Manual, Release 14.0, Release 14.0.3 and Release 17.1
- A.3.9.1-2 CoC 1042 Appendix A, NUHOMS® EOS System Generic Technical Specifications, Amendment 1.

Table A.3.9.1-1
EOS-37PTH/EOS-89BTH DSC Shell Assembly Loads and Load
Combinations
 (2 Sheets)

Loading Type	DSC Orientation	Load for Analysis	Load Combination	Service Level	Load Combination No.	
Dead weight (DW)	Vertical ⁽¹⁾	1g down (axial)	DW+ Normal Pressure+ Normal Thermal ⁽²⁾	A	1	
Blowdown/ Pressure Test		20 psig internal pressure				
Thermal		Normal vertical orientation thermal				
Dead weight (DW)	Horizontal ⁽³⁾	1g down	DW + H + Pressure+ Thermal (117 °F)	A	2	
Thermal-Off Normal Hot		Off-Normal –Hot (117 °F)				
Thermal–Off Normal Cold		Off-Normal Cold (-40 °F)	DW + H + Pressure+ Thermal (-40 °F)		3	
Internal Pressure-Off Normal		20 psig				
Handling in transfer cask (H) ⁽¹⁵⁾		H=± 1g axial± 1 g trans.±1 g vertical				
Dead weight (DW)	Horizontal ⁽³⁾	1g down	DW+ Ram (135 kips insertion)+ Pressure +Thermal	A/B ⁽⁷⁾	4	
Ram Loads (push/pull)		135 kips (push) ⁽⁵⁾ , 80 kips (pull) ⁽⁶⁾				
Internal pressure-Off-Normal		20 psig ⁽⁹⁾	DW + Ram (80 kips, retrieval) + Pressure + Thermal		5	
Thermal—Off Normal		Thermal –Off Normal ⁽⁸⁾				
Dead weight (DW)	Horizontal ⁽³⁾	1g down	DW + Ram (135 kips retrieval) + Pressure	D	6	
Ram Loads (pull)		135 kips ⁽⁶⁾				
Internal pressure-Off-Normal		20 psig ⁽⁹⁾				

Table A.3.9.1-1
EOS-37PTH/EOS-89BTH DSC Shell Assembly Loads and Load
Combinations
(2 Sheets)

Loading Type	DSC Orientation	Load for Analysis	Load Combination	Service Level	Load Combination No.
Dead Weight (DW)	Horizontal ⁽³⁾ Vertical ⁽³⁾	1g down	DW + Pressure+ 65 inch Accident Drop	D	7A
Internal pressure-Off-Normal		20 psig ⁽⁹⁾			
Accident Side/corner drop ⁽¹⁷⁾		65 inch drop			7B
Dead Weight (DW)	Horizontal	1g down	DW + Accident Pressure	D	8
Internal pressure-Accident		130 psig ⁽³⁾⁽⁹⁾⁽¹⁰⁾			
Dead Weight (DW)	Horizontal ⁽¹¹⁾	1g down	DW + Pressure+ Thermal	A	9
Internal Pressure-Off-Normal		20 psig			
Thermal-Off Normal		Thermal-Off Normal			
Dead Weight (DW)	Horizontal ⁽¹¹⁾	1g down	DW + Pressure+ Seismic (S)	D	10
Internal Pressure-Off-Normal		20 psig			
Seismic (S)		S=±1.7g(axial) ±1.7g(transverse ±0.8g(vertical) ⁽¹⁶⁾			
Test Pressure at fabricator—23 psig ⁽¹²⁾	Vertical	23 psig internal pressure	23 psig (15x1.5=23 psig) internal pressure	Test	11
External pressure	Horizontal	See Note ⁽¹⁴⁾		D	12

Notes

- DSC in Transfer cask in vertical orientation. Only inner top cover is installed.
- Use bounding thermal case for normal operations of transfer cask in vertical orientation.
- DSC in Transfer Cask; Transfer Cask is in horizontal orientation. In case of End drop, the orientation is vertical supported by IBS in case of Bottom End drop and TSP in case of Top End drop.
- Not used.
- The push loads are applied at the canister bottom surface within the grapple ring support.
- The pull loads are applied at the inner surface of the grapple ring.

7. Level B evaluations may take credit for 10% increase in allowable per NB-3223(a). Level B is used for the case with internal pressure. Level A is used for the case without internal pressure.
8. Use controlling thermal off-normal case.
9. Load combination results to bound cases with and without internal pressure. Use bounding pressure of HSM blocked vent accident or transfer cask accident fire conditions.
10. Use bounding pressure of HSM blocked vent accident or transfer cask accident fire conditions.
11. DSC in HSM supported on the DSC supports.
12. Conservatively use 23 psig as the test pressure; test configuration is circular shell and inner bottom welded to shell; a top end lid with a 155 kips clamping force may be used to seal the test assembly.
13. Not Used.
14. The maximum accident condition external pressure before DSC collapse/buckling is to be determined from the analysis.
15. These handling loads in conjunction with Level A limits bounds case of transfer cask in fuel building under seismic loads (Level D accident condition).
16. Unless lower g loads can be justified based on frequency analysis of HSM loaded with bounding DSC.
17. The top end drop and bottom end drop are not credible events under 10 CFR Part 72, therefore these drop analyzes are not required. However, consideration of end drops (for 10 CFR Part 71 conditions) and the 65" side drop to conservatively envelope the effects of a corner drop.

Table A.3.9.1-2
DSC Results - Load Combinations
(2 Sheets)

Load Combination Number	Service Level	Loads	Components		Stress Category [ksi]				
					P _m	P _m +P _b	P _L	P _m (or P _L)+P _b +Q	P _m (or P _L)+P _b +Q+P _e
9	A	DW+IP (20psi)	DSC Shell (Confinement)	Stress Intensity	6.77	12.11	18.07	27.90	45.44
				Allowable Stress	17.50	26.25	26.25	52.50	52.50
				Stress Ratio	0.39	0.46	0.69	0.53	0.87
			DSC Shell (Non-Confinement)	Stress Intensity	4.99	6.87	7.46	11.61	31.00
				Allowable Stress	17.50	26.25	26.25	52.50	52.50
				Stress Ratio	0.29	0.26	0.28	0.22	0.59
			OTCP	Stress Intensity	1.81	7.01	2.99	8.46	15.08
				Allowable Stress	17.50	26.25	26.25	52.50	52.50
				Stress Ratio	0.10	0.27	0.11	0.16	0.29
			ITCP	Stress Intensity	1.96	7.12	3.62	10.96	17.30
				Allowable Stress	17.50	26.25	26.25	52.50	52.50
				Stress Ratio	0.11	0.27	0.14	0.21	0.33
			OBCP	Stress Intensity	1.10	2.71	1.91	5.61	20.15
				Allowable Stress	17.50	26.25	26.25	52.50	52.50
				Stress Ratio	0.06	0.10	0.07	0.11	0.38
			IBCP	Stress Intensity	2.87	4.72	5.23	8.20	24.42
				Allowable Stress	17.50	26.25	26.25	52.50	52.50
				Stress Ratio	0.16	0.18	0.20	0.16	0.47

Table A.3.9.1-2
DSC Results - Load Combinations
 (2 Sheets)

Load Combination Number	Service Level	Loads	Components		Stress Category[ksi]		
					P_m	P_m+P_b	P_L
10	D	DW+ Seismic+ IP(20psi)	DSC Shell (Confinement)	Stress Intensity	22.10	29.10	34.00
				Allowable Stress	44.38	57.06	57.06
				Stress Ratio	0.50	0.51	0.60
			DSC Shell (Non- Confinement)	Stress Intensity	20.10	22.60	20.30
				Allowable Stress	44.38	57.06	57.06
				Stress Ratio	0.45	0.40	0.36
			OTCP	Stress Intensity	7.13	13.00	14.30
				Allowable Stress	44.38	57.06	57.06
				Stress Ratio	0.16	0.23	0.25
			ITCP	Stress Intensity	5.53	11.20	9.27
				Allowable Stress	44.38	57.06	57.06
				Stress Ratio	0.12	0.20	0.16
			OBCP	Stress Intensity	19.80	26.70	5.60
				Allowable Stress	44.38	57.06	57.06
				Stress Ratio	0.45	0.47	0.10
			IBCP	Stress Intensity	11.10	16.10	18.60
				Allowable Stress	44.38	57.06	57.06
				Stress Ratio	0.25	0.28	0.33

Table A.3.9.1-3
DSC Weld Stress Results- Load Combinations

Load Combination Number	Service Level	Loads	Weld Components	Stress Category	Stress Intensity [ksi]	Allowable Stress [ksi]	Stress Ratio
9	A	DW+IP (20psi)	DSC-ITCP	P_L	16.50	23.2	0.71
				$P_L+P_b+Q+P_e$	40.19	46.3	0.87
			DSC-OTCP	P_L	11.57	23.2	0.50
				$P_L+P_b+Q+P_e$	30.24	46.3	0.65
			DSC-OBCP	P_L	5.46	23.2	0.24
				$P_L+P_b+Q+P_e$	25.77	46.3	0.56
10	D	DW+ Seismic + IP (20psi)	DSC-ITCP	P_L	25.0	46.9	0.53
			DSC-OTCP	P_L	38.8	46.9	0.83
			DSC-OBCP	P_L	17.30	46.9	0.37

Table A.3.9.1-4
DSC-OTCP Maximum Radial Weld Stress (S_x) Results- Load Combinations

Load Combination Number	Service Level	Loads	Maximum Radial Stress [ksi]
9	A	DW+IP (20psi)	0.14
10	D	DW+Seismic +IP(20psi)	4.22

Table A.3.9.1-5
Controlling DSC Load Combination Results Summary

Components / Welds	Controlling Load Combination ⁽¹⁾		Service Level	Max. Stress Ratio
	Number	Description		
DSC Shell Containment	9	DW + IP + Thermal	A	0.87
DSC Shell Non Containment	5	DW + Ram Retrieval+ IP + Thermal	A/B	0.85
OTCP	8	DW + Accident P	D	0.45
ITCP	8	DW + Accident P	D	0.45
OBCP	5	DW + Ram Retrieval + IP + Thermal	A/B	0.78
IBCP	4	DW + Ram Insert + IP + Thermal	A/B	0.47
Grapple Support	5	DW + Ram Retrieval + IP + Thermal	A/B	0.92
Grapple Ring	5	DW + Ram Retrieval + IP + Thermal	A/B	0.81
OTCP-DSC Shell Weld	10	DW + IP + max (HS_TOP, HS_BOT)	D	0.83
ITCP-DSC Shell Weld	9	DW + IP	A	0.87
OBCP-DSC Shell Weld	5	DW + Ram Retrieval + IP + Thermal	A/B	0.75

Note: ⁽¹⁾ See Table A.3.9.1-1 for the load combination description.

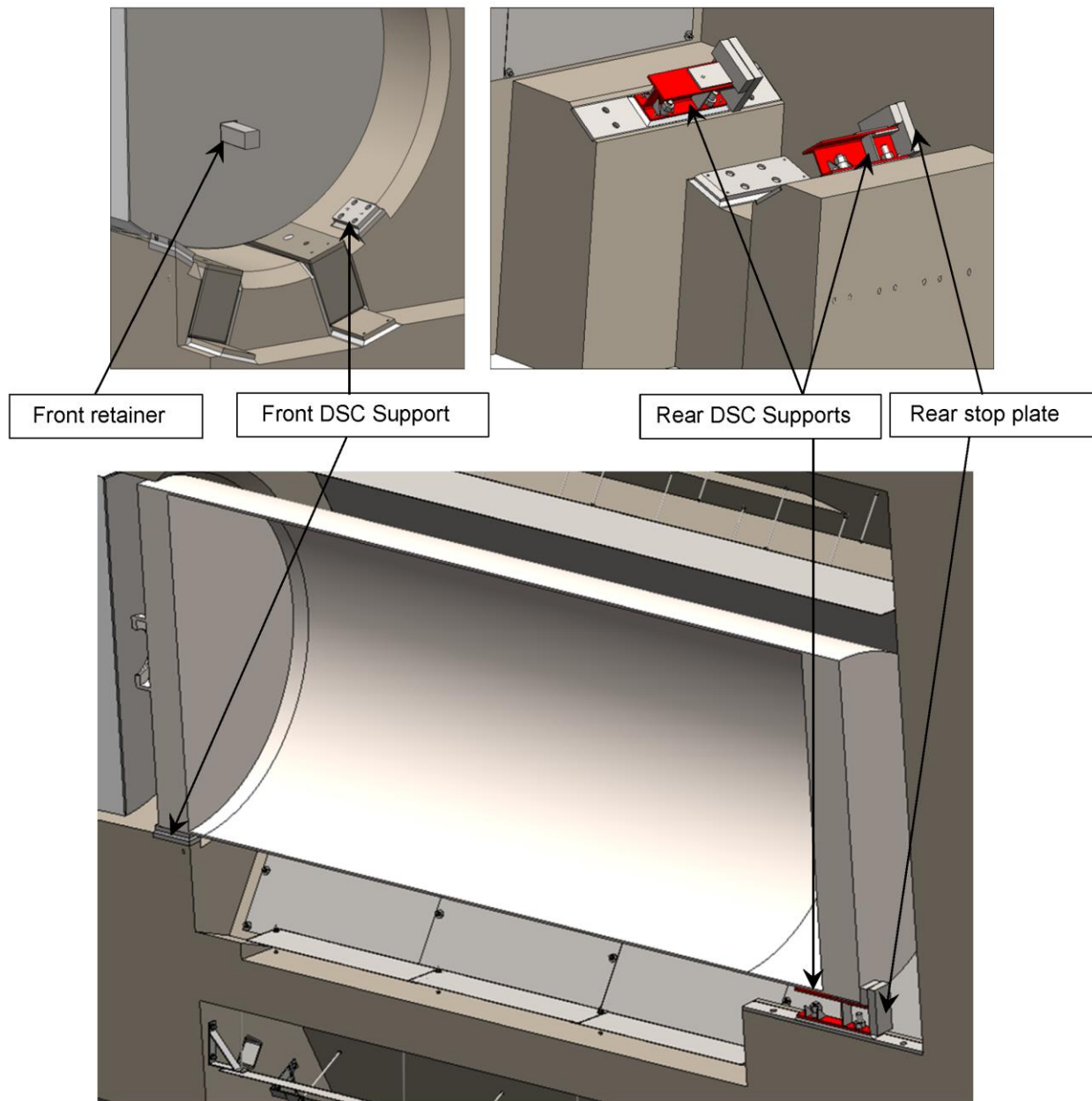


Figure A.3.9.1-1
DSC Supports and Axial Retainers

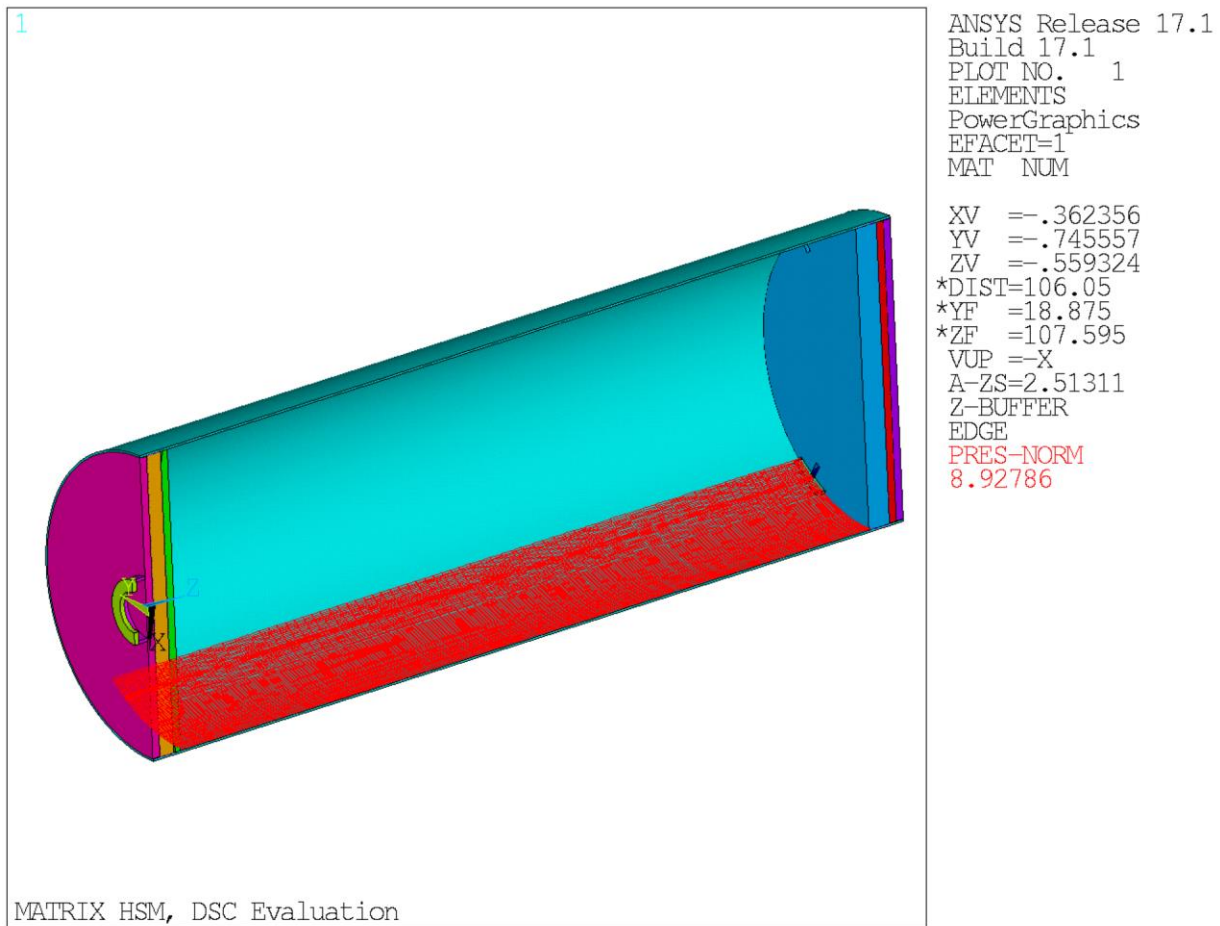


Figure A.3.9.1-2
DSC Dead Weight Equivalent Pressure

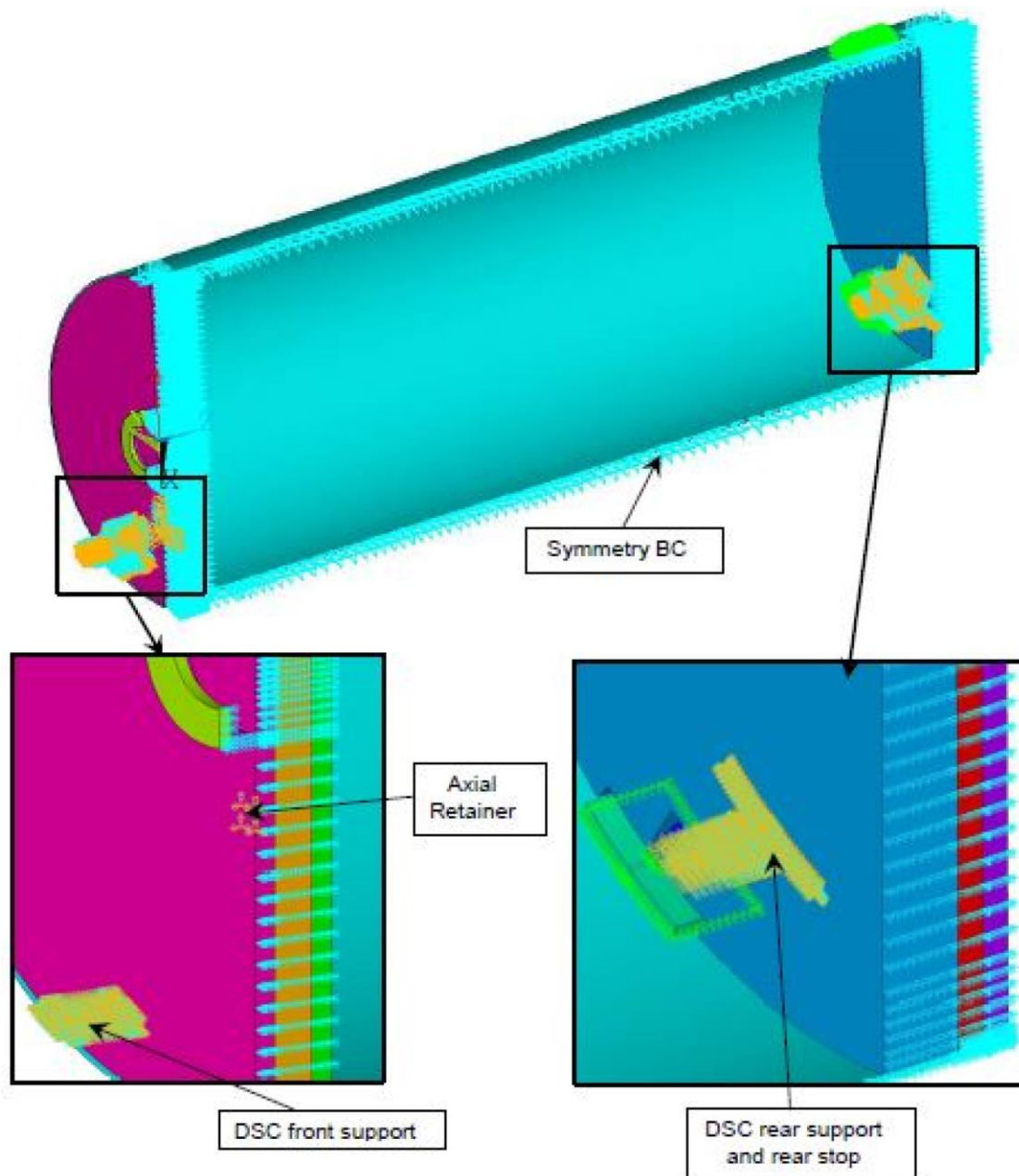


Figure A.3.9.1-3
DSC Boundary Conditions in HSM-MX

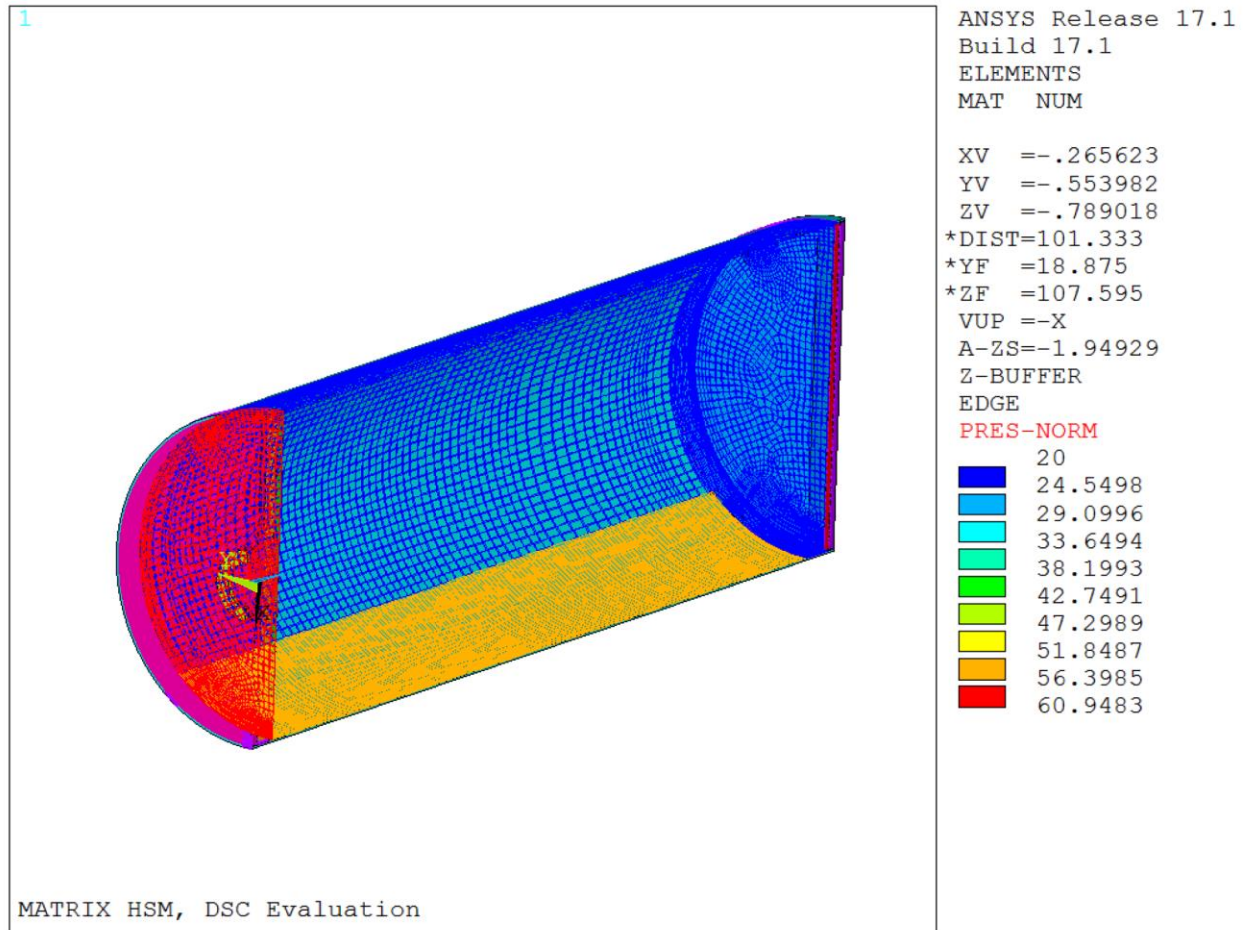


Figure A.3.9.1-4
Internals Seismic Equivalent Pressures with Internal Pressure, Load Case 2

A.3.9.2 EOS-37PTH AND EOS-89BTH BASKET STRUCTURAL ANALYSIS

There is no change to the EOS-37PTH and EOS-89BTH Basket Structural evaluation documented in Sections 3.9.2 due to the addition of the NUHOMS® MATRIX.

A.3.9.3 NUHOMS® EOS SYSTEM ACCIDENT DROP EVALUATION

There is no change to the EOS-37PTH DSC and EOS-89BTH DSC within the EOS-TC108 for drop evaluation documented in Sections 3.9.3 due to the addition of the NUHOMS® MATRIX.

APPENDIX A.3.9.4 HSM-MX STRUCTURAL ANALYSIS

Table of Contents

A.3.9.4 HSM-MX STRUCTURAL ANALYSIS.....	A.3.9.4-1
A.3.9.4.1 General Description	A.3.9.4-1
A.3.9.4.2 Material Properties	A.3.9.4-1
A.3.9.4.3 Design Criteria	A.3.9.4-1
A.3.9.4.4 Load Cases	A.3.9.4-2
A.3.9.4.5 Load Combination	A.3.9.4-2
A.3.9.4.6 Finite Element Models	A.3.9.4-2
A.3.9.4.7 Normal Operation Structural Analysis.....	A.3.9.4-4
A.3.9.4.8 Off-Normal Operation Structural Analysis.....	A.3.9.4-5
A.3.9.4.9 Accident Condition Structural Analysis	A.3.9.4-6
A.3.9.4.10 Structural Evaluation	A.3.9.4-11
A.3.9.4.11 Conclusions.....	A.3.9.4-21
A.3.9.4.12 References	A.3.9.4-22

List of Tables

Table A.3.9.4-1	Design Pressures for Tornado Wind Flowing from Front Wall to Rear Wall and Vice Versa.....	A.3.9.4-23
Table A.3.9.4-2	Design Pressures for Tornado Wind Flowing from Right Side to Left Side Wall and Vice Versa	A.3.9.4-24
Table A.3.9.4-3	Spectral Acceleration Applicable to Different Components of HSM-MX for Seismic Analysis.....	A.3.9.4-25
Table A.3.9.4-4	Load Cases for HSM-MX Concrete Components Evaluation	A.3.9.4-26
Table A.3.9.4-5	Load Combination for HSM-MX Concrete Components Evaluation	A.3.9.4-27
Table A.3.9.4-6	Demand to Capacity Ratios for HSM-MX Longitudinal Reinforcement Areas	A.3.9.4-28

List of Figures

Figure A.3.9.4-1	HSM-MX (Back-to-Back) CAD Model	A.3.9.4-29
Figure A.3.9.4-2	HSM-MX (Back-to-Back) Meshed Model	A.3.9.4-30
Figure A.3.9.4-3	Temperature Distribution of HSM-MX for Normal Thermal Hot Condition.....	A.3.9.4-31
Figure A.3.9.4-4	Temperature Distribution of HSM-MXS for Blocked Vent Accident Thermal Condition.....	A.3.9.4-32
Figure A.3.9.4-5	HSM-MX Concrete Reinforcement Directions	A.3.9.4-33
Figure A.3.9.4-6	Analytical Model of Heat Shield (a) Coupled Lower Side Heat Shield and Studs (b) Coupled Lower Top Heat Shield and Studs ..	A.3.9.4-34
Figure A.3.9.4-7	Horizontal Target and 5% Spectral Match (Horizontal 1, Hector Mine Earthquake).....	A.3.9.4-35
Figure A.3.9.4-8	Baseline Corrected Acceleration, Velocity and Displacement Time Histories (Horizontal 1, Hector Mine Earthquake)	A.3.9.4-36
Figure A.3.9.4-9	Horizontal Target and 5% Spectral Match (Horizontal 2, Hector Mine Earthquake).....	A.3.9.4-37
Figure A.3.9.4-10	Baseline Corrected Acceleration, Velocity and Displacement Time Histories (Horizontal 2, Hector Mine Earthquake)	A.3.9.4-38
Figure A.3.9.4-11	Vertical Target and 5% Spectral Match (Vertical Up, Hector Mine Earthquake).....	A.3.9.4-39
Figure A.3.9.4-12	Baseline Corrected Acceleration, Velocity and Displacement Time Histories (Vertical Up, Hector Mine Earthquake).....	A.3.9.4-40
Figure A.3.9.4-13	Lower Top Heat Shield Support Node ISRS due to Envelope of Four Earthquake-Based Motions Compatible with Enhanced RG1.60 Spectra, 4% Damping, X-Direction	A.3.9.4-41
Figure A.3.9.4-14	Lower Top Heat Shield Support Node ISRS due to Envelope of Four Earthquake-Based Motions Compatible with Enhanced RG1.60 Spectra, 4% Damping, Y-Direction	A.3.9.4-42
Figure A.3.9.4-15	Lower Top Heat Shield Support Node ISRS due to Envelope of Four Earthquake-Based Motions Compatible with Enhanced RG1.60 Spectra, 4% Damping, Z-Direction.....	A.3.9.4-43

A.3.9.4 HSM-MX STRUCTURAL ANALYSIS

The purpose of this appendix is to present the structural evaluation of the NUHOMS® MATRIX (HSM-MX) due to all applied loads during storage and transfer operations.

A.3.9.4.1 General Description

General description and operational features for the HSM-MX is provided in Appendix A.1. The HSM-MX is a freestanding, staggered reinforced concrete structure, designed to provide environmental protection and radiological shielding for the EOS-37PTH/EOS-89BTH DSC. The drawings of the HSM-MX, showing different components and overall dimensions, are provided in Appendix A.1.3

The HSM-MX is one of the three main components of the NUHOMS® MATRIX System. The system consists of the dual purpose (Transportation/Storage) EOS-37PTH/EOS-89BTH DSC, the HSM-MX, and the onsite transfer cask (EOS-TC) with associated ancillary equipment.

The HSM-MX overpack system comprises the MATRIX Horizontal Storage Modules, the MATRIX retractable roller tray (MX-RRT), the MATRIX loading crane (MX-LC) and associated trailer interface for storing dry shielded canisters (DSCs).

The HSM-MX is a staggered, two-tiered, high density, high-heat rejection, storage overpack that provides a self-contained modular structure for storage of DSCs. The HSM-MX is constructed from reinforced concrete and structural steel. The thick concrete roof and walls of the HSM-MX provide substantial neutron and gamma shielding. The monolithic structure increases resistance to earthquakes and offers significant self-shielding. The MX-RRT delivers the DSC from the transfer cask to the HSM-MX and places it on the front and rear DSC supports.

The HSM-MX can be arranged in both single-row or back-to-back row arrays.

For thermal protection of the HSM-MX concrete, stainless steel heat shields are installed inside the HSM-MX. The primary function of the heat shields is to limit the temperature of the surrounding concrete walls. The heat shields guide the cooling airflow through the HSM-MX.

A.3.9.4.2 Material Properties

The material properties used in the analysis and design of the HSM-MX and its components are discussed in detail in Chapter 8 and Appendix A.8.

A.3.9.4.3 Design Criteria

No change to Section 3.9.4.3.

A.3.9.4.4 Load Cases

A summary of the design loads for HSM-MX concrete component evaluation is similar to Table 3.9.4-4 except the definition of normal handling (R_o) and off-normal handling (R_a) loads, and is provided in Table A.3.9.4-4 for information only. This table also presents the applicable codes and standards for specific load.

A.3.9.4.5 Load Combination

The load combinations used in the structural analysis of the HSM-MX structure comply with the requirements of 10 CFR 72.122 [A.3.9.4-1] and ANSI 57.9-84 [A.3.9.4-8] and are provided in Table A.3.9.4-5.

A.3.9.4.6 Finite Element Models

The structural analysis of HSM-MX storage modules arranged in a back-to-back row array provides a conservative estimate of the response of the HSM-MX under the postulated static and dynamic loads for any HSM-MX array configurations. The frame and shear wall action of the HSM-MX concrete components are considered to be the primary load carrying mechanism of the structural system. The analytical model is evaluated for normal operating, off-normal, and postulated accident loads acting on the HSM-MX.

A single Finite Element Model (FEM) is developed for the HSM-MX storage arranged in a back-to-back row array, where each row consists of three lower compartments and two upper compartments. This is a configuration with the minimum number of storage modules that an HSM-MX array can have. A back-to-back row array, instead of a single row array, is considered because the back wall shared by two rows is only 30 inch whereas, for a single row array, the thickness of the rear shield wall at the modules back end is 44 inch. Moreover, an array with additional storage modules would have a greater natural frequency in the transverse direction (that is, the direction of array expansion), resulting in a lower seismic loads. Therefore, the model based on a back-to-back row array with each row consisting of three lower compartments and two upper compartments provides a conservative estimate of the response of the HSM-MX structural elements under various static and dynamic loads.

The analysis results from ANSYS are post-processed using CivilFEM® [A.3.9.4-18] software. CivilFEM® defines the shell elements at the mid-planes of the walls and slabs that are represented by the 3D solid elements in the ANSYS model. Forces and moments on the shell elements that are equivalent to the displacement results on solid elements are computed by CivilFEM®. Then the results of the shell forces and moments are utilized to determine reinforcement areas.

A.3.9.4.6.1 Finite Element Model to Evaluate HSM-MX Concrete Components for Mechanical Loads

A three-dimensional (3D) finite element model (FEM) of the HSM-MX, including all the concrete components, is developed in the computer program ANSYS [A.3.9.4-14]. The eight-node brick element (ANSYS element type SOLID185) is used to model the concrete structure. Each node of the eight-node brick element has three translational degrees of freedom. A global element dimension of 4-inch is used in the model. As demonstrated in A.3.9.4.6, the model can accurately simulate the frame and shear wall action of the HSM-MX concrete components, which are the primary load-resisting mechanisms. The mass of the DSC is evenly distributed over the four supports using lumped mass elements (ANSYS element type MASS21). The mass of the door is included as lumped mass elements placed around the recessed door opening at the five embedment locations of the door. The mass of the vent cover is also included as lumped mass elements at the vent cover support locations on the roof. A plot of the CAD model and ANSYS FEM of the HSM-MX back-to-back array are shown in Figure A.3.9.4-1 and Figure A.3.9.4-2, respectively. The coordinate system for the model is shown in Figure A.3.9.4-2, where the origin is located at the bottom left corner on the front.

The model is assumed to neither uplift due to dead weight nor slide due to friction with the ISFSI pad. Therefore, the model is restrained vertically at all nodes on the bottom of the model, and also restrained laterally and axially at all nodes on the bottom of the model to prevent rigid body movement.

A.3.9.4.6.2 Finite Element Model of the HSM-MX Concrete Structure for Thermal Stress Analysis

Thermal stress analyses of the HSM-MX were performed using a 3D FEM, which includes only the concrete components developed in Section A.3.9.4.6.1. The connections of the door to the HSM-MX concrete structure are designed so that free thermal growth is permitted in these members when the HSM-MX is subjected to thermal loads. Because of their free thermal growth, the doors do not induce thermal stresses in the concrete components of the HSM-MX. Therefore, the analytical model of the HSM-MX for thermal stress analysis of the concrete components does not include doors. The ANSYS models with temperature profile, which are used to perform thermal stress analysis of the concrete components for normal thermal hot and blocked vent accident thermal conditions, are shown in Figure A.3.9.4-3 and Figure A.3.9.4-4, respectively.

For thermal stress analysis, the FEM has Z-degrees of freedom restrained along the bottom front edge of the module ($Z=0$ and $Y=0$ in the ANSYS model), X-degrees of freedom restrained along the bottom left side edge of the module ($X=0$ and $Y=0$ in the ANSYS model), and Y-degrees of freedom restrained at the base of the module ($Y=0$ in the ANSYS model).

A.3.9.4.6.3 Finite Element Model for Structural Analysis of Heat Shield Panels and supporting brackets for the heat shields

The primary function of the heat shields is to limit the temperature of the surrounding concrete walls to acceptable values. The stainless steel heat shields are evaluated for their ability to sustain structural integrity after being subjected to two loads: a combination of 1g dead load due to its own weight, and a seismic load that is dependent upon its natural frequency as well as the in-structure response spectra (ISRS) at the supports.

The FEMs of the HSM-MX (single and back-to-back double) arrays developed in Section A.3.9.4.6.1 are used for the modal time-history analysis using ANSYS. In order to determine the appropriate seismic loading for the heat shields, ISRS are determined for the locations of the various heat shield attachments. The ISRS are determined by performing modal time history analysis of the entire HSM-MX structures. ANSYS is used to determine the natural vibration frequencies of the coupled panel-stud system. Shell elements (ANSYS element type SHELL63) are used to model the heat shield panels and support brackets and beam elements (ANSYS element type BEAM4) are used for the studs. The analytical models of the coupled lower side heat shield (LSHS) and Studs, and coupled lower top heat shield (LTHS) and studs are shown in Figure A.3.9.4-6. Similar models were used for the upper bottom heat shields (UBHS), upper side heat shield (USHS), and upper top heat shield (UTHS).

A.3.9.4.7 Normal Operation Structural Analysis

This section describes the design basis normal operation events for the HSM-MX components and presents analyses that demonstrate the adequacy of the design safety features of the HSM-MX. The normal operating loads for which the HSM-MX components are designed include dead load, live load, normal handling loads, normal thermal loads, and wind load. The ANSYS FEM described in Section A.3.9.4.6.1 is used to evaluate concrete forces and moments due to these normal loads. The methodology used to evaluate the effects of these normal loads is addressed in the following paragraphs.

A.3.9.4.7.1 HSM-MX Dead Load (DL) Analysis

Dead loads are applied to the analytical model by application of 1g acceleration in the vertical direction where g is the gravitational acceleration (386.4 in/sec²). The 5% variation of dead load as indicated in ANSI/ANS 57.9 is not used because the heaviest design weight is used for analysis.

A.3.9.4.7.2 HSM-MX Live load (LL) Analysis

Live load analysis is performed by applying 200 psf pressure on the roof. The DSC weight is also applied on the DSC supports as a live load.

A.3.9.4.7.3 HSM-MX Normal Operational Handling Load (R_o) Analysis

Normal operation assumes the canister is sliding over the MX-RRT due to a hydraulic ram force of up to 135,000 lbs (insertion) and 80,000 lbs (extraction) applied at the grapple ring and resisted by an axial load of 70,000 lb (insertion) and 40,000 lb (extraction) developing at each side of the MX-RRT supports. Here the total resisting axial load of 140,000 lbs is greater than the hydraulic ram force of 135,000 lbs. Only the insertion load is applied in the ANSYS FEM, since the extraction load is bounded by the insertion load. In addition, the DSC weight is applied to the MX-RRT support locations on both sides (4 points).

A.3.9.4.7.4 HSM-MX Normal Operating Thermal (T_o) Stress Analysis

The normal operating thermal (T_o) loads on the HSM-MX include the effect of design basis heat load of up to 50 kW generated by the DSC, plus the effect of normal ambient temperature. To evaluate the effects of normal thermal loads on the HSM-MX, heat transfer analyses for a range of normal ambient temperatures (-20 °F and 100 °F) are performed with a DSC heat load of 50 kW. The normal thermal cold condition (-20 °F) is bounded by the off-normal thermal cold condition (-40 °F). Therefore, the off-normal thermal cold condition is used in place of the normal thermal cold condition. The ambient condition that causes the maximum temperature and maximum gradients in the concrete components is used in the analysis. The normal thermal hot condition is the governing case for this load case. The HSM-MX thermal stress analysis was performed using thermal profiles and maximum temperatures that bound those reported in Section A.4.5. The ANSYS FEM described in Section A.3.9.4.6.2 is used for the normal thermal load analysis.

A.3.9.4.7.5 HSM-MX Design Basis Wind Load (W) Analysis

The DSCs inside the HSM-MX are not affected by wind load. The concrete structure forces and moments due to the design basis wind load (W) are bounded by the result of tornado generated wind load discussed in Section A.3.9.4.9.1. Therefore, no separate analysis is performed for this case.

A.3.9.4.8 Off-Normal Operation Structural Analysis

This section describes the design basis off-normal events for the HSM-MX components and presents analyses that demonstrate the adequacy of the design safety features of the HSM-MX.

The off-normal operating loads for which the HSM-MX components are designed include off-normal handling load and off-normal thermal load.

For an operating NUHOMS® MATRIX System, off-normal events could occur during fuel loading, TC handling, canister transfer, trailer towing, and other operational events. Two credible off-normal events bound the range of off-normal conditions for the HSM-MX. The limiting off-normal events as defined above are defined as a jammed DSC during loading or unloading from the HSM-MX and the extreme ambient temperatures of -40 °F (winter) and +117 °F (summer). These events bound the range of expected off-normal structural loads and off-normal temperatures acting on the HSM-MX. The ANSYS FEM described in Section A.3.9.4.6.1 is used to evaluate concrete forces and moments due to these loads.

A.3.9.4.8.1 HSM-MX Off-Normal Handling Loads (R_a) Analysis

This load case assumes that the EOS-TC is not accurately aligned with respect to the HSM-MX resulting in binding of the DSC during a transfer operation causing the hydraulic pressure in the ram to increase. The ram force is limited to a maximum load of 135,000 lbs during insertion, as well as during retrieval. Therefore, for the DSC, the off-normal jammed canister load (R_a) is defined as an axial load of 135,000 lbs on one side of MX-RRT supports. In addition, the DSC weight is applied to MX-RRT support locations of the loaded MX-RRT rail (2 points).

A.3.9.4.8.2 HSM-MX Off-Normal Thermal Loads Analysis

This load case is the same as the normal thermal load, but with an ambient temperature range from -40 °F to 117 °F. The temperature distributions for the extreme ambient conditions are considered for the concrete component evaluation. The concrete forces and moments due to this load case are bounded by the results of the accident blocked vent condition discussed in Section A.3.9.4.9.4. Therefore, no separate analysis is performed for this case.

A.3.9.4.9 Accident Condition Structural Analysis

The design basis accident events specified by ANSI/ANS 57.9-1984, and other credible accidents postulated to affect the normal safe operation of the HSM-MX are addressed in this section.

Each accident condition is analyzed to demonstrate that the requirements of 10 CFR 72.122 are met and that adequate safety margins exist for the HSM-MX design. The resulting accident condition stresses, forces and moments in the HSM-MX components are evaluated and compared with the applicable code limits. The postulated accident conditions addressed in this section include:

- Tornado winds and tornado generated missiles (W_t , W_m)
- Design basis earthquake (E)
- Design basis flood (FL)
- Blocked Vent Accident Thermal (T_a)

The ANSYS FEM described in Section A.3.9.4.6.1 is used to evaluate concrete forces and moments due to these loads.

A.3.9.4.9.1 Tornado Winds/Tornado Missile Load (W_t , W_m) Analysis

The most severe tornado generated wind and missile loads selected for analysis are specified by U.S. NRC (NRC) Regulatory Guide 1.76 [A.3.9.4-4] and NUREG-0800 [A.3.9.4-5]. The extreme design basis wind loads are less severe than tornado generated wind loads and, therefore, do not need to be addressed.

The tornado wind intensities used for the HSM-MX analysis are obtained from NRC Regulatory Guide 1.76, Rev. 0 [A.3.9.4-4], which bound the design basis requirements. Region I intensities are utilized since they result in the most severe loading parameters. For this region, the maximum wind speed is 360 mph, the rotational speed is 290 mph, and the maximum translational speed is 70 mph. The radius of the maximum rotational speed is 150 ft, the pressure drop across the tornado is 3 psi and the rate of pressure drop is 2 psi per second [A.3.9.4-4].

The maximum wind speed used of 360 mph provides substantial conservatism relative to the maximum wind speed of 230 mph prescribed in current regulatory guidance in NRC Regulatory Guide 1.76 Revision 1 [A.3.9.4-17]. For the purposes of the structural evaluation as described in Appendix A.3, as well as the accident evaluation as described in Appendix A.12 the design basis tornado (DBT) refers to the bounding criteria from Regulatory Guide 1.76, Rev. 0 used in the analysis.

Tornado loads are generated for three separate loading phenomena:

- Pressure or suction forces created by drag as air impinges and flows past the HSM-MX. These pressure or suction forces are due to tornado-generated wind with maximum wind speed of 360 mph.
- Pressure or suction forces created by drag due to tornado-generated pressure drop or differential pressure load of 3 psi.
- Impact, penetration and spalling forces created by tornado-generated missiles impinging on the HSM-MX.

The determination of impact forces created by tornado missiles for the HSM-MX is consistent with that presented in Section 2.3.1.2. The four types of missiles listed below envelope the missile spectrum of NUREG-0800, Revision 2, Section 3.5.1.4 [A.3.9.4-5]. These missiles also bound the design basis missile spectrum of NRC Regulatory Guide 1.76, Revision 1 [A.3.9.4-17] and NUREG 0800, Revision 3, Section 3.5.1.4 [A.3.9.4-6]. Evaluation of the effects of small diameter spherical missiles (artillery) is not required because there are no openings in the HSM-MX leading directly to the DSC through which such missiles could pass.

1. Utility wooden pole, 13.5" diameter, 35' long, Weight = 1124 lbs, Impact velocity = 180 fps.
2. Armor piercing artillery shell 8" diameter, Weight = 276 lbs, Impact velocity = 185 fps.
3. Steel pipe, 12.75" diameter, Schedule 40, 15 ft long, Weight = 750 lbs, Impact velocity = 154 fps.

4. Automobile traveling through the air not more than 25 ft above the ground and having contact area of 20 sq. ft, Weight = 4000 lbs, Impact Horizontal Velocity = 195 fps.

Stability and stress analyses are performed to determine the response of the HSM-MX to tornado wind pressure loads. The stability analyses are discussed in detail in Appendix A.3.9.7. The stress analyses are performed using the ANSYS FEM of the HSM-MX to determine design forces and moments. These conservative analyses envelope the effects of wind pressures on the HSM-MX in other array configurations. Thus, the requirements of 10 CFR 72.122 are met.

The HSM-MX is qualified for maximum design basis tornado (DBT) generated design wind loads of 238 psf and 167 psf on the windward and leeward HSM-MX walls (See Table A.3.9.4-1 and Table A.3.9.4-2), respectively, and a pressure drop of 3 psi.

An HSM-MX array is protected by end side walls, shield walls, or an adjacent module. For an HSM-MX array, the module on the windward end of the array has either an end side wall or an end shield wall to protect the module from tornado missile impacts. The end walls are also subjected to the 238 psf windward pressure load. The 167 psf suction load is applicable to the end side wall on the opposite end module in the array. A suction of 355 psf is also applied to the roof of each HSM-MX in the array.

For the stress analyses, the DBT wind pressures are applied to the HSM-MX as uniformly distributed loads. The bending moments and shear forces at critical locations in the HSM-MX concrete components are calculated by performing an analysis using the ANSYS analytical model of the HSM-MX as described in Section A.3.9.4.6. The wind and tornado loads are identified as load combination C2 and C5 as provided in Table A.3.9.4-5. The demand to capacity ratios in terms of reinforcement areas for the bounding load combinations are presented in Table A.3.9.4-6 for each of the HSM-MX components.

Conservatively, the design basis extreme wind pressure loads are assumed to be equal to those calculated for the DBT (based on 360 mph wind speed) in the formulation of HSM-MX load combination results.

In addition, the adequacy of the HSM-MX to resist tornado missile loads is checked using the modified National Defense Research Committee (NDRC) empirical formulae [A.3.9.4-10] for local damage evaluation, and response chart solution method [A.3.9.4-13] for global response. These evaluations are described in Section A.3.9.4.10.5.

A.3.9.4.9.2 Earthquake (Seismic) Load (E) Analysis

The design basis seismic load used for analysis of the HSM-MX components is as discussed in Section A.2.3.4. Based on NRC Regulatory Guide 1.61 [A.3.9.4-3], a damping value of 4% is used for seismic analysis of steel structural components and a damping value of 7% is used for seismic analysis of concrete components of the HSM-MX. An evaluation of the frequency content of the loaded HSM-MX is performed to determine the amplified accelerations associated with the design basis seismic response spectra for the HSM-MX. The results of the frequency analysis of the HSM-MX structure (which includes a simplified model of the DSC) yield a lowest frequency of 23.94 Hz in the transverse direction and 24.08 Hz in the longitudinal direction. The lowest vertical frequency exceeds 45 Hz; therefore, the spectral acceleration is not amplified in the vertical direction. Thus, based on the enhanced Regulatory Guide 1.60 response spectra amplifications, the corresponding seismic accelerations used for the design of the HSM-MX are 1.33g and 1.33g in the transverse and longitudinal directions, respectively, and 0.800g in the vertical direction. The resulting amplified accelerations are given in Table A.3.9.4-3.

An equivalent static analysis of the HSM-MX is performed using the ANSYS FEM described in Section A.3.9.4.6.1 by applying the amplified seismic accelerations load. The dominant frequencies are lower for the double row array in the X and Y directions, whereas the single row array has a lower frequency in the Z direction. Therefore, the spectral accelerations to be used in seismic analysis are taken from the double row array model for the X and Y directions, and from the single row array model for the Z direction.

The responses for each orthogonal direction are combined using the square root of the sum of the squares (SRSS) method. The resulting moments and forces due to the combined seismic load are included in the HSM-MX load combination results.

For sites having a higher zero period acceleration than analyzed, the reinforcement requirement may need to be reviewed, and additional rebar may be added for such sites.

The stability evaluation of the HSM-MX due to seismic load is discussed in Appendix A.3.9.7.

Seismic analysis of the HSM-MX heat shields consists of a modal time-history analysis of the HSM-MX using the seismic acceleration load corresponding to the ISRS with $\pm 15\%$ peak-broadening and the frequency response of each type of heat shield. The ground motion time histories used in the modal time-history analysis of the HSM-MX are based on four earthquakes,

- Hector Mine,
- Chi-Chi,
- Denali,
- Mianzhuqingping.

The time histories are compatible with the enhanced NRC Regulatory Guide 1.60 [A.3.9.4-2] response spectra. The acceleration, velocity, and displacement time histories and corresponding spectra in the two horizontal and vertical directions, all with 1.0g zero period acceleration (ZPA), are shown for the ground motion based on the Hector Mine earthquake in Figure A.3.9.4-7 through Figure A.3.9.4-12 for information only. The time histories are scaled down in the modal time-history analyses because their response spectra are anchored at 1.0g ZPA whereas the seismic criteria for the HSM-MX are based on 0.85g ZPA in the horizontal directions and 0.80g ZPA in the vertical direction. The envelopes of the ISRS of heat shield support nodes due to the four ground motions are shown in Figure A.3.9.4-13 through Figure A.3.9.4-15 for lower top heat shield (LTHS) only.

A.3.9.4.9.3 Flood Load (FL) Analysis

Since the source of flooding is site specific, the exact source, or quantity of flood water, should be established by the licensee. However, for this generic evaluation of the HSM-MX, bounding flooding conditions are specified that envelope those that are postulated for most plant sites. As described in Section 2.3.3, the design basis flooding load is specified as a 50-foot static head of water and a maximum flow velocity of 15 feet per second. Each licensee should confirm that this represents a bounding design basis for their specific ISFSI site.

Since the HSM-MX is open to the atmosphere, static differential pressure due to flooding is not a design load.

The maximum drag pressure, D , acting on the HSM-MX due to a 15 fps flood water velocity is calculated as follows:

$$D = \frac{C_D \rho_w V^2}{2g} \quad [A.3.9.4-15]$$

Where:

- V = 15 fps, Flood water velocity
- C_D = 2.0, Drag coefficient for flat plate
- ρ_w = 62.4 lb/ft³, Flood water density
- g = 32.2 ft/sec², Acceleration due to gravity
- D = Drag pressure (psf)

The resulting flood induced drag pressure is: $D = 436$ psf.

The following flood load cases are considered to account for different flow direction:

- Case 1: Flood water flowing longitudinally from the front row to the back row of the module or vice versa.

- Case 2: Flood water flowing transversely from the right side wall to the left side wall of the module or vice versa.

The ANSYS FEM described in Section A.3.9.4.6.1 is used for the structural evaluation. The results for the flood load case are obtained by enveloping results from the above load cases.

The stability evaluation of the HSM-MX due to flood load is discussed in Appendix A.3.9.7.

A.3.9.4.9.4 Accident Blocked Vent Thermal (T_a) Stress Analysis

The postulated accident thermal event occurs due to blockage of the air inlet and outlet vents under off-normal ambient temperatures range from -40 °F to 117 °F. The HSM-MX thermal stress analysis was performed using the thermal profiles and maximum temperatures reported in Section A.4.5.

The ANSYS FEM described in Section A.3.9.4.6.2 is used for the structural analysis for the accident blocked vent condition.

A.3.9.4.10 Structural Evaluation

The load categories associated with normal operating conditions, off-normal conditions and postulated accident conditions are described previously. The load combination results and design strengths of HSM-MX components are presented in this section.

A.3.9.4.10.1 HSM-MX Concrete Components

To determine the required strength (internal axial forces, shear forces, and bending moments) for each HSM-MX concrete component, linear elastic finite element analyses are performed for the normal, off-normal, and accident loads using the analytical models described in Sections A.3.9.4.6.1 and A.3.9.4.6.2 for mechanical and thermal loads, respectively.

The concrete design loads are multiplied by load factors and combined to simulate the most adverse load conditions. The load combinations listed in Table A.3.9.4-5 are used to evaluate the concrete components. The demand to capacity ratios (in terms of reinforcement areas) for the bounding load combinations are presented in Table A.3.9.4-6 for each HSM-MX component. The reinforcement directions are shown in Figure A.3.9.4-5. The thermal stresses of HSM-MX concrete components used in the load combination results are based on thermal results that bound those reported in Section A.4.5.

The required longitudinal reinforcement areas for the critical sections of concrete are calculated in accordance with the requirements of ANSI 57.9 [A.3.9.4-8] and ACI 349-06 [A.3.9.4-9], including the strength reduction factors defined in ACI 349-06, Section 9.3. The longitudinal reinforcement areas provided for the HSM-MX concrete components exceed the required reinforcement areas as shown in Table A.3.9.4-6.

A.3.9.4.10.2 HSM-MX Shield Door

The shield door is free to grow in the radial direction when subjected to thermal loads. Therefore, there are no stresses in the door due to thermal growth. The dead weight, differential pressure, flood and seismic loads cause insignificant stresses in the door compared to stresses due to missile impact load. Therefore, the door is evaluated only for the missile impact load.

The minimum thickness of a concrete component to prevent perforation and scabbing are 18.5 inches and 27.7 inches, respectively. Thus, the 28-inch thick door is adequate to protect from local damage due to missile impact. The computed maximum ductility ratio for the door is less than 2, which satisfies the ductility requirement if compared against the allowable ductility ratio of 10 as per ACI 349-06 [A.3.9.4-9]. Therefore, the concrete door meets the ductility requirement and is adequate to protect from the global effect of missile impact.

A.3.9.4.10.3 HSM-MX Heat Shield

The heat shield panels are connected by bolts and threaded studs to the support brackets and surrounding concrete walls. The HSM-MX heat shield consists of different variations such as lower cavity side heat shield (LSHS), lower cavity top heat shield (LTHS), upper cavity bottom heat shield (UBHS), upper cavity side heat shield (USHS) and upper cavity top heat shield (UTHS).

The heat shield panels consists of 12 gauge 0.1054-inch thick stainless steel.

The maximum interaction ratio for the combined axial and bending stress for all bolts is 0.98, which is less than 1.0, in the UBHS and maximum bending stress in the panel is 30.0 ksi, which is less than the allowable stress of 32.2 ksi.

The maximum temperature used in the stress analysis of the heat shields bounds the maximum temperatures reported in Section A.4.5. Expansion due to off-normal and accident condition for all heat shields will not be restrained by the supporting elements.

A.3.9.4.10.4 HSM-MX DSC Axial Retainer

The DSC axial retainer consists of a 3.5 in x 3.5 in solid steel square rod. The axial retainer slides horizontally through the HSM-MX door and stops the forward motion of the DSC towards the door. The anchor plate of the axial retainer (2 ½ in. thick, in the middle and 2 in. thick near the edge 6 in. x 15 in. plate), which is bolted to the door, supports the axial motion of the retainer and transfers the DSC seismic load to the door. The motion towards the back wall is controlled by the rear stop plate.

The calculated compressive strength of the axial retainer rod is 280.3 kips which is greater than the equivalent force of 270.5 kips, due to seismic load. The maximum seismically induced shear load in the anchor plate is 135.3 kips. The allowable shear strength of the anchor plate is 498.6 kips. The bounding seismically induced moment in the anchor plate is 507.2 in-kips. The allowable flexural strength of the anchor plate at that location is 714.0 in-kips. Hence, the DSC axial retainer design is adequate to perform its intended function.

A.3.9.4.10.5 Evaluation of Concrete Components for Missile Loading

Missile impact effects are assessed in terms of local damage and overall structural response. Local damage that occurs in the immediate vicinity of the impact area is assessed in terms of penetration, perforation, spalling and scabbing. Evaluation of local effects is essential to ensure that protected items (the DSC and fuel) would not be damaged by a missile perforating a protective barrier, or by secondary missiles such as scabbing particles. Evaluation of overall structural response is essential to ensure that protected items are not damaged or functionally impaired by deformation or collapse of the impacted structure.

The tornado-generated missiles are conservatively assumed to strike normal to the surface with the long axis of the missile parallel to the line of flight to maximize the local effects. Plastic deformation to absorb the energy input by the tornado-generated missile load is desirable and acceptable, provided that the overall integrity of the structure is not impaired. Due to complex physical process associated with missile impact effects, the HSM-MX structure is primarily evaluated conservatively by application of empirical formulae.

A.3.9.4.10.5.1 Local Damage Evaluation

Local missile impact effects consist of (a) missile penetration into the target, (b) missile perforation through the target, and (c) spalling and scabbing of the target. This also includes punching shear in the region of the target. Per F.7.2.3 of ACI 349-06 [A.3.9.4-9], if the concrete thickness is at least 20% greater than that required to prevent perforation, the punching shear requirement of the code need not be checked.

The following enveloping missiles are considered for local damage:

- Utility wooden pole
- Armor piercing artillery shell

- 12-inch diameter schedule 40 steel pipe

Large deformable missiles such as automobiles are incapable of producing significant local damage. Concrete thickness satisfying the global structural response requirements including punching shear is considered to preclude unacceptable local damage. Therefore, the local effects from an automobile are evaluated using punching shear criteria of ACI 349-06 [A.3.9.4-9]

The following empirical formulae are used to determine the local damage effects on reinforced concrete target:

A. Modified NDRC formulas for penetration depth [A.3.9.4-10]:

$$x = \sqrt{4KNWd \left(\frac{v_o}{1000 d} \right)^{1.8}}, \text{ for } x/d \leq 2.0$$

$$x = \left[KNW \left(\frac{v_o}{1000 d} \right)^{1.8} \right] + d, \text{ for } x/d > 2.0$$

Where,

x = Missile penetration depth, inches

K = concrete penetrability factor = $\frac{180}{\sqrt{f'_c}}$

N = projectile shape factor

= 0.72 flat nosed

= 0.84 blunt nosed

= 1.0 bullet nosed (spherical end)

= 1.14 very sharp nose

W = weight of missile, lb

v_o = striking velocity of missile, fps

d = effective projectile diameter, inches.

for a solid cylinder, d = diameter of projectile and

for a non-solid cylinder, $d = (4A_c/\pi)^{1/2}$

A_c = projectile impact area, in²

B. Modified NDRC formula for perforation thickness [A.3.9.4-10]:

$$\frac{e}{d} = 3.19 \left(\frac{x}{d} \right) - 0.718 \left(\frac{x}{d} \right)^2, \text{ for } x/d \leq 1.35$$

$$\frac{e}{d} = 1.32 + 1.24 \left(\frac{x}{d} \right), \text{ for } 1.35 \leq x/d \leq 13.5$$

Where,

e = perforation thickness, in.

In order to provide an adequate margin of safety the design thickness $t_d = 1.2e$
[A.3.9.4-9]

C. Modified NDRC formula for scabbing thickness [A.3.9.4-10]:

$$\frac{s}{d} = 7.91 \left(\frac{x}{d} \right) - 5.06 \left(\frac{x}{d} \right)^2, \text{ for } x/d \leq 0.65$$

$$\frac{s}{d} = 2.12 + 1.36 \left(\frac{x}{d} \right), \text{ for } 0.65 \leq x/d \leq 11.75$$

Where,

s = scabbing thickness, in.

In order to provide an adequate margin of safety the design thickness $t_d = 1.2s$
[A.3.9.4-9]

The concrete targets of the HSM-MX that may be subjected to local damage due to missile impact are:

- 24-inch thick roof panel
- 44-inch thick roof side wall
- 39-inch thick (minimum) front wall
- 36-inch thick end shield wall
- 36-inch thick end shield wall with 11-inch thick (minimum) side wall (upper compartment)
- 44-inch thick end wall (lower compartment)
- 82-inch thick end wall (upper compartment)
- 44-inch thick rear wall (for the case of single row array)

The minimum thickness of concrete target components listed above is 36 inches and 24 inches for horizontal and vertical missiles impacts, respectively. So, the required perforation thickness and required scabbing thickness are compared against 36 inches and 24 inches for horizontal and vertical missiles impacts, respectively, to ensure the adequacy of design.

Local Impact Effects of Utility Wooden Pole Missile

Per section 6.4.1.2.5 of [A.3.9.4-10], utility wooden pole missiles do not have sufficient strength to penetrate a concrete target and that the scabbing thickness required for wood missiles is substantially less than that required for a steel missile with the same mass and velocity. Practically, wooden pole missiles do not appear to be capable of causing local damage to the 12-inch or thicker walls (also see Section 2.1.1 of [A.3.9.4-13]). Since none of the concrete targets are less than 12 inches thick, the postulated wood missiles do not cause any local damage to the HSM-MX concrete component.

Local Impact Effects of Armor Piercing Artillery Shell Missile

The penetration depth for this missile is calculated using the NDRC Formula as given in Section A.3.9.4.10.5.1 (a) and the parameters used in the formula are as listed below:

$d = 8.0$ in. effective diameter of missile

$W = 276$ lb weight of missile

$v_o = 185$ fps striking velocity of missile

$f'_c = 5000$ psi concrete compressive strength

$K = 180/\sqrt{5000} = 2.55$ concrete penetrability factor

$N = 0.84$ projectile shape factor (blunt nosed)

Penetration depth, $x = 4.6$ in. for $x/d (= 0.58) \leq 2.0$

Perforation thickness, $e = 12.9$ in. for $x/d (= 0.58) \leq 1.35$

Required perforation thickness = $1.2 * 12.9 = 15.5$ in. < 36 in.

Scabbing thickness, $s = 23.1$ in. for $x/d (= 0.58) \leq 0.65$

Required scabbing thickness = $1.2 * 23.1 = 27.7$ in. < 36 in.

Similarly, for vertical impact:

Required perforation thickness = 11.2 in. < 24 in

Required scabbing thickness = 22.7 in. < 24 in

Therefore, penetration and perforation of the concrete components of the HSM-MX do not occur due to this missile impact.

Local Impact Effects of 12-Inch Diameter Schedule 40 Steel Pipe Missile

The penetration depth for this missile is calculated using the NDRC Formula as given in Section A.3.9.4.10.5.1 and the parameters used in the formula are as listed below:

$\phi = 12.75$ in. outer diameter of 12-inch dia. schedule 40 steel pipe.

$A_c = 15.74$ in² missile impact area (cross sectional area of steel)

$d = (4 \cdot 15.74 / \pi)^{1/2} = 4.5$ in. effective diameter of missile

$W = 750$ lb weight of missile

$v_o = 154$ fps striking velocity of missile

$f_c = 5000$ psi concrete compressive strength

$K = 180 / \sqrt{5000} = 2.55$ concrete penetrability factor

$N = 0.72$ projectile shape factor (flat nosed)

Penetration depth, $x = 7.6$ in. for $x/d (= 1.69) \leq 2.0$

Perforation thickness, $e = 15.4$ in. for $1.35 \leq x/d (= 1.69) \leq 13.5$

Required perforation thickness = $1.2 \cdot 15.4 = 18.5$ in. < 36 in.

Scabbing thickness, $s = 19.9$ in. for $0.65 \leq x/d (= 1.69) \leq 11.75$

Required scabbing thickness = $1.2 \cdot 19.9 = 23.9$ in. < 36 in.

Similarly, for vertical impact:

Required perforation thickness = 14.8 in. < 24 in

Required scabbing thickness = 20 in. < 24 in

Therefore, penetration and perforation of the concrete components of the HSM-MX do not occur due to this missile impact.

A.3.9.4.10.5.2 Global Structural Response

When a missile strikes a structure, large forces develop at the missile-structure interface, which decelerate the missile and accelerate the structure. The response of the structure depends on the dynamic properties of the structure and the time dependent nature of the applied loading (interface force-time function). The force-time function is, in turn, dependent on the type of impact (elastic or plastic) and the nature and extent of local damage.

In an elastic impact, the missile and the structure deform elastically, remain in contact for a short period of time (duration of impact), and subsequently disengage due to the action of elastic interface restoring forces.

In a plastic impact, the missile or the structure (or both) may sustain permanent deformation or damage (local damage). Elastic restoring forces are small, and the missile and the structure tend to remain in contact after impact. Plastic impact is much more common than elastic impact, which is rarely encountered. Test data have indicated that the impact from all postulated tornado-generated missiles can be characterized as a plastic impact.

If the interface forcing function can be defined or conservatively idealized, the structure can be modeled mathematically, and conventional analytical or numerical techniques can be used to predict structural response. If the interface forcing function cannot be defined, the same mathematical model of the structure can be used to determine structural response by application of conservation of momentum and energy balance techniques with due consideration for type of impact (elastic or plastic).

In either case, in lieu of a more rigorous analysis, a conservative estimate of structural response can be obtained by first determining the response of the impacted structural element, and then applying its reaction forces to the structure. The predicted structural response enables assessment of structural design adequacy in terms of strain energy capacity, deformation limits, stability and structural integrity.

The overall structural response of each component as a whole (global response) is determined by single degree of freedom analysis using response charts solution method of [A.3.9.4-13].

The following enveloping missiles are considered for global structural response:

- Utility wooden pole
- Armor piercing artillery shell
- 12-inch diameter schedule 40 steel pipe
- Automobile missile

The peak interface force and impact duration for each missile are calculated as follows:

A. Utility Wooden Pole Missile

For wooden missile, the interface forcing function is a rectangular pulse having a force magnitude of F and duration t_i , per Section 2.3.1 of [A.3.9.4-13]

$$F = PA$$

$$t_i = M_m v_c / F$$

Where,

F = interface force (lb)

P = interface pressure (psi) = 2500 psi for wood missiles [A.3.9.4-13]

A = cross sectional area of the missile (in^2) = $\pi * 13.5^2 / 4 = 143.1 \text{ in}^2$

t_i = impact duration (sec)

W_m = weight of missile (lb) = 1124 lb

M_m = missile mass ($\text{lb-sec}^2/\text{ft}$) = $W_m / g = 1124 \text{ lb} / 32.2 \text{ ft/sec}^2 = 34.9 \text{ lb-sec}^2/\text{ft}$

v_c = change in velocity during impact (conservatively = v_s) (fps) = 180 fps

Therefore,

$$F = 358 \text{ kip and } t_i = 0.0175 \text{ sec}$$

For the missile with vertical velocity, F is the same and $t_i = 0.0117 \text{ sec}$

B. Armor Piercing Artillery Shell

For solid steel missile, the concrete is a soft target per section 6.4.2 of [A.3.9.4-10] with a penetration depth of 4.6 in. The interface forcing function is a rectangular pulse per Section 6.4.2.1.1 of [A.3.9.4-10].

$$F = W_m V_0^2 / 2gX$$

$$t_i = 2X/V_0$$

Where,

F = interface force (lb)

t_i = impact duration (sec)

W_m = missile weight (lb) = 276 lb

V_0 = initial velocity of the missile (fps) = 185 fps

X = penetration depth = 4.6 in.

Therefore,

$$F = 383 \text{ kip and } t_i = 0.00414 \text{ sec}$$

For the missile with vertical velocity,

$$F = 170 \text{ kip and } t_i = 0.00622 \text{ sec}$$

C. 12-Inch Diameter Schedule 40 Steel Pipe

For steel pipe missile, the interface forcing function is a triangular pulse per Section 2.3.2 of [A.3.9.4-13].

$$t_i = 400M_m / PA$$

$$F = (2M_m v_s) / t_i$$

Where,

F = peak interface force (lb)

P = collapse stress of pipe (psi) = 60000 psi

A = cross sectional metal area of the missile (in^2) = 15.74 in^2

t_i = impact duration (sec)

$$W_m = \text{weight of missile (lb)} = 750 \text{ lb}$$

$$M_m = \text{missile mass (lb-sec}^2/\text{ft)} = W_m/g = 750 \text{ lb} / 32.2 \text{ ft/sec}^2 = 23.29 \text{ lb-sec}^2/\text{ft}$$

$$v_s = \text{striking velocity of missile} = 154 \text{ fps}$$

Therefore,

$$F = 728 \text{ kip and } t_i = 0.00986 \text{ sec}$$

$$\text{For the missile with vertical velocity } F_{\text{peak}} = 485 \text{ kip}$$

D. Automobile Missile

For automobile missile, the interface forcing function per 2.3.3 of [A.3.9.4-13] is as follows:

$$F_t = 0.625 v_c W \sin(20t) \quad 0 < t \leq 0.0785 \text{ sec}$$

$$F_t = 0 \quad t > 0.0785 \text{ sec}$$

Where,

$$F_t = \text{force as a function of time (lb)}$$

$$W = \text{weight of automobile (lb)} = 4000 \text{ lb}$$

$$v_c = \text{change in velocity during impact (conservatively} = v_s) \text{ (fps)} = 195 \text{ fps}$$

Therefore,

$$F = 488 \text{ kip and } t_i = 0.0785 \text{ sec}$$

$$\text{For the missile with vertical velocity, } F_{\text{peak}} = 325 \text{ kip}$$

The lower compartment module left sidewall, top left sidewall, right shield wall, front wall, rear wall, roof and roof sidewall of the HSM-MX are evaluated for global response, since these components may interface with missile loading. The lower compartment module left side wall, upper compartment module left side wall and rear wall are idealized as a simply supported plate. The roof is idealized as a plate clamped to three sides and free at the other side adjacent to vent opening. The roof sidewall is idealized as a plate clamped to three sides and free at the other side facing the top. The yield resistance and fundamental period of vibration of concrete components are then determined based on the assumed idealized boundary condition using the equations given in Section 4.4 of [A.3.9.4-13]. For the right shield wall and front wall, ANSYS finite element models are used to determine the yield resistance and fundamental period of vibration. The calculated value of yield resistance, R_y , and fundamental period of vibration, T_n , for different concrete components are tabulated below.

Component	R_y (kip)	T_n (sec)
Lower Compartment Module Left Side Wall	1659	0.0048
Upper Compartment Module Left Side Wall	3255	0.0025
Right Shield Wall	359.5	0.016
Front Wall	961.1	0.0079
Rear Wall	1659	0.0030
Roof	453.8	0.0040
Roof Side Wall	1659	0.0015

In the response chart solution method, the structural response is determined by entering the chart with calculated values of C_T and C_R to determine the ductility ratio, μ , which is compared against the allowable ductility ratio as given in Appendix F of ACI 349-06 [A.3.9.4-9]. The dimensionless ratios, C_T and C_R , are defined as follows:

$$C_R = \frac{R_y}{F} \quad C_T = \frac{t_i}{T_n}$$

The maximum value of ductility ratio of all seven components is found to be less than the allowable ductility ratio per ACI 349-06 [A.3.9.4-9], which is 10 if flexure controls the design and 1.3 if shear controls the design. Hence, the global response of HSM-MX is within deformation limit meeting the ductility requirement.

Each component is also evaluated for punching shear capacity with interfacing utility wooden pole missile and automobile missile. All the components have punching shear capacity greater than the peak missile interface force.

A.3.9.4.11 Conclusions

The load categories associated with normal operating conditions, off-normal conditions and postulated accident conditions are described and analyzed in previous sections. The load combination results for HSM-MX components important-to-safety are also presented. Comparison of the results with the corresponding design capacity shows that the design strength of the HSM-MX is greater than the strength required for the most critical load combination.

A.3.9.4.12 References

- A.3.9.4-1 Code of Federal Regulation Title 10, Part 72 (10CFR Part 72), “Licensing Requirements for the Independent Storage of Spent Nuclear Fuel, High-Level Radioactive Waste, and Reactor-Related Greater than Class C Waste.”
- A.3.9.4-2 U.S. Nuclear Regulatory Commission, Regulatory Guide 1.60, “Design Response Spectra for Seismic Design of Nuclear Power Plants,” Revision 1, 1973.
- A.3.9.4-3 U.S. Nuclear Regulatory Commission, Regulatory Guide 1.61, “Damping Values for Seismic Design of Nuclear Power Plants,” Revision 1, March 2007.
- A.3.9.4-4 U.S. Nuclear Regulatory Commission, Regulatory Guide 1.76, “Design Basis Tornado for Nuclear Power Plants,” Revision 0, April 1974.
- A.3.9.4-5 NUREG-0800, Standard Review Plan, Section 3.5.1.4, “Missiles Generated by Natural Phenomena,” Revision 2, July 1981.
- A.3.9.4-6 NUREG-0800, Standard Review Plan, Section 3.3.1, “Wind Loading,” Section 3.3.2 “Tornado Loads,” and Section 3.5.1.4 “Missiles Generated by Tornado and Extreme Winds,” Revision 3, March 2007.
- A.3.9.4-7 Not used.
- A.3.9.4-8 ANSI/ANS 57.9-1984, “Design Criteria for an Independent Spent Fuel Storage Installation (Dry Storage Type),” American National Standards Institute, American Nuclear Society.
- A.3.9.4-9 ACI 349-06, “Code Requirements for Nuclear Safety Related Concrete Structures,” American Concrete Institute.
- A.3.9.4-10 American Society of Civil Engineers, “Structural Analysis and Design of Nuclear Plant Facilities,” ASCE Publication No. 58.
- A.3.9.4-11 Not used.
- A.3.9.4-12 American Society of Civil Engineers, “Minimum Design Loads for Buildings and Other Structures,” ASCE 7-10 (formerly ANSI A58.1).
- A.3.9.4-13 Bechtel Corporation, “Design Guide Number C-2.45 for Design of Structures for Tornado Missile Impact,” Rev. 0, April 1982.
- A.3.9.4-14 “ANSYS Computer Code and User’s Manual”, Release 17.1
- A.3.9.4-15 Binder, Raymond C., “Fluid Mechanics,” 3rd Edition, Prentice-Hall, Inc, 1973.
- A.3.9.4-16 AREVA Inc., “Updated Final Safety Analysis Report For The Standardized Advanced NUHOMS® Horizontal Modular Storage System For Irradiated Nuclear Fuel,” Revision 6, US NRC Docket Number 72-1029, August 2014.
- A.3.9.4-17 U.S. Nuclear Regulatory Commission, Regulatory Guide 1.76, “Design Basis Tornado for Nuclear Power Plants,” Revision 1, March 2007.
- A.3.9.4-18 “CivilFEM® Documentation”, Release 17.1, SP1.

Table A.3.9.4-1
Design Pressures for Tornado Wind Flowing from Front Wall to Rear Wall
and Vice Versa

Component	Velocity Pressure, q_v (psf)	External Pressure Coefficient, C_p	Internal Pressure Coefficient, (GC_{pi})	Max. Design Pressure, $q_v*(G*C_p - GC_{pi})$ (psf)
Windward (Front Row Front Wall)	276	0.80	± 0.18	238
Leeward (Back Row Front Wall)		-0.47 ⁽¹⁾		-160
Side (Right Side Wall)		-0.70		-214
Side (Left Side Wall)		-0.70		-214
Roof		-1.30		-355

Notes:

1. The C_p value is taken for $L/B = 496''/438'' \approx 1.13$.
2. The gust effect factor, $G=0.85$ considering the HSM-MX as rigid.

Table A.3.9.4-2
Design Pressures for Tornado Wind Flowing from Right Side to Left Side
Wall and Vice Versa

Component	Velocity Pressure, q_v (psf)	External Pressure Coefficient, C_p	Internal Pressure Coefficient, (GC_{pi})	Max. Design Pressure, $q_v*(G*C_p - GC_{pi})$ (psf)
Side (Front Row Front Wall)	276	-0.70	± 0.18	-214
Side (Back Row Front Wall)		-0.70		-214
Windward (Right Side Wall)		0.80		238
Leeward (Left Side Wall)		-0.50 ⁽¹⁾		-167
Roof		-1.30		-355

Notes:

1. The C_p value is taken for $L/B = 431''/438'' \approx 0.88$
2. The gust effect factor, $G=0.85$ considering the HSM-MX as rigid.

Table A.3.9.4-3
Spectral Acceleration Applicable to Different Components of HSM-MX for
Seismic Analysis

Direction	Frequency (Hz)	Spectral Acceleration Corresponding to Design ZPA (Design ZPA = 0.85g horizontal & 0.80g vertical)		
		at 3% Damping (for DSC)	at 4% Damping (for steel structure)	at 7% Damping (for concrete components)
X (Transverse)	23.94	1.62g	1.53g	1.33g
Y (Vertical)	49.02	0.80g	0.80g	0.80g
Z (Longitudinal)	24.08	1.61g	1.52g	1.33g

Table A.3.9.4-4
Load Cases for HSM-MX Concrete Components Evaluation

Design Load Type	Load Notation	Design Parameters	Applicable Codes / References
Normal			
Dead	DL	Includes self-weight with 160 pcf density for concrete.	ANSI/ANS 57.9-1984 [A.3.9.4-8]
Live	LL	Design live load of 200 psf on roof which includes snow and ice load and DSC weight of 135 kip applied on DSC supports.	ANSI/ANS 57.9-1984 [A.3.9.4-8] & ASCE 7-10 [A.3.9.4-12]
Normal Handling	R _O	140 kip of DSC insertion load is distributed to both sides of the MX-RRT supports. The DSC weight is also applied at both sides of the MX-RRT support locations (4 points).	
Normal Thermal	T _O	DSC with spent fuel rejecting up to 50.0 kW of decay heat. Extreme ambient air temp. -20 °F and 100 °F. Reference temperature = 70 °F.	
Off-Normal/Accidental			
Off-Normal Handling	R _a	135 kip of DSC insertion and retrieval load is applied to one side of the MX-RRT supports. The DSC weight is also applied at one side of the MX-RRT support locations (two points).	
Accidental Thermal	T _a	Enveloped of Off-Normal and Accidental Thermal (vent blocked) condition. Extreme ambient temperatures -40 °F and 117 °F. Reference temperature = 70 °F	
Earthquake	E	ZPA of 0.85g in horizontal and 0.80g in vertical direction with enhancement in frequency above 9 Hz and 7% damping.	NRC Reg. Guide 1.60 [A.3.9.4-2] & Reg. Guide 1.61 [A.3.9.4-3]
Flood	FL	Maximum flood height of 50 ft and max. velocity of water 15 ft/sec	10 CFR Part 72 [A.3.9.4-1]
Wind/Tornado Wind	W/W _t	Maximum wind speed of 360 mph, and a pressure drop of 3 psi	ASCE 7-10 [A.3.9.4-12] & NRC Reg Guide 1.76 [A.3.9.4-4]
Tornado Generated Missile	W _m	Four types of tornado-generated missiles	NUREG-0800 Section 3.5.1.4 [A.3.9.4-5]

Table A.3.9.4-5
Load Combination for HSM-MX Concrete Components Evaluation

Combination Number	Load Combination	Event
C1	$1.4 \text{ DL} + 1.7 (\text{LL} + \text{R}_o)$	Normal
C2	$1.05 \text{ DL} + 1.275 (\text{LL} + \text{T}_o + \text{W})$	Off-Normal – Wind
C3	$1.05 \text{ DL} + 1.275 (\text{LL} + \text{T}_o + \text{R}_a)$	Off-Normal – Handling
C4	$\text{DL} + \text{LL} + \text{T}_o + \text{E}$	Accident – Earthquake
C5	$\text{DL} + \text{LL} + \text{T}_o + \text{W}_t$	Accident – Tornado
C6	$\text{DL} + \text{LL} + \text{T}_o + \text{FL}$	Accident – Flood
C7	$\text{DL} + \text{LL} + \text{Ta}$	Accident – Thermal

Note: See Table A.3.9.4-4 for notation.

Table A.3.9.4-6
Demand to Capacity Ratios for HSM-MX Longitudinal Reinforcement Areas

Component Name	Thickness (in)	Reinforcement	$A_{s,provided}$ (in ² /in)	A_{sx}			A_{sy}			A_{sip}		
				$A_{sx,read}$ (in ² /in)	D/C _{asx}	Governing Load Combination	$A_{sy,read}$ (in ² /in)	D/C _{asy}	Governing Load Combination	$A_{sip,read}$ (in ² /in)	D/C _{asip}	Governing Load Combination ⁽¹⁾
Bottom Unit Front Wall Bottom	51	#9@7"	0.1429	0.1304	0.91	C4	0.0703	0.49	C4	0.1287	0.45	C1
Top Unit Front Wall Bottom	51	#9@8"	0.1250	0.0856	0.68	C4	0.0847	0.68	C4	0.1280	0.51	C1
Front Wall Top	39	#9@8"	0.1250	0.1023	0.82	C4	0.1142	0.91	C4	0.1589	0.64	C4
Bottom Unit Vent Wall	11.5	#5@8"	0.0388	0.0165	0.43	C4	0.0149	0.38	C4	0.0285	0.37	C1
Top Unit Side Vent Wall	11	#5@8"	0.0388	0.0122	0.31	C5	0.0172	0.44	C7	0.0276	0.36	C1
Bottom Unit Side Wall	37	#6@8"	0.0550	0.0243	0.44	C4	0.0239	0.43	C4	0.0925	0.84	C1
Bottom Unit End Side Wall	44	#9@8"	0.1250	0.0990	0.79	C4	0.0715	0.57	C7	0.1102	0.44	C1
Top Unit End Side Wall	82	#9@8"	0.1250	0.0449	0.36	C4	0.0570	0.46	C4	0.2047	0.82	C1
Bottom Unit Rear Wall Bottom	78	#9@8"	0.1250	0.0706	0.56	C4	0.0151	0.12	C4	0.1949	0.78	C1
Rear Wall	30	#9@8"	0.1250	0.0088	0.07	C4	0.0000	0.00	C1	0.1350	0.54	C4
Roof Top Panel	24	#7@9"	0.0667	0.0319	0.48	C2	0.0583	0.87	C5	0.0600	0.45	C1
Roof Bottom Panel	10	#5@8"	0.0388	0.0130	0.34	C5	0.0081	0.21	C7	0.0283	0.37	C3
Roof Side Panel	11	#5@8"	0.0388	0.0066	0.17	C5	0.0072	0.19	C2	0.0276	0.36	C1
Roof Side Panel	10.5	#5@9"	0.0344	0.0038	0.11	C5	0.0126	0.37	C7	0.0551	0.80	C5
Roof Side Wall	44	#9@8"	0.1250	0.0303	0.24	C5	0.1038	0.83	C2	0.1102	0.44	C1
Roof	50	#9@8"	0.1250	0.0973	0.78	C2	0.0711	0.57	C5	0.1250	0.50	C1
Inclined Slab	11.5	#5@8"	0.0388	0.0144	0.37	C4	0.0149	0.38	C4	0.0285	0.37	C1
Pedestal	23.89	#7@8"	0.0750	0.0242	0.32	C4	0.0410	0.55	C4	0.0600	0.40	C1

Note 1:

$A_{\text{sip,required}}$ is governed by minimum in-plane shear reinforcement requirement for most components. C1 is shown for such components.

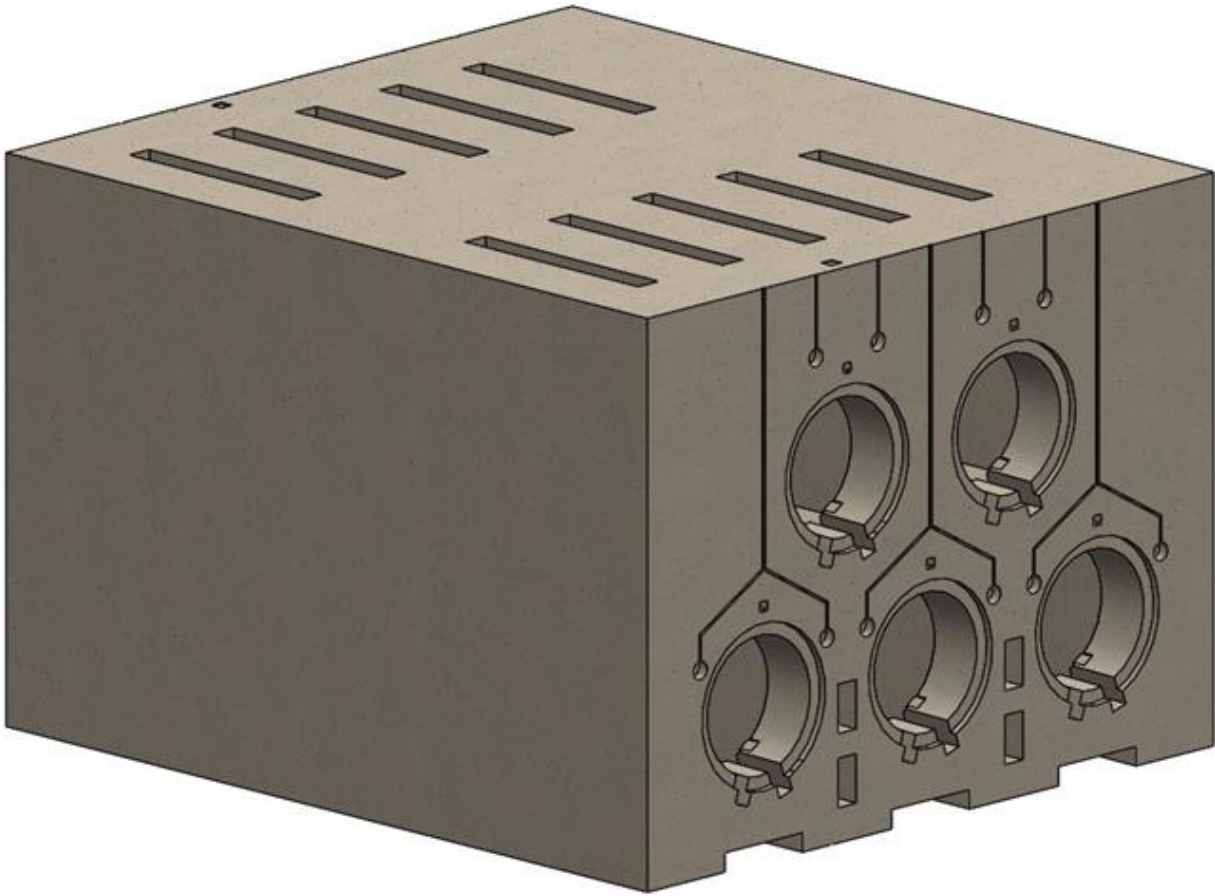


Figure A.3.9.4-1
HSM-MX (Back-to-Back) CAD Model

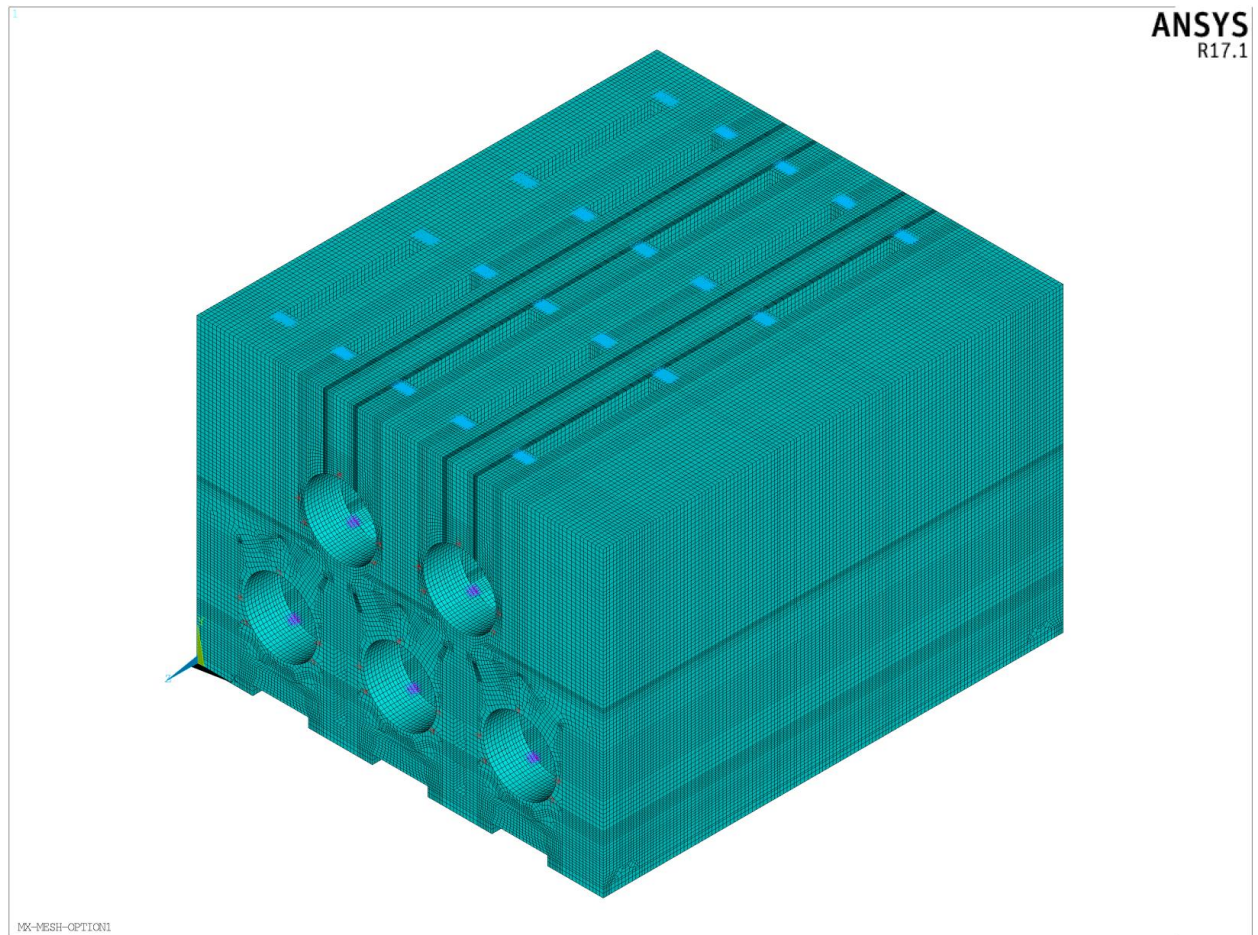


Figure A.3.9.4-2
HSM-MX (Back-to-Back) Meshed Model

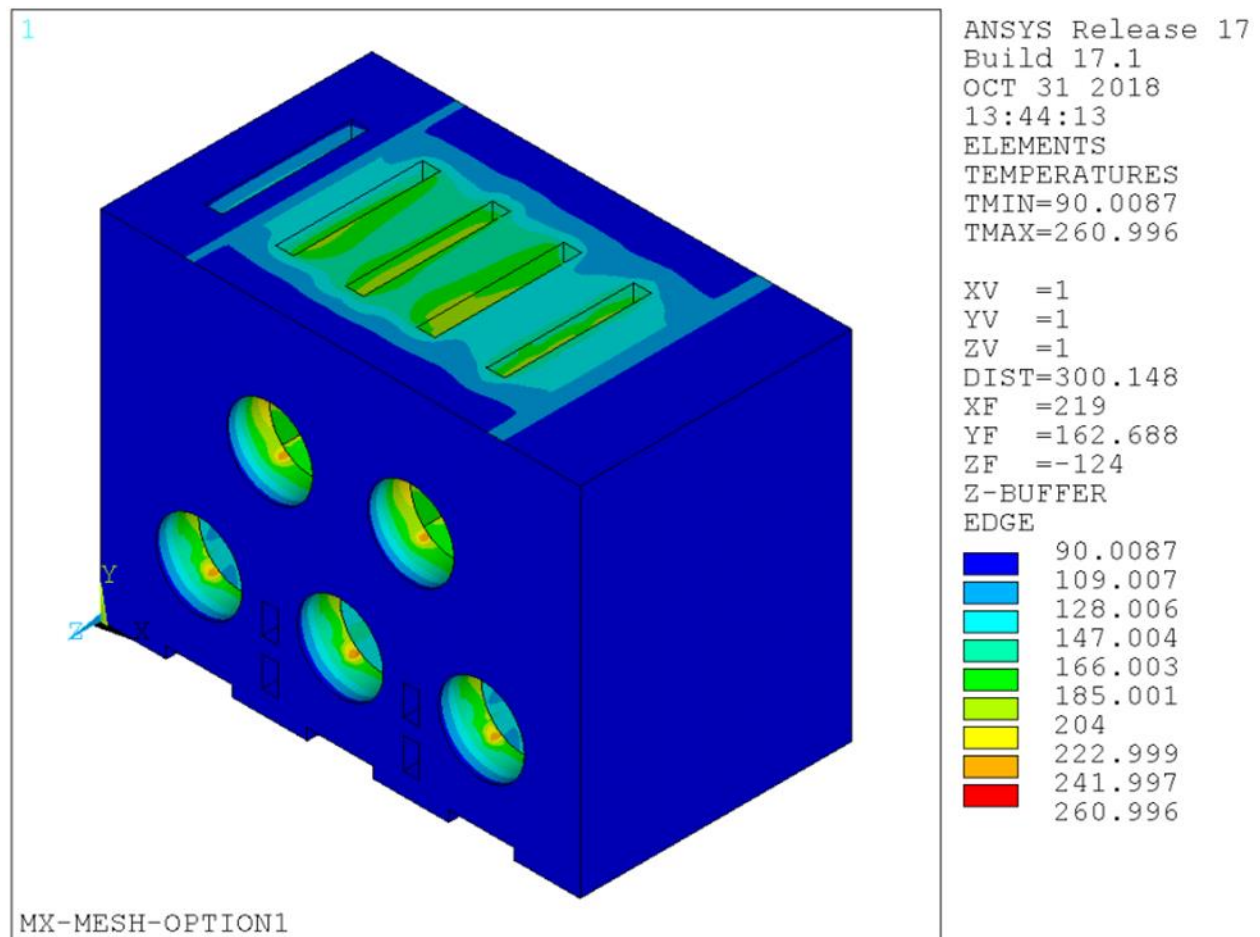


Figure A.3.9.4-3
Temperature Distribution of HSM-MX for Normal Thermal Hot Condition

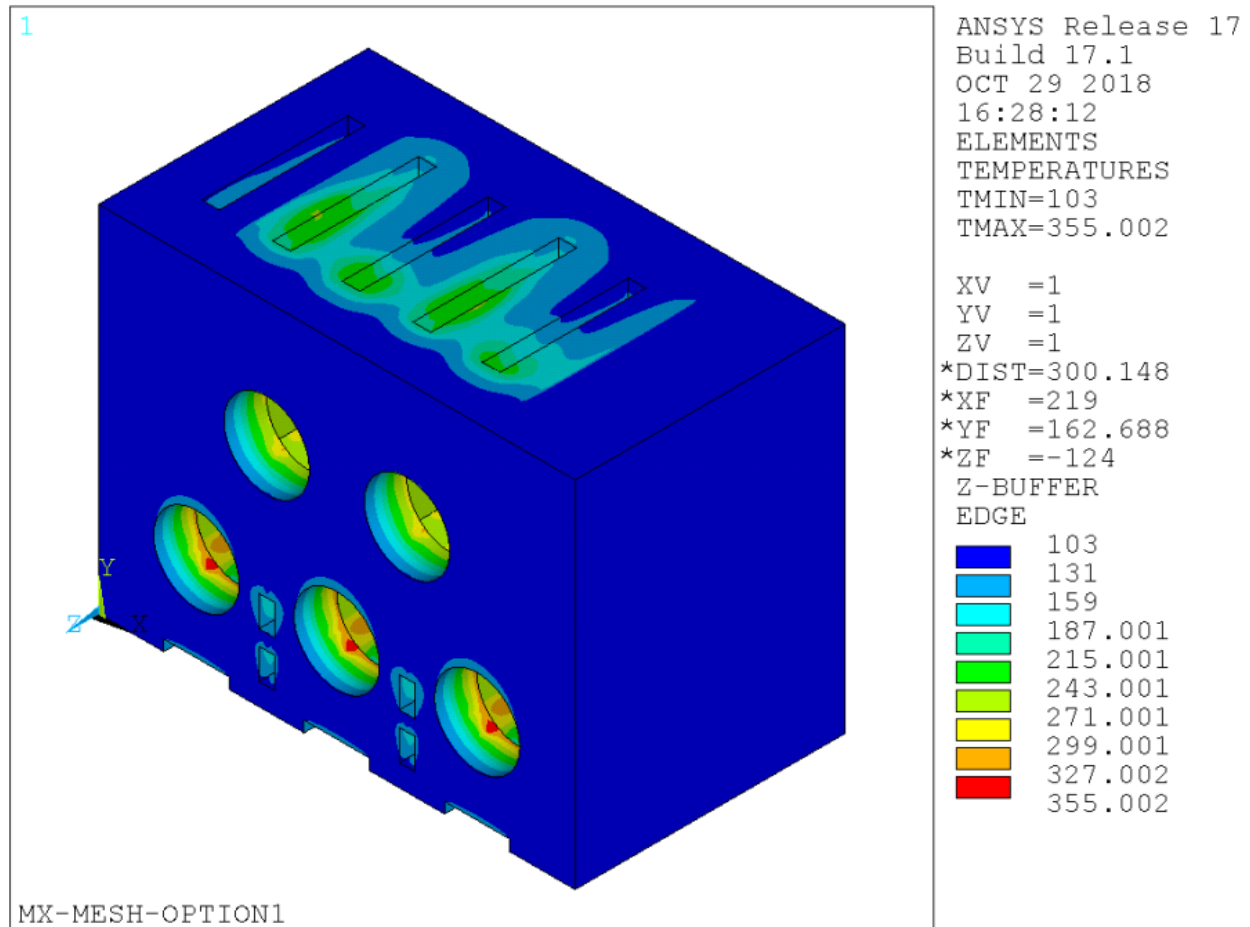


Figure A.3.9.4-4
Temperature Distribution of HSM-MXS for Blocked Vent Accident Thermal Condition

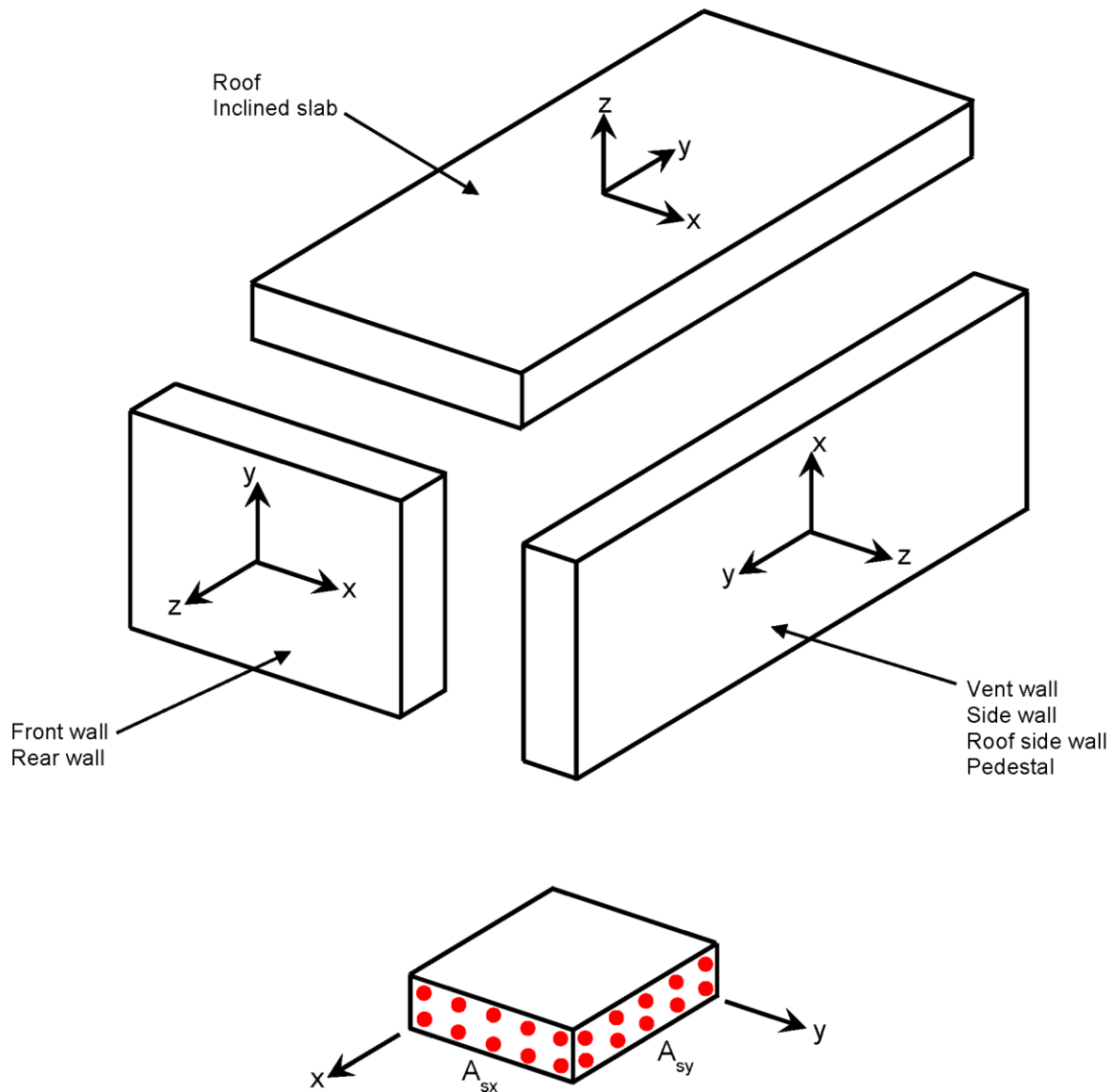
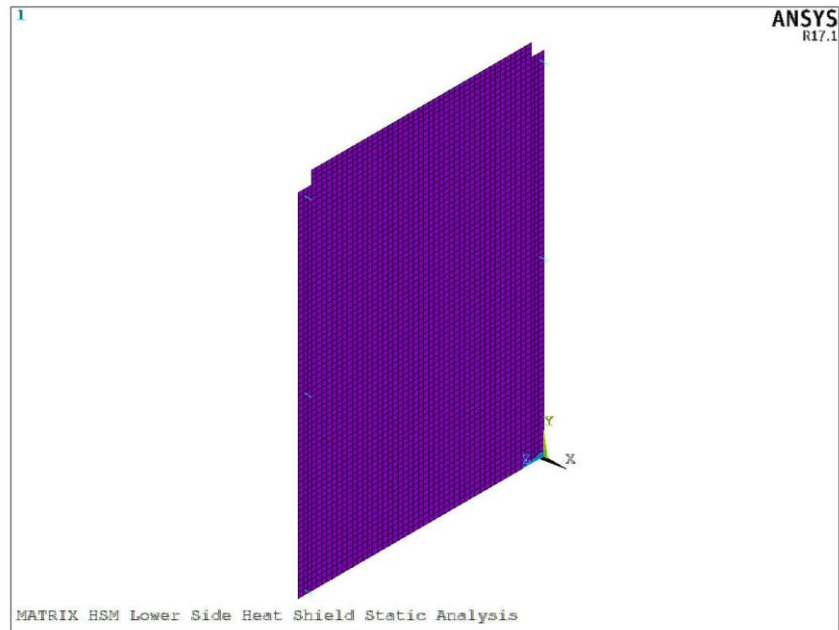
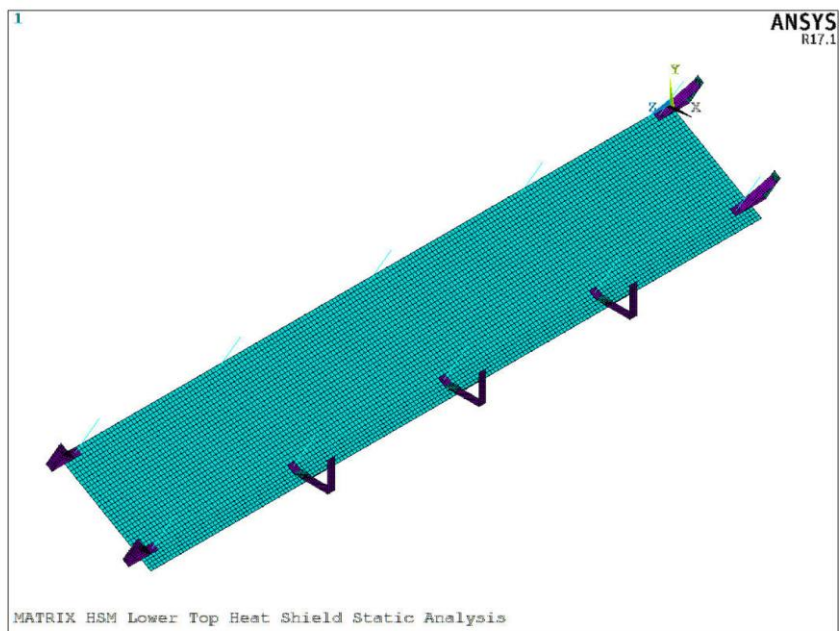


Figure A.3.9.4-5
HSM-MX Concrete Reinforcement Directions



(a)



(b)

Figure A.3.9.4-6
Analytical Model of Heat Shield
(a) Coupled Lower Side Heat Shield and Studs (b) Coupled Lower Top Heat Shield and Studs

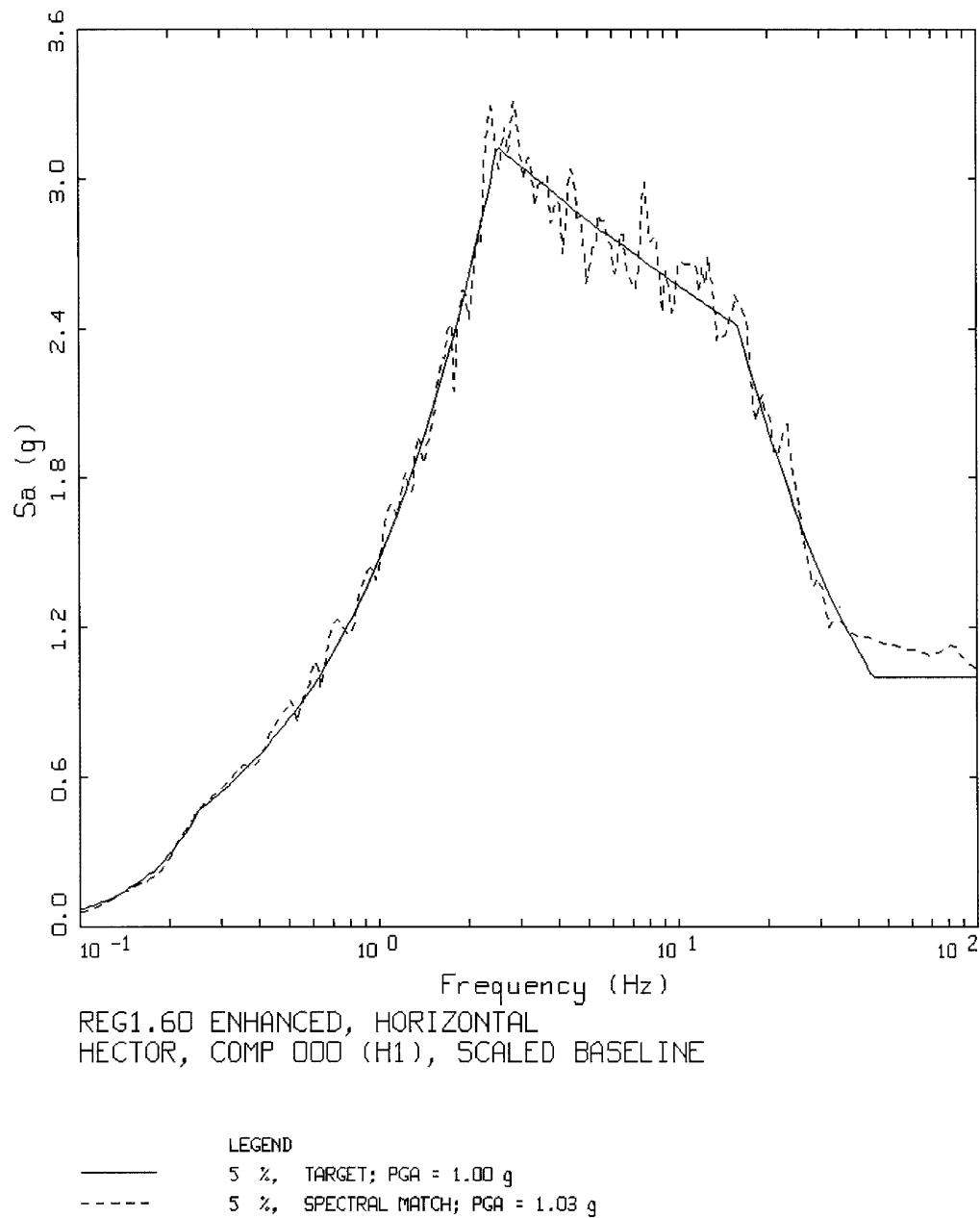


Figure A.3.9.4-7
Horizontal Target and 5% Spectral Match (Horizontal 1, Hector Mine Earthquake)

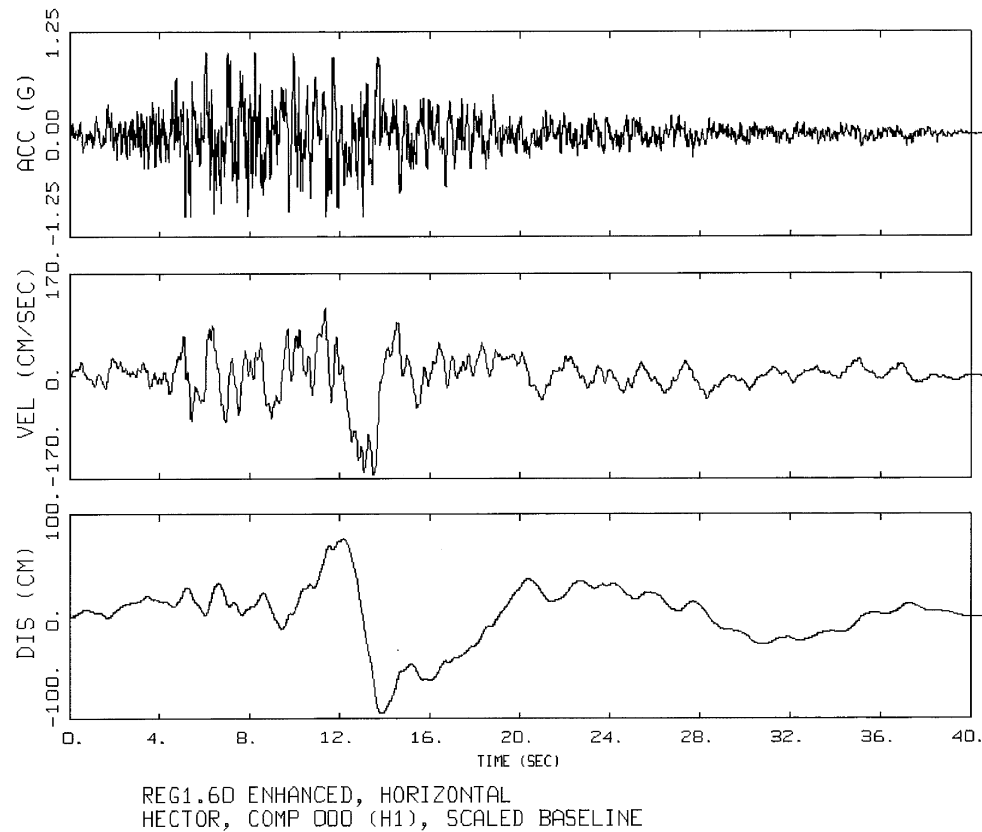
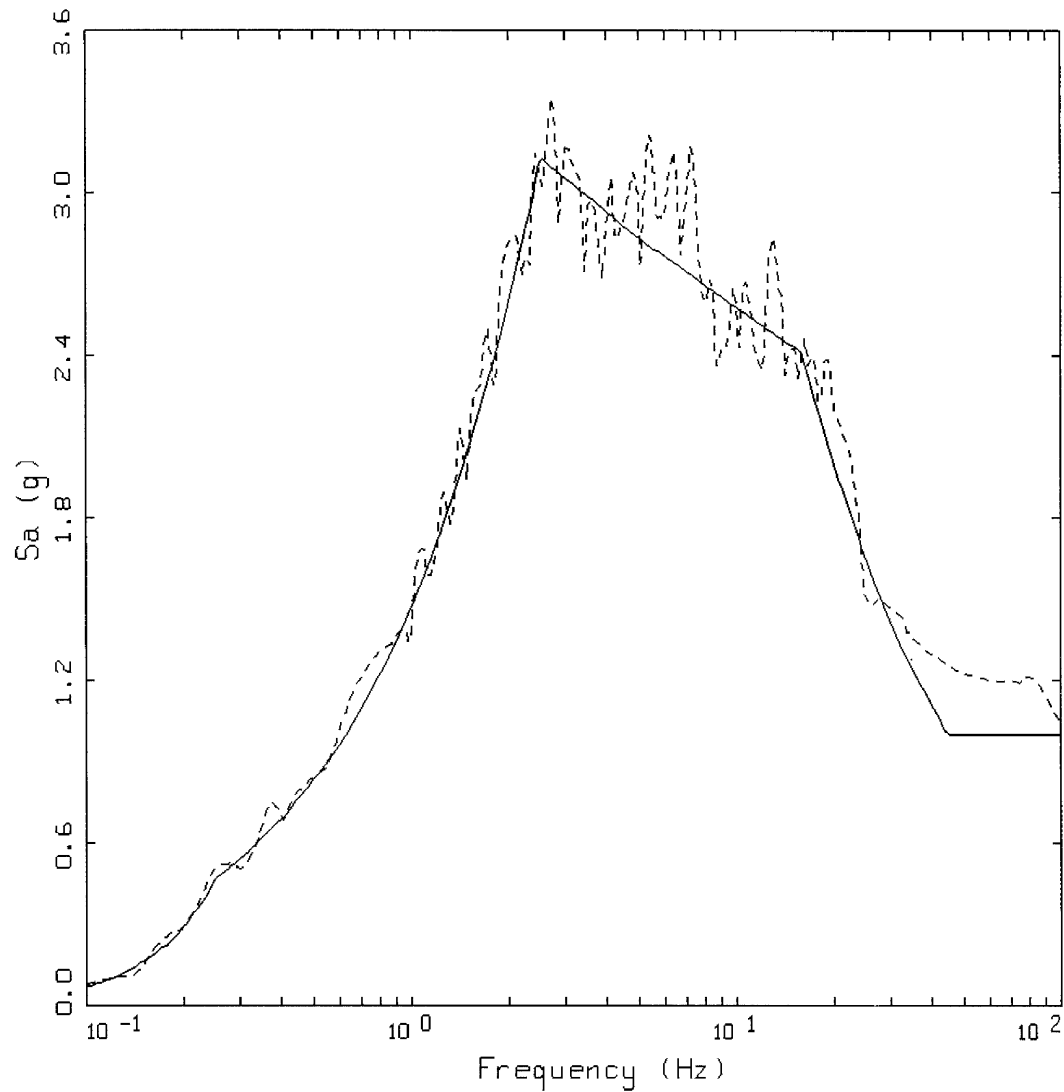


Figure A.3.9.4-8
Baseline Corrected Acceleration, Velocity and Displacement Time Histories
(Horizontal 1, Hector Mine Earthquake)



LEGEND
—— 5 %, TARGET; PGA = 1.00 g
----- 5 %, SPECTRAL MATCH; PGA = 1.05 g

Figure A.3.9.4-9
Horizontal Target and 5% Spectral Match (Horizontal 2, Hector Mine Earthquake)

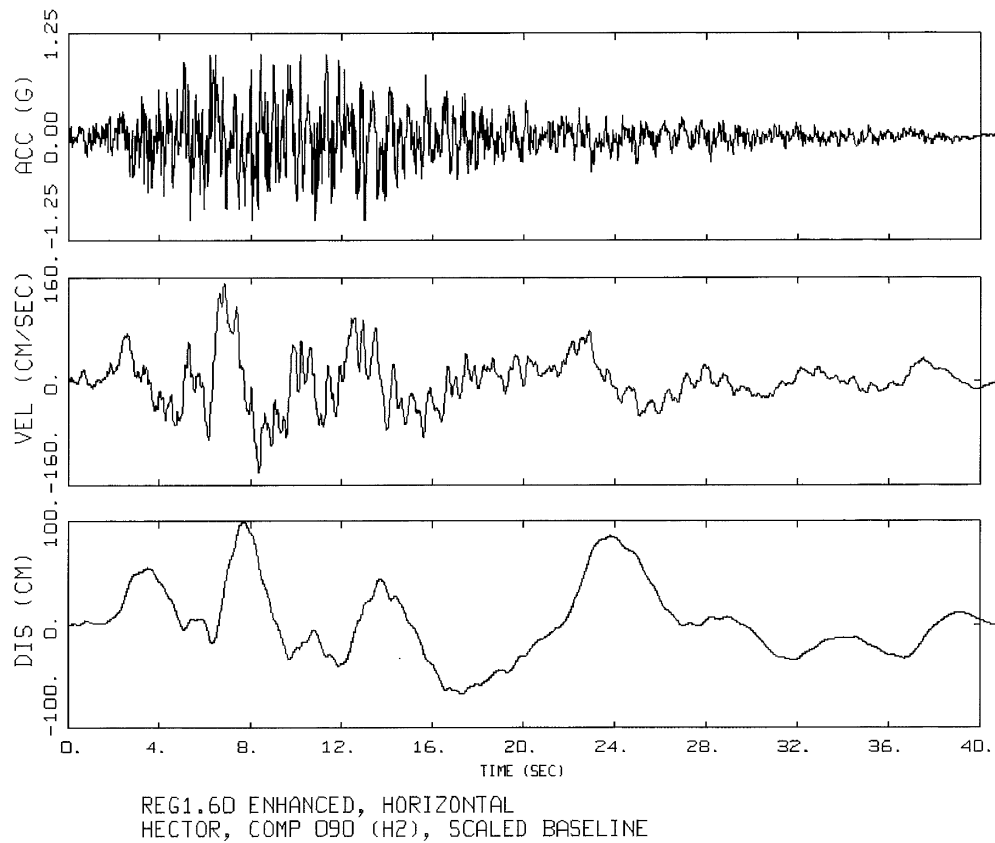


Figure A.3.9.4-10
Baseline Corrected Acceleration, Velocity and Displacement Time Histories
(Horizontal 2, Hector Mine Earthquake)

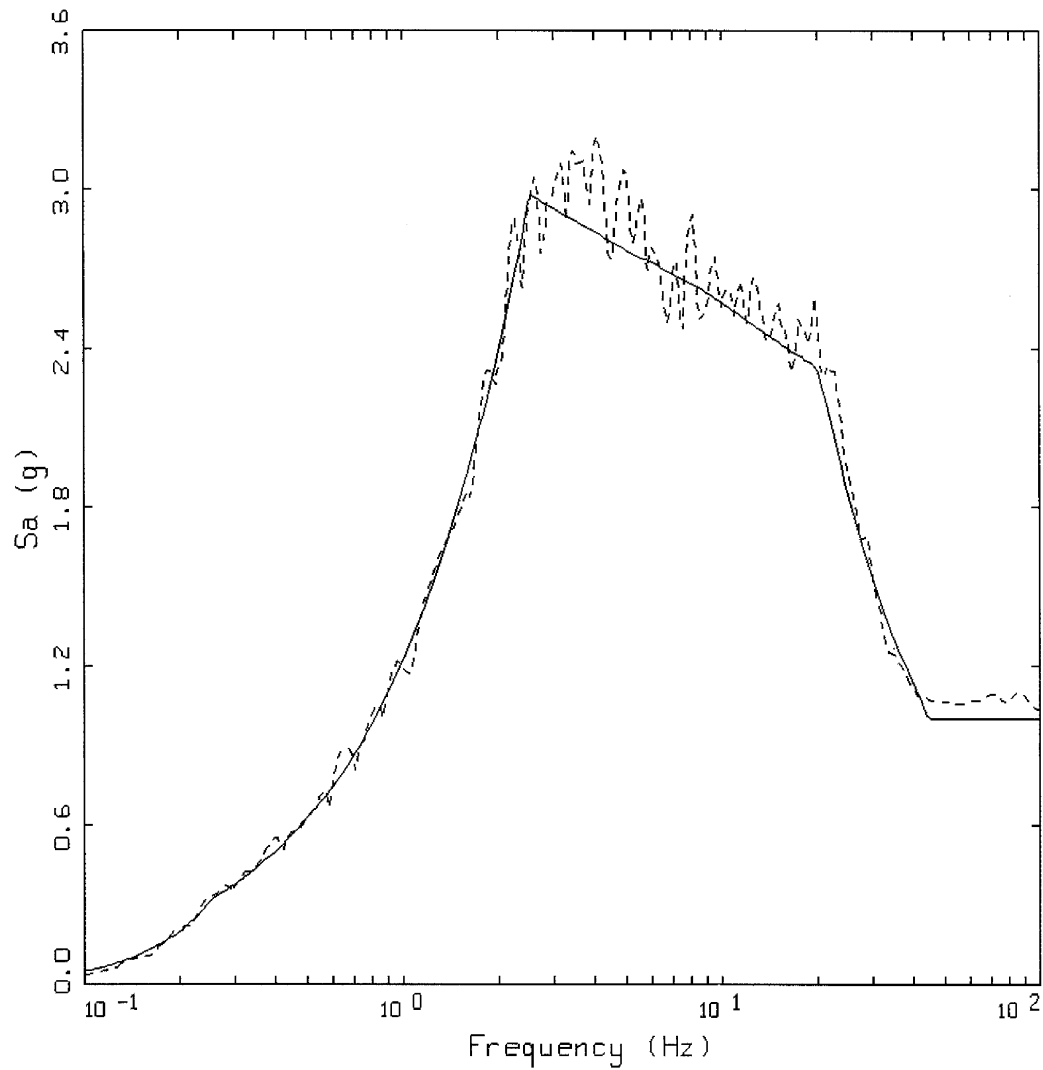


Figure A.3.9.4-11
Vertical Target and 5% Spectral Match (Vertical Up, Hector Mine Earthquake)

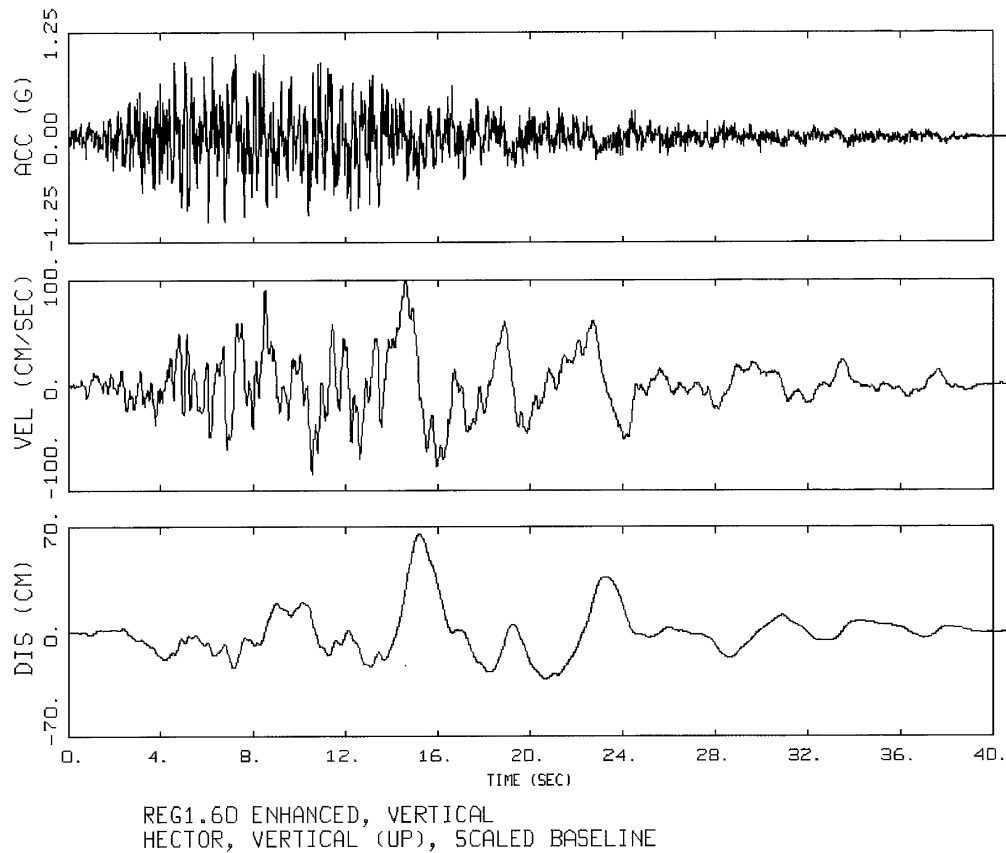


Figure A.3.9.4-12
Baseline Corrected Acceleration, Velocity and Displacement Time Histories
(Vertical Up, Hector Mine Earthquake)

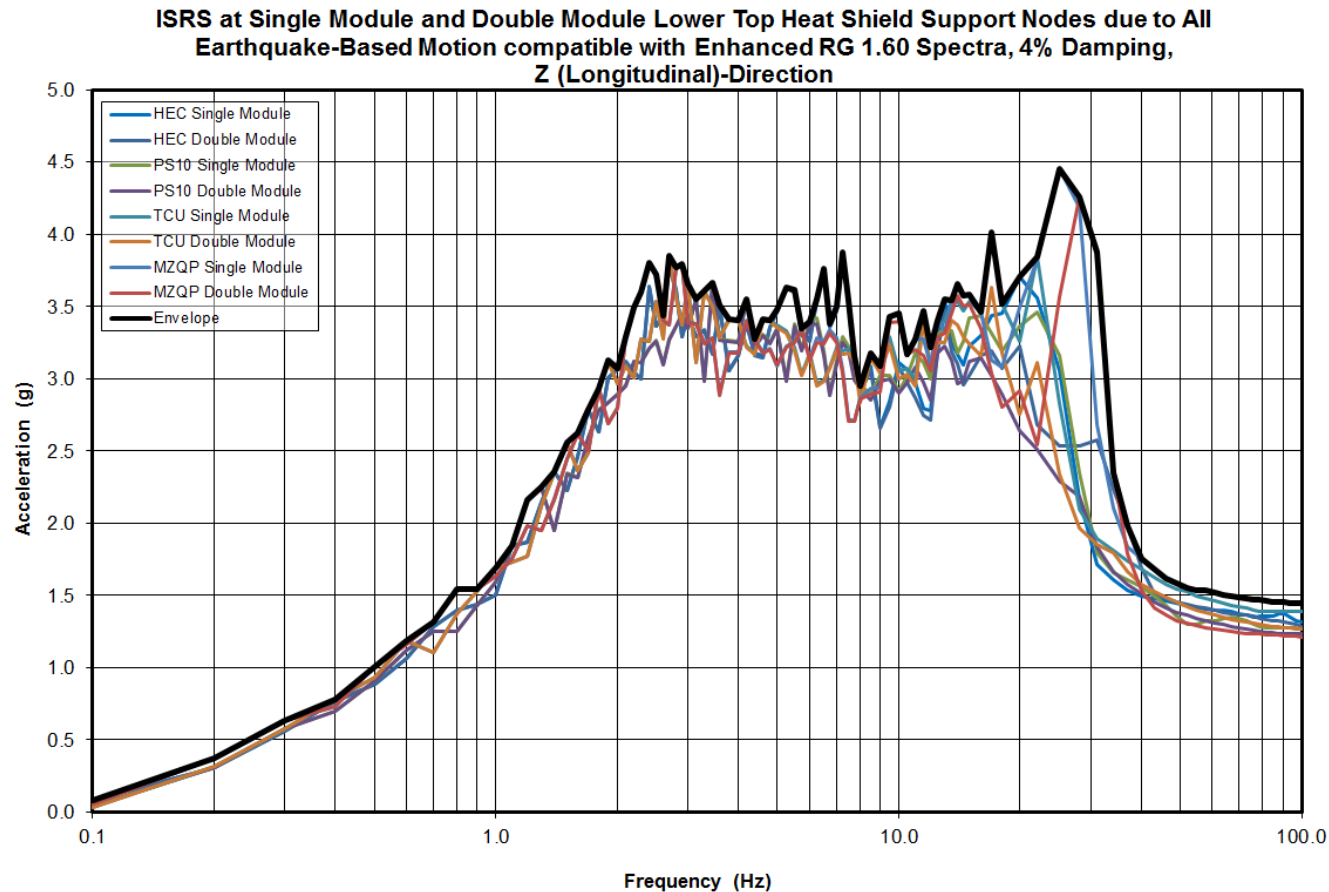


Figure A.3.9.4-13
Lower Top Heat Shield Support Node ISRS due to Envelope of Four Earthquake-Based Motions Compatible with Enhanced RG1.60 Spectra, 4% Damping, X-Direction

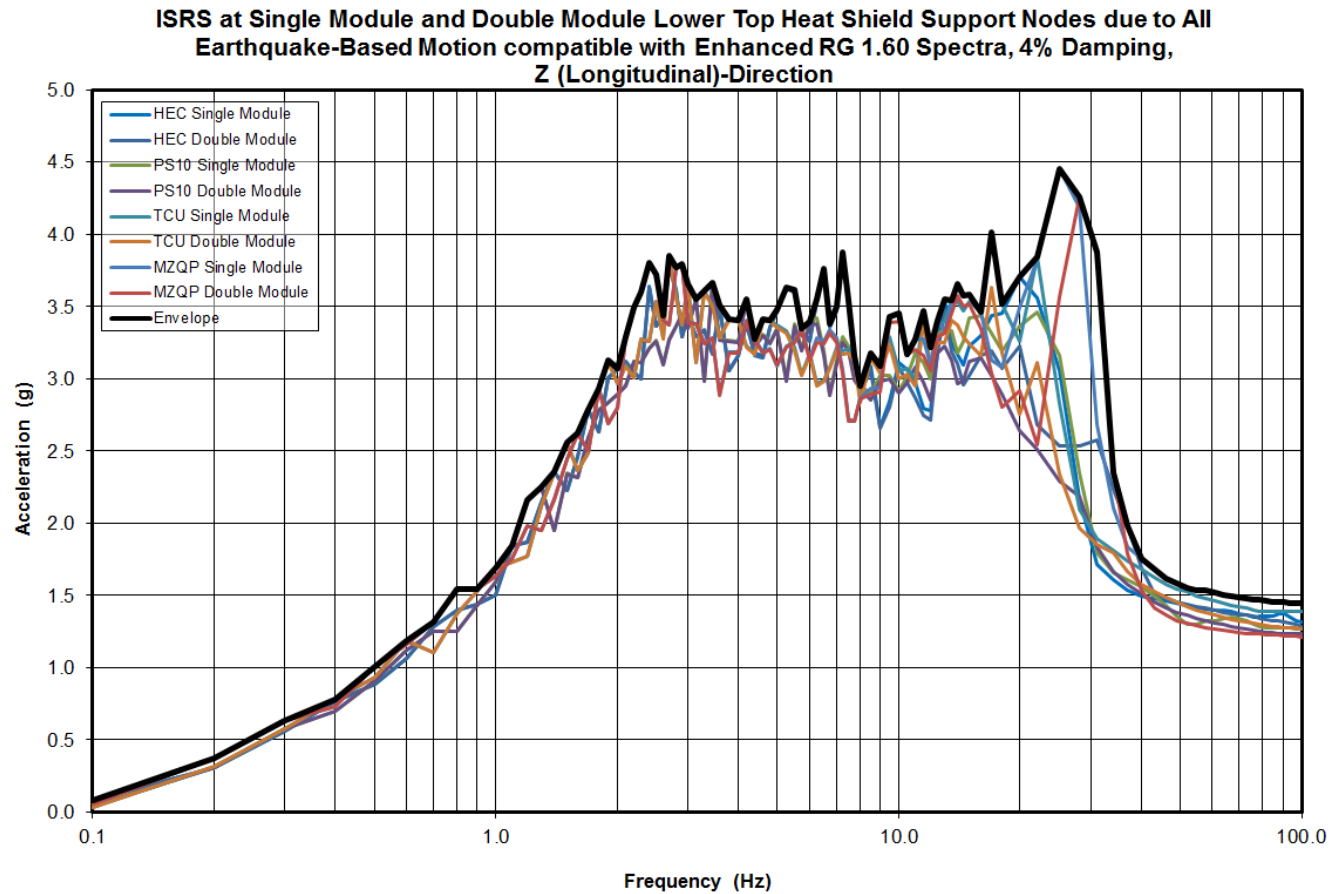


Figure A.3.9.4-14
Lower Top Heat Shield Support Node ISRS due to Envelope of Four Earthquake-Based Motions Compatible with Enhanced RG1.60 Spectra, 4% Damping, Y-Direction

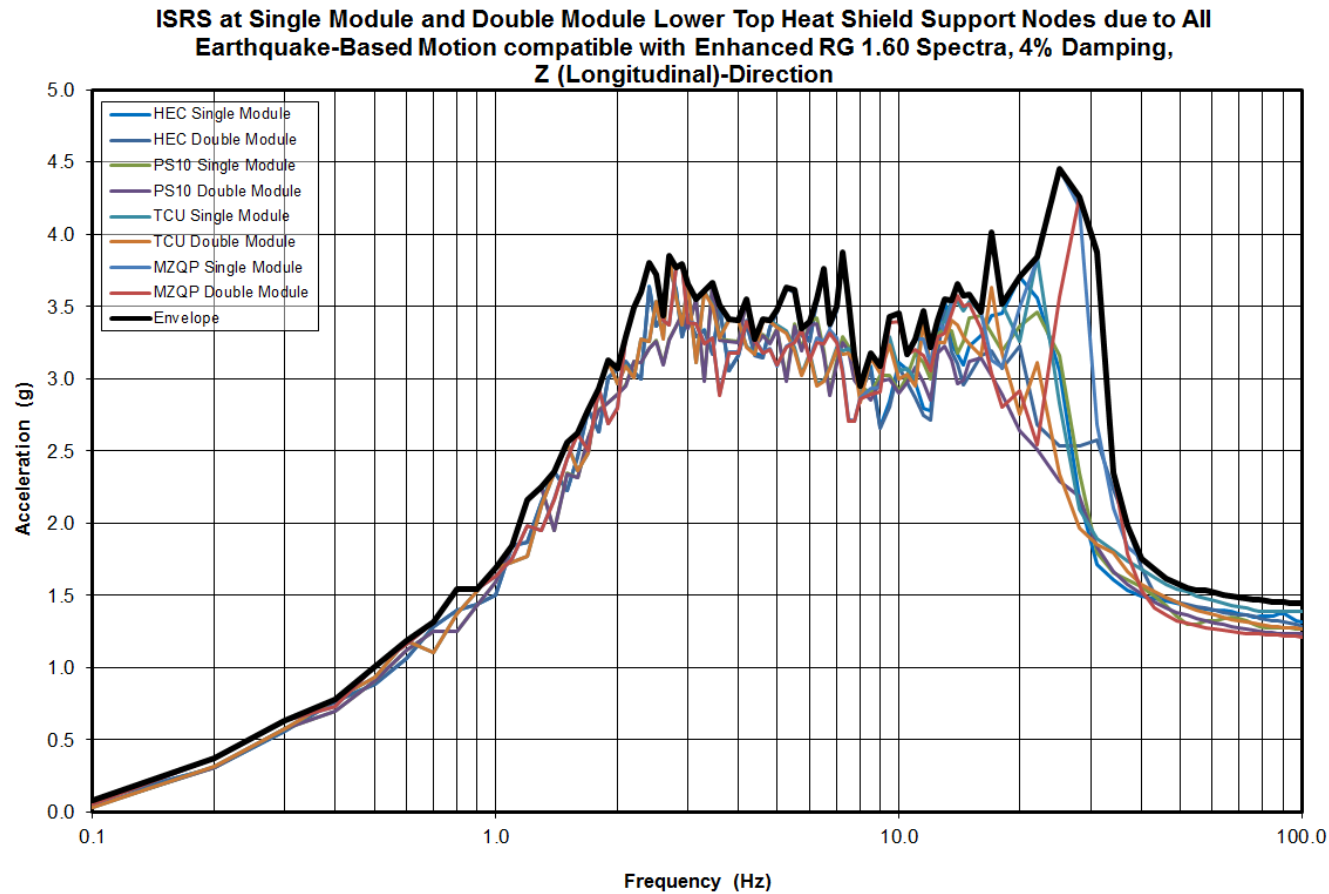


Figure A.3.9.4-15
Lower Top Heat Shield Support Node ISRS due to Envelope of Four Earthquake-Based Motions Compatible with Enhanced RG1.60 Spectra, 4% Damping, Z-Direction

A.3.9.5 NUHOMS® EOS-TC BODY STRUCTURAL ANALYSIS

There is no change to the evaluation of the NUHOMS® EOS-TC Body Structural Analysis documented in Sections 3.9.5 due to the addition of the NUHOMS® MATRIX.

A.3.9.6 NUHOMS® EOS FUEL CLADDING EVALUATION

There is no change to the evaluation of the NUHOMS® EOS fuel Cladding evaluation documented in Sections 3.9.6 due to the addition of the NUHOMS® MATRIX.

APPENDIX A.3.9.7 NUHOMS® MATRIX STABILITY ANALYSIS

Table of Contents

A.3.9.7	NUHOMS® MATRIX STABILITY ANALYSIS.....	A.3.9.7-1
A.3.9.7.1	General Description	A.3.9.7-1
A.3.9.7.2	HSM-MX Stability Analyses	A.3.9.7-4
A.3.9.7.3	EOS Transfer Cask Missile Stability and Stress Evaluation.....	A.3.9.7-14
A.3.9.7.4	References	A.3.9.7-15

List of Tables

Table A.3.9.7-1	Sizes and Weight for Various HSM-MX Models.....	A.3.9.7-16
Table A.3.9.7-2	Missile Load Data for HSM-MX Stability Analysis	A.3.9.7-16
Table A.3.9.7-3	Design Pressures for Tornado Wind Loading of HSM-MX.....	A.3.9.7-17
Table A.3.9.7-4	Summary of HSM-MX Sliding and Stability Results	A.3.9.7-17
Table A.3.9.7-5	Static analysis, Overturning and Sliding of the HSM-MX.....	A.3.9.7-18
Table A.3.9.7-6	Summary of Displacement of HSM-MX relative to the ISFSI pad for nominal concrete density (150 pcf).....	A.3.9.7-19

List of Figures

Figure A.3.9.7-1	HSM-MX Dimensions for Stability Analysis (Static)	A.3.9.7-20
Figure A.3.9.7-2	Not Used	A.3.9.7-21
Figure A.3.9.7-3	Not Used	A.3.9.7-22
Figure A.3.9.7-4	HSM-MX Single Array Design with Five DSCs.....	A.3.9.7-23
Figure A.3.9.7-5	Seismic Stability of DSC on HSM-MX.....	A.3.9.7-24
Figure A.3.9.7-6	Not Used	A.3.9.7-25
Figure A.3.9.7-7	HSM-MX Maximum X-Direction Sliding TAB, $\mu=0.4$	A.3.9.7-26
Figure A.3.9.7-8	HSM-MX Maximum Z-Direction Sliding MIAN, $\mu=0.4$	A.3.9.7-27
Figure A.3.9.7-9	HSM-MX Maximum Rocking PS10, $\mu=0.8$	A.3.9.7-28
Figure A.3.9.7-10	DSC Sliding on Supports during Max. HSM-MX Z-direction Sliding Case: MIAN, $\mu=0.4$	A.3.9.7-29
Figure A.3.9.7-11	DSC Load on Supports during Max. HSM-MX Z-Direction Rocking Case: PS10, $\mu=0.8$	A.3.9.7-30
Figure A.3.9.7-12	DSC Load on Door Opening During Max. HSM-MX Z-Direction Rocking Case: PS10, $\mu=0.8$	A.3.9.7-31
Figure A.3.9.7-13	Horizontal Time History Set 1, HEC – Global X Direction	A.3.9.7-32
Figure A.3.9.7-14	Vertical Time History Set 1, HEC – Global Y Direction	A.3.9.7-33
Figure A.3.9.7-15	Horizontal Time History Set 1, HEC – Global Z Direction	A.3.9.7-34

A.3.9.7 NUHOMS® MATRIX STABILITY ANALYSIS

A.3.9.7.1 General Description

The system consists of the dual-purpose (transportation/storage) EOS-37PTH and EOS-89BTH DSCs, the HSM-MX and the onsite transfer cask (EOS-TC) with associated ancillary equipment. Each NUHOMS® MATRIX (HSM-MX) is designed to store DSCs containing up to either 37 pressurized water reactor (PWR) or 89 boiling water reactor (BWR) spent fuel assemblies (SFAs).

The HSM-MX is a staggered, two-tiered compartment, high density, high-heat rejection, storage overpack that provides a self-contained modular structure for storage of DSCs. The HSM-MX is constructed from reinforced concrete and structural steel. The thick concrete roof and walls of the HSM-MX provide substantial neutron and gamma shielding. The monolithic structure increases resistance to earthquakes and offers significant self-shielding. The NUHOMS® MATRIX retractable roller tray (MX-RRT) delivers the DSC from the transfer cask to the HSM-MX and places it on the DSC supports.

The HSM-MX storage modules can be arranged in both single row or back-to-back row arrays. The HSM-MX assembly considered for the stability evaluation is in a single row array, having three lower compartments and two upper compartments.

A.3.9.7.1.1 HSM-MX Stability Evaluation

The sliding and overturning stability analyses due to design basis wind, flood, and massive missile impact loads are performed using hand calculations. A non-linear dynamic seismic stability analysis is performed using LS-DYNA [A.3.9.7-7].

A.3.9.7.1.2 Material Properties

The HSM-MX assembly is constructed of reinforced concrete and steel. The analyses consider rigid body motions. Therefore, the mechanical properties of the materials are not used as design inputs in the evaluations. The non-linear dynamic evaluation performed using LS-DYNA for the seismic loads, consists of simplified models of the HSM-MX and DSCs representative of their global masses and inertia properties.

A.3.9.7.1.3 Mass Properties

The mass properties of the HSM-MX are listed in Table A.3.9.7-1. Bounding values of concrete density (140 pcf) are considered for static analyses. Nominal concrete density of 150 pcf is considered for the non-linear dynamic seismic evaluation.

A.3.9.7.1.4 Friction Coefficients

The static analyses are performed using a concrete-to-concrete friction coefficient of 0.6. The non-linear dynamic analysis for the seismic loads are performed for a range of friction coefficients for concrete against concrete, varying from 0.8 as the upper bound, 0.6 as the nominal coefficient of friction for concrete poured directly on the independent spent fuel storage installation (ISFSI) pad and 0.4 as the lower bound.

A.3.9.7.1.5 Methodology

The stability of the HSM-MX unit is evaluated for four load cases that may cause overturning and sliding of a freestanding module. These four load cases are:

- Tornado-generated wind loads
- Massive missile impact loads
- Flood loads
- Seismic loads

A.3.9.7.1.6 Assumptions

1. The analyses assume that the dynamic coefficient of friction is equal to the static coefficient. This assumption maximizes the rocking uplift displacements of the HSM-MX (particularly for the high friction coefficient analysis cases).
2. For the non-linear dynamic seismic analysis, coefficients of friction between the HSM-MX and the concrete ISFSI pad are varied between a lower limit of 0.4 and an upper limit of 0.8, with a single intermediate value of 0.6. The coefficients of friction for all other contact surfaces are taken as 0.25.
3. The differential pressure load caused by the tornado pressure drop does not affect the overall stability of the HSM-MX and is ignored. The structure is vented, and so any differential pressure is negligible, as the internal and external pressures equilibrate.
4. This stability evaluation is applicable to both single and double array HSM-MX design.
5. For the non-linear dynamic time history analyses, impact damping coefficients are included in all contact definitions (concrete-to-concrete and steel-to-steel) to obtain a coefficient of restitution (COR) of at least 0.8.

A.3.9.7.1.7 Loads and Boundary Conditions

A.3.9.7.1.7.1 Earthquake Input

The earthquake input motions are in the form of acceleration time histories whose response spectra match the Regulatory Guide 1.60 [A.3.9.7-8] response spectra for 5% damping anchored at 0.85g zero period acceleration (ZPA) in both horizontal directions and 0.80g in the vertical direction and enhanced for frequencies above 9 Hz.

The LS-DYNA [A.3.9.7-7] non-linear dynamic analyses are performed using seven sets of earthquake acceleration time histories. Each set consists of three orthogonal components (2 horizontal and 1 vertical), developed to match the Regulatory Guide 1.60 [A.3.9.7-8] response spectra (enhanced for frequencies above 9 Hz) and have a total approximate duration of 40 seconds. The starting seed for each set consists of actual strong motion recordings whose Fourier spectra are altered to match the target Regulatory Guide 1.60 [A.3.9.7-8] spectra (enhanced for frequencies above 9 Hz) but retains the phase spectra of the actual strong motion record. The horizontal time histories are scaled to 0.85g and the vertical time histories are scaled to 0.80g. The description of each set is as follow:

1. Time History Set number 1 (HEC) is developed based on the Magnitude 7.1 Hector Mine, 1999 earthquake (digitized at 0.01 seconds).
2. Time History Set number 2 (LCN) is based on the Magnitude 7.3 Landers/Lucern earthquake of 1992 (digitized at 0.005 seconds).
3. Time History Set number 3 (PS10) is based on the Magnitude 7.9 Denali earthquake site PS-10 of 2002 (digitized at 0.005 seconds).
4. Time History Set number 4 (TAB) is based on the Magnitude 7.4 Tabas earthquake of 1978 (digitized at 0.02 seconds).
5. Time History Set number 5 (TCU) is based on the Magnitude 7.6 Taiwan, 1999 earthquake (digitized at 0.005 seconds).
6. Time History Set number 6 (SHIF) is based on the Magnitude 7.9 Wenchuan China, 2008 earthquake, Shifangbajiao site (digitized at 0.005 seconds).
7. Time History Set number 7 (MIAN) is based on the Magnitude 7.9 Wenchuan China, 2008 earthquake, Mianzhuqingping site (digitized at 0.005 seconds).

Each component in each of the seven time history sets meets the spectral matching requirements of NUREG/CR-6728 [A.3.9.7-5].

A.3.9.7.1.7.2 Wind and Tornado Input

The HSM-MX is evaluated for overturning and sliding due to the design basis tornado (DBT) specified in Appendix A.2. The DBT is based on the NRC Regulatory Guide 1.76 [0] Region I Intensities. The maximum wind speed is 360 mph. The tornado loads are generated for three separate loading phenomena, as follows, which are combined in accordance with Section 3.3.2 of NUREG-0800 [A.3.9.7-1] (i.e. tornado wind load is concurrent with (additive to) tornado missile loads).

1. Pressure or suction forces created by drag as air impinges and flows past the HSM-MX with a maximum tornado wind speed of 360 mph.
2. Suction forces due to a tornado generated pressure drop or differential pressure load of 3 psi.
3. Impact forces created by tornado-generated missiles impinging on the HSM-MX.

Per NUREG-0800, the total tornado load on a structure is combined as follows:

$$W_t = W_p$$

$$W_t = W_w + 0.5W_p + W_m$$

Where,

- W_t = Total tornado load
- W_w = Load from tornado wind effect
- W_p = Load from tornado atmospheric pressure change effect
- W_m = Load from tornado missile impact effect

Note that W_p is not applicable to the stability analysis as discussed in Section A.3.9.7.1.6. Thus, the load combination for tornado loading for this analysis is simplified to:

$$W_t = W_w + W_m$$

In addition, a 1.1 factor is added to Dead weight + Tornado load. (Table 3-3 of NUREG-1536 [A.3.9.7-3])

The envelope of a range of missiles from Chapter 2 is used for the missile impact load.

As shown in Table A.3.9.7-2, the automobile impact on to the HSM-MX has the maximum momentum and is considered as bounding evaluation.

A.3.9.7.1.7.3 Flood Input

The HSM-MX is evaluated for a flood height of 50 feet with a water velocity of 15 fps.

In addition, a 1.1 factor is added to Dead weight + Flood load (Table 3-3 of NUREG-1536 [A.3.9.7-3]).

A.3.9.7.2 HSM-MX Stability Analyses

The load categories associated with the HSM-MX stability analysis are described in the previous section. The analysis steps and results for each load category are presented in this section.

A.3.9.7.2.1 Design Basis Tornado Wind and Missile Loads

The HSM-MX is evaluated for forces created by drag as air impinges and flows past the HSM-MX with a maximum tornado wind speed of 360 mph.

For sliding and overturning analysis, it is assumed that the module is subjected to the load due to 238 psf windward pressure load acting on the front wall. The leeward side of the same module is subjected to a wind suction load of 167 psf. A suction of 355 psf is applied to the roof. These loads are shown in Table A.3.9.7-3.

In addition, missiles loads are combined with the tornado wind load per NUREG-800 [A.3.9.7-1] and NUREG-1536 [A.3.9.7-3].

Static Overturning Analysis due to Tornado Wind

The empty HSM-MX will rotate about B, shown in Figure A.3.9.7-1.

In the overturning analysis of the HSM-MX, the effects of tornado wind forces are first determined. An overturning moment is then calculated and is compared with a stabilizing moment. The safety factor against overturning computed for the HSM-MX due to tornado wind is 3.28, which includes a factor of 1.1

Dynamic Overturning Analysis of Tornado Wind Concurrent with Massive Missile Impact Loading

A dynamic analysis based on the conservation of energy is conducted for the combined effects of wind and concurrent massive missile impact loading. The effects of the concurrent massive missile impact loads are used in determining the initial angular momentum from the conservation of angular momentum equation using the wind loads from the previous section. Then the angle of rotation is determined from the conservation of energy of the concurrent loading.

The wind loads are calculated conservatively for HSM-MX single array:

$$\text{Horizontal} \quad F_{hw} = (P_{windward} + P_{leeward})(L_{base})(h_{HSM})$$

$$\text{Vertical:} \quad F_{vw} = (P_{roof})(L_{base})(w_{HSM})$$

The concurrent wind loading is accounted for by reducing the inertia that resists motion in the denominator of the equation.

$$\omega_B = \frac{m_m \cdot d_m \cdot v_i}{m_m \cdot d_m^2 + I_{tot} - \left(\frac{F_{hw}}{g}\right)\left(\frac{h}{2}\right)^2 - \left(\frac{F_{vw}}{g}\right)\left(\frac{w}{2}\right)^2}$$

Where,

- F_{hw} = Horizontal tornado wind load
- F_{vw} = Vertical tornado wind load
- ω_B = Angle of rotation
- m_m = Mass of the missile
- d_m = Distance from missile impact to floor
- v_i = Initial missile velocity
- I_{tot} = Total moment of inertia of HSM-MX
- h = Height of HSM-MX
- w = Width of HSM-MX

The conservation of energy is used for overturning.

Rotational Kinetic Energy = Change in Potential Energy – Work Done by Horizontal Wind force

$$\frac{I_{tot}\omega_B^2}{2} = (W - F_{vw}) \cdot r \cdot [\sin(\beta + \theta) - \sin\beta] - F_{hw} \cdot r \cdot [\cos(\beta + \theta) - \cos\beta]$$

Where,

- θ = Angle of tipping
- β = Angle from the horizontal to center of gravity (CG) of HSM-MX (52.1°)
- r = Diagonal distance from CG to point B
- I_{tot} = Total moment of Inertia of HSM-MX
- W = Weight of the empty HSM-MX

The HSM-MX is stable against overturning as tip-over does not occur until the CG rotates past the edge (point B, Figure A.3.9.7-1) of the HSM-MX to an angle of more than $90^\circ - 52.1^\circ = 37.9^\circ$. The HSM-MX rotates a maximum of 0.000029 degrees, which includes a factor of 1.1 and is less than the 37.9 degrees required to overturn the module.

Time-Dependent Overturning Analysis of Tornado Wind Concurrent with Massive Missile Impact Loading

In addition to the dynamic overturning analysis, a time dependent analysis is used to ensure the absence of any overturning.

An approximate relationship for the deceleration of an automobile impacting a rigid wall is given by:

$$-\ddot{x} = 12.5g \cdot x \text{ Eq. D-1 of [A. 3.9.7-4]}$$

where,

- $-\ddot{x}$ = Deceleration (ft/sec²)
- x = Distance automobile crushes into target (ft)

A force time history is obtained:

$$F = 0.625V_s W_m \sin 20t \quad \text{Eq. D - 6 of [A. 3.9.7 - 4]}$$

The overturning moment is:

$$M_{ot} = F \cdot d_m + \frac{F_{hw}h}{2}$$

Where,

- d_m = Distance from missile impact to floor
- h = Vertical height to the top of HSM-MX and is a function of rotation

The stabilizing moment is:

$$M_{st} = (W_{HSM} - F_{vw}) \cdot r \cos(\beta + \theta)$$

Where,

W_{HSM}	=	Weight of the loaded HSM-MX
r	=	Diagonal distance from CG to point B
θ	=	Angle of rotation

The moment causing acceleration is:

$$M_{acc} = M_{ot} - M_{st}$$

The angular velocity is:

$$\omega_i = \left[\frac{M_{acc,i} + M_{acc,i-1}}{2} \cdot (t_i - t_{i-1}) \right] / I_{tot} + \omega_{i-1}$$

Where,

i	=	Index for current time step
$i-1$	=	Index for previous time step
I_{tot}	=	Total moment of Inertia of HSM-MX

The angle of rotation is:

$$\theta_i = \left[\frac{\omega_i + \omega_{i-1}}{2} \cdot (t_i - t_{i-1}) \right] + \theta_{i-1}$$

The angle of rotation is zero as the overturning moment due to missile impact and wind loading is less than the resisting moment.

Sliding Analysis for Tornado Wind Concurrent with Massive Missile Impact loading

The combined wind + missile impact case is considered for HSM-MX sliding analysis based on the conservation of energy.

First, the conservation of momentum is used for the sliding analysis.

$$V = \frac{m \cdot v_i}{M + m - F_{hw}/386.4}$$

Where,

V	=	Initial linear velocity of module after impact
v_i	=	Initial velocity of missile
m	=	Mass of the missile
M	=	Mass of the HSM-MX

Then using the conservation of energy:

$$\text{Friction Energy} = \text{Initial Kinetic Energy of System} + \text{Work done by Wind}$$

$$\mu \cdot (gM - F_{vw})d = \frac{(M + m) \cdot V^2}{2} + F_{hw}d$$

Where,

- μ = 0.6 coefficient of friction for concrete-to-concrete surfaces
- F_{vw} = Uplift force generated by DBT wind pressure on the roof
- d = Sliding distance of HSM-MX
- F_{hw} = Sliding force generated by DBT wind pressure

The sliding distance of the HSM-MX module is calculated to be 0.15 inches, which includes a factor of 1.1.

Time-Dependent Sliding Analysis for Tornado Wind Concurrent with Massive Impact Loading

In addition to the dynamic sliding analysis, a time dependent analysis is used to provide a bounding sliding displacement.

The total force causing sliding is:

$$F_{slide} = F + F_{hw}$$

The resisting force from friction is:

$$F_{resis} = \mu(W - F_{vw})$$

Therefore the force causing acceleration is:

$$F_{acc} = F_{slide} - F_{resis}$$

The velocity is:

$$v_i = \left[\frac{F_{acc,i} + F_{acc,i-1}}{2} \cdot (t_i - t_{i-1}) \right] / m_{tot} + v_{i-1}$$

Where,

- i = Index for current time step
- $i-1$ = Index for previous time step
- m_{tot} = Total mass of empty HSM-MX

The sliding displacement is:

$$x_i = \left[\frac{v_i + v_{i-1}}{2} \cdot (t_i - t_{i-1}) \right] + x_{i-1}$$

The sliding displacement is zero as the sliding force due to missile impact and wind loading is less than the resisting force.

A.3.9.7.2.2 Flood Loads

The HSM-MX is designed for a flood height of 50 feet and water velocity of 15 fps. The module is evaluated for the effects of a water current of 15 fps impinging on the side of a submerged HSM-MX. Under 50 feet of water, the inside of the module is rapidly filled with water. Therefore, the HSM-MX components are not evaluated for the 50 feet static head of water.

Calculation of the drag pressure due to design flood is shown in Appendix A.3.9.4.9.3.

Overturning Analysis

The factor of safety against overturning of an empty HSM-MX, for the postulated flooding conditions, is calculated by summing moments about the bottom outside corner of a single array HSM-MX. The factor of safety against overturning of the HSM-MX due to the postulated design basis flood water velocity is 1.98 inches, which includes a factor of 1.1.

Sliding Analysis

The factor of safety against sliding of a freestanding single array HSM-MX due to the maximum postulated flood water velocity of 15 fps is calculated using methods similar to those described above. The effective weight of the HSM-MX acting vertically downward, less the effects of buoyancy acting vertically upward is calculated. The factor of safety against sliding for a single array HSM-MX due to the postulated design basis flood water velocity is 1.42 inches, which includes a factor of 1.1.

A.3.9.7.2.3 Seismic Loads

The static sliding and overturning analysis for the seismic loads are performed to determine the maximum seismic accelerations before HSM-MX starts sliding or overturning. Non-linear dynamic analysis is performed using LS-DYNA for the earthquake inputs discussed in A.3.9.7.1.7.1 to determine the maximum sliding and overturning distances.

A.3.9.7.2.3.1 Low Seismic Load

HSM-MX static overturning analysis

The stabilizing moment due to the components dead weight and the overturning moment due to the seismic forces are calculated and compared. The 1.1 coefficient of the load combination (Table 3-3 of NUREG-1536 [A.3.9.7-3]) is conservatively applied to the overturning moment only. Both the maximum HSM-MX concrete density (160 pcf) with maximum DSC weight (to maximize the overturning moment) and minimum HSM-MX concrete density (140 pcf) with minimum DSC weight (to minimize the stabilizing moment) are considered. The overturning analysis is done considering the smallest distance from the HSM-MX center of gravity to HSM-MX corner point B (Figure A.3.9.7-1).

Table A.3.9.7-5 shows the results. The safety factor $M_{st}/1.1M_{ot}$ is less than 1, meaning the HSM-MX can have some lifting under the seismic loads. The non-linear dynamic analyses (Section A.3.9.7.2.3.2) estimate the amount of lifting for high seismic loads.

The maximum acceptable accelerations before any lifting occurs are $a_v = 0.40g$ and $a_h = 0.60g$ (assuming $a_v = \frac{2}{3}a_h$)

HSM-MX static sliding analysis

The resisting friction force and horizontal seismic force are calculated and compared. The 1.1 coefficient of the load combination (Table 3-3 of NUREG-1536 [A.3.9.7-3]) is conservatively applied to the horizontal seismic force only.

Resisting friction force: $F_{fr} = \mu W(1 - 0.4a_v)$ μ : Coefficient of friction

Horizontal seismic force: $F_{hs} = a_h W$

Safety factor: $SF = F_{fr}/1.1F_{hs} = \mu(1 - 0.4a_v)/(1.1a_h)$

For static sliding analysis of the HSM-MX, the safety factor is independent of the weight considered. It only depends on the coefficient of friction and accelerations.

Table A.3.9.7-5 shows the results for a nominal coefficient of friction of 0.6 and gives a safety factor of 0.44. The HSM-MX will slide under 0.85g horizontal and 0.80g vertical loads. The non-linear dynamic analyses (Section A.3.9.7.2.3.2) estimate the amount of sliding for high seismic loads.

The maximum acceptable accelerations before any sliding occurs are $a_v = 0.32g$ and $a_h = 0.48g$ (assuming $a_v = \frac{2}{3}a_h$)

Seismic Stability of the DSC on DSC Supports inside the HSM-MX

This evaluation is performed for the DSC resting on the supports inside the HSM-MX, which includes the stability of the DSC against lifting off from one of the support during a seismic event and potential sliding off of the DSC from the supports. The horizontal equivalent static acceleration of 0.85g is applied laterally to the center of gravity of the DSC. The point of rigid body rotation of the DSC is assumed to be the center of the support, point of contact with the DSC (as shown in Figure A.3.9.7-5). The applied moment acting on the DSC is calculated by summing the overturning moments.

The stabilizing moment, acting to oppose the overturning moment, is calculated by subtracting the effects of the upward vertical seismic acceleration of 0.80g from the total weight of the DSC and summing moments at the point of rigid body rotation.

Figure A.3.9.7-5 shows a DSC on its front and rear DSC supports and define the geometric parameters and loads used below.

Stabilizing moment:

$$M_{st} = (W - 1.1F_v)X \quad \text{with} \quad F_v = 0.4Wa_v \quad X = R \sin \theta$$

Overturning moment:

$$M_{ot} = 1.1F_hY \quad \text{with} \quad F_h = Wa_h \quad Y = R \cos \theta$$

Safety coefficient:

$$SF = \frac{M_{st}}{M_{ot}} = \frac{1 - 0.44a_v}{1.1a_h} \tan \theta$$

For DSC overturning analysis, the safety factor is independent of the DSC weight or radius considered. It only depends on the support angle and the accelerations. The minimum support angle θ to avoid DSC overturning (Figure A.3.9.7-5) is 55.3° .

Assuming $a_v = \frac{2}{3} a_h$, the maximum seismic accelerations are 0.54g horizontal and 0.36g vertical before DSC overturning occurs

A.3.9.7.2.3.2 High Seismic Load

Non-Linear Dynamic Time-History Analyses of HSM-MX for High Seismic Loads

LS-DYNA Finite Element Model HSM-MX

A finite element model (FEM) of the HSM-MX monolithic expansion single array design loaded with five DSCs was created for use with LS-DYNA [A.3.9.7-7]. The HSM-MX unit and DSC are constructed with solid 4-node tetrahedral elements for meshing simplicity, whereas the ISFSI pad includes 8-node solids elements. All components are modeled with rigid materials for the stability analysis. The FEM includes the DSC axial retainers modeled with 0.5 inch gap to the DSC, the front and rear DSC supports with stop plates and five front doors and top vent covers.

The model does not include the metallic components (heat shields, etc.) which are not structurally important for the stability analysis. Their weight is accounted for in the total weight of the HSM-MX.

The HSM-MX rests on top of the ISFSI concrete pad and is free to slide or rock when subjected to the forces resulting from the prescribed pad seismic accelerations. In the FEM, contacts are defined between the HSM-MX and the ISFSI pad as well as between the DSCs with their front and rear DSC supports and parts of the HSM-MX concrete that could be in contact with the DSCs if they lift from their supports. Contact definitions are included between all interfacing parts using contacts algorithm in LS-DYNA.

Contacts are defined for the following interfaces:

- HSM-MX to basemat, no initial gap

- DSC to for supports, no initial gap
- DSC to rear stop plate, no initial gap
- DSC to HSM-MX front circular opening, initial 1.5” gap between DSC Ø75.5” and the door opening Ø78.5”
- DSC to front axial retainer, initial gap of 0.5”

Coefficient of Restitution

The coefficient of restitution is defined as the ratio of the velocity of a body immediately after impact to its velocity immediately prior to impact. A coefficient of restitution equal to 0 means a perfectly plastic impact in which the impacting body “sticks” to the impacted body. A coefficient of restitution equal to 1 means a perfectly elastic impact in which the impacting body bounces off the impacted body with no energy loss. For the case of concrete impacting against concrete, a reasonable coefficient of restitution is in the order of 0.1 since a concrete body does not “bounce” upon impacting on a concrete surface. For the LS-DYNA analyses, a coefficient of restitution of at least 0.8 is used as a conservative value. The coefficient of restitution is inputted into LS-DYNA analyses as the parameter viscous damping coefficient ((VDC) in percent of critical) of the surface-to-surface contact.

Non-Linear Dynamic Analyses

The seismic analyses inputs as described in Section A.3.9.7.1.7.1 consist of three components of acceleration in the form of earthquake time histories applied to the ISFSI pad. Thus, all nodal points of the pad move as prescribed by these input motions. Examples of the input motion displacement, velocity and acceleration histories used in LS-DYNA analysis are shown in Figure A.3.9.7-13, Figure A.3.9.7-14 and Figure A.3.9.7-15 in the global X, Y, and Z directions, respectively, for the motion derived from the Hector Mine (HEC) earthquake. The three components of the acceleration time histories are applied simultaneously in each of the three orthogonal directions. Each of the seven time history sets are analyzed with three different coefficients of friction (0.4, 0.6, and 0.8) for a total of 21 computer runs.

In order to obtain the sliding displacement of the HSM-MX relative to the pad, the change in X-lengths and change in Z-lengths (Figure A.3.9.7-4) between the four HSM-MX corner nodes and one ISFSI pad node are plotted over time.

Two uplift values are reported, one each for rotation about the global X and Z axes. For rocking about the X-axis, the change in the vertical (global Y) distance between the +Z and –Z node pairs is plotted and tabulated. For rocking about the Z axis, the change in the vertical distance between the +X and –X node pairs is plotted and tabulated.

The gaps between the DSCs and front axial retainers are verified against the DSC sliding on the support. Also, the loads on the DSC supports are verified against the uplift.

The maximum values over time for sliding and rocking movements from the seven time histories are used to get the “computed” response as the median value plus 1 standard deviation (shown in Table A.3.9.7-6). This methodology is in accordance with NUREG/CR-6865 [A.3.9.7-6]

A.3.9.7.2.4 Results

Table A.3.9.7-4 through Table A.3.9.7-6 show a summary of the results from the analyses performed in Section A.3.9.7.2.

For flood, wind, and missile impact, it is determined that the uplift and sliding values are small for the HSM-MX. Therefore, the DSC remains stable on the front and rear DSC supports inside the HSM-MX.

The maximum seismic acceleration before HSM-MX sliding or overturning occurs are 0.48g horizontal and 0.32g vertical for a coefficient friction of 0.6 between the HSM-MX and the ISFSI pad. The non-linear dynamic analysis shows a maximum resultant sliding of 12.5 inches and a maximum uplift of 0.13 inches for the set of seismic earthquake inputs.

Figure A.3.9.7-7 and Figure A.3.9.7-8 show the maximum sliding results in both horizontal directions, and Figure A.3.9.7-9 shows the maximum rocking for the input earthquake loads. On each sliding plots (Figure A.3.9.7-7 and Figure A.3.9.7-8), the four curves represent the displacement of each bottom corner of the HSM-MX relative to the ISFSI pad. For the rocking plot (Figure A.3.9.7-9), the two curves represents the relative vertical displacement between 2 HSM-MX bottom corners.

Figure A.3.9.7-10 shows the sliding of five DSCs on the front and rear DSC supports. Figure A.3.9.7-11 shows total load on four support for all five DSCs. The sliding fluctuates in the range of 0 to 0.5 inches, which is the initial gap in front axial retainer.

Figure A.3.9.7-12 shows the load between the DSC shell and circular opening on the front door. There is no contact between the DSC and the HSM-MX. Therefore, DSCs do not lift from their supports during a seismic event.

A.3.9.7.3 EOS Transfer Cask Missile Stability and Stress Evaluation

There is no change to the EOS transfer cask missile stability and stress evaluation documented in Sections 3.9.7.2 due to the addition of the HSM-MX.

A.3.9.7.4 References

- A.3.9.7-1 NUREG-0800, Standard Review Plan, “Missiles Generated by Natural Phenomena,” Revision 2, U.S. Nuclear Regulatory Commission, July 1981.
- A.3.9.7-2 American Society of Civil Engineers, ASCE 7-10, “Minimum Design Loads for Buildings and Other Structures.”
- A.3.9.7-3 NUREG-1536 Revision 1, “Standard Review Plan for Spent Fuel Dry Storage Systems at a General License Facility,” July 2010, U.S. Nuclear Regulatory Commission.
- A.3.9.7-4 Bechtel Report BC-TOP-9A Rev. 2, “Topical Report – Design of Structures for Missile Impact,” September 1974.
- A.3.9.7-5 NUREG/CR-6728, “Technical Basis for Revision of Regulatory Guidance on Design Ground Motions: Hazard- and Risk-consistent Ground Motion Spectra Guidelines,” October 2001, Prepared by Risk Engineering, Inc. for U.S. Nuclear Regulatory Commission.
- A.3.9.7-6 NUREG/CR-6865, “Parametric Evaluation of Seismic Behavior of Freestanding Spent Fuel Dry Cask Storage Systems,” February 2005, U.S. Nuclear Regulatory Commission.

U. S. Nuclear Regulatory Commission, Regulatory Guide 1.76, “Design Basis Tornado for Nuclear Power Plants,” Revision 1, March 2007.
- A.3.9.7-7 LS-DYNA Version 7.0.0, Rev. 79055, Livermore Software Technology Corporation (LSTC).
- A.3.9.7-8 NRC Regulatory Guide 1.60, “Design Response Spectra for Seismic Design of Nuclear Power Plants,” Rev. 1, December 1973.
- A.3.9.7-9 U.S. Nuclear Regulatory Commission, Regulatory Guide 1.76, “Design Basis Tornado and Tornado Missiles for Nuclear Power Plants,” Rev. 1, March 2007.

Table A.3.9.7-1
Sizes and Weight for Various HSM-MX Models

HSM-MX Module	Total Length of HSM-MX (in.)	Nominal Weight of Empty HSM-MX (kips)⁽¹⁾
HSM-MX Single Array	277	2.355
HSM-MX Double Array	496	3,945

Notes:

(1) The nominal weights for the HSM-MX are based on concrete density of 150 pcf.

Table A.3.9.7-2
Missile Load Data for HSM-MX Stability Analysis

Missile	Mass (lbs.)	Dimensions	Velocity (fps)	Momentum (lbs-fps)
Utility Wooden Pole	1,124	13.5" Diameter 35' Long	180	202,320
Armor Piercing Artillery Shell	276	8" Diameter	185	51,060
Steel Pipe	750	12" Sch. 40 15' Long	154	115,500
Automobile	4,000	20 ft ² Contact Area	195	780,000

Table A.3.9.7-3
Design Pressures for Tornado Wind Loading of HSM-MX

Wall Orientation ⁽¹⁾	Velocity Pressure (psf)	Ext. Pressure Coefficient ⁽²⁾	Int. Pressure Coefficient ⁽³⁾	Max/Min Design Pressure (psf) ⁽⁴⁾
Front	276.4	0.680	± 0.18	237.7
Left	276.4	-0.595		-214.2
Rear ⁽⁵⁾	276.4	-0.425		-167.2
Right	276.4	-0.595		-214.2
Top	276.4	-1.105		-355.2

Notes:

- (1) Wind direction assumed to be from front. Wind loads from other directions may be found by rotating above table values to desired wind direction.
- (2) These values are calculated using the external pressure coefficients from Figure 27.4-1 of [A.3.9.7-2] times the gust effect factor (0.85) from Section 26.9 of [A.3.9.7-2]
- (3) Internal pressure coefficient taken from Table 26.11-1 of [A.3.9.7-2]
- (4) These values are computed based on Equation 27.4-1 of [A.3.9.7-2]
- (5) The bounding C_p of -0.5 from an L/B ratio of 0-1 is used for wind in all directions from Figure 27.4-1 of [A.3.9.7-2]

Table A.3.9.7-4
Summary of HSM-MX Sliding and Stability Results

Loading	Tornado Wind + Missile ⁽¹⁾		Flood	
Result	Maximum Sliding Distance (in)	Maximum Rocking Uplift (°)	Safety Factor against Sliding	Safety Factor against Tipping
HSM-MX Single Array	0.15	0.000029	1.42	1.98

Notes:

- (1) 1.1 Factor Included.

Table A.3.9.7-5
Static analysis, Overturning and Sliding of the HSM-MX

	Concrete Density [pcf]		140	160
Overturning	Overturning Moment [in.kips]		463,757	523,739
	Stabilizing Moment [in.kips]		344,115	383,056
	Safety Factor ⁽¹⁾		0.67	0.66
	Max accelerations before overturning	$a_v = 2/3 a_h$	0.41	0.40
		a_h	0.61	0.60
Sliding	Horizontal Seismic Force [kips]		2126	2408
	Resisting Friction Force ⁽³⁾ [kips]		1021	1156
	Safety Factor ⁽²⁾		0.44	
	Max accelerations before sliding	$a_v = 2/3 a_h$	0.32	
		a_h	0.48	

Notes:

(1) $SF = M_{st}/1.1M_{ot}$

(2) $SF = F_{fr}/1.1F_{hs}$

(3) Nominal Coefficient of friction 0.6

Table A.3.9.7-6
Summary of Displacement of HSM-MX relative to the ISFSI pad for nominal
concrete density (150 pcf)

Earthquake	Coefficient of Friction	X-Displ. [in] ⁽²⁾	Z-Displ. [in] ⁽²⁾	Resultant [in] ⁽¹⁾	X-Rocking [in]	Z-Rocking [in]
1. HEC	0.4	7.29	3.53	7.61	0.00	0.00
	0.6	2.45	2.08	2.55	0.00	0.02
	0.8	1.59	1.11	1.65	0.01	0.06
2. LCN	0.4	6.79	7.99	9.11	0.00	0.00
	0.6	3.83	5.52	6.65	0.00	0.02
	0.8	2.66	3.12	3.94	0.02	0.13
3. PS10	0.4	9.32	6.76	10.75	0.00	0.00
	0.6	5.13	3.36	6.12	0.00	0.07
	0.8	2.69	1.12	2.91	0.01	0.14
4. TAB	0.4	9.84	7.00	11.51	0.00	0.00
	0.6	5.39	3.78	6.48	0.00	0.02
	0.8	1.98	1.13	2.22	0.01	0.05
5. TCU	0.4	9.14	4.22	9.52	0.00	0.00
	0.6	3.73	1.40	3.77	0.00	0.02
	0.8	1.51	0.51	1.53	0.01	0.07
6. SHIF	0.4	8.49	9.57	12.77	0.00	0.00
	0.6	3.69	7.74	8.57	0.00	0.02
	0.8	2.35	4.63	5.19	0.01	0.10
7. MIAN	0.4	5.13	11.47	11.51	0.00	0.00
	0.6	3.19	7.69	8.11	0.00	0.02
	0.8	1.91	4.54	4.84	0.02	0.11
Maximum	0.4	9.84	11.47	12.77	0.00	0.00
	0.6	5.39	7.74	8.57	0.00	0.07
	0.8	2.69	4.63	5.19	0.02	0.14
Average	0.4	8.00	7.22	10.40	0.00	0.00
	0.6	3.92	4.51	6.04	0.00	0.03
	0.8	2.10	2.31	3.18	0.01	0.09
Median	0.4	8.49	7.00	10.75	0.00	0.00
	0.6	3.73	3.78	6.48	0.00	0.02
	0.8	1.98	1.13	2.91	0.01	0.10
Median + σ	0.4	10.16	9.80	12.50	0.00	0.00
	0.6	4.77	6.33	8.66	0.00	0.04
	0.8	2.46	2.88	4.41	0.01	0.13

- (1) The resultant displacement is the square root of the sum of the squares of the X- and Z-displacements over time. This is not the resultant of the maximum X- and Z-Displacements
- (2) Absolute values are reported = $\max(\text{abs}(u(t)))$

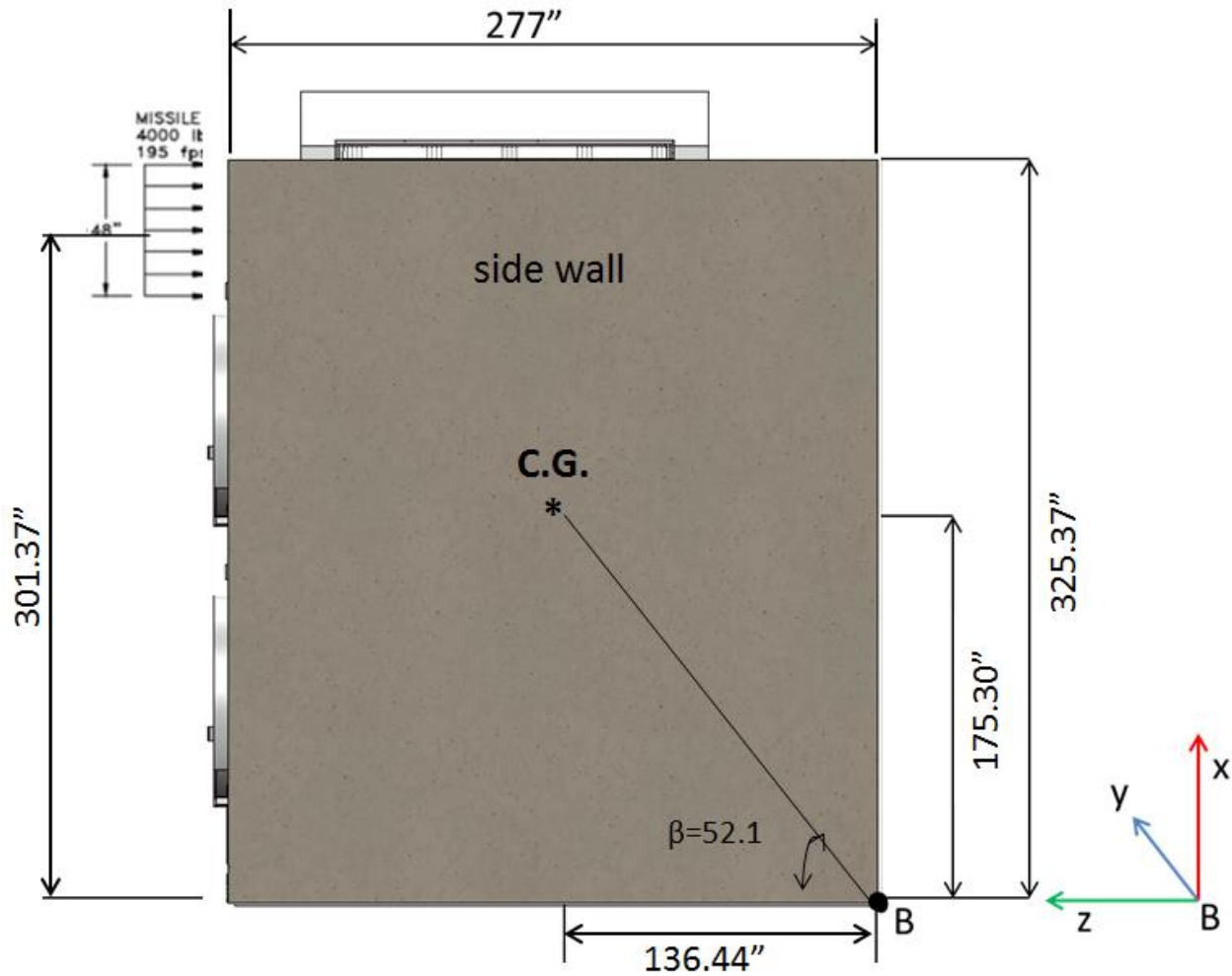


Figure A.3.9.7-1
HSM-MX Dimensions for Stability Analysis (Static)

Figure A.3.9.7-2
Not Used

Figure A.3.9.7-3
Not Used

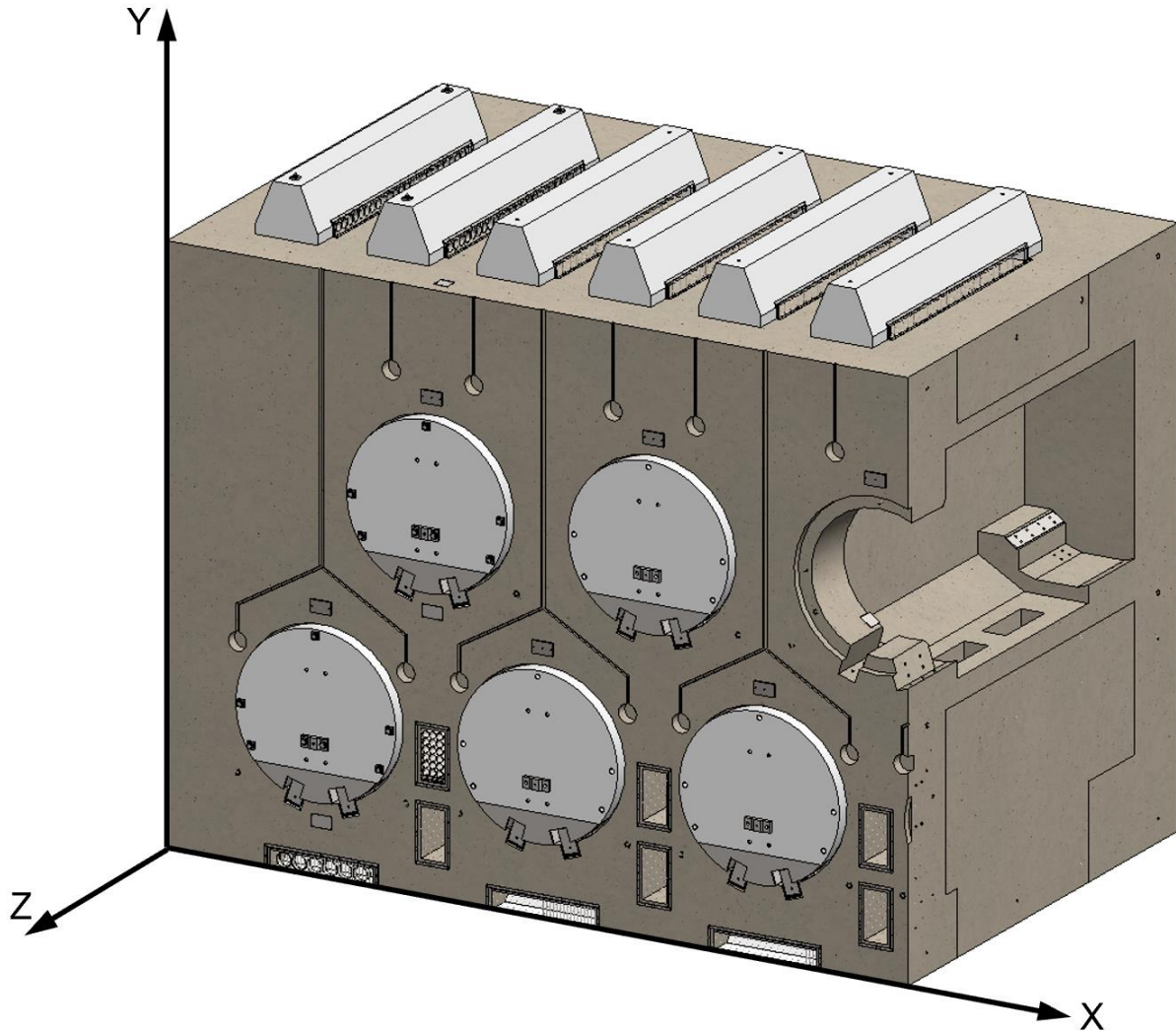


Figure A.3.9.7-4
HSM-MX Single Array Design with Five DSCs

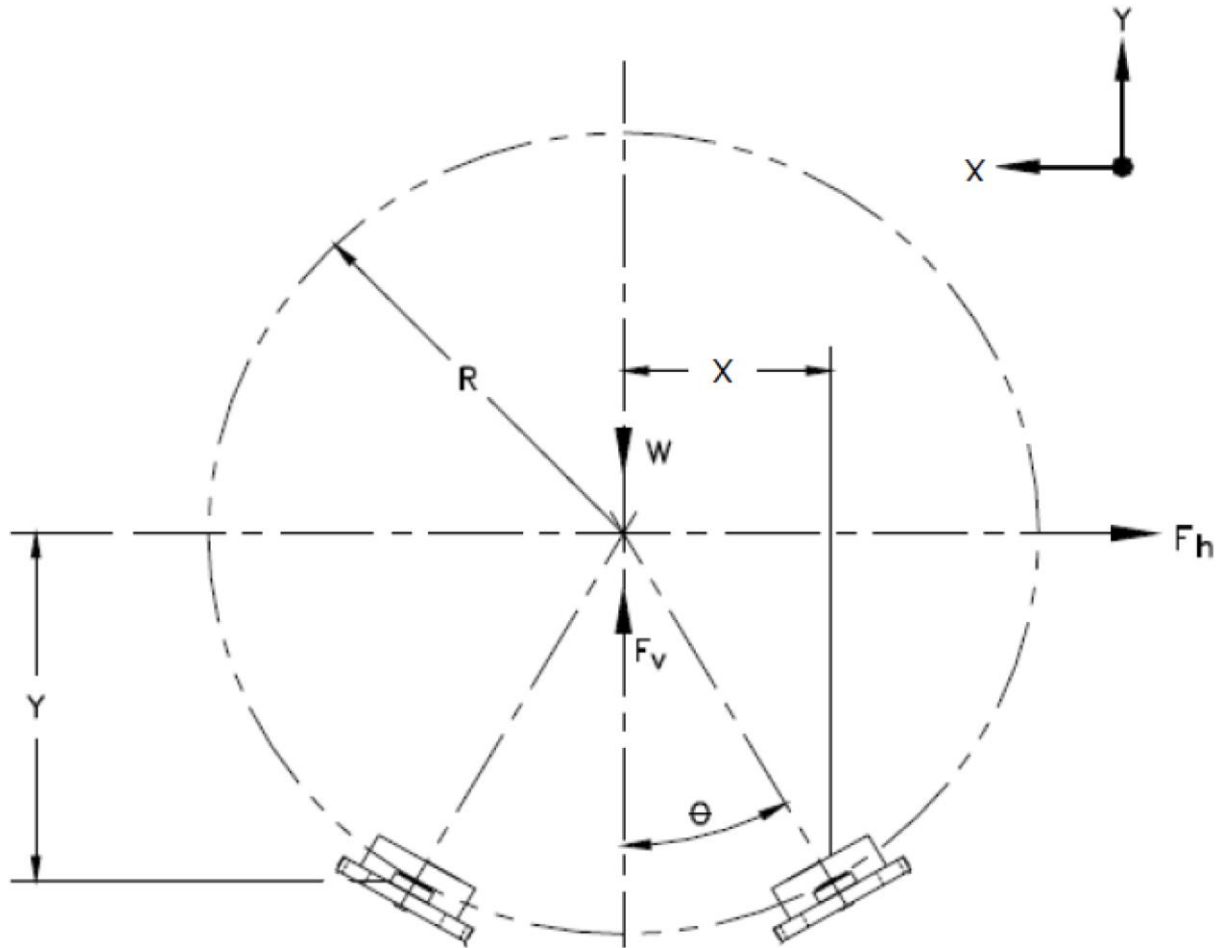


Figure A.3.9.7-5
Seismic Stability of DSC on HSM-MX

Figure A.3.9.7-6
Not Used

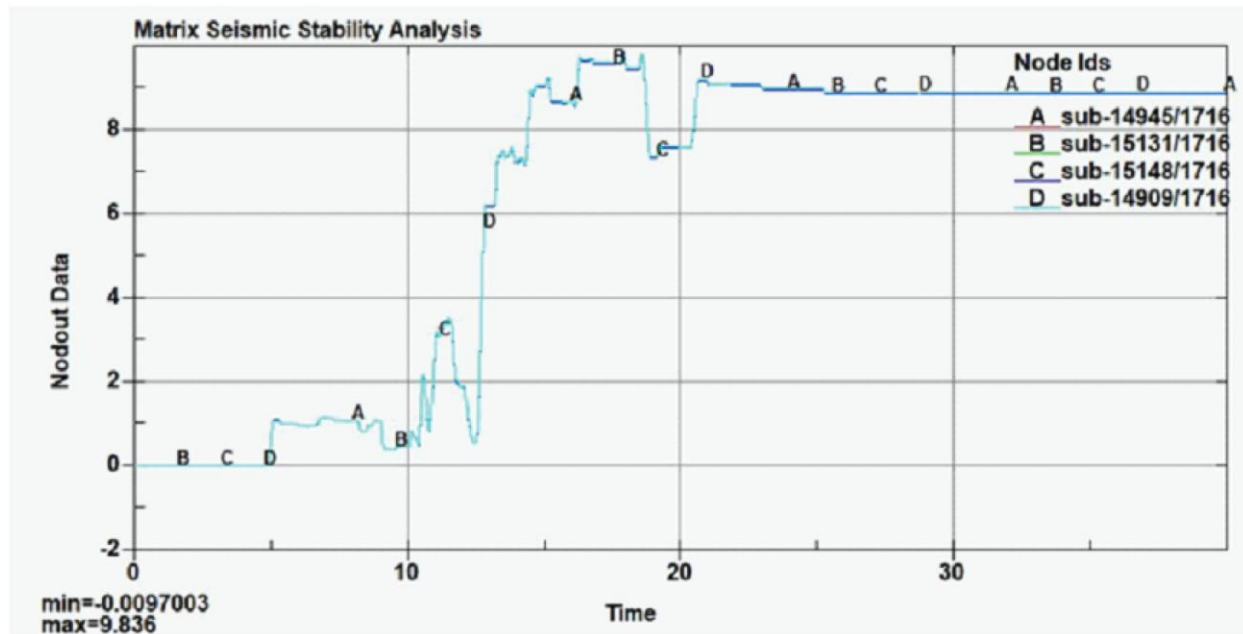


Figure A.3.9.7-7
HSM-MX Maximum X-Direction Sliding TAB, $\mu=0.4$

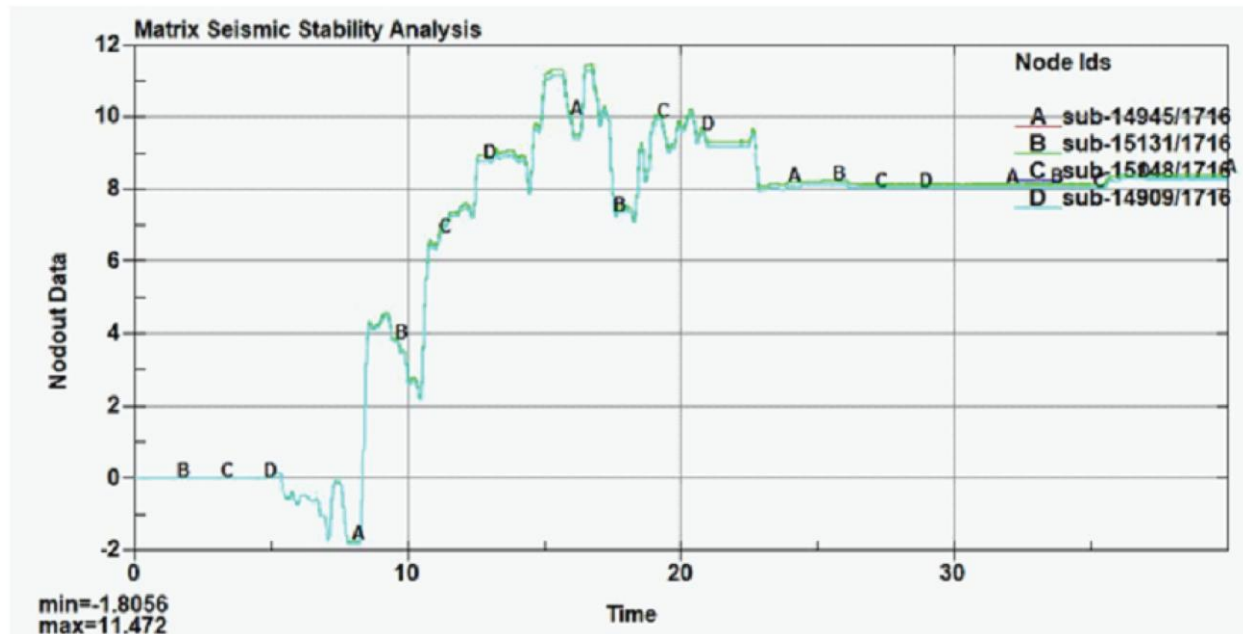


Figure A.3.9.7-8
HSM-MX Maximum Z-Direction Sliding MIAN, $\mu=0.4$

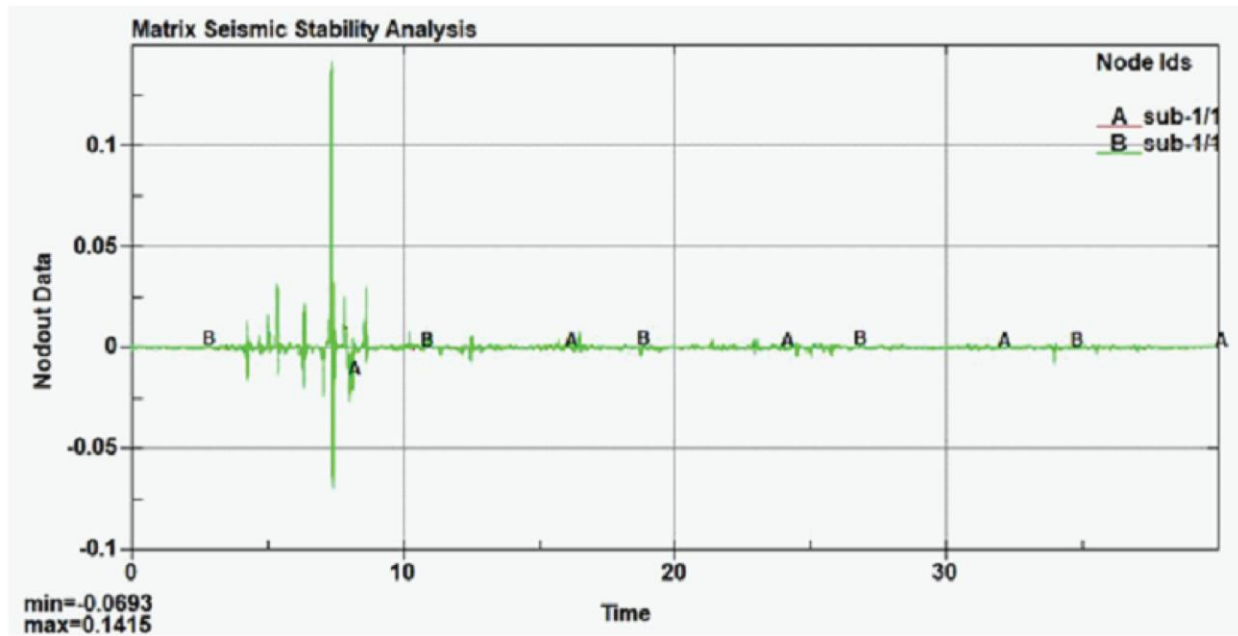


Figure A.3.9.7-9
HSM-MX Maximum Rocking PS10, $\mu=0.8$

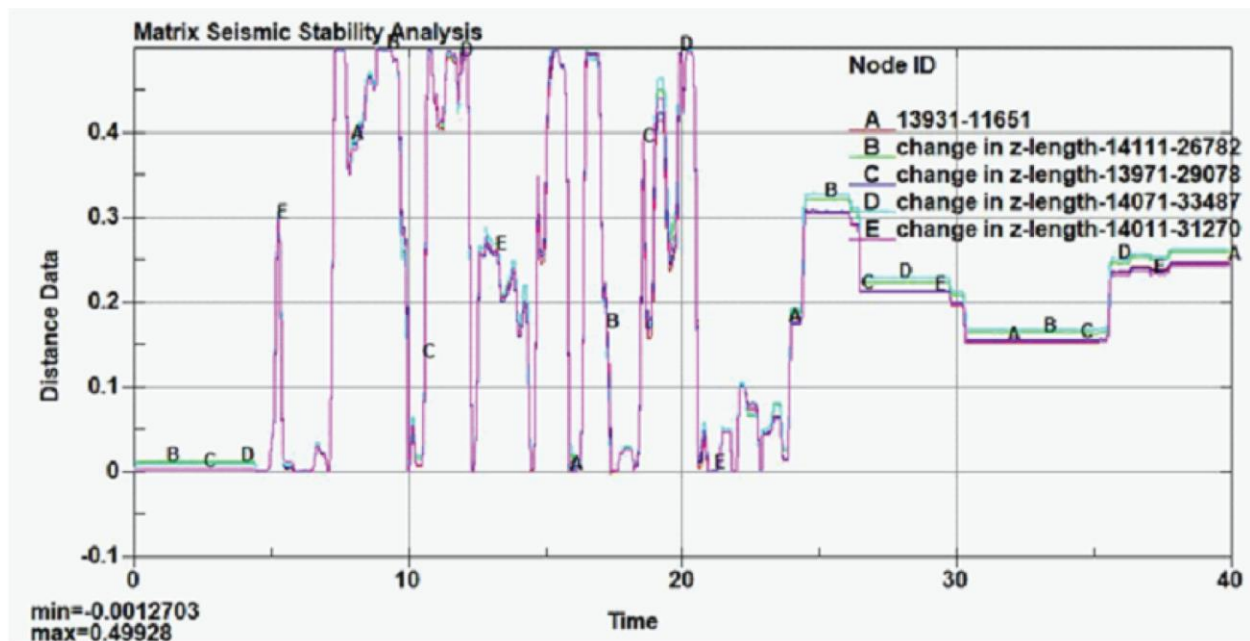


Figure A.3.9.7-10
DSC Sliding on Supports during Max. HSM-MX Z-direction Sliding Case:
MIAN, $\mu=0.4$

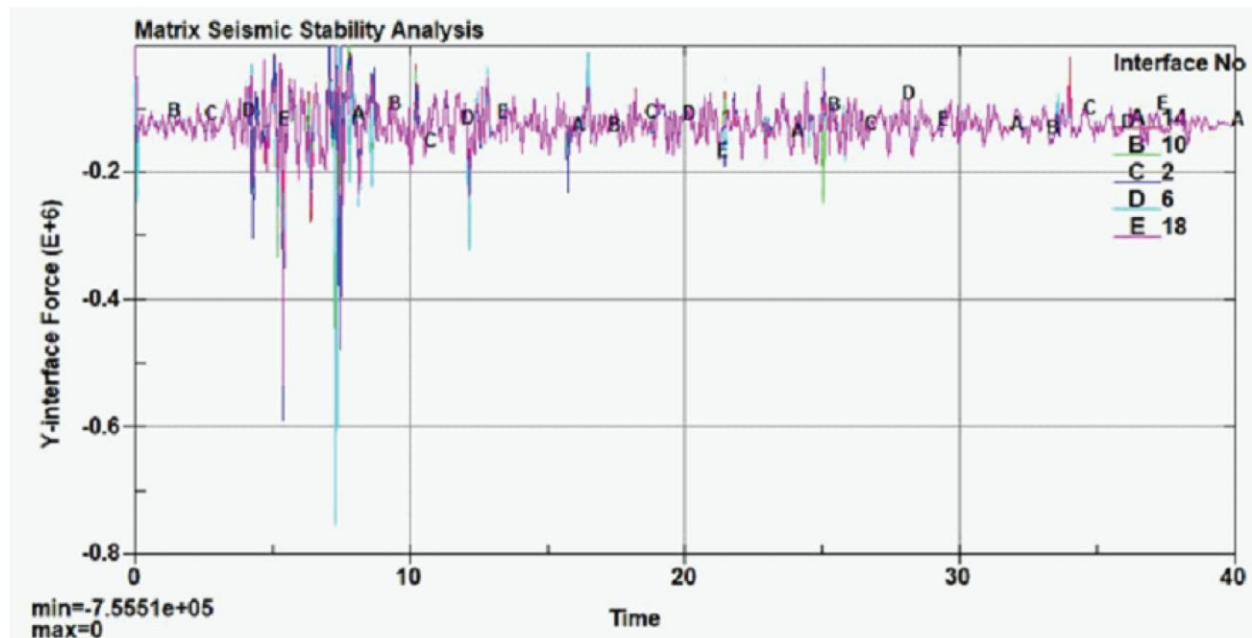


Figure A.3.9.7-11
DSC Load on Supports during Max. HSM-MX Z-Direction Rocking Case:
PS10, $\mu=0.8$

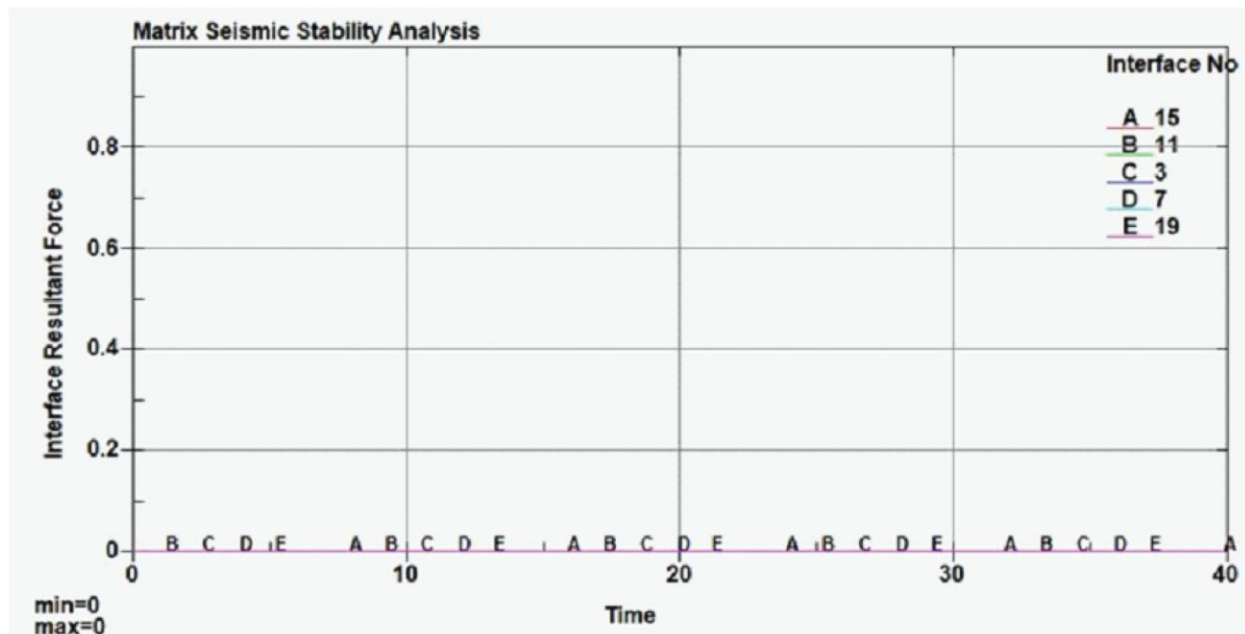


Figure A.3.9.7-12
DSC Load on Door Opening During Max. HSM-MX Z-Direction Rocking
Case: PS10, $\mu=0.8$

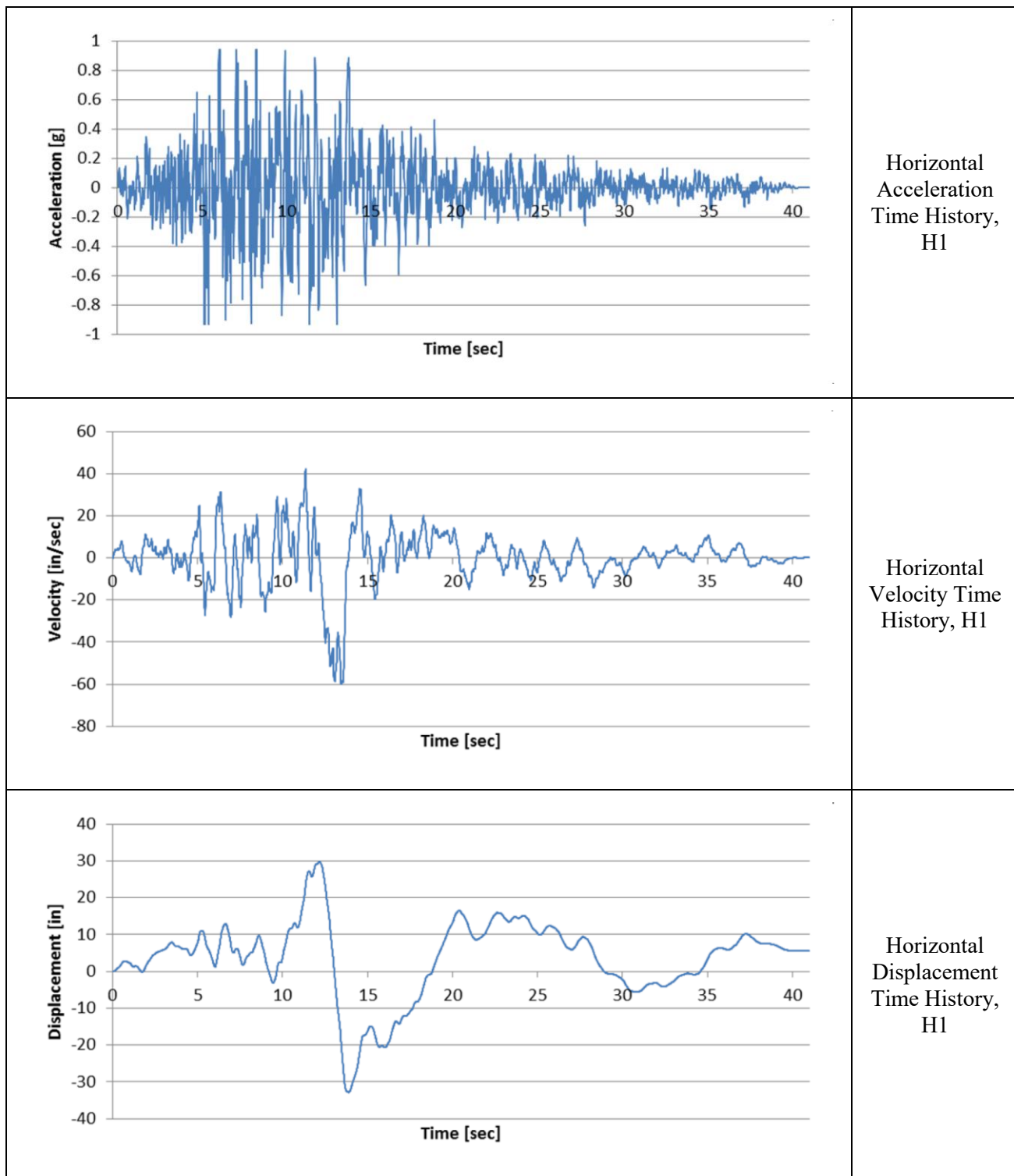


Figure A.3.9.7-13
Horizontal Time History Set 1, HEC – Global X Direction

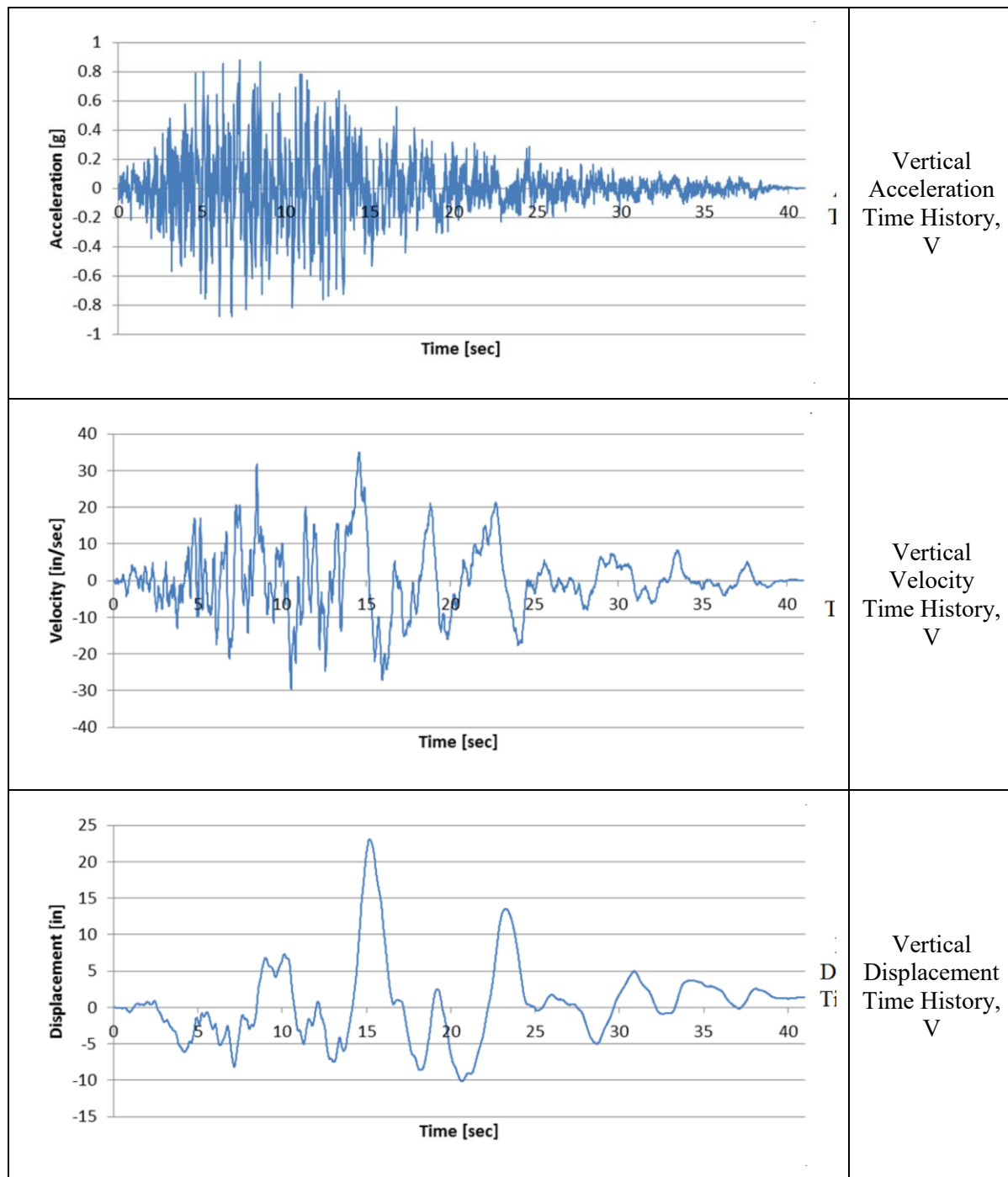


Figure A.3.9.7-14
Vertical Time History Set 1, HEC – Global Y Direction

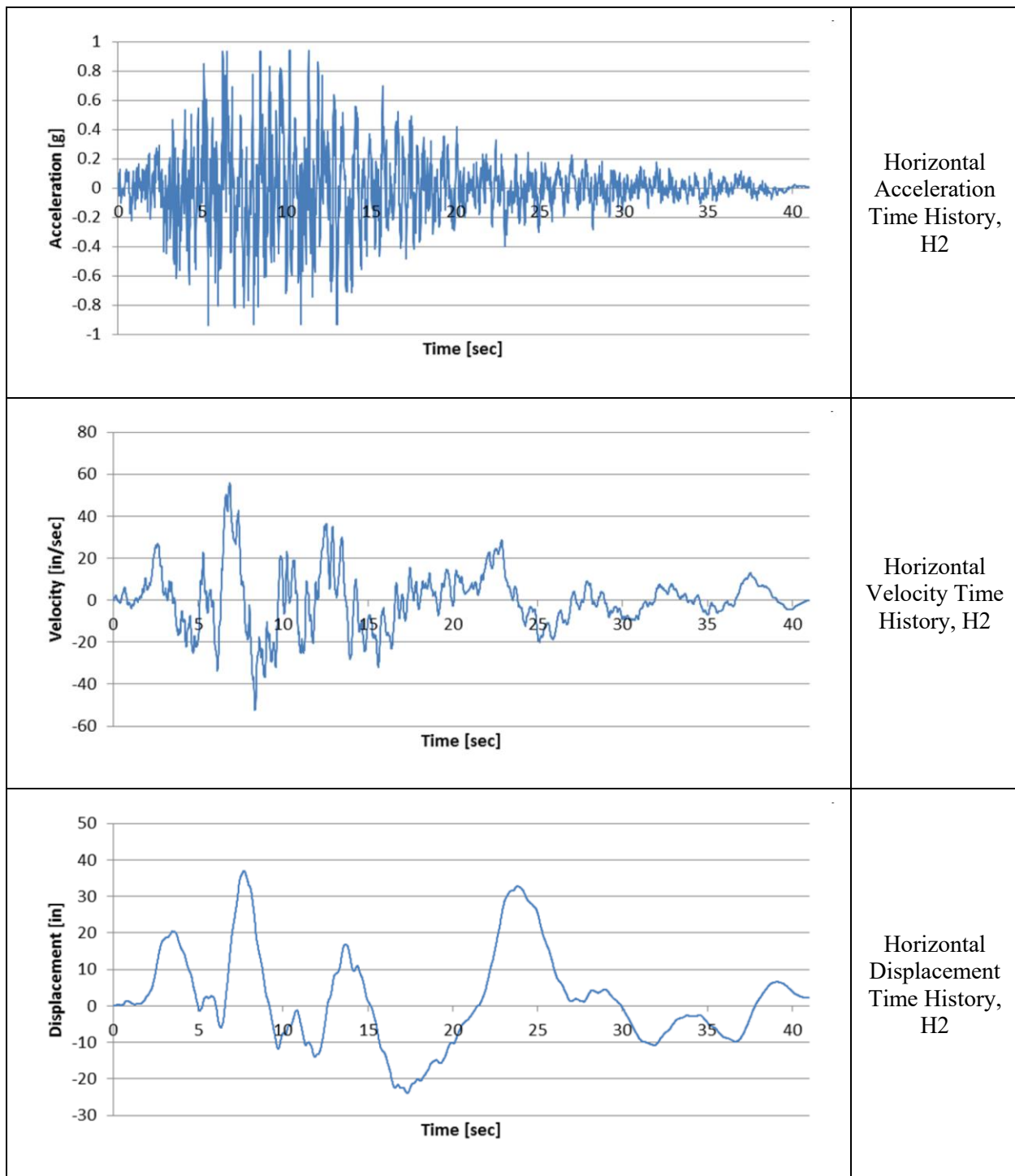


Figure A.3.9.7-15
Horizontal Time History Set 1, HEC – Global Z Direction

APPENDIX A.4 THERMAL EVALUATION

Table of Contents

A.4	THERMAL EVALUATION.....	A.4-1
A.4.1	Discussion of Decay Heat Removal System	A.4-2
A.4.2	Material and Design Limits.....	A.4-3
	A.4.2.1 Summary of Thermal Properties of Materials	A.4-3
A.4.3	Thermal Loads and Environmental Conditions	A.4-4
A.4.4	Thermal Evaluation for Storage.....	A.4-5
	A.4.4.1 EOS-37PTH DSC and Basket Type 4H - Description of Load Cases for Storage	A.4-6
	A.4.4.2 EOS-37PTH DSC with Basket Type 4H - Thermal Model for Storage in HSM-MX.....	A.4-7
	A.4.4.3 EOS-37PTH DSC with Basket Type 4H for HLZC 7 –Storage Evaluation	A.4-17
	A.4.4.4 EOS-37PTH DSC with Basket Type 4L/5 - Storage in HSM- MX	A.4-22
	A.4.4.5 EOS-89BTH DSC with Basket Type 3 - Storage in HSM-MX.....	A.4-26
A.4.5	Thermal Evaluation for Storage in Updated HSM-MX.....	A.4-27
	A.4.5.1 Design Changes in Updated HSM-MX	A.4-27
	A.4.5.2 Description of Load Cases for Storage in Updated HSM-MX	A.4-28
	A.4.5.3 Thermal Model for Storage in Updated HSM-MX.....	A.4-28
	A.4.5.4 EOS-37PTH DSC with Basket Type 4H – Storage in Updated HSM-MX	A.4-29
	A.4.5.5 EOS-37PTH DSC with Basket Type 4L/5 – Storage in Updated HSM-MX	A.4-31
	A.4.5.6 EOS-89BTH DSC with Basket Type 3 - Storage in Updated HSM-MX	A.4-32
	A.4.5.7 Sensitivity Study	A.4-33
A.4.6	References	A.4-38

List of Tables

Table A.4-1	EOS-37PTH DSC in HSM-MX, Design Load Cases for Storage Conditions with HLZC 7	A.4-2
Table A.4-2	Maximum Fuel Cladding and Concrete Temperatures for Storage Conditions of EOS-37PTH DSC in HSM-MX with HLZC 7	A.4-2
Table A.4-3	Maximum Temperatures of Key Components in HSM-MX loaded with EOS-37PTH DSC with HLZC 7	A.4-2
Table A.4-4	Average Temperatures of Key Components in HSM-MX loaded with EOS-37PTH DSC with HLZC 7	A.4-2
Table A.4-5	GCI Calculations Based on LC 1e and LC 1f for HSM-MX Loaded with EOS-37PTH DSC	A.4-2
Table A.4-6	Summary of Air Temperatures and Mass Flow Rates at Inlet and Outlet of EOS-37PTH DSC in HSM-MX with HLZC 7	A.4-2
Table A.4-7	Comparison of Average Gas Temperature in EOS-37PTH DSC Cavity	A.4-2
Table A.4-8	EOS-37PTH DSC in HSM-MX, Design Load Cases for Storage Conditions with HLZCs 8 and 9	A.4-2
Table A.4-9	Maximum Fuel Cladding and Concrete Temperatures for Storage Conditions of EOS-37PTH DSC in HSM-MX with HLZCs 8 and 9	A.4-2
Table A.4-10	Maximum Temperature of Key Components in HSM-MX Loaded with EOS-37PTH DSC with HLZCs 8 and 9	A.4-2
Table A.4-11	Average Temperature of Key Components in HSM-MX Loaded with EOS-37PTH DSC with HLZCs 8 and 9	A.4-2
Table A.4-12	Comparison of Maximum Temperature between HLZCs 8 and 9 with HLZC 7	A.4-2
Table A.4-13	Comparison of EOS-89BTH DSC Temperatures in HSM-MX and EOS-TC125/TC108	A.4-2
Table A.4-14	EOS-37PTH DSC in Updated HSM-MX, Design Load Cases for Storage Conditions with HLZC 7	A.4-2
Table A.4-15	Summary of Convergences of Steady CFD Model of EOS-37PTH DSC in Updated HSM-MX	A.4-2
Table A.4-16	Maximum Fuel Cladding and Concrete Temperatures for Storage Conditions of EOS-37PTH DSC in Updated HSM-MX with HLZC 7	A.4-2
Table A.4-17	Maximum Temperatures of Key Components in Updated HSM-MX loaded with EOS-37PTH DSC with HLZC 7	A.4-2
Table A.4-18	Average Temperatures of Key Components in Updated HSM-MX loaded with EOS-37PTH DSC with HLZC 7	A.4-2

Table A.4-19	GCI Calculations Based on LC 1e-S and LC 1f-S for Updated HSM-MX Loaded with EOS-37PTH DSC	A.4-2
Table A.4-20	Summary of Air Temperatures and Mass Flow Rates at Inlet and Outlet of EOS-37PTH DSC in Updated HSM-MX with HLZC 7	A.4-2
Table A.4-21	Comparison of Average Gas Temperature in EOS-37PTH DSC Cavity	A.4-2
Table A.4-22	EOS-37PTH DSC in Updated HSM-MX, Design Load Cases for Storage Conditions with HLZCs 8 and 9	A.4-2
Table A.4-23	Maximum Fuel Cladding and Concrete Temperatures for Storage Conditions of EOS-37PTH DSC in Updated HSM-MX with HLZCs 8 and 9	A.4-2
Table A.4-24	Maximum Temperature of Key Components in Updated HSM-MX Loaded with EOS-37PTH DSC with HLZCs 8 and 9	A.4-2
Table A.4-25	Average Temperature of Key Components in Updated HSM-MX Loaded with EOS-37PTH DSC with HLZCs 8 and 9	A.4-2
Table A.4-26	Comparison of Maximum Temperature between HLZCs 8 and 9 with HLZC 7	A.4-2
Table A.4-27	Comparison of EOS-89BTH DSC Temperatures in Updated HSM-MX and EOS-TC125/TC108	A.4-2
Table A.4-28	Maximum Fuel Cladding and Concrete Temperatures for Periodic and Symmetric Models	A.4-2
Table A.4-29	Maximum Temperatures of Key Components in HSM-MX Loaded with EOS-37PTH DSC for Periodic and Symmetric Models	A.4-2
Table A.4-30	Average Temperatures of Key Components in HSM-MX Loaded with EOS-37PTH DSC for Periodic and Symmetric Models	A.4-2
Table A.4-31	Maximum Fuel Cladding and Concrete Temperatures for Bounding Storage Conditions of Middle Unit and End Unit Models	A.4-2
Table A.4-32	Maximum Temperatures of Key Components in HSM-MX Loaded with EOS-37PTH DSC for Bounding Storage Conditions of Middle Unit and End Unit Models	A.4-2
Table A.4-33	Average Temperatures of Key Components in HSM-MX Loaded with EOS-37PTH DSC for Bounding Storage Conditions of Middle Unit and End Unit Models	A.4-2
Table A.4-33a	Maximum Fuel Cladding and Concrete Temperatures in HSM-MX Loaded with EOS-37PTH DSC for Periodic and Full Models with Bounding Normal Condition	A.4-2
Table A.4-33b	Maximum Temperatures of Key Components in HSM-MX Loaded with EOS-37PTH DSC for Periodic and Full Models with Bounding Normal Condition	A.4-2

Table A.4-33c	Average Temperatures of Key Components in HSM-MX Loaded with EOS-37PTH DSC for Periodic and Full Models with Bounding Normal Condition	A.4-2
---------------	--	-------

List of Figures

Figure A.4-1	CFD Model for HSM-MX with EOS-37PTH DSC.....	A.4-70
Figure A.4-2	HSM-MX with 90-Degree-Turn Outlet Ducts.....	A.4-71
Figure A.4-3	Axial View of HSM-MX Storage Module with Wind Domain in Symmetrical Mid-Plane for Base Mesh.....	A.4-72
Figure A.4-4	Cross-sectional View of HSM-MX Storage Module with Wind Domain in a Transverse Plane for Base Mesh.....	A.4-73
Figure A.4-5	Histogram of y^+ on the Outer Surface of EOS-37PTH DSC Shell in Lower and Upper Compartments of HSM-MX with HLZC 7	A.4-74
Figure A.4-6	Exterior Boundary Conditions for the Side Wind Load Cases of EOS- 37PTH DSC in HSM-MX.....	A.4-75
Figure A.4-7	Convergence of Maximum Fuel Cladding Temperatures for all Steady- State Load Cases of EOS-37PTH DSC in HSM-MX with HLZC 7	A.4-76
Figure A.4-8	HSM-MX Models Used for Verification of Simplifications within the Thermal Model	A.4-77
Figure A.4-9	Temperature Profiles for HSM-MX loaded with EOS-37PTH DSC at Bounding Normal Hot Storage Condition (Load Case 1e).....	A.4-78
Figure A.4-10	Temperature Profiles for HSM-MX loaded with EOS-37PTH DSC at Off-Normal Hot Storage Condition (Load Case 2)	A.4-81
Figure A.4-11	Temperature Profiles for HSM-MX loaded with EOS-37PTH DSC at Accident Blocked Inlet Vents Storage Condition for 32 hours (Load Case 3)	A.4-84
Figure A.4-12	Maximum Temperature Histories of Key Components in HSM-MX loaded with EOS-37PTH DSC with HLZC 7 at Blocked Inlet Vent Accident Condition (Load Case 3)	A.4-87
Figure A.4-13	Streamlines of Airflow inside the HSM-MX Cavity for Normal Hot Storage Condition (Load Case 1e).....	A.4-88
Figure A.4-14	Temperature Profiles for HSM-MX loaded with EOS-37PTH DSC at Bounding Normal Hot Storage Condition (Load Case 1e for HLZC 8).....	A.4-89
Figure A.4-15	Temperature Profiles for HSM-MX loaded with EOS-37PTH DSC at Bounding Normal Hot Storage Condition (Load Case 1e for HLZC 9).....	A.4-92
Figure A.4-16	Comparison of DSC Support used in the CFD Model in Section A.4.4.2.2 and the Sensitivity Model of HSM-MX in Section A.4.4.3.5.....	A.4-95
Figure A.4-17	Comparison of HSM-MX Door Used in the CFD Model in Section A.4.4.2.2 and the Sensitivity Model in Section A.4.4.3.5	A.4-96
Figure A.4-18	Comparison of DSC Support used in the CFD Model in Section A.4.4.2.2 and the Updated Model of HSM-MX in Section A.4.5	A.4-97

Figure A.4-19	Comparison of Rear Wall close to Rear Support in Lower Compartment in the CFD Model in Section A.4.4.2.2 and the Updated Model of HSM-MX in Section A.4.5	A.4-98
Figure A.4-20	Comparison of Front Retractable Roller Tray Designs in Upper and Lower Compartments in the CFD Model in Section A.4.4.2.2 and the Updated Model of HSM-MX in Section A.4.5.....	A.4-99
Figure A.4-21	Temperature Profiles for Updated HSM-MX loaded with EOS-37PTH DSC at Bounding Normal Hot Storage Condition (Load Case 1e-S)	A.4-100
Figure A.4-22	Temperature Profiles for Updated HSM-MX loaded with EOS-37PTH DSC at Off-Normal Hot Storage Condition (Load Case 2-S)	A.4-103
Figure A.4-23	Temperature Profiles for Updated HSM-MX loaded with EOS-37PTH DSC at Accident Blocked Inlet Vents Storage Condition for 32 hours (Load Case 3-S)	A.4-106
Figure A.4-24	Streamlines of Airflow inside the HSM-MX Cavity for Normal Hot Storage Condition (Load Case 1e-S)	A.4-109
Figure A.4-25	Temperature Profiles for Updated HSM-MX loaded with EOS-37PTH DSC at Bounding Normal Hot Storage Condition (Load Case 1e-S for HLZC 8).....	A.4-110
Figure A.4-26	Temperature Profiles for Updated HSM-MX loaded with EOS-37PTH DSC at Bounding Normal Hot Storage Condition (Load Case 1e-S for HLZC 9).....	A.4-113
Figure A.4-27	Comparison of Designs and Boundary Conditions used in Periodic and Symmetric Models of the HSM-MX in Section A.4.5.7.1	A.4-116
Figure A.4-28	CFD Model for End Unit HSM-MX with EOS-37PTH DSC Loaded in Lower Compartment	A.4-117
Figure A.4-28a	Comparison of Designs and Boundary Conditions used in Periodic Model (Load Case 1e-S in Section A.4.5.3) and Full Model (Load Case 1e-S-full in Section A.4.5.7.3) of the HSM-MX	A.4-118
Figure A.4-28b	Temperature Profiles for Updated HSM-MX loaded with Two Full Upper and One Full Lower EOS-37PTH DSCs at Bounding Normal Hot Storage Condition (Load Case 1e-S-full)	A.4-119

A.4 THERMAL EVALUATION

The thermal evaluation described in this chapter is applicable to the NUHOMS® EOS System that includes EOS-37PTH or EOS-89BTH dry shielded canisters (DSCs) loaded inside the NUHOMS® MATRIX (HSM-MX).

A summary of the EOS-37PTH and EOS-89BTH DSC configurations analyzed in this chapter for storage operations in HSM-MX is shown in the Table in Chapter 4 and also below:

DSC Type	Basket Assembly Type	HLZC	Max. Heat Load (kW)	Transfer Cask	Storage Module
EOS-37PTH	4H	7	50.00	EOS-TC125/ EOS-TC135	HSM-MX
	4L/5	8 ⁽¹⁾	46.40 ⁽²⁾		
	4L/5	9	37.80		
EOS-89BTH	3	3	34.44	EOS-TC125/ EOS-TC108	

Note:

- (1) Basket Type 5 can only accommodate Intact FAs. Therefore, damaged or Failed FAs allowed per HLZC 8 shall only be loaded in Basket Type 4L.
- (2) The maximum decay heat per DSC is limited to 41.8 kW when a damaged or failed FA is loaded

The various basket types within the EOS-37PTH DSC and EOS-89BTH DSC are described in Chapter 1, Section 1.1 and Appendix 4.9.6, Section 4.9.6.1.1.

Descriptions of the detailed analyses performed for normal, off-normal, and hypothetical accident conditions are provided in Section A.4.4 for storage operations. Transfer operations for the EOS-37PTH DSC with HLZCs 7 through 9 are presented in Section 4.9.6.2. Transfer operations for the EOS-89BTH DSC with HLZC 3 are presented in Section 4.5.6.

In order to accommodate lessons learned from the mockup development, the original HSM-MX design has been slightly revised for improved fabricability. Section A.4.5 evaluates the thermal performance of the updated HSM-MX with the EOS-37PTH and EOS-89BTH DSCs under the bounding normal, off-normal, and accident storage conditions.

A.4.1 Discussion of Decay Heat Removal System

Chapter 4, Section 4.1 provides a detailed description of the decay heat removal system within the EOS-37PTH and EOS-89BTH DSCs during storage operations in the EOS-HSM. The decay heat removal system described for storage operations in the EOS-HSM is also applicable for storage operations in the HSM-MX.

Similar to the EOS-HSM described in Chapter 4, Section 4.1, no instrumentation is required to monitor the thermal performance if daily visual inspections of the air inlet and outlet vents are performed. However, in lieu of the daily visual inspections, a direct measurement of the HSM-MX temperature or any other means that would provide an indication of the thermal performance may be used for monitoring in accordance with requirements in Technical Specifications [A.4-13].

A.4.2 Material and Design Limits

To establish the heat removal capability, several thermal design criteria are established for the NUHOMS® EOS System.

- Design criteria for the EOS-37PTH and EOS-89BTH DSCs are identical to those described in Chapter 4, Section 4.2.
- For normal and off-normal conditions, the maximum concrete temperature limit is 300 °F, as noted in Section 3.5.1.2 of [A.4-1]. For the accident conditions, if the concrete temperature exceeds the short-term limit of 350 °F noted in Appendix E.4 of ACI 349-06 [A.4-4], concrete testing will be performed, as described in Chapter A.8, Section A.8.2.1.3.

A.4.2.1 Summary of Thermal Properties of Materials

The thermal properties of the materials used in the thermal evaluation for Type 4H baskets are the same as those specified in Chapter 4, Section 4.2.1. The basket material properties for Type 4L/5 baskets are discussed in Appendix 4.9.6, Section 4.9.6.1.1.

A.4.3 Thermal Loads and Environmental Conditions

For storage operations in the HSM-MX, the maximum temperature is 100 °F for normal storage conditions. A daily average ambient temperature of 90 °F is used in the evaluations, corresponding to a daily maximum temperature of 100 °F for the normal hot storage conditions as discussed in Chapter 4, Section 4.3.

Off-normal ambient temperature is considered in the range of - 40 °F to 117 °F. A daily average ambient temperature of 103 °F is used in the evaluations, corresponding to a daily maximum temperature of 117 °F for the off-normal hot and hypothetical accident storage conditions, as discussed in Chapter 4, Section 4.3. Ambient temperatures of -20 °F and -40 °F are considered for the normal and off-normal cold storage conditions, respectively.

The HSM-MX is located outdoors and is exposed to the environment. Wind is a normal environment variable that varies frequently both in direction and magnitude. For the HSM-MX, low speed wind in the range of 0 to 15 mph is considered for normal storage conditions based on the discussion in Section 2.5 of NUREG-2174 [A.4-2].

A.4.4 Thermal Evaluation for Storage

This section provides an evaluation of the thermal performance of the HSM-MX loaded with the EOS-37PTH DSC for normal, off-normal, and hypothetical accident conditions.

Sections A.4.4.1 through A.4.4.3 present the evaluation for EOS-37PTH DSC with Basket Type 4H and a maximum heat load of 50 kW per HLZC 7 in the HSM-MX. A detailed description of Basket Type 4H is presented in Chapter 1, Section 1.1, Chapter 4, and Appendix 4.9.6, Section 4.9.6.1.1.

Within the HSM-MX, the maximum allowable heat loads differ between the upper and the lower compartments for the same DSC. For an EOS-37PTH DSC with Basket Type 4H, the maximum allowable heat loads in the upper and lower compartments are 41.8 kW and 50 kW, respectively.

Section A.4.4.1 and Section A.4.4.2 present a description of the loading cases and the computational fluid dynamics (CFD) model used for the thermal evaluation of the EOS-37PTH during storage in the HSM-MX, respectively.

Section A.4.4.3 presents the results of the thermal evaluation for the EOS-37PTH DSC with Basket Type 4H during storage operations in the HSM-MX per HLZC 7. Sections A.4.4.3.1, A.4.4.3.2, and A.4.4.3.3 discuss the normal, off-normal, and hypothetical accident conditions of storage, respectively.

Section A.4.4.4 presents the thermal evaluation of the EOS-37PTH DSC with Basket Type 4L/5 during storage operations in the HSM-MX per HLZCs 8 and 9. A description of Basket Type 4L/5 for the EOS-37PTH DSC is presented in Chapter 1, Section 1.1, Chapter 4, and Appendix 4.9.6, Section 4.9.6.1.1.

EOS-37PTH DSC with Basket Type 4L/5 has a maximum heat load of 46.4 and 41.8 kW, respectively, while loaded in the lower and upper compartments of the HSM-MX.

Section A.4.4.5 presents the qualification of the EOS-89BTH DSC with a maximum heat load of 34.44 kW in the HSM-MX.

Proprietary Information on Pages A.4-6 through A.4-17
Withheld Pursuant to 10 CFR 2.390

A.4.4.3.1.2 Temperature Calculations

The maximum temperatures of fuel cladding and concrete of the HSM-MX loaded with the EOS-37PTH DSC for normal storage conditions (LCs 1a through 1e) are summarized in Table A.4-2.

The maximum temperatures of various components of the HSM-MX loaded with the EOS-37PTH DSC for the bounding normal storage condition (LC 1e) are summarized in Table A.4-3. The average temperatures of key components of the HSM-MX loaded with the EOS-37PTH DSC for the bounding normal storage condition (LC 1e) are summarized in Table A.4-4.

Typical temperature plots for the key components in the HSM-MX loaded with the EOS-37PTH DSC are shown in Figure A.4-9 for the bounding normal hot condition.

A.4.4.3.1.3 Airflow Calculations

The streamlines for the airflow inside the HSM-MX loaded with the EOS-37PTH DSC under normal hot storage condition are shown in Figure A.4-13. Cool air enters into the HSM-MX from the inlet, absorbs the heat from the EOS-37PTH DSC, and leaves the HSM-MX through the outlet with higher temperatures. Table A.4-6 summarizes the air temperatures and mass flow rates at the inlet and outlet for the quiescent normal condition of storage.

A.4.4.3.1.4 GCI Calculation

A.4.4.3.2 Off-Normal Conditions of Storage

A.4.4.3.2.1 Temperature Calculations

The maximum temperatures of fuel cladding and concrete of the HSM-MX loaded with the EOS-37PTH DSC for off-normal storage conditions (LC 2) are summarized in Table A.4-2.

The maximum temperatures of various components of the HSM-MX loaded with the EOS-37PTH DSC for off-normal storage conditions (LC 2) are summarized in Table A.4-3. The average temperatures of key components of the HSM-MX loaded with the EOS-37PTH DSC for off-normal storage condition (LC 2) are summarized in Table A.4-4.

Typical temperature plots for the key components in the HSM-MX loaded with the EOS-37PTH DSC are shown in Figure A.4-10 for off-normal hot conditions.

The minimum temperatures for fuel cladding and basket assembly components assuming no credit for decay heat for off-normal cold storage condition is -40 °F. All materials can be subjected to a minimum environment temperature of -40 °F without any adverse effects.

A.4.4.3.2.2 Airflow Calculations

Table A.4-6 summarizes the air temperatures and mass flow rates at the inlet and outlet for LC 2 for off-normal condition of storage.

A.4.4.3.3 Hypothetical Accident Conditions of Storage

A.4.4.3.3.1 Temperature Calculations

The maximum temperatures of fuel cladding and concrete of the HSM-MX loaded with the EOS-37PTH DSC for hypothetical accident condition of storage (LC 3) are summarized in Table A.4-2.

The maximum temperatures of various components of the HSM-MX loaded with the EOS-37PTH DSC for hypothetical accident condition of storage (LC 3) are summarized in Table A.4-3. The average temperatures of key components of the HSM-MX loaded with the EOS-37PTH DSC for hypothetical accident condition of storage (LC 3) are summarized in Table A.4-4. The values listed in Table A.4-3 and Table A.4-4 for LC 3 are based on transient simulation results at 32 hours.

Typical temperature plots for the key components in the HSM-MX loaded with the EOS-37PTH DSC are shown in Figure A.4-11 for hypothetical accident conditions.

For the accident blocked vent condition, the time histories of the maximum and average temperatures for the key components are shown in Figure A.4-12. All the temperatures increase steadily during the 32 hours of the blocked vent event.

A.4.4.3.4 Internal Pressure

Chapter 4, Section 4.7.1 calculates the maximum internal pressure of the EOS-37PTH DSC during storage in the EOS-HSM and transfer in EOS-TC125/135/108. For the EOS-37PTH DSC during storage in HSM-MX, the average gas temperature in the DSC cavity is computed using the same approach presented in Chapter 4, Section 4.7.1.2 and listed in Table A.4-7. As shown in Table A.4-7, the average helium temperatures determined for the EOS-37PTH DSC in HSM-MX with HLZC 7 are lower than the temperatures determined for HLZCs 1 through 3. Therefore, the maximum internal pressures in Chapter 4, Table 4-45 remain bounding for HLZC 7 under normal, off-normal, and accident storage conditions, respectively.

A.4.4.3.5 Impact of Design Changes

The original HSM-MX design has been slightly revised for improved fabricability as described in Section A.4.5.1. Detailed thermal evaluations for the storage in the updated HSM-MX are presented in Section A.4.5. This section evaluates the discrepancy of the original HSM-MX and the thermal model in Section A.4.4.2.2. The evaluation in this section is obsolete and no longer applicable.

Proprietary Information on This Page
Withheld Pursuant to 10 CFR 2.390

A.4.4.4 EOS-37PTH DSC with Basket Type 4L/5 - Storage in HSM-MX

This section presents the thermal evaluation of the EOS-37PTH DSC with Basket Type 4L/5 during storage operations in the HSM-MX. A description of Basket Type 4L/5 for the EOS-37PTH DSC is presented in Chapter 1, Section 1.1 and Appendix 4.9.6, Section 4.9.6.1.1.

This evaluation considers HLZC 8 with a maximum heat load of 46.4 kW and HLZC 9 with a maximum heat load of 37.8 kW. HLZC 8 and HLZC 9 are shown in Figure 1H and Figure 1I of the Technical Specifications [A.4-13], respectively.

HLZC 8 can accommodate either damaged or failed FAs along with intact FAs but not both. In addition, when damaged or failed FAs are loaded per HLZC 8, the maximum heat load is limited to 41.8 kW per DSC. As discussed in Chapter 1, Section 1.1, damaged/failed FAs shall only be loaded in the EOS-37PTH DSC with Basket Type 4L.

EOS-37PTH DSC with Basket Type 4L/5 has a maximum heat load of 46.4 kW while loaded in the lower compartment of the HSM-MX. The maximum heat load for the EOS-37PTH DSC with Basket Type 4L/5 while loaded in the upper compartment of the HSM-MX is 41.8 kW.

Utilizing these new HLZCs, this section evaluates the thermal performance of the HSM-MX loaded with the EOS-37PTH DSC for normal, off-normal, and accident conditions.

Proprietary Information on Pages A.4-23 and A.4-24
Withheld Pursuant to 10 CFR 2.390

A.4.4.4.2 EOS-37PTH DSC with Basket Type 4L/5 - Thermal Model for Storage in HSM-MX

To evaluate the thermal performance of the EOS-37PTH DSC with Basket Type 4L/5 based on HLZCs 8 and 9 during storage operations in HSM-MX, the thermal model from Section A.4.4.2 is modified to simulate LCs described in Section A.4.4.4.1. The modifications in the LCs described in Section A.4.4.4.1 are limited to the changes in material properties of the basket components as described in Appendix 4.9.6, Section 4.9.6.1.1, and heat generation rates based on the new HLZCs, but no changes are considered to the mesh.

A.4.4.4.3 EOS-37PTH DSC with Basket Type 4L/5 for HLZC 8 and 9 –Storage Evaluation

Table A.4-9 and Table A.4-10 present the maximum temperatures of fuel cladding and key components of the EOS-37PTH DSC with Basket Type 4L/5 loaded in the HSM-MX based on HLZCs 8 and 9 during storage operations.

Table A.4-11 presents the average temperatures of fuel cladding and key components of the EOS-37PTH DSC with Basket Type 4L/5 loaded in the HSM-MX based on HLZCs 8 and 9 during storage operations.

Figure A.4-14 and Figure A.4-15 present the temperature profiles of key components in the HSM-MX loaded with the EOS-37PTH DSC for HLZCs 8 and 9, respectively.

Comparison with HLZC 7

Table A.4-12 presents a comparison of the maximum temperatures for HLZCs 8 and 9 with the bounding design basis values from HLZC 7. As shown in the comparison, the maximum temperatures determined for HLZC 7 with 50 kW, remain bounding for HLZCs 8 and 9.

Similar to the normal condition, the maximum temperatures during off-normal and accident storage conditions for HLZCs 8 or 9 will also remain bounded by HLZC 7. Therefore, no further evaluation is required for off-normal and accident storage condition with HLZCs 8 and 9.

Based on this discussion, all design criteria are satisfied for storage of the EOS-37PTH DSC with HLZCs 8 or 9 in the HSM-MX.

Proprietary Information on Pages A.4-26 through A.4-28
Withheld Pursuant to 10 CFR 2.390

A.4.5.4 EOS-37PTH DSC with Basket Type 4H – Storage in Updated HSM-MX

A.4.5.4.1 Convergence of the CFD Model

A.4.5.4.2 Temperature Calculations

The maximum temperatures of fuel cladding and concrete of the updated HSM-MX loaded with the EOS-37PTH DSC for the bounding normal, off-normal, and accident storage conditions are summarized in Table A.4-16.

The maximum temperatures of various components of the HSM-MX loaded with the EOS-37PTH DSC for the bounding normal, off-normal, and accident storage conditions are summarized in Table A.4-17. The average temperatures of key components of the HSM-MX loaded with the EOS-37PTH DSC for the bounding normal, off-normal, and accident storage conditions are summarized in Table A.4-18.

Typical temperature plots for the key components in the HSM-MX loaded with the EOS-37PTH DSC are shown in Figure A.4-21, Figure A.4-22, and Figure A.4-23, respectively, for the bounding normal hot, off-normal hot, and accident conditions.

A.4.5.4.3 Airflow Calculations

The streamlines for the airflow inside the updated HSM-MX loaded with the EOS-37PTH DSC under normal hot storage condition are shown in Figure A.4-24. Cool air enters into the HSM-MX from the inlet, absorbs the heat from the EOS-37PTH DSC, and leaves the HSM-MX through the outlet with higher temperatures. Table A.4-20 summarizes the air temperatures and mass flow rates at the inlet and outlet for the normal and off-normal hot conditions of storage.

A.4.5.4.4 GCI Calculation

A.4.5.4.5 Internal Pressure

Chapter 4, Section 4.7.1 calculates the maximum internal pressure of the EOS-37PTH DSC during storage in the EOS-HSM and transfer in EOS-TC125/135/108. For the EOS-37PTH DSC during storage in the updated HSM-MX, the average gas temperature in the DSC cavity is computed using the same approach presented in Chapter 4, Section 4.7.1.2 and listed in Table A.4-21. As shown in Table A.4-21, the average helium temperatures determined for the EOS-37PTH DSC in the updated HSM-MX with HLZC 7 are lower than the temperatures determined for HLZCs 1 through 3. Therefore, the maximum internal pressures in Chapter 4, Table 4-45 remain bounding for HLZC 7 under normal, off-normal, and accident storage conditions, respectively.

A.4.5.5 EOS-37PTH DSC with Basket Type 4L/5 – Storage in Updated HSM-MX

This section presents the thermal evaluation of the EOS-37PTH DSC with Basket Type 4L/5 during storage operations in the updated HSM-MX. This section follows the same methodology as discussed in Section A.4.4.4. The only difference is the design changes that made to HSM-MX as discussed in Section A.4.5.1.

Same as Section A.4.4.4, this evaluation considers HLZC 8 with a maximum heat load of 46.4 kW and HLZC 9 with a maximum heat load of 37.8 kW. HLZCs 8 and 9 are discussed in Section A.4.4.4.

A.4.5.5.1 EOS-37PTH DSC and Basket Type 4L - Description of Load Cases for Storage

A.4.5.5.2 EOS-37PTH DSC with Basket Type 4L/5 - Thermal Model for Storage in HSM-MX

To evaluate the thermal performance of the EOS-37PTH DSC with Basket Type 4L/5 based on HLZCs 8 and 9 during storage operations in the updated HSM-MX, the thermal model from Section A.4.5.3 is modified to simulate LCs described in Section A.4.5.5.1. The modifications in the LCs described in Section A.4.5.5.1 are limited to the changes in material properties of the basket components as described in Appendix 4.9.6, Section 4.9.6.1.1, and heat generation rates based on the new HLZCs, but no changes are considered to the mesh.

A.4.5.5.3 EOS-37PTH DSC with Basket Type 4L/5 for HLZCs 8 and 9 –Storage Evaluation

Figure A.4-23 and Figure A.4-24 present the maximum temperatures of fuel cladding and key components of the EOS-37PTH DSC with Basket Type 4L/5 loaded in the updated HSM-MX based on HLZCs 8 and 9 during storage operations.

Figure A.4-25 presents the average temperatures of fuel cladding and key components of the EOS-37PTH DSC with Basket Type 4L/5 loaded in the updated HSM-MX based on HLZCs 8 and 9 during storage operations.

Figure A.4-25 and Figure A.4-26 present the temperature profiles of key components in the HSM-MX loaded with the EOS-37PTH DSC for HLZCs 8 and 9, respectively.

Comparison with HLZC 7

Table A.4-26 presents a comparison of the maximum temperatures for HLZCs 8 and 9 with the bounding design basis values from HLZC 7. As shown in the comparison, the majority of the maximum component temperatures determined for HLZC 7 with 50 kW remain bounding for HLZCs 8 and 9. The maximum temperature of the heat shield in the upper compartment for HLZC 8 is slightly higher (2 °F) than that for HLZC 7.

Similar to the normal condition, the maximum temperatures during off-normal and accident storage conditions for HLZCs 8 or 9 will also remain bounded by HLZC 7. Therefore, no further evaluation is required for off-normal and accident storage condition with HLZCs 8 and 9.

Based on this discussion, all design criteria are satisfied for storage of the EOS-37PTH DSC with HLZCs 8 or 9 in the updated HSM-MX.

A.4.5.6 EOS-89BTH DSC with Basket Type 3 - Storage in Updated HSM-MX



Proprietary Information on Pages A.4-33 through A.4-37
Withheld Pursuant to 10 CFR 2.390

A.4.6 References

- A.4-1 NUREG-1536, “Standard Review Plan for Spent Fuel Dry Cask Storage Systems at a General License Facility,” Revision 1, U.S. Nuclear Regulatory Commission, July 2010.
- A.4-2 NUREG-2174, “Impact of Variation in Environmental Conditions on the Thermal Performance of Dry Storage Casks - Final Report,” U.S. Nuclear Regulatory Commission, March 2016.
- A.4-3 J.M. Cuta, U.P. Jenquin, and M.A. McKinnon, “Evaluation of Effect of Fuel Assembly Loading Patterns on Thermal and Shielding Performance of a Spent Fuel Storage/Transportation Cask,” , PNNL-13583, Pacific Northwest National Laboratory, November 2001.
- A.4-4 ACI 349-06, “Code Requirements for Nuclear Safety Related Concrete Structures” American Concrete Institute.
- A.4-5 ANSYS FLUENT, ANSYS FLUENT Users Guide, Version 17.1, ANSYS, Inc.
- A.4-6 ANSYS ICEM CFD, Version 17.1, ANSYS, Inc.
- A.4-7 NUREG-2152, “Computational Fluid Dynamics Best Practice Guidelines for Dry Cask Applications,” U.S. Nuclear Regulatory Commission, March 2013.
- A.4-8 American Society of Mechanical Engineers, “Standard for Verification and Validation in Computational Fluid Dynamics and Heat Transfer,” ASME V&V 20-2009, November 30th, 2009.
- A.4-9 I. E. Idelchik, “Handbook of Hydraulic Resistance,” 3rd Edition, Begell House, Inc., 1996.
- A.4-10 A Zigh, J Solis, “Computational Fluid Dynamics Best Practice Guidelines in Analysis of Dry Storage Cask,” WM2008 Conference, Phoenix, AZ, February 24-28, 2008.
- A.4-11 ASHRAE Handbook, Fundamentals, SI Edition, American Society of Heating, Refrigerating and Air-Conditioning Engineers, Inc., 1997.
- A.4-12 P. J. Roache, “Quantification of Uncertainty in Computational Fluid Dynamics,” Annual Review of Fluid Mechanics, Vol. 29, 123-160, 1997.
- A.4-13 CoC 1042 Appendix A, NUHOMS® EOS System Generic Technical Specifications, Amendment 1.

Table A.4-1
EOS-37PTH DSC in HSM-MX, Design Load Cases for Storage Conditions
with HLZC 7

Load Case	Operating Condition	Description	Mesh	Ambient Temperature (°F)
1a	Normal		Base	100 ⁽¹⁾
1b				
1c				
1d				
1e				
1f			Fine	
2	Off-Normal		Base	117 ⁽¹⁾
3 ⁽²⁾	Accident		Base	117 ⁽¹⁾

Notes:

(1) Daily average temperatures are used as noted in Section A.4.3.

(2) Initial temperatures are taken from steady-state results of Load Case 2.

Table A.4-2
Maximum Fuel Cladding and Concrete Temperatures for Storage
Conditions of EOS-37PTH DSC in HSM-MX with HLZC 7

Load Case ⁽¹⁾	Description	Max Fuel Cladding Temperature (°F)			Concrete Temperature (°F)	
		Upper Compartment	Lower Compartment	Limit	Maximum ⁽⁴⁾	Limit
1a		641	686	752 ⁽²⁾	246	300 ⁽²⁾
1b		651	684		245	
1c		660	690		250	
1d		671	699		260	
1e		676	708		273	
1f		676	707		273	
2		653	696	1058 ⁽²⁾	263	500 ⁽³⁾
3		724	777		371	

Notes:

- (1) See Table A.4-1 for the description of the LCs.
- (2) The temperature limits are from NUREG-1536 [A.4-1].
- (3) The temperature limit for concrete at accident condition is 500 °F. The maximum concrete temperature for accident conditions is above the 350 °F limit given in ACI 349-06 [A.4-4]. Testing will be performed, as described in Chapter A.8, Section A.8.2.1.3.
- (4) According to the sensitivity study in Section A.4.4.3.5, the maximum concrete temperatures are added by 9 °F for conservatism.

Proprietary Information on Pages A.4-41 through A.4-46
Withheld Pursuant to 10 CFR 2.390

Table A.4-9
Maximum Fuel Cladding and Concrete Temperatures for Storage
Conditions of EOS-37PTH DSC in HSM-MX with HLZCs 8 and 9

Load Case ⁽¹⁾	Max Fuel Cladding Temperature (°F)			Concrete Temperature (°F)	
	Upper Compartment	Lower Compartment	Limit	Maximum ⁽⁴⁾	Limit
LC1e for HLZC 8	679	698	752 ⁽²⁾	262	300 ⁽²⁾
LC1e for HLZC 9 ⁽³⁾	675	698		262	

Notes:

- (1) See Table A.4-8 for the description of the LCs.
- (2) The temperature limits are from NUREG-1536 [A.4-1].
- (3) DSC in the upper compartment is modeled per HLZC 9, whereas DSC in the lower compartment is modeled per HLZC 8 as discussed in Section A.4.4.4.1.
- (4) According to the sensitivity study in Section A.4.4.3.5, the maximum concrete temperatures are added by 9 °F for conservatism.

Proprietary Information on Pages A.4-48 through A.4-51
Withheld Pursuant to 10 CFR 2.390

Table A.4-14
EOS-37PTH DSC in Updated HSM-MX, Design Load Cases for Storage
Conditions with HLZC 7

Load Case	Operating Condition	Description	Mesh	Ambient Temperature (°F)
1e-S	Normal		Base	100 ⁽¹⁾
1f-S			Fine	
2-S	Off-Normal		Base	117 ⁽¹⁾
3-S ⁽²⁾	Accident		Base	117 ⁽¹⁾

Notes:

- (1) Daily average temperatures are used as noted in Section A.4.3.
- (2) Initial temperatures are taken from steady-state results of Load Case 2-S.

Proprietary Information on This Page
Withheld Pursuant to 10 CFR 2.390

Table A.4-16
Maximum Fuel Cladding and Concrete Temperatures for Storage Conditions of EOS-37PTH DSC in Updated HSM-MX with HLZC 7

Load Case ⁽¹⁾	Description	Max Fuel Cladding Temperature (°F)			Concrete Temperature (°F)	
		Upper Compartment	Lower Compartment	Limit	Maximum ⁽⁴⁾	Limit
1e		676	708	752 ⁽²⁾	264	300 ⁽²⁾
1e-S		680	704		261	
		4	-4		-3	
2		653	696	1058 ⁽²⁾	254	
2-S		648	685		245	
		-5	-11		-9	
3		724	777		362	
3-S		699	770		355	500 ⁽³⁾
		-25	-7		-7	

Notes:

- (1) See Table A.4-1 and Table A.4-14 for the description of the LCs.
- (2) The temperature limits are from NUREG-1536 [A.4-1].
- (3) The temperature limit for concrete at accident condition is 500 °F. The maximum concrete temperature for accident conditions is above the 350 °F limit given in ACI 349-06 [A.4-4]. Testing will be performed, as described in Chapter A.8, Section A.8.2.1.3.

Proprietary Information on Pages A.4-55 through A.4-59
Withheld Pursuant to 10 CFR 2.390

Table A.4-23
Maximum Fuel Cladding and Concrete Temperatures for Storage
Conditions of EOS-37PTH DSC in Updated HSM-MX with HLZCs 8 and 9

Load Case ⁽¹⁾	Max Fuel Cladding Temperature (°F)			Concrete Temperature (°F)	
	Upper Compartment	Lower Compartment	Limit	Maximum	Limit
LC 1e-S for HLZC 8	682	694	752 ⁽²⁾	256	300 ⁽²⁾
LC 1e-S for HLZC 9 ⁽³⁾	677	694		252	

Notes:

- (1) See Table A.4-22 for the description of the LCs.
- (2) The temperature limits are from NUREG-1536 [A.4-1].
- (3) DSC in the upper compartment is modeled per HLZC 9, whereas DSC in the lower compartment is modeled per HLZC 8 as discussed in Section A.4.4.4.1.

Proprietary Information on Pages A.4-61 through A.4-121
Withheld Pursuant to 10 CFR 2.390

APPENDIX A.5 CONFINEMENT

There is no change to the confinement assessment documented in Chapter 5 due to the addition of the NUHOMS® MATRIX.

APPENDIX A.6 SHIELDING EVALUATION

Table of Contents

A.6	SHIELDING EVALUATION.....	A.6-1
A.6.1	Discussions and Results	A.6-2
A.6.2	Source Specification.....	A.6-4
A.6.2.1	Computer Programs	A.6-4
A.6.2.2	PWR and BWR Source Terms.....	A.6-4
A.6.2.3	Axial Source Distributions and Subcritical Neutron Multiplication.....	A.6-4
A.6.2.4	Control Components	A.6-4
A.6.2.5	Blended Low Enriched Uranium Fuel	A.6-4
A.6.2.6	Reconstituted Fuel	A.6-4
A.6.2.7	Irradiation Gases	A.6-4
A.6.3	Model Specification.....	A.6-5
A.6.3.1	Material Properties.....	A.6-5
A.6.3.2	MCNP Model Geometry for the EOS-TC	A.6-5
A.6.3.3	MCNP Model Geometry for the HSM-MX.....	A.6-5
A.6.4	Shielding Analysis	A.6-8
A.6.4.1	Computer Codes.....	A.6-8
A.6.4.2	Flux-to-Dose Rate Conversion	A.6-8
A.6.4.3	EOS-TC Dose Rates	A.6-8
A.6.4.4	HSM-MX Dose Rates	A.6-8
A.6.5	Supplemental Information	A.6-11
A.6.5.1	References.....	A.6-11

List of Tables

Table A.6-1	HSM-MX Key As-Modeled Dimensions (Inches)	A.6-12
Table A.6-2	HSM-MX Dose Rate Results (mrem/hr)	A.6-13
Table A.6-3	HSM-MX Primary Gamma Average Fluxes and Dose Rates, Normal Conditions	A.6-14
Table A.6-4	HSM-MX Secondary Gamma Average Fluxes and Dose Rates, Normal Conditions	A.6-16
Table A.6-5	HSM-MX Neutron Average Fluxes and Dose Rates, Normal Conditions	A.6-18
Table A.6-6	HSM-MX Primary Gamma Flux from the EOS-89BTH DSC, Accident Conditions	A.6-19
Table A.6-7	HSM-MX Secondary Gamma Flux from the EOS-89BTH DSC, Accident Conditions	A.6-21
Table A.6-8	HSM-MX Neutron Flux from the EOS-89BTH DSC, Accident Conditions	A.6-23

List of Figures

Figure A.6-1	HSM-MX MCNP Single-Reflection Model, X-Y View	A.6-24
Figure A.6-2	HSM-MX MCNP Single-Reflection Model, Z-Y View through Lower Compartment.....	A.6-25
Figure A.6-3	HSM-MX MCNP Single-Reflection Model, Z-Y View through Upper Compartment.....	A.6-26
Figure A.6-4	HSM-MX MCNP Single-Reflection Model, X-Z Views	A.6-27
Figure A.6-5	HSM-MX MCNP Double-Reflection Model.....	A.6-28
Figure A.6-6	HSM-MX MCNP Triple-Reflection Model.....	A.6-29
Figure A.6-7	Dose Reduction Hardware	A.6-30
Figure A.6-8	HSM-MX MCNP Array Expansion Model	A.6-31
Figure A.6-9	HSM-MX MCNP Array Expansion Model, Accident Configuration	A.6-32
Figure A.6-10	HSM-MX Key Dose Rate Results	A.6-33

A.6 SHIELDING EVALUATION

The radiation shielding evaluation for the NUHOMS® EOS System for transfer of an EOS dry shielded canister (EOS-DSC) and storage in an EOS horizontal storage module (EOS-HSM) is documented in Chapter 6. The following radiation shielding evaluation addresses the storage of an EOS-DSC in a NUHOMS® MATRIX (HSM-MX). Detailed three-dimensional (3D) dose rate evaluations are performed to determine the dose rate fields around an HSM-MX. These near-field dose rates are used as input to the dose assessment documented in Chapter A.11.

The methodology, source terms, and dose rates presented in this chapter are developed to be reasonably bounding for general licensee implementation of the EOS System. These results may be used in lieu of near-field evaluations by the general licensee, although the inputs utilized in this chapter should be evaluated for applicability by each site. Site-specific HSM-MX near-field evaluations may be performed by the general licensee to modify key input parameters.

Site dose evaluations for the HSM-MX under normal, off-normal, and accident conditions are documented in Chapter A.11, based on the near-field HSM-MX results presented in this chapter. Because the arrangement and the distance to the site boundary is site-specific, compliance with 10 CFR 72.104 and 10 CFR 72.106 for the HSM-MX can only be demonstrated using a site-specific evaluation. Inputs for the site dose evaluations developed in the current chapter may be directly used as input to a site-specific dose evaluation by the general licensee.

A.6.1 Discussions and Results

The following is a summary of the methodology and results of the shielding analysis of HSM-MX. More detailed information is presented in the body of the chapter.

Source Terms

For the HSM-MX, the DSC in the lower compartment is limited to 50.0 kW, while the DSC in the upper compartment is limited to 41.8 kW. PWR heat load zoning configurations (HLZC) 7, 8, and 9 are used with the HSM-MX, as well as boiling water reactor (BWR) HLZC 3. The HLZCs are defined in the Technical Specifications, Figure 1G through Figure 2 [A.6-2].

In the EOS-HSM analysis documented in Chapter 6, Section 6.4.4, it is demonstrated that the vent dose rates are approximately 50% larger for the EOS-89BTH DSC compared to the EOS-37PTH DSC. Because the EOS-HSM and HSM-MX both feature thick concrete shielding with vents and the maximum dose rates occur at the vents, the EOS-89BTH DSC also bounds the EOS-37PTH DSC in the HSM-MX. Therefore, detailed dose rate evaluations are performed only for the EOS-89BTH DSC.

Detailed EOS-89BTH DSC source terms are developed for the EOS-HSM analysis in Section 6.2 for HLZC 1. These source terms are used without modification in the HSM-MX analysis in both the lower and upper compartments. BWR HLZC 1, which has a heat load of 43.6 kW, is conservatively modeled in the upper HSM-MX compartment, although the upper compartment is limited to a lower decay heat. Note that BWR HLZC 1 is not an allowed content for the HSM-MX, as the only BWR HLZC authorized for storage in the HSM-MX is HLZC 3. Utilizing HLZC 1 sources in the HSM-MX adds a large degree of conservatism in the dose rate results, because HLZC 1 accepts stronger sources compared to HLZC 3.

Dose Rates

The EOS-37PTH and EOS-89BTH DSCs are transferred to the HSM-MX using the EOS-TC. The EOS-TC dose rates provided in Chapter 6 are applicable to transfer to the HSM-MX. Therefore, the dose rates reported in this appendix are limited to the HSM-MX.

The Monte Carlo transport code, MCNP5 [A.6-1], is used to compute dose fields around the HSM-MX using detailed 3D models. [

] A summary of the limiting HSM-MX dose rates is provided in Table A.6-2. The dose rate excluding the contribution from the inlet and outlet vents is small, as the dose rates are due primarily to streaming from the vents. The maximum dose rates at the inlet and outlet vents are 1,470 mrem/hr and 993 mrem/hr, respectively. The average dose rate on the front face of the module is 47.0 mrem/hr, and the average dose rate on the roof above the vent covers is 141 mrem/hr. The dose rate at the door centerline is 1.97 mrem/hr. The fluxes and dose rates on the surface of the HSM-MX are used as input to a generic site dose evaluation documented in Chapter A.11.

The shielding effectiveness of the HSM-MX is not affected by any off-normal events. The following geometry changes may occur in an accident:

- Loss of outlet vent covers
- Loss of dose reduction hardware
- Damage to interior walls due to missile impact when the HSM-MX is in the construction joint expansion configuration with the removable end shield wall absent

10 CFR 72.106 limits the dose to an individual at the site boundary to be less than 5 rem due to an accident. Monte Carlo N-Particle (MCNP) cases are developed for the HSM-MX, in which all vent covers and dose reduction hardware are absent, which is not credible. An MCNP case is also developed for a missile impact when the HSM-MX is in the construction joint expansion configuration with the removable end shield wall absent. In this configuration, it is conservatively assumed that two interior walls are penetrated. The HSM-MX accident increases the average dose rate on the front, roof, and end of the module to 92.9 mrem/hr, 4,730 mrem/hr, and 425 mrem/hr, respectively. The fluxes and dose rates on the surface of the HSM-MX in an accident condition are used as input to an accident site dose evaluation documented in Chapter A.11.

A.6.2 Source Specification

Source term information in Section 6.2 is applicable to the HSM-MX evaluation.

A.6.2.1 Computer Programs

No change to Section 6.2.1.

A.6.2.2 PWR and BWR Source Terms

The EOS-89BTH DSC bounds the EOS-37PTH DSC for storage in the EOS-HSM, see the discussion in Section 6.4.4. Because the EOS-HSM and HSM-MX both feature thick concrete shielding with vents and the maximum dose rates occur at the vents, the EOS-89BTH DSC also bounds the EOS-37PTH DSC in the HSM-MX. Therefore, detailed HSM-MX dose rate evaluations are performed only for the EOS-89BTH DSC.

Detailed EOS-89BTH DSC source terms are developed for the EOS-HSM analysis in Section 6.2 for HLZC 1. These source terms are provided in Table 6-27 through Table 6-29 and maximize the dose rates at the vents. These source terms are used without modification in the HSM-MX analysis in both the lower and upper compartments. BWR HLZC 1, which has a heat load of 43.6 kW, is conservatively modeled in the upper HSM-MX compartment, although the upper compartment is limited to 41.8 kW. Note that BWR HLZC 1 is not an allowed content for the HSM-MX, because the only BWR HLZC authorized for storage in the HSM-MX is HLZC 3. Utilizing HLZC 1 sources in the HSM-MX adds a large degree of conservatism in the dose rate results, because HLZC 1 accepts stronger sources compared to HLZC 3.

A.6.2.3 Axial Source Distributions and Subcritical Neutron Multiplication

No change to Section 6.2.3.

A.6.2.4 Control Components

No change to Section 6.2.4.

A.6.2.5 Blended Low Enriched Uranium Fuel

No change to Section 6.2.5.

A.6.2.6 Reconstituted Fuel

No change to Section 6.2.6.

A.6.2.7 Irradiation Gases

No change to Section 6.2.7.

A.6.3 Model Specification

MCNP5 is used to perform detailed 3D near-field dose rate evaluations for the HSM-MX. All relevant details of the EOS-89BTH DSC and HSM-MX are modeled explicitly.

Separate primary gamma and neutron models are developed. The HSM-MX neutron models are run in coupled neutron-photon mode so that the secondary gamma dose rate from (n, γ) reactions may be computed. The secondary gamma dose rates from the HSM-MX are negligible but are computed for completeness.

The treatment of subcritical neutron multiplication is suppressed in MCNP by using the NONU card. This is done because the fuel assemblies are modeled as fresh fuel and homogenized for simplicity, which would cause inaccurate treatment of subcritical neutron multiplication by MCNP. Subcritical neutron multiplication is accounted for in the neutron source magnitude.

A.6.3.1 Material Properties

The HSM-MX models use the same material properties documented in Section 6.3.1 with the exception of the concrete density. Concrete used in the HSM-MX is modeled without steel rebar at a conservatively low density of 138 pcf (2.22 g/cm³) compared to 140 pcf (2.24 g/cm³) for the EOS-HSM.

A.6.3.2 MCNP Model Geometry for the EOS-TC

The EOS-TC models documented in Section 6.3.2 are applicable for transfer to the HSM-MX.

A.6.3.3 MCNP Model Geometry for the HSM-MX

Detailed HSM-MX MCNP models are developed for an EOS-89BTH DSC in the upper and lower compartments. The EOS-89BTH DSC models developed in Section A.6.3.2 are used without modification in the HSM-MX models. BWR source terms are as described in Section A.6.2.2.

The HSM-MXs are modeled explicitly, including the inlet (front) and outlet (roof) vents. The lower compartment features a single horizontal inlet vent at ground level directly under the DSC, while the upper compartment features two vertical inlet vents that are located between the lower compartments. Key dimensions used to develop the HSM-MX models are summarized in Table A.6-1, and figures illustrating the MCNP models with key features labeled are provided in Figure A.6-1 through Figure A.6-6.

The HSM-MX is a monolithic design of two tiers of DSCs. The length of the monolith is arbitrary and determined by the customer. The roof is integral to the HSM-MX, as well as the end shield walls and the rear shield wall. The monolith may be either a single row or a double row (i.e., back-to-back arrangement).

The minimum thickness of the roof is 4 feet 2 inches. The minimum thickness of the integral end shield wall is 3 feet 8 inches. The minimum thickness of the optional removable end shield wall is 3 feet. In the single-row design, the thickness of the integral rear shield wall is 3 feet 8 inches. In the back-to-back design, the wall thickness between rows is 2 feet 6 inches.

Air inlet vents are located on the front and air outlet vents are located on the roof. Because little radiation directly penetrates the thick concrete shielding, essentially all of the dose rate is due to gamma radiation streaming from the vents. Radiation streaming through the outlet vents is mitigated by the use of vent covers, see Figure A.6-1. Under normal and off-normal conditions the vent covers are always in place.

The baseline MCNP configuration features an HSM-MX with a rear shield wall. On the left side (-x direction) an end shield wall is modeled, while on the right side (+x direction) a mirror boundary is modeled at the centerline of the DSC in the upper compartment, see Figure A.6-1 through Figure A.6-4. The length of the DSC is in the z-direction. This configuration is used to compute dose rates and fluxes on the end shield wall.

A second MCNP configuration features mirror boundaries on both the left and right sides of the model through the centerline of the DSCs in the lower compartments, although the rear shield wall is modeled explicitly, see Figure A.6-5. This configuration is used to simulate the interior region of a single row and is used to compute dose rates and fluxes on the rear shield wall.

A third MCNP configuration features mirror boundaries on the left, right, and rear of the model, see Figure A.6-6. This configuration is used to simulate the interior region of a double row (i.e., back-to-back arrangement) and is used to compute front and roof vent dose rates, as well as average front and roof dose rates and fluxes.

[

]

When an HSM-MX is to be expanded in the future, construction may be terminated at a construction joint and a 3 feet thick removable end shield wall is attached. The two complete compartments (one upper and one lower) nearest the end must remain empty when the HSM-MX is loaded, as indicated in Figure A.6-8. This configuration is explicitly modeled to determine the end dose rate when the removable end shield wall is absent. If an array to be expanded terminates at an expansion joint rather than a construction joint, the two compartments (one upper and one lower) nearest the end wall must remain empty. End dose rates for this configuration are bounded by the construction joint option with the end shield wall removed.

ADVANTG [A.6-3] is used to develop weight windows to accelerate problem convergence for all models.

The average fluxes on the faces of the HSM-MX are used as input to a generic site dose evaluation that is documented in Chapter A.11. These average fluxes are computed on the surface of a box that envelops the HSM-MX model, including the vent covers and door.

[

]

A.6.4 Shielding Analysis

A.6.4.1 Computer Codes

MCNP5 v1.40 is used in the shielding analysis [A.6-1]. MCNP5 is a Monte Carlo transport program that allows full 3D modeling of the HSM-MX. Therefore, no geometrical approximations are necessary when developing the shielding models.

A.6.4.2 Flux-to-Dose Rate Conversion

No change to Section 6.4.2.

A.6.4.3 EOS-TC Dose Rates

No change to Section 6.4.3.

A.6.4.4 HSM-MX Dose Rates

The maximum dose rate at the roof outlet vent is 993 mrem/hr. The maximum dose rate at the lower compartment inlet vent is 1,470 mrem/hr, while the maximum dose rate at the upper compartment inlet vent is 1,350 mrem/hr.

The total dose rate is dominated by primary gammas, while the dose rate from neutrons and secondary gammas is negligible. The bulk shielding of the HSM-MX is very effective in the absence of streaming. The average dose rate on the rear and end (side) shield walls is 0.484 mrem/hr and 0.632 mrem/hr, respectively. The dose rate at the door centerline is 1.97 mrem/hr. These surfaces do not contain streaming paths, although the average rear and end dose rates are computed to the top of the vent covers and include contribution from the roof vents. The average dose rate on the front face of the module is 47.0 mrem/hr, and the average dose rate on the roof above the vent covers is 141 mrem/hr.

Input for Site Dose Evaluation

The average dose rate and flux on the surface of the HSM-MX is of interest for use in the generic site dose evaluations. The site dose evaluations are documented in Chapter A.11, although the inputs to the site dose evaluation are obtained from the HSM-MX evaluations described in the current chapter.

[

]

Average fluxes and dose rates on the end, rear, front, and roof of the HSM-MX with the EOS-89BTH DSC are reported in Table A.6-3, Table A.6-4, and Table A.6-5, for primary gamma, secondary gamma, and neutron radiation, respectively. These dose rates and fluxes are applicable to normal and off-normal conditions.

[

]

Expansion Considerations

As shown in Figure A.6-8, when an array is in the construction joint expansion configuration, the two complete compartments (one upper and one lower) at the end of the module must remain empty. A removable end shield wall is attached. These empty compartments are required to maintain low dose rates when the removable end shield wall is absent during subsequent construction activities. If an array to be expanded terminates at an expansion joint rather than a construction joint, the two compartments (one upper and one lower) nearest the end wall must remain empty. End dose rates for this configuration are bounded by the construction joint option with the end shield wall removed.

Use of Low-Density Grout for HSM-MX Repair

[

]

A.6.5 Supplemental Information

A.6.5.1 References

- A.6-1 Oak Ridge National Laboratory, “MCNP/MCNPX – Monte Carlo N-Particle Transport Code System Including MCNP5 1.40 and MCNPX 2.5.0 and Data Libraries,” CCC-730, RSICC Computer Code Collection, January 2006.
- A.6-2 CoC 1042 Appendix A, NUHOMS® EOS System Generic Technical Specifications, Amendment 1.
- A.6-3 ADVANTG – An Automated Variance Reduction Parameter Generator, Oak Ridge National Laboratory, August 2015.

Proprietary Information on Pages A.6-12 through A.6-33
Withheld Pursuant to 10 CFR 2.390

APPENDIX A.7

CRITICALITY EVALUATION

There is no change to the criticality evaluation documented in Chapter 7 due to the addition of the NUHOMS[®] MATRIX.

APPENDIX A.8 MATERIALS EVALUATION

Table of Contents

A.8 MATERIALS EVALUATION	A.8-1
A.8.1 General Information	A.8-2
A.8.1.1 HSM-MX Materials	A.8-2
A.8.1.2 Environmental Conditions	A.8-2
A.8.1.3 Engineering Drawings	A.8-2
A.8.2 Materials Selection	A.8-3
A.8.2.1 Applicable Codes and Standards and Alternatives	A.8-3
A.8.2.2 Material Properties	A.8-4
A.8.2.3 Materials for ISFSI Sites with Experience of Atmospheric Chloride Corrosion	A.8-5
A.8.2.4 Weld Design and Inspection	A.8-5
A.8.2.5 Galvanic and Corrosive Reactions	A.8-6
A.8.2.6 Creep Behavior of Aluminum	A.8-6
A.8.2.7 Bolt Applications	A.8-7
A.8.2.8 Protective Coatings and Surface Treatments	A.8-7
A.8.2.9 Neutron Shielding Materials	A.8-7
A.8.2.10 Materials for Criticality Control	A.8-7
A.8.2.11 Concrete and Reinforcing Steel	A.8-7
A.8.2.12 Seals	A.8-7
A.8.2.13 Low Temperature Ductility of Ferritic Steels	A.8-7
A.8.3 Fuel Cladding	A.8-8
A.8.4 Prevention of Oxidation Damage During Loading of Fuel	A.8-9
A.8.5 Flammable Gas Generation	A.8-10
A.8.6 DSC Closure Weld Testing	A.8-11
A.8.7 References	A.8-12

List of Tables

Table A.8-1	HSM-MX Materials	A.8-13
Table A.8-2	Material Properties, ASTM A572 Grade 50 Steel	A.8-14
Table A.8-3	Material Properties, ASTM A992 Grade 50	A.8-15
Table A.8-4	Material Properties, ASTM A588.....	A.8-16

A.8 MATERIALS EVALUATION

This chapter only provides the material evaluation for the NUHOMS[®] MATRIX (HSM-MX) in accordance with the guidance outlined in NUREG-1536, Revision 1 [A.8-1]. There are no changes to the materials evaluation of other components in the NUHOMS[®] EOS System in Chapter 8.

A.8.1 General Information

A.8.1.1 HSM-MX Materials

Steel materials employed in the various components of the HSM-MX, particularly those that are relied on for structural integrity, are based on American Society for Testing and Materials (ASTM) and American Society of Mechanical Engineers (ASME) specifications. Horizontal storage module (HSM) concrete is based on American Concrete Institute (ACI) specifications.

A.8.1.2 Environmental Conditions

The dry shielded canister (DSC) and NUHOMS® MATRIX (HSM-MX) are exposed to the ambient weather conditions at the licensee site for the duration of the licensing period. Depending on the licensee local conditions, the environment may include chloride aerosols, precipitation, and freezing temperatures. The monolith roof, front wall, door, sides, rear (for single row arrays) and shield walls (if applicable) of the HSM-MX concrete are directly exposed to the weather. The HSM-MX interior, and the DSC exterior surfaces are sheltered from direct effects of weather, though moisture and aerosols present in the air pass through the HSM-MX interior via natural convection. Material temperatures of the storage system components are presented in Chapter A.4.

During storage, the interior of the DSC is exposed to an inert helium environment. The DSC is vacuum-dried and backfilled with helium after loading the fuel and welding the inner top cover plate.

The DSC and TC are unchanged from the NUHOMS® EOS System; therefore, there are no changes to the environmental conditions relative to the DSC and TC discussed in Section 8.1.2.

A.8.1.3 Engineering Drawings

The drawings for HSM-MX are provided in Chapter A.1, Section A.1.3. The material specification, governing code, and quality category are specified in the parts list for each component.

There are no changes to the EOS-37PTH, EOS-89BTH and TC drawings provided in Chapter 1, Section 1.3.

A.8.2 Materials Selection

This section discusses the materials used in the HSM-MX components. Table A.8-1 summarizes the materials selected for HSM-MX. Materials utilized in the HSM-MX are largely the same as those used in the EOS-HSM, and the materials for the EOS-DSCs and EOS-TCs have not changed. Therefore, the tables described in Section 8.2 also applicable to HSM-MX. Temperature-dependent mechanical and thermal properties for the materials listed in Table A.8-1 are presented in Table A.8-2 through Table A.8-4.

A.8.2.1 Applicable Codes and Standards and Alternatives

A.8.2.1.1 EOS-37PTH and EOS-89BTH DSC

No change from Section 8.2.1.1.

A.8.2.1.2 EOS-TC Transfer Cask

No change from Section 8.2.1.2.

A.8.2.1.3 HSM-MX Horizontal Storage Module

The applicable codes for the HSM-MX are:

- Concrete construction per ACI-318-08 [A.8-4].
- Concrete Design per ACI-349-06 [A.8-5].
- DSC Support design per AISC Manual of Steel Construction [A.8-7].

Cement, aggregate, reinforcing steel, and steel structures conform to ASTM specifications.

The HSM-MX concrete subcomponents are designed and constructed using a specified 28-day compressive strength of 5,000 psi, normal weight concrete. The cement is Type II or Type III Portland cement meeting the requirements of ASTM C150. The concrete aggregate meets the specifications of ASTM C33. The reinforcing steel is ASTM A615 or A706 Gr. 60 deformed bars placed vertically and horizontally at each face of the walls, roof and slabs.

The concrete surface temperature limits criteria are based on the provisions in Section 3.5.1.2 of NUREG-1536, as follows:

- If concrete temperatures in general or local areas are at or below 200 °F for normal/off-normal conditions/occurrences, no tests to prove capability at elevated temperatures or reduction of concrete strength are required.
- If concrete temperatures, in general, or local areas exceed 200 °F, but do not exceed 300 °F, no tests to prove capability at elevated temperatures or reduction of concrete strength are required if the aggregates have a coefficient of thermal expansion (CTE) no greater than 6×10^{-6} in/in/°F, or are one of the following materials: limestone, dolomite, marble, basalt, granite, gabbro, or rhyolite.

The above criteria in lieu of the ACI 349-06 requirements do not extend above 300 °F for normal/off-normal conditions and do not modify the ACI 349-06 requirements for accident conditions. Per E.4.2 of ACI 349-06 [A.8-5], the accident conditions or short-term period (i.e., blocked vent accident transient) concrete temperatures are limited to 350 °F. Higher temperatures are allowed per E.4.3 if tests are provided to evaluate the reduction in strength and this reduction is applied to design allowables. HSM-MX concrete compressive tests are performed on specimens heated to or above that maximum accident temperature for no less than 40 hours. HSM-MX concrete temperature testing is performed whenever there is a significant change in the cement, aggregate, or water-cement ratio of the concrete mix design. See Section 5.3 of the Technical Specifications [A.8-17].

Alternatively, per the ACI 349-13 [A.8-10] commentary Section RE.4, the specified 28-day compressive strength can be increased to 7,000 psi for HSM fabrication, in lieu of the above aggregate types or coefficient of thermal expansion requirements, so that any losses in properties (e.g., compressive strength, modulus of elasticity) resulting from long-term thermal exposure will not affect the safety margins based on the specified 5,000 psi compressive strength used in the design evaluations. Additionally, also as indicated in Section RE.4, short, randomly oriented steel fibers may be used to provide increased ductility, dynamic strength, toughness, tensile strength, and improved resistance to spalling. See Section 4.4.4 of the Technical Specifications [A.8-17].

The rear DSC supports consists of a W6 x 25 structural beam of ASTM A992 Gr.50 material or equivalent built-up I-Beam of ASTM A572 Gr. 50 material coated with an inorganic zinc-rich primer and a high-build epoxy enamel finish. The DSC rests on an ASTM A240 Type 304 support plate welded to the beam. A corrosion allowance of 1/16 inch is used in the design calculations. Welding procedures are in accordance with ASME Code Section IX or AWS D1.1 [A.8-11].

At coastal sites with operational experience of corrosion due to atmospheric chlorides, the front and rear DSC supports steel and weld filler metal have a minimum of 0.20% copper content or are stainless steel. For carbon steels, weld material with 1% or more nickel is acceptable in lieu of 0.20% copper content. The copper content is equivalent to weathering steel [A.8-12], and nickel-bearing weld materials show equivalent corrosion resistance [A.8-13].

A.8.2.2 Material Properties

The material properties used in the HSM-MX design analyses are listed in Table 8-4 through Table 8-6, Table 8-13, Table 8-23, and Table 8-24. Additionally, new materials used in the HSM-MX are provided in Table A.8-2 through Table A.8-4. Each table cites the source for the properties. Table A.8-1 ties these materials to the individual components.

A.8.2.2.1 EOS-37PTH and EOS-89BTH DSC

No change from Section 8.2.2.1.

A.8.2.2.2 EOS TC Transfer Cask

No change from Section 8.2.2.2.

A.8.2.2.3 HSM-MX Horizontal Storage Module

In accordance with ACI 349-06, Section E.4.3, the strength properties of the concrete and reinforcing steel used in the HSM-MX structural analysis are taken at the maximum calculated temperature. Temperature-dependent mechanical properties of concrete and reinforcing steel are taken from [A.8-3] and presented in Table 8-23, and Table 8-24.

The material properties of the ASTM A992 Gr 50 steel used for the rear DSC support are listed in Table A.8-3, and the material properties for the ASTM A572 Gr. 50 front and rear stop plate and optional built-up I-beam are listed in Table A.8-2. The material properties used for the Type 304 stainless steel used for the front DSC supports and heat shields are provided in Table 8-5. The material properties used for the Type 316 stainless steel used as an option for the front DSC supports and heat shields are listed in Table 8-5.

The properties ASTM A588 for the axial retainer is provided in Table A.8-4.

A.8.2.2.4 NUHOMS® EOS System Materials Employed in the Shielding Analysis

Shielding properties of steel and concrete are obtained from [A.8-6] and are summarized in Table 8-30. Concrete used in the HSM-MX is modeled without steel rebar at a density of 138 pcf (2.211 g/cm³).

A.8.2.2.5 NUHOMS® EOS System Materials Employed in the Criticality Analysis

No change to Section 8.2.2.5.

A.8.2.3 Materials for ISFSI Sites with Experience of Atmospheric Chloride Corrosion

Front and rear DSC supports at sites with operational experience of corrosion caused by atmospheric chlorides are fabricated from steels equivalent to weathering steel or stainless steel.

A.8.2.4 Weld Design and Inspection

There are no changes to the weld design and inspection for the DSC and TC described in Section 8.2.4.

The rear DSC supports are bolted inside the HSM. The welds of the rear DSC supports are designed in accordance with the Manual of Steel Construction [8-7], and visually inspected in accordance with AWS D1.1 with acceptance criteria for statically loaded, non-tubular structures.

A.8.2.5 Galvanic and Corrosive Reactions

A.8.2.5.1 Behavior of Aluminum and Neutron Absorbers in Water and Boric Acid

No change to Section 8.2.5.1.

A.8.2.5.2 Behavior of Stainless Steel in Deionized Water and Weak Boric Acid

No change to Section 8.2.5.2.

A.8.2.5.3 Behavior of Low-Alloy Steel in Deionized Water and Weak Boric Acid

No change to Section 8.2.5.3.

A.8.2.5.4 Lubricants and Cleaning Agents

No change to Section 8.2.5.4.

A.8.2.5.5 Corrosion of Canister Shell During Storage

No change to Section 8.2.5.4.

A.8.2.5.6 Corrosion of DSC Front and Rear Supports

The DSC front and rear supports are protected from direct exposure to precipitation, and are exposed only to the humidity and aerosols in the cooling air that flows through the HSM-MX. Exposed surfaces are coated with an inorganic zinc-rich rimer and high build epoxy enamel finish or galvanized, except for the stainless steel contact plates. The front DSC support is a stainless steel contact plate that sits atop a galvanized steel plate. Epoxy enamels such as Carboguard® 890 are suitable for continuous service to 300 °F, while inorganic zinc primers such as Carbozinc 11 have much higher temperature resistance. The maximum temperature on the rear DSC supports is about 270 °F. The top coat is expected to experience chalking and other effects of radiation over 10^6 rad, but the inorganic primer coat is insensitive to radiation. Inspections for license extension [A.8-15, A.8-16] have found only minor local rusting. Nonetheless, the stress analysis removes 1/16 inch from all surfaces to account for corrosion. At independent spent fuel storage installations (ISFSIs) with operational experience of corrosion with atmospheric chlorides, additional protection is provided by specifying a minimum 0.2% copper content, which results in an adherent self-protecting oxide layer equivalent to weathering steel [A.8-12].

A.8.2.5.7 Corrosion of Transfer Cask

No change to Section 8.2.5.7.

A.8.2.6 Creep Behavior of Aluminum

No change to Section 8.2.6.

A.8.2.7 Bolt Applications

No change to Section 8.2.7.

A.8.2.8 Protective Coatings and Surface Treatments

No change to Section 8.2.8.

A.8.2.9 Neutron Shielding Materials

No change to Section 8.2.9.

A.8.2.10 Materials for Criticality Control

No change to Section 8.2.10.

A.8.2.11 Concrete and Reinforcing Steel

No change to Section 8.2.11.

A.8.2.12 Seals

No change to Section 8.2.12.

A.8.2.13 Low Temperature Ductility of Ferritic Steels

No change to Section 8.2.13.

A.8.3 Fuel Cladding

No change to Section 8.3.

A.8.4 Prevention of Oxidation Damage During Loading of Fuel

No change to Section 8.4.

A.8.5 Flammable Gas Generation

No change to Section 8.5.

A.8.6 DSC Closure Weld Testing

No change to Section 8.6.

A.8.7 References

- A.8-1 NUREG-1536, “Standard Review Plan for Spent Fuel Dry Storage Systems at a General license Facility,” Revision 1, U.S. Nuclear Regulatory Commission, July 2010.
- A.8-2 American Society of Mechanical Engineers, ASME Boiler and Pressure Vessel Code, 2010 Edition with 2011 Addenda.
- A.8-3 Mark Fintel, “Handbook of Concrete Engineering,” September 1974.
- A.8-4 ACI-318-08, “Building Code Requirement for Structural Concrete and Commentary,” American Concrete Institute.
- A.8-5 American Concrete Institute, “Code Requirements for Nuclear Safety Related Concrete Structures”, ACI-349-06.
- A.8-6 PNNL-15870, Re. 1, “Compendium of Material Composition Data for Radiation Transport Modeling,” Pacific Northwest National Laboratory, March 2011.
- A.8-7 American Institute of Steel Construction, Manual of Steel Construction, 13th Edition or 14th Edition.
- A.8-8 Mark Fintel, “Handbook of Concrete Engineering, Second Edition,” September 1985.
- A.8-9 ASTM A572/A572M, “Standard Specification for High-Strength Low-Alloy Columbium-Vanadium Structural Steel,” Latest Edition.
- A.8-10 ACI-349-13, “Code Requirements for Nuclear Safety Related Concrete Structures and Commentary,” American Concrete Institute.
- A.8-11 American Welding Society, AWS D1.1, March 2010, Structural Welding Code-Steel.
- A.8-12 []
- A.8-13 C. P. Larrabee, S. K. Coburn, “The Atmospheric Corrosion of Steels as Influenced by Changes in Chemical Composition,” First International Congress on Metallic Corrosion, 1962
- A.8-14 ASTM A992, “Standard Specification for Structural Steel Shapes.”
- A.8-15 Duke Energy Carolinas, LLC, Oconee Nuclear Station, Docket No. 72-4, License No. SNM-2503, License Renewal Application for the Site-Specific Independent Spent Fuel Storage Installation (ISFSI) - Response to Requests for Additional Information, License Amendment Request No. 2007-06, ADAMS ML090370066, January 30, 2009 (Response to Question A-4).
- A.8-16 Calvert Cliffs Nuclear Power Plant, Independent Spent Fuel Storage Installation, Material License No. SNM-2505, Docket No. 72-8, Response to Request for Supplemental Information, RE: Calvert Cliffs Independent Spent Fuel Storage Installation License Renewal Application (TAC No. L24475), ADAMS ML12212A216, July 27, 2012.
- A.8-17 CoC 1042 Appendix A, NUHOMS® EOS System Generic Technical Specifications, Amendment 1.

A.8-18 ASTM A588/A588M, "Standard Specification for High-Strength Low-Alloy Structural Steel, up to 50 ksi [345 MPa] Minimum Yield Point, with Atmospheric Corrosion Resistance."

Table A.8-1
HSM-MX Materials

HSM Subcomponents	Material
HSM-MX walls, roof, floor, end shield walls	Reinforced concrete with ASTM A615 or A706 Gr 60 reinforcing steel
DSC Support Pedestal	ASTM A992 Gr. 50 or ASTM A572 Gr. 50
DSC Support Pedestal Stop Plate	ASTM A572 Gr. 50
DSC Support Pedestal Support Plate	ASTM A240 Type 304 or 316
HSM-MX Door	Reinforced concrete
Door Steel Liner Assembly	Steel
Threaded Inserts	Steel
Inspection Penetration Sleeve Door	Steel
Axial Retainer Rod	ASTM A588
Axial Retainer miscellaneous plate (fastener plate, spacer plate)	Steel
HSM-MX Heat Shields	Stainless steel ASTM A240 Type 304 or 316
HSM-MX Outlet Vent Cover	Reinforced concrete
HSM-MX Outlet Vent Liners	Carbon Steel
HSM Inlet Vent Screen Assembly	Carbon Steel
Bird Screens and Dose Reduction Hardware	Stainless steel or Carbon Steel
Fasteners:	
Bolts	ASTM A193 Gr B7/ A325/A563/A490/A108
Washers	ASTM A36/F436/F844/ Stainless Steel
Nuts	ASTM A194/A563/A194/ Carbon Steel
Threaded Embedments:	
Stud Bolt	ASTM A193-Gr. B7, ASTM A193-B8 CL 2 or ASTM A193-B8M CL 2
Sleeve Nut	ASTM A194 Gr 2H or A563 Gr A
Nut	ASTM A194 Gr 8M or A563 Gr A

Table A.8-2
Material Properties, ASTM A572 Grade 50 Steel

Temp (°F)	E ⁽²⁾ (10 ³ ksi)	S _y ⁽³⁾ (ksi)	S _u ⁽⁴⁾ (ksi)	α_{AVG} ⁽⁵⁾ (10 ⁻⁶ °F ⁻¹)	ρ (lb/in ³) ⁽⁶⁾
-20					0.280
70	29.0 ⁽⁷⁾	50.0 ⁽¹⁾	65.0 ⁽¹⁾		
100	29.0	48.5	65.0	6.3	
150					
200	28.4	46.0	63.7	6.5	
250					
300	27.8	44.0	65.0	6.7	
350					
400	27.3	42.5	65.0	6.9	
450					
500	26.7	41.5	65.0	7.1	
550					
600	26.1	41.0	62.4	7.2	
650					
700	25.5	40.0	53.3	7.4	

Notes

1. Reference [A.8-9].
2. Based on lowest rate of reduction provided in [A.8-8] Figure 7.5.
3. Based on lowest rate of reduction provided in [A.8-8] Figure 7.3.
4. Based on lowest rate of reduction provided in [A.8-8] Figure 7.4.
5. Based on lowest rate of reduction provided in [A.8-8] Figure 7.6.
6. ASME Section II Part D [A.8-2].
7. Based on AISC, Table B4.1 [A.8-7].

Table A.8-3
Material Properties, ASTM A992 Grade 50

Temp (°F)	E ⁽²⁾ (10 ³ ksi)	Yield Strength ⁽³⁾ (ksi)	Tensile Strength ⁽⁴⁾ (ksi)	ρ ⁽⁵⁾ (lb/in ³)
-20				0.280
70	29.0 ⁽⁶⁾	50.0 ⁽¹⁾	65.0 ⁽¹⁾	
100	29.0	48.5	65.0	
150				
200	28.4	46.0	63.7	
250				
300	27.8	44.0	65.0	
350				
400	27.3	42.5	65.0	
450				
500	26.7	41.5	65.0	

Notes

1. Reference [A.8-14].
2. Based on lowest rate of reduction provided in [A.8-8] Figure 7.5.
3. Based on lowest rate of reduction provided in [A.8-8] Figure 7.3.
4. Based on lowest rate of reduction provided in [A.8-8] Figure 7.4.
5. ASME Section II Part D, Table PRD [A.8-2].
6. Based on AISC, Table B4.1 [A.8-7]

Table A.8-4
Material Properties, ASTM A588

Temp (°F)	E ⁽²⁾ (10³ ksi)	Yield Strength⁽³⁾ (ksi)	Tensile Strength⁽⁴⁾ (ksi)	Density⁽⁵⁾ (lb/in³)
-20				0.280
70	29.0 ⁽⁶⁾	50.0 ⁽¹⁾	70.0 ⁽¹⁾	
100	29.0	48.5	70.0	
150				
200	28.4	46.0	68.6	
250				
300	27.8	44.0	70.0	
350				
400	27.3	42.5	70.0	
450				
500	26.7	41.5	70.0	

Notes

1. Reference [A.8-18].
2. Based on lowest rate of reduction provided in [A.8-8] Figure 7.5.
3. Based on lowest rate of reduction provided in [A.8-8] Figure 7.3.
4. Based on lowest rate of reduction provided in [A.8-8] Figure 7.4.
5. ASME Section II Part D, Table PRD [A.8-2].
6. Based on AISC, Table B4.1 [A.8-7]

APPENDIX A.9 OPERATING PROCEDURES

Table of Contents

A.9	OPERATING PROCEDURES.....	A.9-1
A.9.1	Procedures for Loading the DSC and Transfer to the HSM-MX.....	A.9-2
A.9.1.1	TC and DSC Preparation	A.9-2
A.9.1.2	DSC Fuel Loading	A.9-2
A.9.1.3	DSC Drying and Backfilling.....	A.9-2
A.9.1.4	DSC Sealing Operations	A.9-2
A.9.1.5	TC Downending and Transfer to ISFSI.....	A.9-2
A.9.1.6	DSC Transfer to the HSM-MX.....	A.9-2
A.9.1.7	Monitoring Operations.....	A.9-4
A.9.2	Procedures for Unloading the DSC	A.9-5
A.9.2.1	DSC Retrieval from the HSM-MX.....	A.9-5
A.9.2.2	Removal of Fuel from the DSC	A.9-7
A.9.3	References.....	A.9-8

List of Figures

Figure A.9-1	HSM-MX System Loading Operations	A.9-9
--------------	--	-------

A.9 OPERATING PROCEDURES

This chapter presents the operating procedures for the NUHOMS® MATRIX (HSM-MX) described in previous chapters and shown on the drawings in Chapter A.1, Section A.1.3. The procedures include preparation of the NUHOMS® EOS system dry shielded canister (DSC) and fuel loading, closure of the DSC, transfer to the independent spent fuel storage installation (ISFSI) using the transfer cask (TC), DSC transfer into HSM-MX, monitoring operations, and DSC retrieval from the HSM-MX. The NUHOMS® EOS transfer equipment, MATRIX loading crane (MX-LC), MATRIX retractable roller tray (MX-RRT), and the existing plant systems and equipment are used to accomplish these operations.

The generic NUHOMS® HSM-MX procedures described in this chapter have been developed to minimize the amount of time required to complete the subject operations, to minimize personnel exposure, and to assure that all operations required for DSC loading, closure, transfer, and storage are performed safely. Plant-specific ISFSI procedures are to be developed by each licensee in accordance with the requirements of 10 CFR 72.212(b) and the guidance of Regulatory Guide 3.61 [A.9-4]. These generic procedures are provided as a guide for the preparation of plant-specific procedures and serve to explain how the HSM-MX system operations are to be accomplished. They are not intended to be limiting in that the licensee may judge that alternate acceptable means are available to accomplish the same operational objective.

Pictograms of the HSM-MX System operations are presented in Figure A.9-1. The location of the various operations may vary with individual plant requirements. Chapter A.9 provides a description as to how these operations are to be performed for the HSM-MX system.

See Chapter 1 for description of components.

The generic terms used throughout this section are as follows.

- TC, or transfer cask is used for the TC125 transfer cask.
- DSC is used for the EOS-37PTH DSC or EOS-89BTH DSC.
- HSM-MX is used for the storage module.
- MX-RRT is used to insert/retrieve DSC into/from HSM-MX module.
- MX-LC is used to lift and position DSC with HSM-MX.

Note: If applicable to the planned DSC heat zone loading configuration per Figure 1a - 2 of the Technical Specifications [A.9-5], the forced cooling (FC) system should be verified operational prior to initiating the transfer operations and installed as soon as practical once the cask is on the transfer skid.

A.9.1 Procedures for Loading the DSC and Transfer to the HSM-MX

The following steps describe the recommended operating procedures for HSM-MX system. A pictorial representation of key phases of this process is provided in Figure A.9-1.

A.9.1.1 TC and DSC Preparation

No change. See Section 9.1.1.

A.9.1.2 DSC Fuel Loading

No change. See Section 9.1.2.

A.9.1.3 DSC Drying and Backfilling

No change. See Section 9.1.3.

A.9.1.4 DSC Sealing Operations

No change. See Section 9.1.4.

A.9.1.5 TC Downending and Transfer to ISFSI

No change. See Section 9.1.5.

A.9.1.6 DSC Transfer to the HSM-MX

CAUTION: The insides of empty compartments have the potential for high dose rates due to adjacent loaded compartments. Proper as low as reasonably achievable (ALARA) practices should be followed for operations inside these compartments and in the areas outside these compartments whenever the door from the empty compartment has been removed.

1. MX-LC Rails are installed, aligned and verified on the pad for the loading campaign. Alignment is verified to the specifically designated features on the face of HSM-MX.
2. Prior to transporting the TC to the ISFSI, remove the HSM-MX door, inspect the compartment of the HSM-MX, removing any debris and ready the HSM-MX to receive a DSC. The doors on adjacent compartments should remain in place.
3. Inspect the DSC, and MX-RRT support pads inside HSM-MX compartment.
4. For ALARA purposes, reinstall the HSM-MX door.
5. Inspect the HSM-MX air inlet and outlets to ensure that they are clear of debris. Inspect the screens on the air inlet and outlets for damage.

CAUTION: The insides of empty compartments have the potential for high dose rates due to adjacent loaded compartments. Proper ALARA practices should be followed for operations inside these compartments and in the areas outside these compartments whenever the MX-RRT operations are being performed.

6. Remove the MX-RRT cover plates and shield plugs.
7. Insert and install MX-RRT into HSM-MX. Extend the MX-RRT rollers, secure and verify that the rollers are extended.
8. Transport the TC from the plant's fuel/reactor building to the ISFSI along the designated transfer route.
9. Once at the ISFSI, move the transfer trailer inside the MX-LC at "home" position between the skid and the MX-LC grappling mechanism.
10. Use the MX-LC grappling mechanism to capture the skid along with TC, disengage the skid positioning system, move the skid up in the vertical direction to clear it from the transfer trailer, and then the transfer trailer is moved from MX-LC.
11. Remove the FC system, and install the ram cylinder assembly.
12. Remove the HSM-MX door.
13. Unbolt and remove the TC top cover plate.
14. Move MX-LC along the rail in front of HSM-MX until the TC is completely against the face of HSM-MX.
15. The skid is moved until the target compartment is reached. If necessary, adjust the MX-LC position until the MX-LC is properly aligned with the targeted compartment.
16. Secure the MX-LC/skid/cask to the front wall embeddings of the HSM-MX using the restraints.
17. The hydraulic power unit is connected to the ram cylinder. The grapple is moved until it engages with grapple ring of the canister. Using the ram cylinder, fully insert the DSC into the HSM-MX compartment.
18. Disengage the ram grapple mechanism so that the grapple is retracted away from the DSC grapple ring.
19. Retract the MX-RRT rollers; the DSC is lowered onto the HSM-MX front and rear DSC supports.

Note: The time limit for transfer operations, if any, starts with the initiation of the TC/DSC annulus water draining described in Step 9 of Section 9.1.4 and ends when the DSC is fully seated onto the front and rear DSC supports.

CAUTION: Verify that the applicable time limits for transfer operations of Section 3.1.3 of the Technical Specifications [A.9-5] are met.

20. Remove the wall embedments from the HSM-MX.
21. Retract the skid with TC from docking position and lower it.
22. Place the HSM-MX door. Verify that the HSM dose rates are compliant with the limits specified in Section 5.1.2 of the Technical Specifications [A.9-5].
23. Move MX-LC to its “home” position, and the transfer trailer is moved into accepting position.
24. Lower the Skid along with TC onto the transfer trailer. Reconnect the skid positioning system. Remove the ram cylinder assembly.
25. Bolt the TC cover plate into place, tightening the bolts to the required torque in a star pattern.

CAUTION: The insides of empty compartments have the potential for high dose rates due to adjacent loaded compartments. Proper ALARA practices should be followed for operations inside these compartments and in the areas outside these compartments whenever the MX-RRT operations are being performed.

26. Remove the MX-RRT from the HSM-MX.
27. Place MX-RRT shield plugs and cover plates for the MX-RRT accesses.
28. Move the transfer trailer from MX-LC to the designated equipment storage area. Return the remaining transfer equipment to the storage area.
29. Close and lock the ISFSI access gate and activate the ISFSI security measures.

A.9.1.7 Monitoring Operations

1. Perform routine security surveillance in accordance with the licensee's ISFSI security plan.
2. Perform a daily visual surveillance of the HSM-MX air inlets and outlets (bird screens) to verify that no debris is obstructing the HSM-MX vents in accordance with Section 5.1.3.2(a) of the Technical Specification [A.9-5] requirements, or, perform a temperature measurement for each EOS-HSM in accordance with Section 5.1.3.2(b) of the Technical Specification [A.9-5] requirements.

A.9.2 Procedures for Unloading the DSC

The following section outlines the procedures for retrieving the DSC from the HSM-MX. The procedures for removing the FAs from the DSC are the same as described in Section 9.2.

A.9.2.1 DSC Retrieval from the HSM-MX

1. Ready the TC, transfer trailer, loading crane, and skid for service. Fill the TC liquid neutron shield and remove the top cover plate from the TC. Transport the trailer into the ISFSI.

Note: Verify that a TC spacer of appropriate height is placed inside the TC to provide the correct airflow and interface at the top of the TC during cutting and unloading operations for DSCs that are shorter than the TC cavity length.

2. MATRIX MX-LC rails are installed, aligned and verified on the pad for the unloading campaign. Alignment is verified to the specifically designated features on the face of HSM-MX.
3. Move the transfer trailer inside the MX-LC “home” position between the skid and the MX-LC grappling mechanism.
4. Use the MX-LC grappling mechanism to capture the skid along with TC, disengage the skid positioning system, move the skid up vertically to clear it from the transfer trailer, then move the transfer trailer from the MX-LC.
5. Install the ram cylinder assembly.

CAUTION: The insides of empty compartments have the potential for high dose rates due to adjacent loaded compartments. Proper ALARA practices should be followed for operations inside these compartments and in the areas outside these compartments whenever the MX-RRT operations are being performed.

6. Remove the MX-RRT shield blocks plugs and cover plates.
7. Insert and install MX-RRT into HSM-MX. Extend the MX-RRT rollers, secure and verify that the rollers are extended.

CAUTION: The insides of empty compartments have the potential for high dose rates due to adjacent loaded compartments. Proper ALARA practices should be followed for operations inside these compartments and in the areas outside these compartments whenever the door from the empty compartment has been removed.

8. Remove the HSM-MX door.

9. Unbolt and remove the TC top cover plate.
10. Move MX-LC along the rail in front of HSM-MX until the TC is completely against the face of HSM-MX.
11. Move MX-LC along the face of the HSM-MX to the target HSM-MX compartment.
12. The skid is moved in to the target compartment. If necessary, adjust the MX-LC position until the MX-LC is properly aligned with the targeted cavity.
13. Secure the MX-LC/skid/cask to the front wall embedments of the HSM-MX using the restraints.
14. The hydraulic power unit is connected to the ram cylinder. The grapple is moved until it engages with the grapple ring of the canister. Using ram cylinder, fully insert the ram into HSM-MX compartment.
15. Operate the ram grapple and engage the grapple arms with the DSC grapple ring.
16. Recheck all alignment marks and ready all systems for DSC transfer.

CAUTION: The time limits for the unloading of the DSC should be determined using the heat loads at the time of the unloading operation and the methodology presented in Sections 4.5 and 4.6 before pulling the DSC out of the HSM-MX.

17. Activate the ram to pull the DSC into the TC.
18. Disengage the ram grapple mechanism so that the grapple is retracted away from the DSC grapple ring.
19. Retract and disengage the ram system from the TC and move it clear of the TC. Remove the TC embedments from the HSM-MX.
20. Retract the skid with TC from docking position and lower it.
21. Move MX-LC to its “home” position, and move the transfer trailer to accepting position.
22. Lower the skid along with TC onto the transfer trailer. Reconnect the skid positioning system, remove the ram cylinder assembly, and reinstall the FC system.
23. Bolt the TC cover plate into place, tightening the bolts to the required torque in a star pattern.

CAUTION: The insides of empty compartments have the potential for high dose rates due to adjacent loaded compartments. Proper ALARA practices should be followed for operations inside these compartments and in the areas outside these compartments whenever the MX-RRT operations are being performed.

24. Disconnect MX-RRT operating mechanism and retract MX-RRT to MX-RRT handling device.
25. Place MX-RRT shield plugs and cover plates for the MX-RRT accesses.
26. Move the transfer trailer from MX-LC and ready the trailer for transfer.
27. Replace the HSM-MX door.

A.9.2.2 Removal of Fuel from the DSC

No change, see Section 9.2.2.

A.9.3 References

- A.9-1 U.S. Nuclear Regulatory Commission, Office of the Nuclear Material Safety and Safeguards, “Safety Evaluation of VECTRA Technologies’ Response to Nuclear Regulatory Commission Bulletin 96-04 For the NUHOMS®-24P and NUHOMS®-7P.
- A.9-2 U.S. Nuclear Regulatory Commission Bulletin 96-04, “Chemical, Galvanic or Other Reactions in Spent Fuel Storage and Transportation Casks,” July 5, 1996.
- A.9-3 SNT-TC-1A, “American Society for Nondestructive Testing, Personnel Qualification and Certification in Nondestructive Testing,” 2006.
- A.9-4 U.S. Nuclear Regulatory Commission, Regulatory Guide 3.61 “Standard Format and Content for a Topical Safety Analysis Report for a Spent Fuel Dry Storage Container,” February 1989.
- A.9-5 CoC 1042 Appendix A, NUHOMS® EOS System Generic Technical Specifications, Amendment 1.

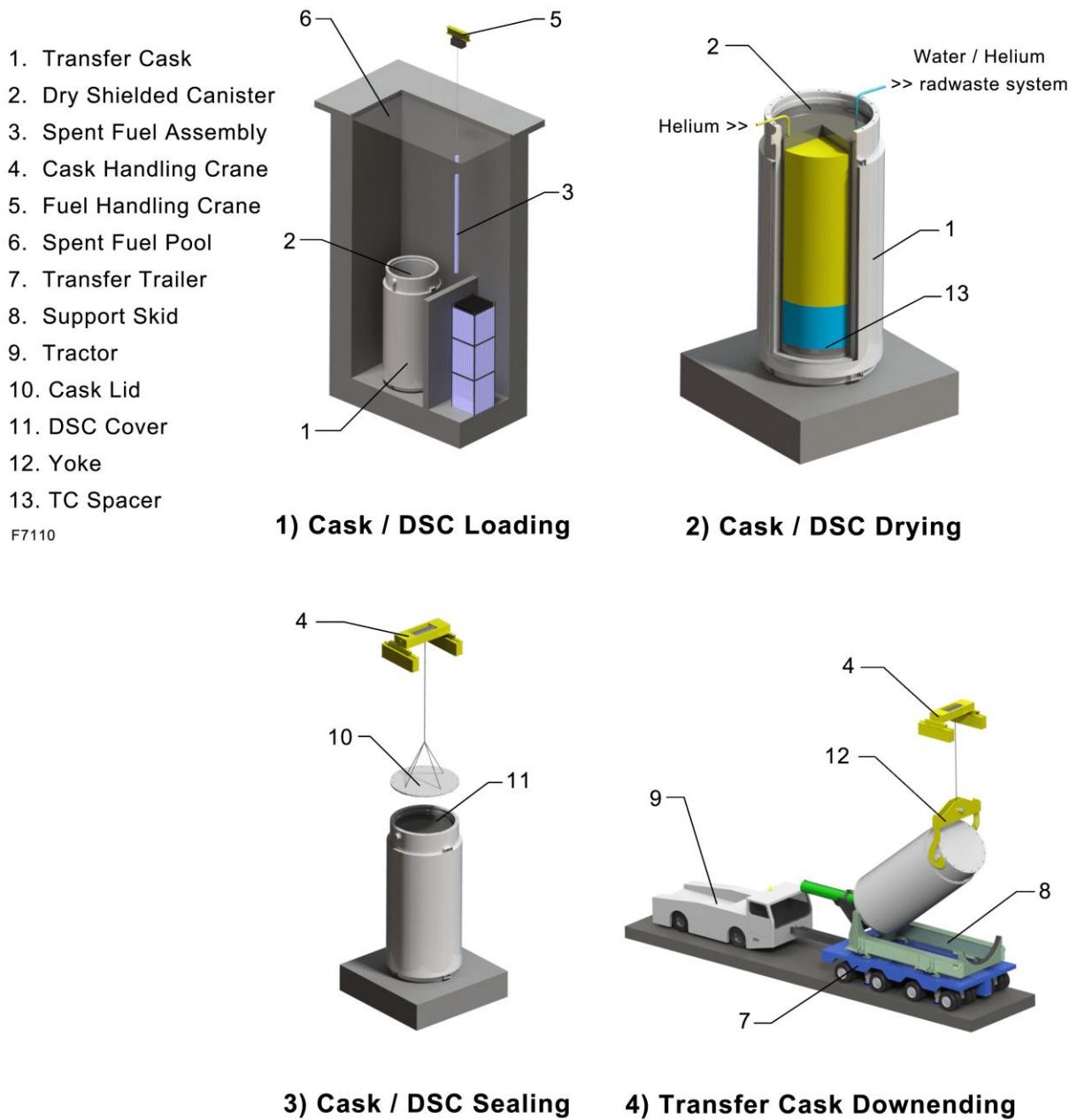
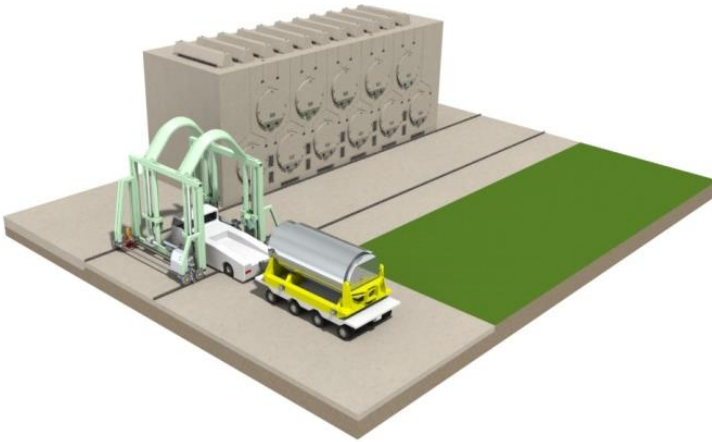
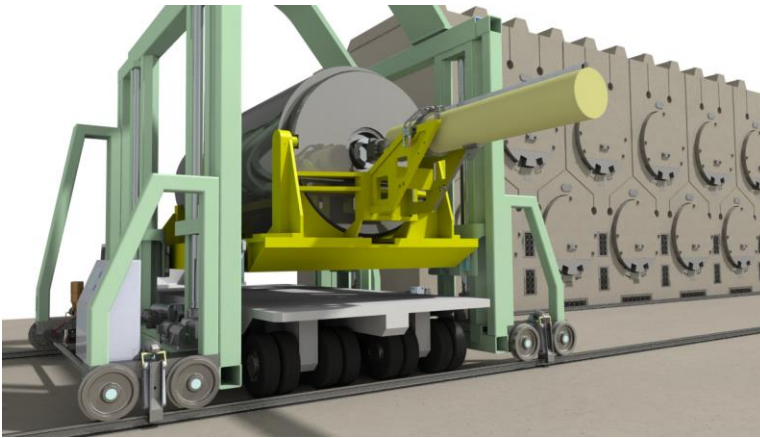


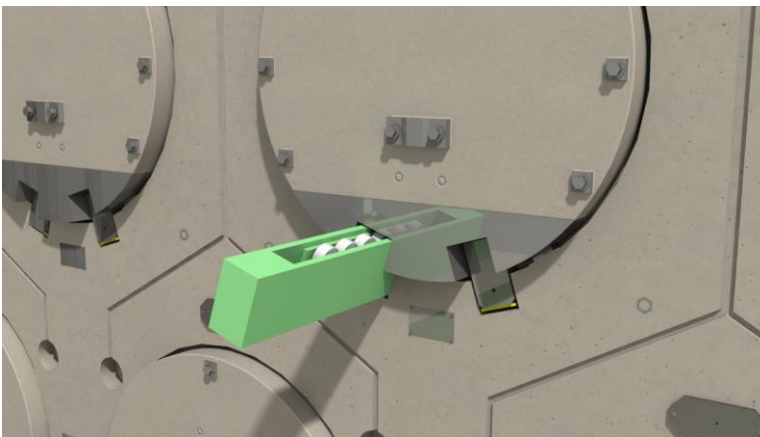
Figure A.9-1
NUHOMS® MATRIX Loading Operations
4 Pages



5) Tow Trailer to Loading Crane at ISFSI

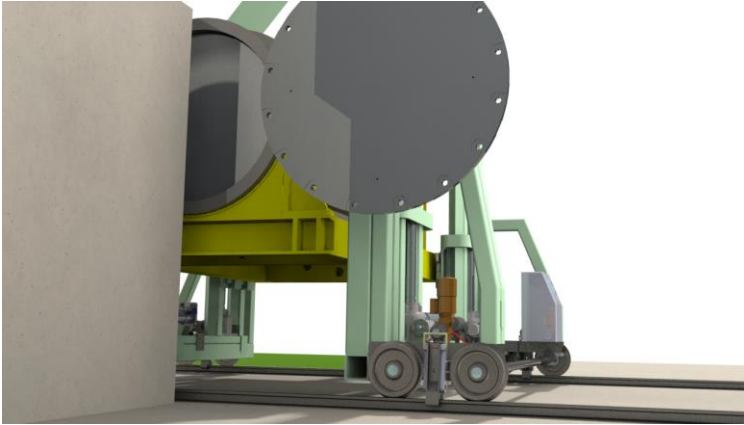


6) Transfer TC from Trailer to Loading Crane



7) Insert and Install Retrievable Roller Tray (MX-RRT)

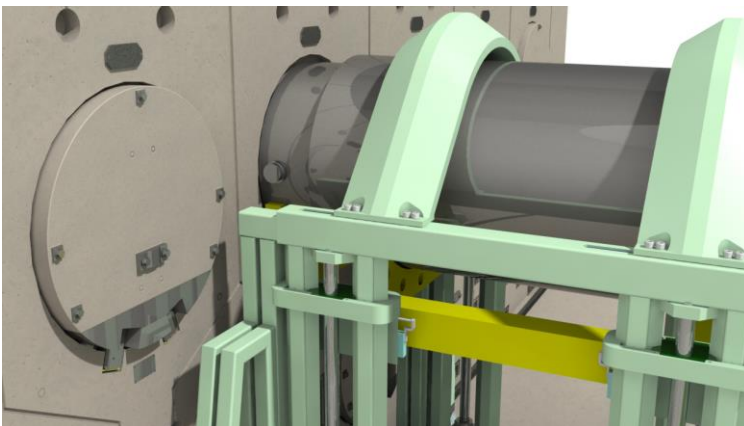
Figure A.9-1
NUHOMS® MATRIX Loading Operations
 4 Pages



8) Remove the Transfer Cask Cover.

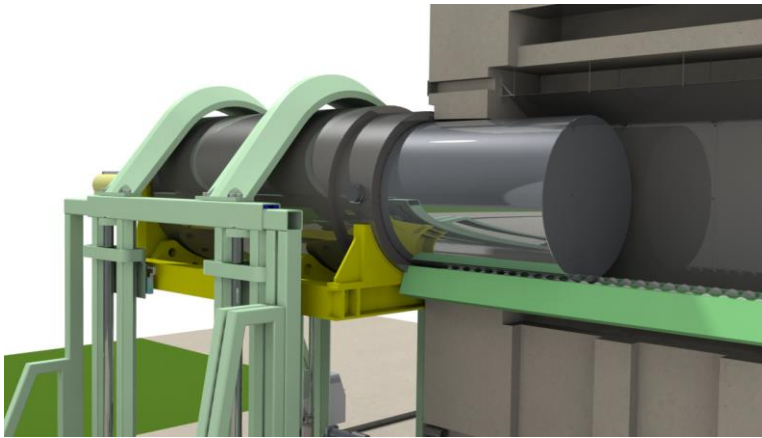


9) Align Transfer Cask at X-Plane Direction, Engage Ram Grapple with Canister, HSM Door Is Removed.

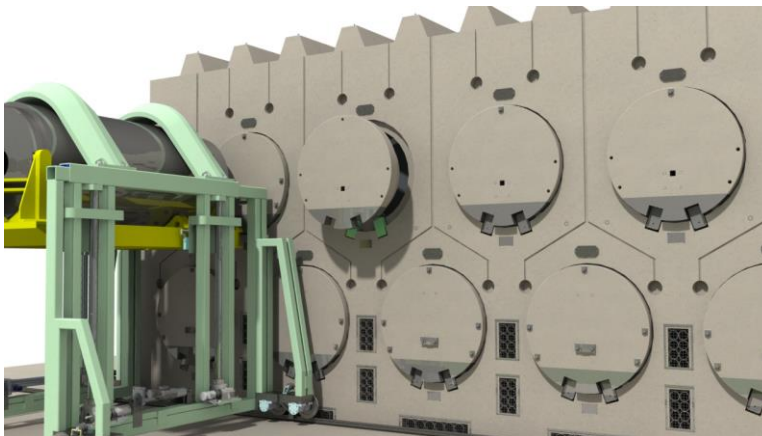


10) Align Transfer Cask at Z-Direction.

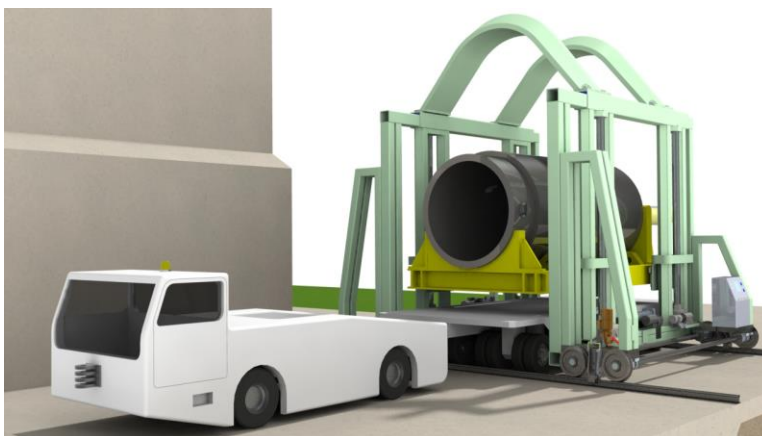
Figure A.9-1
NUHOMS® MATRIX Loading Operations
 4 Pages



11) Transfer Canister to HSM-MX



12) Remove Cask and Install HSM-MX Door



13) Transfer Cask from Loading Crane to Trailer

Figure A.9-1
NUHOMS® MATRIX Loading Operations
 4 Pages

APPENDIX A.10 ACCEPTANCE TESTS AND MAINTENANCE PROGRAM

Table of Contents

A.10 ACCEPTANCE TESTS AND MAINTENANCE PROGRAM.....	A.10-1
A.10.1 Acceptance Tests	A.10-2
A.10.1.2 Leak Tests	A.10-2
A.10.1.3 Visual Inspection and Non-Destructive Examinations	A.10-2
A.10.1.4 Shielding Tests	A.10-2
A.10.1.5 Neutron Absorber Tests	A.10-2
A.10.1.6 Thermal Acceptance Tests	A.10-3
A.10.1.7 Low Alloy High Strength Steel for Basket Structure	A.10-3
A.10.1.8 Cask Identification	A.10-3
A.10.2 Maintenance Program	A.10-4
A.10.3 Repair, Replacement, and Maintenance.....	A.10-5
A.10.4 References	A.10-6

A.10 ACCEPTANCE TESTS AND MAINTENANCE PROGRAM

This chapter specifies the acceptance testing and maintenance program for important-to-safety (ITS) components of the NUHOMS® MATRIX (HSM-MX).

A.10.1 Acceptance Tests

The addition of the HSM-MX to the standardized NUHOMS® EOS system does not result in any change to the pre-operational tests described in Section 10.1, since the EOS-DSCs and EOS-TCs involved are not changed.

A.10.1.1.1 DSC

No change to Section 10.1.1.1.

A.10.1.1.2 HSM-MX

Concrete mix design, placement, and testing are performed in accordance with ACI-318 [A.10-1]. The minimum 28-day compressive strength is 5000 psi if controls are placed on the aggregate type or coefficient of thermal expansion as described in Section 8.2.1.3. If the alternative described in that section is used, the minimum is 7000 psi. In accordance with American Concrete Institute (ACI) 349 Appendix E, paragraph E.4.3 [A.10-2], compressive testing of the concrete mix design for the monolith, and doors is conducted after heating the test cylinders prior to testing. For the HSM-MX, the testing of the specimens are performed at a temperature of 500 °F per Table 4-17. See Sections 4.4.4 and 5.3 of the Technical Specifications [A.10-4].

The reinforcing steel, ITS fasteners, and steel for the door and the front and rear DSC supports are tested for mechanical properties in accordance with the governing specifications called out on the drawings in Chapter A.1.

Weld procedures and welders for the front and rear DSC supports are qualified in accordance with ASME Code Section IX or American Welding Society (AWS) D1.1 [A.10-3].

A.10.1.1.3 Transfer Cask

No change to Section 10.1.1.3.

A.10.1.2 Leak Tests

No change to Section 10.1.2.

A.10.1.3 Visual Inspection and Non-Destructive Examinations

No change to Section 10.1.3.

A.10.1.4 Shielding Tests

No change to Section 10.1.4.

A.10.1.5 Neutron Absorber Tests

No change to Section 10.1.5.

A.10.1.6 Thermal Acceptance Tests

No change to Section 10.1.6.

A.10.1.7 Low Alloy High Strength Steel for Basket Structure

No change to Section 10.1.7.

A.10.1.8 Cask Identification

No change to Section 10.1.8.

A.10.2 Maintenance Program

No change to Section 10.2 associated with the addition of the HSM-MX. HSM inspections from Section 10.2.1.2 are applicable to the HSM-MX.

A.10.3 Repair, Replacement, and Maintenance

No change to Section 10.3 associated with the addition of the HSM-MX.
Requirements of Section 10.3.2 for the HSM are applicable to the HSM-MX.

A.10.4 References

- A.10-1 ACI 318-08, “Building Code Requirements for Structural Concrete and Commentary,” American Concrete Institute, Detroit, MI.
- A.10-2 ACI 349-06, “Code Requirements for Nuclear Safety Related Structures,” American Concrete Institute, Detroit, MI.
- A.10-3 American Welding Society, AWS D1.1/D1.1M, “Structural Welding Code – Steel.”
- A.10-4 CoC 1042 Appendix A, NUHOMS® EOS System Generic Technical Specifications, Amendment 1.

APPENDIX A.11 RADIATION PROTECTION

Table of Contents

A.11 RADIATION PROTECTION	A.11-1
A.11.1 Radiation Protection Design Features	A.11-2
A.11.2 Occupational Dose Assessment.....	A.11-3
A.11.2.1 EOS-DSC Loading, Transfer, and Storage Operations	A.11-3
A.11.2.2 EOS-DSC Retrieval Operations.....	A.11-3
A.11.2.3 Fuel Unloading Operations	A.11-4
A.11.2.4 Maintenance Operations	A.11-4
A.11.2.5 Doses during ISFSI Expansion	A.11-4
A.11.3 Offsite Dose Calculations	A.11-5
A.11.3.1 Normal Conditions (10 CFR 72.104)	A.11-5
A.11.3.2 Accident Conditions (10 CFR 72.106)	A.11-8
A.11.4 Ensuring that Occupational Radiation Exposures Are ALARA.....	A.11-9
A.11.4.1 Policy Considerations	A.11-9
A.11.4.2 Design Considerations	A.11-9
A.11.4.3 Operational Considerations.....	A.11-9
A.11.5 References	A.11-10

List of Tables

Table A.11-1	Occupational Dose Rates	A.11-11
Table A.11-2	Occupational Exposure, EOS-TC108 with EOS-89BTH DSC	A.11-12
Table A.11-3	Occupational Exposure, EOS-TC125/135 with EOS-37PTH DSC.....	A.11-14
Table A.11-4	Occupational Exposure, EOS-TC125 with EOS-89BTH DSC	A.11-16
Table A.11-5	Total Annual Exposure from ISFSI	A.11-18
Table A.11-6	ISFSI Surface Sources	A.11-19
Table A.11-7	2x11 Back-to-Back Dose Rates	A.11-20
Table A.11-8	Two 1x11 Front-to-Front Dose Rates	A.11-22
Table A.11-9	2x11 Back-to-Back Accident Dose Rates.....	A.11-24

List of Figures

Figure A.11-1	Total Annual Exposure from the ISFSI	A.11-26
Figure A.11-2	2x11 ISFSI MCNP Geometry	A.11-27
Figure A.11-3	Two 1x11 ISFSI MCNP Geometry.....	A.11-28

A.11 RADIATION PROTECTION

This chapter describes the design features of the NUHOMS® MATRIX (HSM-MX) that maintain radiation exposure to site personnel as low as reasonably achievable (ALARA), as well as minimize exposure to the public. An occupational dose assessment for operation of the HSM-MX is provided. Radiation exposures to offsite individuals are also computed for both normal and accident conditions of an independent spent fuel storage installation (ISFSI). This chapter provides an example of how to demonstrate compliance with the relevant radiological requirements of 10 CFR Part 20 [A.11-1], 10 CFR Part 72 [A.11-2], and 40 CFR Part 190 [A.11-3]. Each user must perform site-specific calculations to account for the actual layout of the HSM-MXs and fuel source.

A.11.1 Radiation Protection Design Features

The HSM-MX has design features that ensure a high degree of integrity for the confinement of radioactive materials and reduction of direct radiation exposures during storage. These features are described in Section A.11.4.2.

A.11.2 Occupational Dose Assessment

This section provides estimates of occupational dose for typical EOS transfer cask (EOS-TC) and ISFSI loading operations. Assumed annual occupancy times, including the anticipated maximum total hours per year for any individual, and total person-hours per year for all personnel for each radiation area during normal operation and anticipated operational occurrences, will be evaluated by the licensee in a 10 CFR 72.212 evaluation to address the site-specific ISFSI layout, inspection, and maintenance requirements. In addition, the estimated annual collective doses associated with loading operations will be addressed by the licensee in a 10 CFR 72.212 evaluation.

A.11.2.1 EOS-DSC Loading, Transfer, and Storage Operations

The dose rates used in the occupational dose assessment are summarized in Table A.11-1. The EOS-TC loading and transfer dose rates are unchanged from the values presented in Chapter 11. The HSM-MX dose rate reported in Table A.11-1 is the average dose rate on the front surface of an HSM-MX and is obtained from Chapter A.6.

The estimated occupational exposures to ISFSI personnel during loading, transfer, and storage operations using the EOS-TC108 (time and number of workers may vary depending on individual ISFSI practices) are provided in Table A.11-2 for the EOS-89BTH DSC. Similar operations for the EOS-TC125/135 are provided in Table A.11-3 and Table A.11-4. Transfer of the EOS-37PTH DSC to the HSM-MX using the EOS-TC108 is not currently authorized. The task times, number of personnel required, and total doses are listed in these tables. The total exposure results are as follows:

- EOS-TC108 with EOS-89BTH DSC: 4,535 person-mrem (~4.5 person-rem)
- EOS-TC125/135 with EOS-37PTH DSC: 3,200 person-mrem (~3.2 person-rem)
- EOS-TC125 with EOS-89BTH DSC: 2,523 person-mrem (~2.5 person-rem)

The exposures provided above are bounding estimates. Measured exposures from typical NUHOMS® System loading campaigns have been 600 mrem or lower per canister for normal operations, and exposures for the HSM-MX are expected to be similar.

Regulatory Guide 8.34 [A.11-4] is to be used to define the onsite occupational dose and monitoring requirements.

A.11.2.2 EOS-DSC Retrieval Operations

Occupational exposures to ISFSI personnel during EOS-DSC retrieval are similar to those exposures calculated for EOS-DSC insertion. Dose rates for retrieval operations will be lower than those for insertion operations due to radioactive decay of the spent fuel inside the HSM-MX. Therefore, the dose rates for EOS-DSC retrieval are bounded by the dose rates calculated for insertion.

A.11.2.3 Fuel Unloading Operations

No change to Section 11.2.3.

A.11.2.4 Maintenance Operations

The dose rates for surveillance activities are shown in Table A.11-7 and Table A.11-8 for dose rates 6.1 m from the front of an HSM-MX. The 6.1-meter dose rate is a conservative estimate for surveillance activities. The HSM-MX surface dose rates provided in Chapter A.6 can be used for temperature sensor maintenance activities, including calibration and repair.

The general licensee will evaluate the additional dose to personnel from ISFSI operations, based on the particular storage configuration and site personnel requirements.

A.11.2.5 Doses during ISFSI Expansion

During the ISFSI expansion using the construction joint option, the removable end shield wall is absent, and the two complete compartments (one upper and one lower) at the end of the module are empty. The maximum dose rate at the end of the module for the array expansion configuration is 3.64 mrem/hr, which is low (see Section A.6.4.4). If the array terminates at an expansion joint, two empty compartments (one upper and one lower) are also required at the end of the array, and dose rates are bounded by the construction joint option. The maximum dose rate on the surface of the integral shield wall is 4.20 mrem/hr (see Table A.6-2). Therefore, the end dose rate during array expansion activities is approximately the same as the end dose rate with an integral end shield wall, and elevated dose rates during array expansion activities are not anticipated.

A.11.3 Offsite Dose Calculations

Calculated dose rates in the immediate vicinity of the HSM-MX are presented in Chapter A.6, which provides a detailed description of source term configuration, analysis models, and bounding dose rates. The HSM-MX dose rates reported in Chapter A.6 are conservatively based on the EOS-89BTH DSC HLZC #1, which is not authorized for storage in the HSM-MX. Offsite dose rates and annual exposures are presented in this section. Neutron and gamma-ray offsite dose rates are computed, including skyshine, in the vicinity of the two generic ISFSI layouts containing design-basis contents.

A.11.3.1 Normal Conditions (10 CFR 72.104)

Offsite dose rates are a result of direct radiation from the ISFSI. The operation of loading an HSM-MX occurs over a very short time period and contributes negligibly to the offsite dose rates. Therefore, normal condition offsite dose rate calculations are computed only for a loaded ISFSI. No off-normal conditions have been identified that affect offsite dose rates.

Two generic ISFSI configurations are considered that each store 22 EOS-DSCs. In the first configuration, the 22 DSCs are stored in a single HSM-MX with the DSCs in a 2x11 back-to-back configuration. In the 2x11 back-to-back configuration, the front of the modules face outward and the rows are separated by a wall of concrete. In the second configuration, the 22 DSCs are stored in two HSM-MX systems that each contain 11 DSCs in a 1x11 configuration. In the two 1x11 front-to-front configuration, the modules are aligned with the rear shield walls facing outward and the front of the modules facing inward, separated by 32 ft. This configuration has the advantage of minimizing the dose rate near the ISFSI because the inlet vents are directed inward in an area that would not normally be occupied.

It is noted in Chapter A.6 that HSM-MX dose rates are larger for the EOS-89BTH DSC compared to the EOS-37PTH DSC. Therefore, offsite dose rates are computed only for the bounding EOS-DSC. This evaluation provides results for distances ranging from 6.1 to 600 m from each face for the two configurations.

The Monte Carlo computer code Monte Carlo N-Particle Version 5 (MCNP5) [A.11-5] is used to calculate the dose rates at the specified locations around the HSM-MX. The results of this evaluation provide an example of how to demonstrate compliance with the relevant radiological requirements of 10 CFR 20, 10 CFR 72, and 40 CFR 190 for a specific site. Each user must perform site-specific calculations to account for the actual layout of the HSM-MXs and fuel source.

The total annual exposure for each ISFSI layout as a function of distance from each face is given in Table A.11-5 and plotted in Figure A.11-1. The total annual exposure estimates are based on 100% occupancy for 365 days. At large distances, the annual exposure from the 2x11 back-to-back configuration is similar to the two 1x11 front-to-front configuration. Per 10 CFR 72.104, the annual whole-body dose to an individual at the site boundary is limited to 25 mrem. Based on the data shown in Table A.11-5, the offsite dose rate drops below 25 mrem at a distance of approximately 349 m from the ISFSI. Therefore, 349 m is the minimum distance with design basis fuel to the site boundary for the HSM-MX system with 22-DSCs; however, a shorter distance can be demonstrated in a site-specific calculation.

The methodology, inputs, and assumptions for the MCNP analyses are summarized in the following paragraphs.

- The 2x11 back-to-back configuration is modeled as a box enveloping the HSM-MX, including the 44 inch thick shield walls on the two ends. Source particles are started on the surfaces of the box. A sketch of this geometry is shown in Figure A.11-2. The interiors of the HSM-MX and shield walls are modeled as air. Most particles that enter the interiors of the HSM-MX and shield walls will, therefore, pass through unhindered.
- The HSM-MXs in the two 1x11 front-to-front configuration are modeled as two boxes that envelop each 1x11 row, including the 44-inch thick shield walls on the two ends and 44 inch thick rear shield wall in each row. Source particles are started on the surfaces of one of the modules, which is modeled as air. The opposite module is modeled as solid concrete. A sketch of this geometry is shown in Figure A.11-3. The dose field is then created for a source in both modules by accounting for model symmetry, as indicated in Figure A.11-3.
- The ISFSI approach slab is modeled as concrete. Because the ground composition has, at best, only a secondary impact on the dose rates at the detectors, any differences between this assumed layout and the actual layout would not have a significant effect on the site dose rates.
- The “universe” is a sphere surrounding the ISFSI. To account for skyshine, the radius of this sphere ($r=500,000$ cm) is more than 10 mean free paths for neutrons and 50 mean free paths for gammas in air, thus ensuring that the model is of a sufficient size to include all interactions, including skyshine, affecting the dose rate at the detectors.
- The 2x11 and two 1x11 surface sources are input to reproduce the average dose rate and spectrum on the surface of the HSM-MX, as computed in Chapter A.6. The surface average fluxes on the front, roof, side, and rear of the HSM-MXs are explicitly computed and are provided in Tables A.6-3 through A.6-5. The primary and secondary gamma fluxes are simply summed in the gamma input file. These surface spectra are directly input to MCNP for each face.
- Source particles on the ISFSI surface are specified with a cosine distribution. For a cosine distribution, the outward particle current is equal to half of the flux. The MCNP source description requires the number of source particles per second emitted on each face (particle current). Because the current is half of the flux for a cosine distribution, and the flux at each face is known, the input current for each

face (particles/s) is computed as $A \cdot F/2$, where A is the area of the face (cm^2) and F is the total flux on each face (particles/ cm^2 -s). The surface source evaluations are summarized in Table A.11-6.

- ANSI/ANS 6.1.1-1977 flux-to-dose rate factors are utilized [A.11-6]. These factors are provided in Table 6-51.
- For the 2x11 back-to-back configuration with end shield walls, the “box” dimensions are 1260 cm wide, 2096 cm long, and 903 cm high. For the two 1x11 front-to-front configuration with end and back shield walls, the “box” dimensions are 704 cm wide, 2096 cm long, and 903 cm high. The two 1x11 rows are 975 cm (32 ft) apart.
- Dose rates are calculated for distances of 6.1 m (20 ft) to 600 m from the edges of the two ISFSI configurations. Point detectors are placed at the following locations, as measured from each face of the “box”: 6.095 m (20 ft), 10 m, 20 m, 30 m, 40 m, 50 m, 60 m, 70 m, 80 m, 90 m, 100 m, 200 m, 300 m, 400 m, 500 m, and 600 m. Each point detector is placed 91 cm (~3 ft) above the ground.

The MCNP results for the 2x11 back-to-back and two 1x11 front-to-front configurations are summarized in Table A.11-7 and Table A.11-8, respectively. At near distances, the 2x11 configuration results in larger front dose rates than the outward rear of the two 1x11 configuration. For example, the 6.1 m front dose rate is 16.5 mrem/hr for the 2x11 configuration compared to 1.15 mrem/hr for the two 1x11 configuration. However, at near distances, the two 1x11 configuration results in nominally larger side dose rates than the 2x11 configuration.

At large distances, the dose rates are approximately the same, regardless of configuration or direction from the ISFSI, as the dose rate at large distances is dominated by skyshine from the radiation streaming from the roof outlet vents. Also, note that the neutron dose rate is negligible compared to the gamma dose rate at all dose rate locations.

The total Monte Carlo uncertainty is < 5% for all dose rate locations. The annual exposures reported in Table A.11-5 are simply the computed dose rates multiplied by 8760 hours (1 year).

The preceding analyses and results are intended to provide high estimates of dose rates for generic ISFSI layouts. The written evaluations performed by a general licensee for the actual ISFSI must consider the type and number of storage units, layout, characteristics of the irradiated fuel to be stored, site characteristics (e.g., berms, distance to the controlled area boundary, etc.), and reactor operations at the site in order to demonstrate compliance with 10 CFR 72.104.

A.11.3.2 Accident Conditions (10 CFR 72.106)

Per 10 CFR 72.106, the exposure to an individual at the site boundary due to an accident is limited to 5 rem. In an accident, the HSM-MX outlet vent covers and all dose reduction hardware may be lost. In addition, it is assumed that the HSM-MX is in an expansion configuration with the removable end shield wall absent and that a missile strike has damaged two interior walls. This accident scenario results in elevated dose rates on the front, roof, and side of the ISFSI. The average HSM-MX roof, front, and side dose rates and fluxes in an accident are provided in Chapter A.6, Tables A.6-6 through A.6-8.

Table A.11-9 shows the bounding dose rate as a function of distance from a 2x11 back-to-back configuration of HSM-MXs for the accident configuration described above. These dose rates are calculated assuming damage to every module in the array. This is a highly conservative scenario that is not credible, as an accident is not expected to damage every module.

MCNP inputs for a 2x11 ISFSI accident configuration are prepared using the same method as described for the normal condition models. At a distance of 200 m and 349 m from the ISFSI, the accident dose rate is approximately 0.436 mrem/hr and 0.061 mrem/hr, respectively. It is assumed that the recovery time for this accident is five days (120 hours). Therefore, the total exposure to an individual at a distance of 200 m and 349 m is approximately 52 mrem and 7.3 mrem, respectively. This is significantly less than the 10 CFR 72.106 limit of 5 rem.

The EOS-TC may also be damaged in an accident during transfer operations, which would result in an offsite dose, see the discussion in Section 11.3.2.

A.11.4 Ensuring that Occupational Radiation Exposures Are ALARA

A.11.4.1 Policy Considerations

No change to Section 11.4.1.

A.11.4.2 Design Considerations

No change to the EOS-DSC and EOS-TC, see Section 11.4.2.

The HSM-MX storage modules include no active components that require periodic maintenance, thereby minimizing potential personnel dose due to maintenance activities.

The HSM-MXs provide thick concrete shielding, and the shielding design features of the storage modules minimize occupational exposure for any activities on or near the ISFSI.

Regulatory Position 2 of Regulatory Guide 8.8 is incorporated into the design considerations, see Section 11.4.2.

A.11.4.3 Operational Considerations

The areas of highest operational dose of HSM-MX are the front of a loaded HSM-MX at the air inlet vent. Operating procedures, temporary shielding, and personnel training are put into practice to minimize personnel exposure in this area.

The HSM-MX is designed to be essentially maintenance free. It is a passive system with no moving parts. The only anticipated maintenance procedures are the visual inspection of the bird screens on the HSM-MX ventilation inlet and outlet openings, and periodic maintenance of the temperature sensors.

A.11.5 References

- A.11-1 Title 10, Code of Federal Regulations, Part 20, “Standards for Protection Against Radiation.”
- A.11-2 Title 10, Code of Federal Regulations Part 72, “Licensing Requirements for the Independent Storage of Spent Nuclear Fuel and High-Level Radioactive Waste, and Reactor-Related greater than Class C Waste.”
- A.11-3 Title 40, Code of Federal Regulations, Part 190, “Environmental Radiation Protection Standards for Nuclear Power Operations.”
- A.11-4 U.S. Nuclear Regulatory Commission, Regulatory Guide 8.34, “Monitoring Criteria and Methods to Calculate Occupational Radiation Doses,” July 1992.
- A.11-5 Oak Ridge National Laboratory, “MCNP/MCNPX – Monte Carlo N-Particle Transport Code System Including MCNP5 1.40 and MCNPX 2.5.0 and Data Libraries,” CCC-730, RSICC Computer Code Collection, January 2006.
- A.11-6 ANSI/ANS-6.1.1-1977, “Neutron and Gamma-Ray Fluence-to-Dose Factors, American Nuclear Society, LaGrange Park, Illinois, March 1977.

Table A.11-1
Occupational Dose Rates

			Dose Rate (mrem/hr)		
			EOS-TC108	EOS-TC125/135	
Dose Rate Location	Averaged Segments	Config.	EOS-89BTH DSC	EOS-37PTH DSC	EOS-89BTH DSC
DRL1 through DRL10	(1)	(1)	(1)	(1)	(1)
HSM-MX (HMX)	Front face surface average	-	50	50	50

Note 1: Information pertaining to dose rate locations DRL1 through DRL10 is provided in Table 11-1.

Table A.11-2
Occupational Exposure, EOS-TC108 with EOS-89BTH DSC
 (2 Pages)

No. ⁽²⁾	Operation	Configuration	Dose Rate Location	No. of People	Duration (hr)	Dose Rate (mrem/hr)	Dose (person-mrem)	% of Total Dose
1	Place an empty EOS-DSC into an EOS-TC and prepare the EOS-TC for placement into the spent fuel pool.	N/A	N/A	6	4.00	0	0	0%
2	Move the EOS-TC containing an EOS-DSC without fuel into the spent fuel pool.	N/A	N/A	6	1.50	0	0	0%
3	Remove the loaded EOS-TC from the fuel pool and place in the decontamination area.	Decon.	DRL1	2	0.25	194	97	2.1%
4	Install neutron shield. Fill neutron shield with water.	Decon.	DRL4	3	0.33	1050	1040	22.9%
5	Prep and weld inner top cover plate.	Welding	DRL3	2	0.75	198	297	6.5%
6	Vacuum dry and backfill with helium.	Welding	DRL3	2	0.50	198	198	4.4%
7	Weld outer top cover plate and port covers, perform non-destructive examination.	Welding	DRL3	2	0.50	198	198	4.4%
8	Drain annulus. Install EOS-TC aluminum top cover. Ready the support skid and transfer trailer.	Transfer	DRL5	1	0.50	586	293	6.5%
9	Place the EOS-TC onto the skid and trailer. Secure the EOS-TC to the skid.	Transfer	DRL2	2	0.33	747	498	11.0%
10	Install retractable roller tray (RRT).	Transfer	HMX	2	2.00	50	200	4.4%
11	Remove aluminum top cover and replace with steel top cover.	Transfer	DRL3	2	0.33	199	133	2.9%
12	Transfer the EOS-TC to ISFSI.	N/A	N/A	6	1.83	0	0	0%

Table A.11-2
Occupational Exposure, EOS-TC108 with EOS-89BTH DSC
 (2 Pages)

No. ⁽²⁾	Operation	Configuration	Dose Rate Location	No. of People	Duration (hr)	Dose Rate (mrem/hr)	Dose (person-mrem)	% of Total Dose
13	Position the EOS-TC inside the loading crane (MX-LC).	Transfer	HMX+DRL2	2	0.50	797	797	17.6%
14	Remove forced cooling system (if used) and install the ram cylinder assembly.	Transfer	DRL9	2	0.50	137	137	3.0%
15	Remove HSM-MX door.	Transfer	HMX	2	0.50	50	50	1.1%
16	Remove the EOS-TC top cover.	Transfer	HMX+DRL6	2	0.67	150	200	4.4%
17	Align and dock the EOS-TC with the HSM-MX. Secure the EOS-TC to the HSM-MX.	Transfer	HMX+DRL7	2	0.25	239	120	2.6%
18	Transfer the EOS-DSC from the EOS-TC to the HSM-MX using the ram cylinder.	N/A	N/A	3	0.50	0	0	0%
19	Disengage the ram and un-dock the EOS-TC from the HSM-MX.	Transfer	HMX+DRL10	2	0.08	171	29	0.6%
20	Install HSM-MX access door. Move EOS-TC to the transfer skid for removal.	Transfer	HMX	2	0.50	50	50	1.1%
21	Uninstall RRT.	Transfer	HMX	2	2.00	50	200	4.4%
						Total ⁽¹⁾	4535	

Note:

(1) A building crane hang-up off-normal event adds 776 person-mrem (DRL1/decon * 4 workers * 1 hour).

(2) Occupational exposures for steps 1 through 9 are consistent with Chapter 11, Table 11-3.

Table A.11-3
Occupational Exposure, EOS-TC125/135 with EOS-37PTH DSC
 (2 Pages)

No. ⁽²⁾	Operation	Configuration	Dose Rate Location	No. of People	Duration (hr)	Dose Rate (mrem/hr)	Dose (person -mrem)	% of Total Dose
1	Drain neutron shield if necessary. Place an empty EOS-DSC into an EOS-TC and prepare the EOS-TC for placement into the spent fuel pool.	N/A	N/A	6	4.00	0	0	0%
2	Move the EOS-TC containing an EOS-DSC without fuel into the spent fuel pool.	N/A	N/A	6	1.50	0	0	0%
3	Remove a loaded EOS-TC from the fuel pool and place in the decontamination area. Refill neutron shield tank if necessary.	Decon.	DRL1	2	0.25	101	50	1.6%
4	Decontaminate the EOS-TC and prepare welds.	Decon.	DRL2	2	1.75	315	1104	34.5%
		Decon.	DRL3	2	0.50	232	232	7.2%
5	Weld inner top cover plate.	Welding	DRL3	2	0.75	127	191	6.0%
6	Vacuum dry and backfill with helium.	Welding	DRL3	2	0.50	127	127	4.0%
7	Weld outer top cover plate and port covers, perform non-destructive examination.	Welding	DRL3	2	0.50	127	127	4.0%
8	Drain annulus. Install EOS-TC top cover. Ready the support skid and transfer trailer.	Transfer	DRL5	1	0.50	196	98	3.1%
9	Place the EOS-TC onto the skid and trailer. Secure the EOS-TC to the skid.	Transfer	DRL2	2	0.33	248	164	5.1%
10	Install RRT.	Transfer	HMX	2	2.00	50	200	6.2%

Table A.11-3
Occupational Exposure, EOS-TC125/135 with EOS-37PTH DSC
 (2 Pages)

No. ⁽²⁾	Operation	Configuration	Dose Rate Location	No. of People	Duration (hr)	Dose Rate (mrem/hr)	Dose (person-mrem)	% of Total Dose
11	Transfer the EOS-TC to ISFSI.	N/A	N/A	6	1.83	0	0	0%
12	Position the EOS-TC inside the loading crane (MX-LC).	Transfer	HMX+DRL2	2	0.50	298	298	9.3%
13	Remove forced cooling system (if used) and install the ram cylinder assembly.	Transfer	DRL9	2	0.50	76	76	2.4%
14	Remove HSM-MX door.	Transfer	HMX	2	0.50	50	50	1.6%
15	Remove the EOS-TC top cover.	Transfer	HMX+DRL6	2	0.67	108	145	4.5%
16	Align and dock the EOS-TC with the HSM-MX. Secure the EOS-TC to the HSM-MX.	Transfer	HMX+DRL7	2	0.25	147	74	2.3%
17	Transfer the EOS-DSC from the EOS-TC to the HSM-MX using the ram cylinder.	N/A	N/A	3	0.50	0	0	0%
18	Disengage the ram and un-dock the EOS-TC from the HSM-MX.	Transfer	HMX+DRL10	2	0.08	88	14	0.4%
19	Install HSM-MX access door. Move EOS-TC to the transfer skid for removal.	Transfer	HMX	2	0.50	50	50	1.6%
20	Uninstall RRT.	Transfer	HMX	2	2.00	50	200	6.2%
						Total	3200 ⁽¹⁾	

Note:

- (1) Use of aluminum cask lid increases total occupational dose by approximately ~95 person-mrem.
 (2) Occupational exposures for steps 1 through 9 are consistent with Chapter 11, Table 11-4.

Table A.11-4
Occupational Exposure, EOS-TC125 with EOS-89BTH DSC
 (2 Pages)

No. ⁽¹⁾	Operation	Configuration	Dose Rate Location	No. of People	Duration (hr)	Dose Rate (mrem/hr)	Dose (person-mrem)	% of Total Dose
1	Drain neutron shield if necessary. Place an empty EOS-DSC into an EOS-TC and prepare the EOS-TC for placement into the spent fuel pool.	N/A	N/A	6	4.00	0	0	0%
2	Move the EOS-TC containing an EOS-DSC without fuel into the spent fuel pool.	N/A	N/A	6	1.50	0	0	0%
3	Remove a loaded EOS-TC from the fuel pool and place in the decontamination area. Refill neutron shield tank if necessary.	Decon.	DRL1	2	0.25	62	31	1.2%
4	Decontaminate the EOS-TC and prepare welds.	Decon.	DRL2	2	1.75	181	634	25.1%
		Decon.	DRL3	2	0.50	98	98	3.9%
5	Weld inner top cover plate.	Welding	DRL3	2	0.75	113	170	6.7%
6	Vacuum dry and backfill with helium.	Welding	DRL3	2	0.50	113	113	4.5%
7	Weld outer top cover plate and port covers, perform non-destructive examination.	Welding	DRL3	2	0.50	113	113	4.5%
8	Drain annulus. Install EOS-TC top cover. Ready the support skid and transfer trailer.	Transfer	DRL5	1	0.50	191	96	3.8%
9	Place the EOS-TC onto the skid and trailer. Secure the EOS-TC to the skid.	Transfer	DRL2	2	0.33	239	158	6.3%
10	Install RRT.	Transfer	HMX	2	2.00	50	200	7.9%
11	Transfer the EOS-TC to ISFSI.	N/A	N/A	6	1.83	0	0	0%

Table A.11-4
Occupational Exposure, EOS-TC125 with EOS-89BTH DSC
 (2 Pages)

No. ⁽¹⁾	Operation	Configuration	Dose Rate Location	No. of People	Duration (hr)	Dose Rate (mrem/hr)	Dose (person-mrem)	% of Total Dose
12	Position the EOS-TC inside the loading crane (MX-LC).	Transfer	HMX+DRL2	2	0.50	289	289	11.5%
13	Remove forced cooling system (if used) and install the ram cylinder assembly.	Transfer	DRL9	2	0.50	114	114	4.5%
14	Remove HSM-MX door.	Transfer	HMX	2	0.50	50	50	2.0%
15	Remove the EOS-TC top cover.	Transfer	HMX+DRL6	2	0.67	93	125	4.9%
16	Align and dock the EOS-TC with the HSM-MX. Secure the EOS-TC to the HSM-MX.	Transfer	HMX+DRL7	2	0.25	141	71	2.8%
17	Transfer the EOS-DSC from the EOS-TC to the HSM-MX using the ram cylinder.	N/A	N/A	3	0.50	0	0	0%
18	Disengage the ram and un-dock the EOS-TC from the HSM-MX.	Transfer	HMX+DRL10	2	0.08	88	14	0.6%
19	Install HSM-MX access door. Move EOS-TC to the transfer skid for removal.	Transfer	HMX	2	0.50	50	50	2.0%
20	Uninstall RRT.	Transfer	HMX	2	2.00	50	200	7.9%
						Total ⁽²⁾	2523	

Note:

- (1) Occupational exposures for steps 1 through 9 are consistent with Chapter 11, Table 11-5.
- (2) Use of an aluminum cask lid increases the total occupational exposure by approximately 70 person-mrem.

Table A.11-5
Total Annual Exposure from ISFSI

Distance (m)	2x11		Two 1x11	
	Front Total Dose (mrem)	Side Total Dose (mrem)	Back Total Dose (mrem)	Side Total Dose (mrem)
6.1	144687	12069	10042	58090
10	88673	9504	8176	30971
20	32767	5876	5366	11061
30	16063	4035	3807	5937
40	9324	2925	2826	3815
50	6007	2205	2157	2689
60	4137	1703	1679	1992
70	2979	1338	1331	1520
80	2221	1087	1071	1197
90	1698	867	869	961
100	1323	706	714	776
200	191	126	131	135
300	43	31	32	32
400	12	8	9	9
500	4	3	3	3
600	1	1	1	1

Table A.11-6
ISFSI Surface Sources

2x11 Back-to-Back Configuration			
Source	Area (cm²)	Neutron Source (n/s)	Gamma Source (γ/s)
Roof	2.640E+06	2.157E+08	2.414E+11
Front 1	1.892E+06	1.145E+08	9.324E+10
Front 2	1.892E+06	1.145E+08	9.324E+10
Side 1	1.137E+06	8.005E+05	3.898E+08
Side 2	1.137E+06	8.005E+05	3.898E+08
Total	8.697E+06	4.464E+08	4.287E+11
Two 1x11 Front-to-Front Arrays (source for one of the two rows)			
Source	Area (cm²)	Neutron Source (n/s)	Gamma Source (γ/s)
Roof	1.474E+06	1.205E+08	1.348E+11
Front	1.892E+06	1.145E+08	9.324E+10
Back	1.892E+06	1.195E+06	8.996E+08
Side 1	6.351E+05	4.470E+05	2.177E+08
Side 2	6.351E+05	4.470E+05	2.177E+08
Total	6.528E+06	2.371E+08	2.294E+11

Table A.11-7
2x11 Back-to-Back Dose Rates
 (2 Pages)

In Front of ISFSI				
Distance (m)	Gamma Dose Rate (mrem/hr)	Neutron Dose Rate (mrem/hr)	Total Dose Rate (mrem/hr)	σ
6.1	1.62E+01	3.58E-01	1.65E+01	0.02%
10	9.90E+00	2.21E-01	1.01E+01	0.03%
20	3.66E+00	8.23E-02	3.74E+00	0.05%
30	1.79E+00	4.05E-02	1.83E+00	0.1%
40	1.04E+00	2.32E-02	1.06E+00	0.1%
50	6.71E-01	1.46E-02	6.86E-01	0.1%
60	4.62E-01	9.84E-03	4.72E-01	0.2%
70	3.33E-01	6.88E-03	3.40E-01	0.1%
80	2.49E-01	4.97E-03	2.54E-01	0.2%
90	1.90E-01	3.74E-03	1.94E-01	0.2%
100	1.48E-01	2.87E-03	1.51E-01	0.2%
200	2.14E-02	4.23E-04	2.18E-02	0.3%
300	4.78E-03	1.18E-04	4.90E-03	0.7%
400	1.28E-03	4.74E-05	1.33E-03	1.2%
500	4.18E-04	1.87E-05	4.37E-04	4.9%
600	1.33E-04	6.57E-06	1.40E-04	1.6%

Table A.11-7
2x11 Back-to-Back Dose Rates
 (2 Pages)

At Side of ISFSI				
Distance (m)	Gamma Dose Rate (mrem/hr)	Neutron Dose Rate (mrem/hr)	Total Dose Rate (mrem/hr)	σ
6.1	1.31E+00	6.67E-02	1.38E+00	0.1%
10	1.03E+00	5.15E-02	1.08E+00	0.1%
20	6.42E-01	2.93E-02	6.71E-01	0.1%
30	4.43E-01	1.81E-02	4.61E-01	0.2%
40	3.22E-01	1.19E-02	3.34E-01	0.1%
50	2.43E-01	8.20E-03	2.52E-01	0.2%
60	1.89E-01	5.89E-03	1.94E-01	0.2%
70	1.48E-01	4.34E-03	1.53E-01	0.2%
80	1.21E-01	3.29E-03	1.24E-01	1.6%
90	9.65E-02	2.53E-03	9.90E-02	0.3%
100	7.85E-02	2.00E-03	8.05E-02	0.2%
200	1.40E-02	3.66E-04	1.44E-02	0.4%
300	3.40E-03	9.85E-05	3.50E-03	1.2%
400	9.26E-04	3.66E-05	9.62E-04	0.9%
500	2.92E-04	1.41E-05	3.06E-04	1.9%
600	9.88E-05	6.59E-06	1.05E-04	1.9%

Table A.11-8
Two 1x11 Front-to-Front Dose Rates
 (2 Pages)

In Back of ISFSI				
Distance (m)	Gamma Dose Rate (mrem/hr)	Neutron Dose Rate (mrem/hr)	Total Dose Rate (mrem/hr)	σ
6.1	1.09E+00	5.54E-02	1.15E+00	0.3%
10	8.89E-01	4.43E-02	9.33E-01	0.1%
20	5.86E-01	2.63E-02	6.13E-01	0.1%
30	4.18E-01	1.66E-02	4.35E-01	0.1%
40	3.11E-01	1.12E-02	3.23E-01	0.1%
50	2.39E-01	7.72E-03	2.46E-01	0.1%
60	1.86E-01	5.54E-03	1.92E-01	0.2%
70	1.48E-01	4.08E-03	1.52E-01	0.2%
80	1.19E-01	3.08E-03	1.22E-01	0.3%
90	9.68E-02	2.44E-03	9.92E-02	0.2%
100	7.96E-02	1.87E-03	8.15E-02	0.3%
200	1.46E-02	3.34E-04	1.50E-02	0.5%
300	3.53E-03	1.09E-04	3.63E-03	0.8%
400	1.01E-03	3.61E-05	1.05E-03	1.4%
500	3.17E-04	1.40E-05	3.31E-04	1.9%
600	1.11E-04	5.94E-06	1.17E-04	3.8%

Table A.11-8
Two 1x11 Front-to-Front Dose Rates
 (2 Pages)

At Side of ISFSI				
Distance (m)	Gamma Dose Rate (mrem/hr)	Neutron Dose Rate (mrem/hr)	Total Dose Rate (mrem/hr)	σ
6.1	6.46E+00	1.70E-01	6.63E+00	0.02%
10	3.44E+00	9.81E-02	3.54E+00	0.03%
20	1.22E+00	3.94E-02	1.26E+00	0.1%
30	6.56E-01	2.13E-02	6.78E-01	0.1%
40	4.22E-01	1.32E-02	4.36E-01	0.1%
50	2.98E-01	8.82E-03	3.07E-01	0.1%
60	2.21E-01	6.19E-03	2.27E-01	0.1%
70	1.69E-01	4.54E-03	1.74E-01	0.1%
80	1.33E-01	3.30E-03	1.37E-01	0.1%
90	1.07E-01	2.57E-03	1.10E-01	0.2%
100	8.66E-02	2.00E-03	8.86E-02	0.2%
200	1.50E-02	3.62E-04	1.54E-02	0.3%
300	3.55E-03	1.02E-04	3.65E-03	0.6%
400	9.99E-04	3.21E-05	1.03E-03	0.7%
500	3.21E-04	1.46E-05	3.36E-04	1.4%
600	1.06E-04	5.52E-06	1.12E-04	1.3%

Table A.11-9
2x11 Back-to-Back Accident Dose Rates
 (2 Pages)

In Front of ISFSI				
Distance (m)	Gamma Dose Rate (mrem/hr)	Neutron Dose Rate (mrem/hr)	Total Dose Rate (mrem/hr)	σ
6.1	5.74E+01	7.25E-01	5.81E+01	0.05%
10	4.11E+01	5.01E-01	4.16E+01	0.1%
20	2.18E+01	2.39E-01	2.20E+01	0.1%
30	1.40E+01	1.39E-01	1.41E+01	0.1%
40	9.80E+00	9.00E-02	9.89E+00	0.1%
50	7.25E+00	6.09E-02	7.32E+00	0.1%
60	5.56E+00	4.39E-02	5.60E+00	0.2%
70	4.36E+00	3.24E-02	4.39E+00	0.2%
80	3.48E+00	2.50E-02	3.51E+00	0.2%
90	2.82E+00	1.94E-02	2.84E+00	0.2%
100	2.30E+00	1.56E-02	2.32E+00	0.3%
200	4.19E-01	2.94E-03	4.22E-01	0.4%
300	1.03E-01	8.40E-04	1.04E-01	0.8%
400	2.91E-02	3.28E-04	2.94E-02	0.9%
500	8.83E-03	1.41E-04	8.97E-03	1.3%
600	2.92E-03	5.79E-05	2.98E-03	2.0%

Table A.11-9
2x11 Back-to-Back Accident Dose Rates
 (2 Pages)

At Side of ISFSI				
Distance (m)	Gamma Dose Rate (mrem/hr)	Neutron Dose Rate (mrem/hr)	Total Dose Rate (mrem/hr)	σ
6.1	1.33E+02	7.31E-01	1.34E+02	0.04%
10	7.96E+01	4.72E-01	8.01E+01	0.1%
20	3.21E+01	2.16E-01	3.23E+01	0.1%
30	1.81E+01	1.25E-01	1.82E+01	0.4%
40	1.17E+01	8.07E-02	1.18E+01	0.1%
50	8.34E+00	5.60E-02	8.39E+00	0.1%
60	6.19E+00	4.04E-02	6.23E+00	0.1%
70	4.76E+00	3.04E-02	4.79E+00	0.2%
80	3.76E+00	2.34E-02	3.78E+00	0.2%
90	3.00E+00	1.84E-02	3.01E+00	0.2%
100	2.42E+00	1.46E-02	2.44E+00	0.2%
200	4.33E-01	2.95E-03	4.36E-01	0.4%
300	1.05E-01	8.18E-04	1.06E-01	0.7%
400	3.00E-02	3.02E-04	3.03E-02	1.1%
500	9.36E-03	1.36E-04	9.49E-03	2.1%
600	3.09E-03	5.60E-05	3.15E-03	1.6%

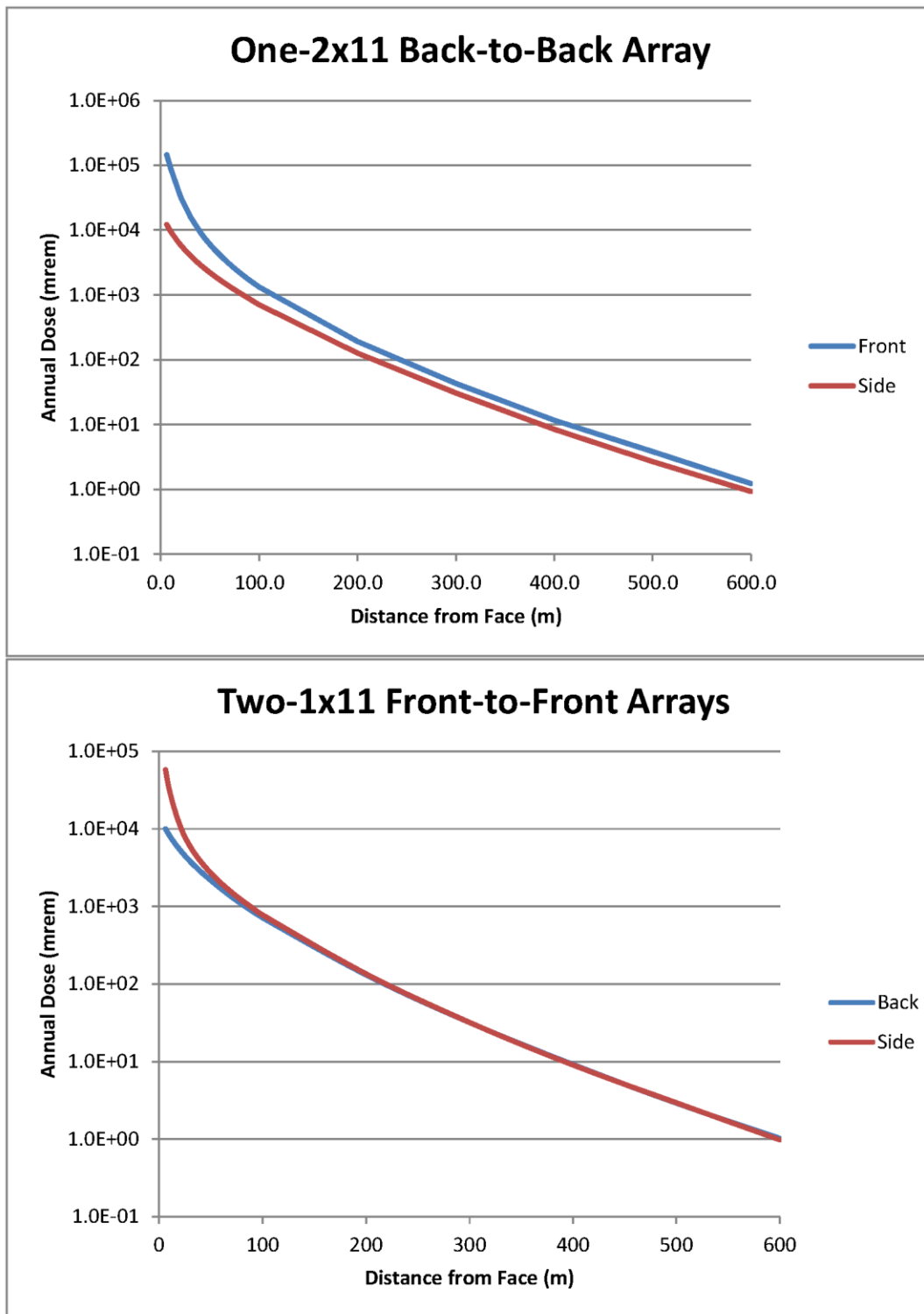


Figure A.11-1
Total Annual Exposure from the ISFSI

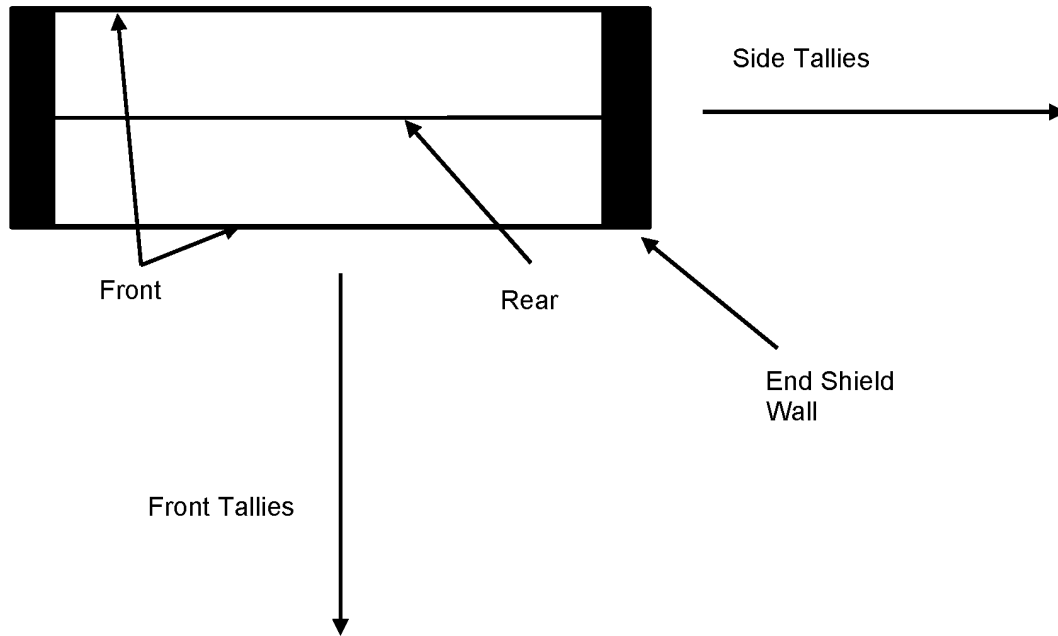
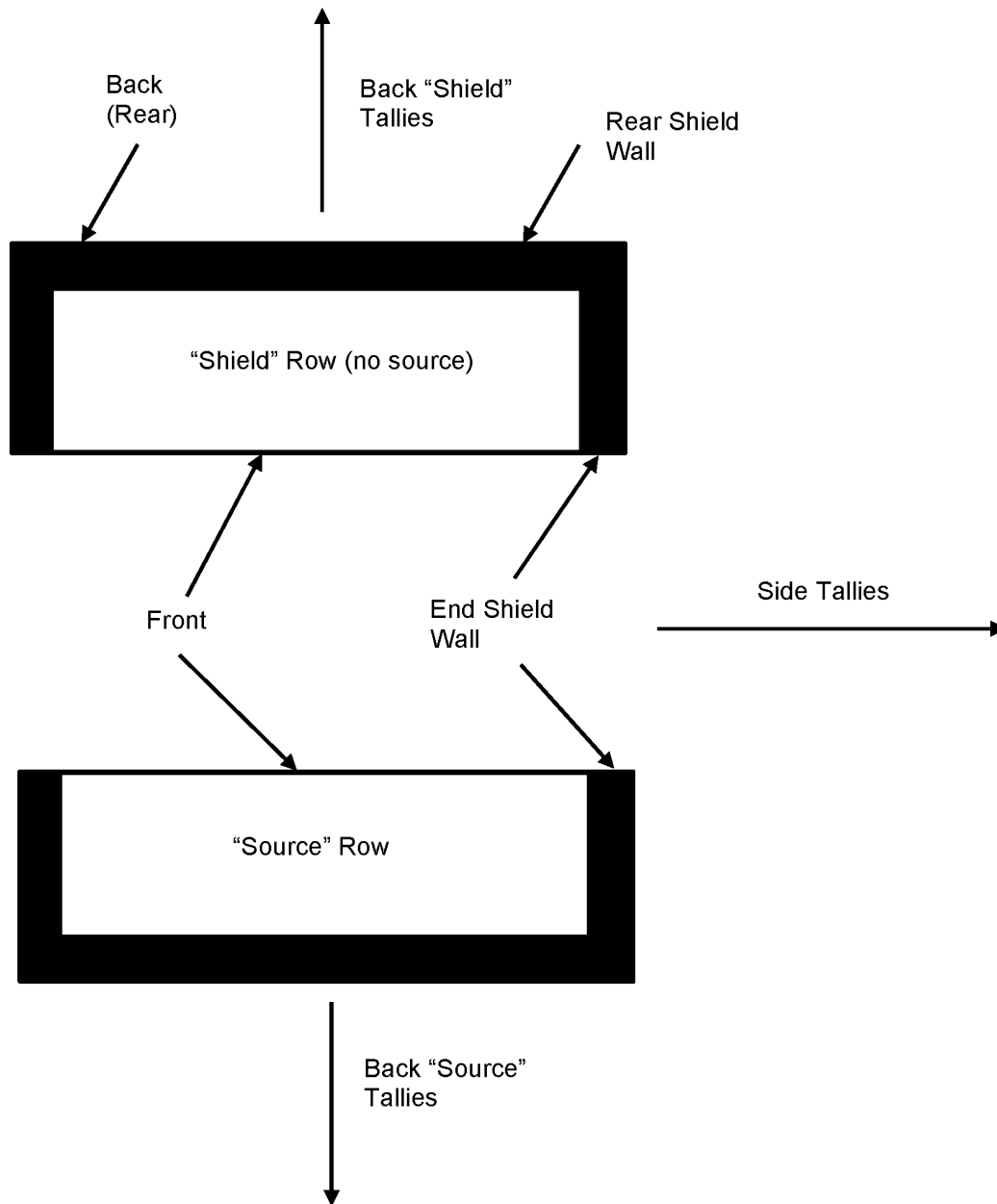


Figure A.11-2
2x11 ISFSI MCNP Geometry



Note: Back "Source" Tallies and Back "Shield" Tallies are summed to create the total back dose rates. Side Tallies are multiplied by two to create the total side dose rates.

Figure A.11-3
Two 1x11 ISFSI MCNP Geometry

APPENDIX A.12 ACCIDENT ANALYSES

Table of Contents

A.12 ACCIDENT ANALYSES.....	A.12-1
A.12.1 Introduction.....	A.12-1
A.12.2 Off-Normal Events.....	A.12-2
A.12.2.1 Off-Normal Transfer Load.....	A.12-2
A.12.2.2 Extreme Temperatures	A.12-4
A.12.3 Postulated Accidents.....	A.12-5
A.12.3.1 EOS-TC Drop	A.12-5
A.12.3.2 Earthquake	A.12-7
A.12.3.3 Tornado Wind and Tornado Missiles Effect on HSM-MX	A.12-7
A.12.3.4 Tornado Wind and Tornado Missiles Effect on EOS-TC.....	A.12-9
A.12.3.5 Flood	A.12-9
A.12.3.6 Blockage of HSM-MX Air Inlet Openings.....	A.12-9
A.12.3.7 Lightning.....	A.12-10
A.12.3.8 Fire/Explosion.....	A.12-10
A.12.4 References.....	A.12-12

A.12 ACCIDENT ANALYSES

A.12.1 Introduction

No change to Section 12.1, except that this appendix is updated to include the NUHOMS® MATRIX (HSM-MX).

A.12.2 Off-Normal Events

Off-normal events are design events of the second type (Design Event II) as defined in ANSI/ANS 57.9 [A.12-2]. Design Event II conditions consist of a set of events that do not occur regularly, but can be expected to occur with a moderate frequency, or about once during a calendar year of independent spent fuel storage installation (ISFSI) operation.

For the HSM-MX, off-normal events could occur during trailer movement, EOS-37PTH dry shielded canister (DSC) or EOS-89BTH DSC transfer and other operational events. The two off-normal events, which bound the range of off-normal conditions, are:

- A “jammed” DSC during loading or unloading from the HSM-MX
- The extreme ambient temperatures of -40 °F (winter) and +117 °F (summer)

These two events envelop the range of expected off-normal structural loads and temperatures acting on the HSM-MX.

A.12.2.1 Off-Normal Transfer Load

Although unlikely, the postulated off-normal handling event assumes that the leading edge of the DSC becomes jammed against some element of the support structure during transfer between the EOS transfer cask (EOS-TC) and the HSM-MX.

Cause of Event

It is postulated that if the EOS-TC is not accurately aligned with respect to the HSM-MX, may bind or jam the DSC during transfer operations.

The interiors of the EOS-TC and the HSM-MX are inspected prior to transfer operations to ensure there are no obstacles. Also, the DSC has beveled lead-ins on each end, designed to avoid binding or sticking on small (less than 0.25-inch) obstacles. The EOS-TC and the MATRIX retractable roller tray (MX-RRT) supports are designed to minimize binding or obstruction during DSC transfer. The postulated off-normal handling load event considers that the leading edge of the DSC becomes jammed against some element of the MX-RRT because of an unlikely gross misalignment of the EOS-TC.

The interfacing dimensions of the top end of the EOS-TC and the HSM-MX access opening sleeve are specified so that docking the EOS-TC with the HSM-MX is not possible should gross misalignments between the EOS-TC and HSM-MX exist.

Detection of Event

The normal load to push/pull the DSC in and out of the EOS-TC/HSM-MX is 135 kips and 80 kips, respectively, applied at the grapple ring and resisted by an axial load of 70 kips push and 40 kips pull on each of the MX-RRT. This movement is performed at a very low speed. System operating procedures and technical specification limits defining the safeguards to be provided ensure that the system design margins are not compromised. If the DSC were to jam or bind during transfer, the pressure increases. The off-normal load set for the “jammed DSC” for both insertion and retrieval are 135 kips and 80 kips, respectively. This load is administratively controlled to ensure that during the transfer operation this load is not exceeded.

During the transfer operation, the force exerted on the DSC by the ram is that required to first overcome the static frictional resisting force between the EOS-TC rails and the MX-RRT rollers. Once the DSC begins to slide on the rollers, the resisting force is a function of sliding friction between the DSC and the EOS-TC rails or between the DSC and the MX-RRT. If motion is prevented, the pressure increases, thereby increasing the force on the DSC until the ram system pressure limit is reached. This limit is controlled so that adequate force is available but is sufficiently low to ensure that component damage does not occur.

Analysis of Effects and Consequences

The DSC and the HSM-MX are designed and analyzed for off-normal transfer loads of 135 kips for insertion and 80 kips for retrieval during insertion and retrieval (unloading) operations. These analyses are discussed in Appendix A.3.9.1 for DSC and A.3.9.4 for HSM-MX. For either loading or unloading of the DSC under off-normal conditions, the stresses on the shell assembly components are demonstrated to be within the ASME allowable stress limits. Therefore, permanent deformation of the DSC shell components does not occur. The internal basket assembly components are unaffected by these loads based on clearances provided between the basket and DSC internal cavity.

There is no breach of the confinement pressure boundary and, therefore, no potential for release of radioactive material exists.

Corrective Actions

No changes to corrective actions described in Section 12.2.1.

A.12.2.2 Extreme Temperatures

The HSM-MX is designed for use at ambient temperatures of -40 °F (winter) and 117 °F (summer). Even though these extreme temperatures are likely to occur for a short period of time, it is conservatively assumed that these temperatures occur for a sufficient duration to produce steady state temperature distributions in HSM-MX. Each licensee should verify that this range of ambient temperatures envelopes the design basis ambient temperatures for the ISFSI site. The components affected by the postulated extreme ambient temperatures are the EOS-TC and DSC during their transfer from the plant's fuel/reactor building to the ISFSI site, and the HSM-MX during storage of a DSC.

Cause of Event

Off-normal ambient temperatures are natural phenomena.

Detection of Event

Off-normal ambient temperature conditions are confirmed by the licensee to be bounding for their site.

Analysis of Effects and Consequences

The thermal evaluation of the HSM-MX for extreme ambient conditions is presented in Chapter A.4. The effects of extreme ambient temperatures on the NUHOMS® MATRIX System are analyzed in sections as follows:

Components	UFSAR Sections
EOS-37PTH DSC and EOS-89BTH DSC Shell	Appendix 3.9.1 and A.3.9.1
EOS-37PTH Basket and EOS-89BTH Basket	Appendix 3.9.2
HSM-MX	Appendix A.3.9.4 & A.3.9.7
EOS-TC	Appendix 3.9.5

Corrective Actions

None

A.12.3 Postulated Accidents

The design basis accident events specified by ANSI/ANS 57.9-1984 [A.12-2] and other postulated accidents that may affect the normal safe operation of the HSM-MX are addressed in this section.

The following sections provide descriptions of the analyses performed for each accident condition. The analyses demonstrate that the requirements of 10 CFR 72.122 [A.12-1] are met and that adequate safety margins exist for the HSM-MX System design. The resulting accident condition stresses in the HSM-MX components are evaluated and compared with the applicable code limits set forth in Chapter A.2.

Radiological calculations are performed to confirm that on-site and off-site dose rates are within acceptable limits. Similarly seismic calculations are performed to confirm that seismic stresses are within acceptable stress limits.

The postulated accident conditions addressed in this section include:

- EOS-TC drop
- Earthquake
- Tornado wind pressure and tornado-generated missiles
- Flood
- Blockage of HSM-MX air inlet openings
- Lightning
- Fire/Explosion

A.12.3.1 EOS-TC Drop

Cause of Accident

As described in Chapter A.9, handling operations involving hoisting and movement of EOS-TC loaded with the EOS-37PTH or EOS-89BTH DSC is typically performed inside the plant's fuel handling building. These include utilizing the crane for placement of the empty DSC into the EOS-TC cavity, lifting the EOS-TC/DSC onto the transfer skid/trailer. An analysis of the plant's lifting devices used for these operations, including the crane and lifting yoke, is needed to address a postulated drop accident for the EOS-TC and its contents. The postulated drop accident scenarios addressed in the plant's 10 CFR Part 50 [A.12-3] licensing basis are plant-specific and should be addressed by the licensee.

Once the EOS-TC is loaded onto the transfer skid/trailer and secured, it is pulled to the HSM-MX site by a tractor vehicle. A predetermined route is chosen to minimize the potential hazards that could occur during transfer. This movement is performed at very low speeds. System operating procedures and technical specification limits defining the safeguards to be provided ensure that the system design margins are not compromised. As a result, it is highly unlikely that any plausible incidents leading to an EOS-TC drop accident could occur. At the ISFSI site, the transfer skid/trailer is used in conjunction with the MATRIX loading crane (MX-LC). The MX-LC is used to assist in loading the DSC into the HSM. The MX-LC is designed, fabricated, installed, tested, inspected and qualified in accordance with ASME NOG-1, as a Type I gantry type of crane, as per the guidance provided in NUREG-0612 [A.12-4]. The transfer skid/trailer is backed up to, and aligned with, the HSM-MX using transfer equipment. The EOS-TC/MX-LC is docked with, and secured to, the HSM-MX access opening. The MX-RRT rollers are extended into HSM-MX through front wall slots for the MX-RRT and secured. The loaded DSC is transferred to or from the HSM-MX using a transfer equipment. The MX-RRT is then lowered to place the DSC on the front and rear DSC supports in the HSM-MX. As a result, for a loaded EOS-TC drop accident to occur during these operations is considered non credible.

Lifts of the EOS-TC loaded with the dry storage canister are made within the existing heavy loads requirements and procedures of the licensed nuclear power plant. The EOS-TC design meets requirements of NUREG-0612 [A.12-4] and American National Standards Institute (ANSI) N14.6 [A.12-4].

The EOS-TC is transferred to the ISFSI in a horizontal configuration. Therefore, the only drop accident evaluated during storage or transfer operations is a side drop or a corner drop.

The EOS-TC and DSC are evaluated for a postulated side and corner drops to demonstrate structural integrity during transfer and plant handling.

Accident Analysis

No change to accident analysis in Section 12.3.1.

Accident Dose Calculation

No change to the accident dose calculation described in Section 12.3.1.

Corrective Actions

No change to corrective actions described in Section 12.3.1.

A.12.3.2 Earthquake

Cause of Accident

The explicitly evaluated seismic response spectra for the NUHOMS® HSM-MX consist of the U.S. Nuclear Regulatory Commission (NRC) Regulatory Guide 1.60 (Reg. Guide 1.60) [A.12-6] with enhanced spectral accelerations above 9 Hz, and anchored to a maximum ground acceleration of 0.85g horizontal and 0.80g for the vertical peak accelerations. The results of the frequency analysis of the HSM-MX structure (which includes a simplified model of the DSC) yield a lowest frequency of 23.94 Hz in the transverse direction and 24.08 Hz in the longitudinal direction. The lowest vertical frequency is 49.02 Hz. Thus, based on the Reg. Guide 1.60 response spectra amplifications, the corresponding seismic accelerations used for the design of the HSM-MX are 1.33g and 1.33g in the transverse and longitudinal directions, respectively, and 0.80g in the vertical direction. The corresponding accelerations applicable to the DSC are 1.62g and 1.61g in the transverse and longitudinal directions, respectively, and 0.80g in the vertical direction.

Accident Analysis

The seismic analyses of the components that are important to safety are analyzed as follow:

Components	UFSAR Sections
EOS-37PTH DSC and EOS-89BTH DSC Shell	Appendix 3.9.1 and A.3.9.1
EOS-37PTH Basket and EOS-89BTH Basket	Appendix 3.9.2
HSM-MX	Appendices A.3.9.4 & A.3.9.7
EOS-TC	Appendix 3.9.5

The results of these analyses show that seismic stresses are well below the applicable stress limits.

Accident Dose Calculations

The dose rate increase is bounded by Section A.12.3.3.

Corrective Actions

No change to corrective actions described in Section 12.3.2.

A.12.3.3 Tornado Wind and Tornado Missiles Effect on HSM-MX

Cause of Accident

No change to the cause of accident described in Section 12.3.3.

Accident Analysis

Stability and stress analyses are performed to determine the response of the HSM-MX to flood, massive missile impact and tornado wind pressure loads.

The stress analyses are performed using the ANSYS [A.12-7]. HSM-MX storage modules arranged in a back-to-back row array provides a conservative estimate of the response of the HSM-MX under postulated static and dynamic loads for any HSM-MX array configurations. These analyses are described in Appendix A.3.9.4.

The sliding and overturning stability analyses due to wind, flood and massive impact loads are performed using closed-form calculation methods to determine the sliding and overturning response of the HSM-MX. A non-linear seismic stability analysis is performed using LS-DYNA [A.12-8]. These analyses are described in Appendix A.3.9.7, Section A.3.9.7.1.

Thus, the requirements of 10 CFR 72.122 are met.

Accident Dose Calculation

As discussed in the evaluations, the tornado wind and tornado missiles do not breach the HSM-MX to the extent that the DSC confinement boundary is compromised. Localized scabbing of the end shield wall of a HSM-MX array may be possible. When the array is in the expansion configuration with the removable end shield wall absent, two inner walls may be damaged as a result of a missile impact.

The HSM-MX outlet vent covers and all dose reduction hardware (DRH) may be lost due to a tornado or tornado missile event. The assumed accident damage increases the dose rates on the front, roof, and end (side) of the HSM-MX. The effect on the average rear dose rate is negligible because the rear surface does not contain vents and sustains little damage in an accident. The HSM-MX accident increases the average dose rate on the front, roof, and end of the module to 92.9 mrem/hr, 4,730 mrem/hr, and 425 mrem/hr, respectively (see Section A.6.1).

The evaluation for the impact on public exposure, a 2x11 ISFSI configuration and a distance to the site boundary of 349 m is used. As documented in Chapter A.11, Section A.11.3.2, for a 2x11 ISFSI configuration, the accident dose rate is approximately 0.436 mrem/hour and 0.061 mrem/hr at a distance of 200 m and 349 m, respectively, from the ISFSI. It is assumed that the recovery time for this accident is five days (120 hours). Therefore, the total exposure to an individual at a distance of 200 m and 349 m is 52 mrem and 7.3 mrem, respectively. This is significantly less than the 10 CFR 72.106 limit of 5 rem. Note that the dose is bounded by the EOS-HSM accident dose documented in Section 12.3.3.

Corrective Action

No change to corrective actions described in Section 12.3.3.

A.12.3.4 Tornado Wind and Tornado Missiles Effect on EOS-TC

Cause of Accident

No change to cause of accident described in Section 12.3.4.

Accident Analysis

No change to accident analysis described in Section 12.3.4.

Accident Dose Calculation

No change to accident dose calculation described in Section 12.3.4.

Corrective Actions

No change to corrective actions described in Section 12.3.4.

A.12.3.5 Flood

Cause of Accident

This event is described in Section 12.3.5.

Accident Analysis

The HSM-MX is evaluated for flooding in Appendix A.3.9.4. Based on the evaluation presented in that section, the HSM-MX can withstand the design basis flood.

Accident Dose Calculation

No change to accident dose calculation described in Section 12.3.5.

Corrective Actions

No change to corrective actions described in Section 12.3.5.

A.12.3.6 Blockage of HSM-MX Air Inlet Openings

This accident conservatively postulates the complete blockage of the air inlet openings of the HSM-MX.

Cause of Accident

Since the HSM-MX is located outdoors, there is a remote probability that the air inlet or outlet openings could become blocked by debris from such unlikely events as floods and tornadoes. There are no credible scenarios that could block both the inlet and outlet vents at the same time due to the significant height difference between the inlet and out vent locations. Therefore, only blockage of the inlet vents is considered in the UFSAR. The HSM-MX design features, such as the perimeter security fence and the redundant protected location of the air inlet and outlet openings, reduce the probability of occurrence of such an accident. Nevertheless, for this conservative generic analysis, such an accident is postulated to occur and is analyzed.

Accident Analysis

The thermal evaluation of this event is presented in Chapter A.4, Section A.4.5 for the EOS-37PTH DSC stored inside an HSM-MX. The analysis performed for the EOS-37PTH DSC bounds the values for the EOS-89BTH DSC. Therefore, the temperatures determined for Load Case #3-S in Section A.4.5 are used in the HSM-MX structural evaluation of this event. The HSM-MX structural analysis, presented in Appendix A.3.9.4, demonstrates that the HSM-MX component stresses remain below allowable values.

Accident Dose Calculation

There are no offsite dose consequences as a result of this accident.

Corrective Actions

No change to corrective actions described in Section 12.3.6.

A.12.3.7 Lightning

Cause of Accident

No change to cause of accident described in Section 12.3.7.

Accident Analysis

No change to accident analysis described in Section 12.3.7.

Corrective Actions

No change to corrective actions described in Section 12.3.7.

A.12.3.8 Fire/Explosion

Cause of Accident

No change to cause of accident described in Section 12.3.8.

Accident Analysis

No change to accident analysis described in Section 12.3.8.

Accident Dose Calculation

No change to the accident dose calculation described in Section 12.3.8.

Corrective Actions

No change to corrective actions described in Section 12.3.8.

A.12.4 References

- A.12-1 Title 10, Code of Federal Regulations, Part 72, “Licensing Requirements for the Independent Storage of Spent Nuclear Fuel, High-Level Radioactive Waste, and Reactor-Related Greater than Class C Waste.”
- A.12-2 ANSI/ANS-57.9-1984, “Design Criteria for an Independent Spent Fuel Storage Installation (Dry Storage Type),” American National Standards Institute, American Nuclear Society.
- A.12-3 Title 10, Code of Federal Regulations, Part 50, “Domestic Licensing of Production and Utilization Facilities.”
- A.12-4 NUREG-0612, “Control of Heavy Loads at Nuclear Power Plants,” U.S. Nuclear Regulatory Commission, July 1980.
- A.12-5 ANSI N14.6-1993, “American National Standards for Special Lifting Device for Shipping Containers Weighing 10,000 lbs. or More for Nuclear Materials,” American National Standards Institute.
- A.12-6 U.S. Nuclear Regulatory Commission, Regulatory Guide 1.60, “Design Response Spectra for Seismic Design of Nuclear Power Plants,” U.S. Atomic Energy Commission, Revision 1, December 1973.
- A.12-7 ANSYS Computer Code and User’s Manual, Release 14.0 and 17.1.
- A.12-8 LS-DYNA Version 7.0.0, Rev. 79055, Livermore Software Technology Corporation (LSTC)

APPENDIX A.13

OPERATING CONTROLS AND LIMITS

The operating controls and limits, including those for the NUHOMS® MATRIX are described in Chapter 13.

APPENDIX A.14 QUALITY ASSURANCE

The addition of the NUHOMS® MATRIX to the NUHOMS® EOS system does not require any changes to the quality assurance requirements stipulated in Chapter 14. Chapter 14 provides the Quality Assurance Program applied to the design, purchase, fabrication, handling, shipping, storing, cleaning, assembly, inspection, testing, operation, maintenance, repair, and modification of the NUHOMS® EOS System and components identified as “important-to-safety” and “safety-related.”